Accepted Manuscript

Submission Date: 2020-10-19
Accepted Date: 2020-11-13
Publication Date: 2020-11-13

Synlett

Enantioselective Halocyclization of Indole Derivatives: Using 1,3-Dihalohydantoins with Anionic Chiral Co(III) Complexes

Ting-Ting Sun, Kun Liu, Shun-Xin Zhang, Chun-Ru Wang, Chuan-Zhi Yao, Jie Yu.

Affiliations below.

DOI: 10.1055/a-1310-5213

Please cite this article as: Sun T-T, Liu K, Zhang S-X et al. Enantioselective Halocyclization of Indole Derivatives: Using 1,3-Dihalohydantoins with Anionic Chiral Co(III) Complexes. Synlett 2020. doi: 10.1055/a-1310-5213

Conflict of Interest: The authors declare that they have no conflict of interest.

This study was supported by National Natural Science Foundation of China (http://dx.doi.org/10.13039/501100001809), 21672002, Anhui Provincial Natural Science Funds for Distinguished Young Scholar, 1908085J07

Abstract:
The highly enantioselective halocyclization reactions of indole derivatives, including tryptophols and tryptamines, have been accomplished by means of anionic chiral Co(III) complexes and 1,3-dihalohydantoins (as little as 0.50 equiv). 3-Halo fused indolines were obtained in excellent yields (up to 98%) and enantioselectivities (up to 98% ee), employing the chiral anion phase-transfer catalysis strategy.

Corresponding Author:
Jie Yu, Anhui Agricultural University, Depart. of Applied Chemistry, Hefei, China, jieyu@ahau.edu.cn

Affiliations:
Ting-Ting Sun, Anhui Agricultural University, Dept. of Applied Chemistry, Hefei, China
Kun Liu, Anhui Agricultural University, applied chemistry, Hefei, China
Shun-Xin Zhang, Anhui Agricultural University, Dept. of Applied Chemistry, Hefei, China
[...]
Jie Yu, Anhui Agricultural University, Depart. of Applied Chemistry, Hefei, China

Enantioselective Halocyclization of Indole Derivatives: Using 1,3-Dihalohydantoins with Anionic Chiral Co(III) Complexes

Ting-Ting Sun [◊a]
Kun Liu [◊a]
Shun-Xin Zhang [◊a]
Chun-Ru Wang [a]
Chuan-Zhi Yao [a]
Jie Yu *[a]

[a] Department of Applied Chemistry, Anhui Agricultural University, Hefei, 230036, China
jieyu@ahau.edu.cn

[◊] These authors contributed equally to this work.

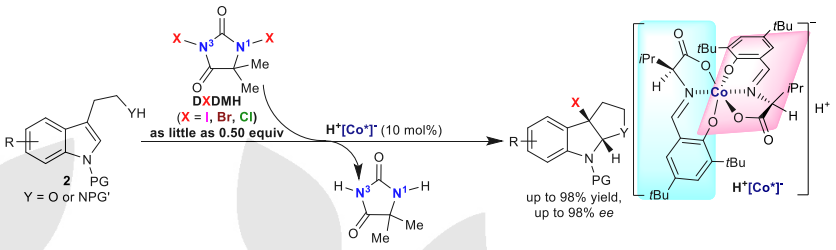

Received:
Accepted:
Published online:
DOI:

Abstract The highly enantioselective halocyclization reactions of indole derivatives, including tryptophols and tryptamines, have been accomplished by means of anionic chiral Co(III) complexes and 1,3-dihalohydantoins (as little as 0.50 equiv). 3-Halo fused indolines were obtained in excellent yields (up to 98%) and enantioselectivities (up to 98% *ee*), employing the chiral anion phase-transfer catalysis strategy.

Key words anion phase-transfer catalysis, chiral Co(III) complex, Brønsted acid, indole derivatives, halocyclization

Asymmetric electrophilic halogenations of olefins are the most fundamental transformations for building up various kinds of enantioenriched heterocyclic molecules, enabled by either organocatalysts or chiral metal-complexes.[1,2] Tremendous efforts have been made on the asymmetric halofunctionalization that mostly relies on the easy handling *N*-halo reagents, such as *N*-haloamides, *N*-haloimides (especially *N*-halosuccinimides), and 1,3-dihalo-5,5-dimethylhydantoins (DXDMHs, X = I, Br, I).[3] Among these reagents, *N*-halosuccinimides (NXS) are the most studied group of N-halo compounds, which can be utilized for the highly stereoselective reactions under mild conditions. [3a-3d] Besides, the commercially available DXDMHs, which possess the same selectivity as NXS and equal or better halogenating ability, are also frequently used.[3g] The traditional activation mode of DXDMHs is believed to form enhanced electrophilic N^3-halogen species, which were generated through protonation or coordination of the C-2 carbonyl moiety by chiral Brønsted or Lewis acid catalysts or the interaction between the halogenating reagents with nucleophilic Lewis bases (Scheme 1A).[1d,3g,4-6] Despite these elegant achievements, the study of the activation manner of DXDMHs remains limited, and the asymmetric versions using the more reactive DBDMH[5] or DIDMH[6] have been less recognized due to the rapid background reactions. Thus, the exploration of novel chiral catalyst systems with DXDMHs bearing two N^1,N^3-X bonds in an atom-economical manner is still desirable to offer new opportunities for the development of enantioselective halogenations.

In our previous works on asymmetric halofunctionalization,[7] we have developed the chiral Co(III) complexes as bifunctional phase-transfer catalysts (Scheme 1, Λ-(*S*,*S*)-**1**) for either intramolecular bromocyclization [7a,7b] or intermolecular iodofunctionalization [7c,7d] with high stereoselectivities. It turned out that Brønsted acids of anionic chiral Co(III) complexes can function like chiral-anion-mediated catalysts[8,9] to undergo exchange reactions with NBS or NIS, leading to the formation of the halogen cation-anionic chiral Co(III) complex species {$X^+[Co^*]^-$} (Scheme 1B).[7] Therefore, we speculated that the anionic chiral Co(III) complexes which are highly soluble in nonpolar media could also act as solid-liquid biphasic transfer catalysts to shuttle the less-soluble DXDMHs (especially the DIDMH) across the solvent interface to control the stereochemistry. The uncatalyzed reaction may be slower than the phase-transfer catalyzed process, as the insoluble parent achiral halogenating agent should be much less reactive with respect to the in situ generated soluble chiral $X^+[Co^*]^-$ species. Moreover, the exchange reaction between chiral Co(III) complexes and DXDMHs with two N^1,N^3-halo groups could make DXDMHs more economical in comparison to NXS (Scheme 1C).

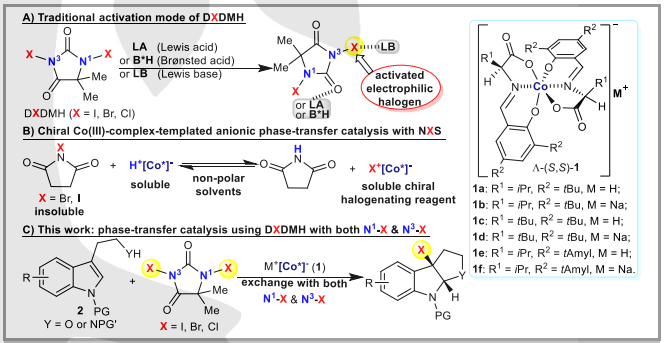

Scheme 1 Asymmetric halogenation with anionic chiral Co(III) complexes.

The asymmetric halocyclizations of indole derivatives, including tryptamines and tryptophols, could provide convenient access to enatioenriched halo-substituted fused indolines, pivotal intermediates in the synthesis of natural alkaloids and other biological active molecules.[10,11] In 2011, Gouverneur reported an elegant asymmetric fluorocyclization of indole derivatives with a chiral amine Lewis base catalyst.[11a] Then Ma, Xie and Lai made a milestone contribution on the enantioselective bromocyclization of tryptamines and tryptophols catalyzed by chiral phosphoric acid.[11b-d] Recently, You and coworkers established the asymmetric fluorocyclization of indole derivatives with chiral phosphoric acid.[11f-g] Despite these progresses, the development

of enantioselective iodo- and chloro-functionalization of indole derivatives and the exploration of the novel activation mode of *N*-halo reagents are still highly desirable. Herein, we present the enantioselective halocyclization of indole derivatives with anionic chiral Co(III) complexes, employing DXDMHs (as little as 0.50 equiv, X = I, Br, Cl) as the halogenating reagents. Chiral Co(III)-complex-templated Brønsted acid enabled the synthesis of the 3-halo fused indoline products with up to 98% yield and with 98% *ee*.

Our studies commenced with the iodocyclization of *N*-Boc protected tryptophol **2a**, a substrate which allows the creation of a stereogenic iodinated quaternary carbon center. The iodocyclization reactions of **2a** with various iodinating reagents, such as DIDMH, NIS and *N*-iodosaccharin (NISC), were initially tested in the presence of 10 mol% of Brønsted acid of anionic chiral Co(III) complexes Λ-**1a** (Table 1, entries 1-3). As anticipated, the more reactive DIDMH turned out to be the best iodine source for this iodocyclization by premixing Λ-**1a** with iodinating reagent and following slow addition of tryptophol **2a** (entries 1-3). Other reaction parameters were then evaluated, including Chiral Co(III)-complex-templated Brønsted acids and sodium salts (Λ-**1b**-**1f**) and solvents, which were found to be less efficient (entries 4-10). Increasing the solvent volume enabled a slightly improved enantioselectivity (entry 11 vs entry 1). To our delight, the utilization of CCl_4 rendered the iodocyclization reaction in 98% yield, furnishing 3-iodofuroindoline **3a** with 95% *ee* (entry 12). Employing toluene as a co-solvent in CCl_4 at lower temperature led to a little decline in stereoselectivity (entry 13). It is noteworthy that the addition of DIDMH in one portion to the mixture of Λ-**1** and **2a** proved detrimental (entry 14).

Table 1 Optimization of the iodocyclization conditions of **2a**.[a]

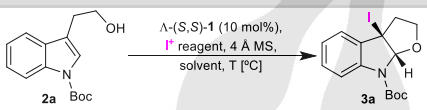

entry	Λ-**1**	I⁺ reagent	solvent	T [°C]	Yield[b] (%)	*ee*[c] (%)
1	**1a**	DIDMH	PhMe	-30	79	79
2	**1a**	NIS	PhMe	-30	93	62
3	**1a**	NISC	PhMe	-30	90	67
4	**1b**	DIDMH	PhMe	-30	84	70
5	**1c**	DIDMH	PhMe	-30	5	3
6	**1d**	DIDMH	PhMe	-30	70	3
7	**1e**	DIDMH	PhMe	-30	54	39
8	**1f**	DIDMH	PhMe	-30	50	68
9	**1a**	DIDMH	$CHCl_3$	-30	75	50
10	**1a**	DIDMH	MTBE	-30	70	61
11[d]	**1a**	DIDMH	PhMe	-30	90	86
12[d]	**1a**	DIDMH	CCl_4	-20	98	95
13[d]	**1a**	DIDMH	CCl_4/PhMe (20:1)	-30	83	88
14[e]	**1a**	DIDMH	CCl_4	-20	86	81

[a] Unless otherwise noted, reactions were carried out by slow addition (over 20 minutes) of **2a** (0.10 mmol) in solvent (0.50 mL) to a mixture of I⁺ reagent (0.10 mmol), Λ-**1** (0.01 mmol) and 4 Å MS (100 mg) in solvent (0.50 mL) under an air atmosphere in the absence of light for 48 h. [b] Isolated yield. [c] Determined by HPLC analysis. [d] The reaction was carried out by slow addition of **2a** in solvent (1.0 mL) to the reaction mixture in solvent (4.0 mL) for 72 h. [e] Solid DIDMH was added in one portion to the reaction mixture of **2a** with **1a** in CCl_4 (5.0 mL).

Table 2 Substrate scope of enantioselective iodocyclization.[a]

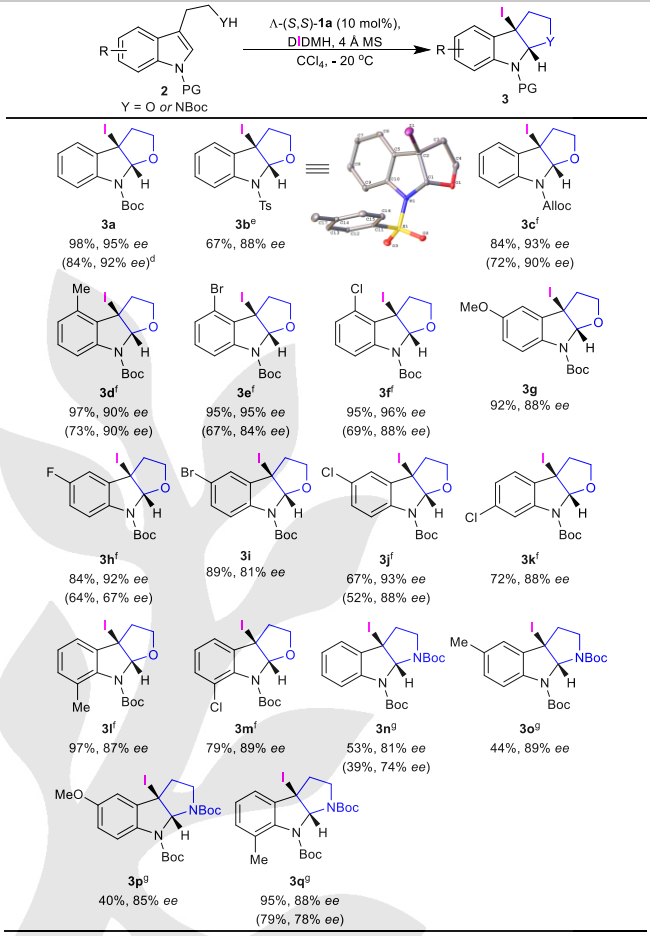

[a] Unless otherwise noted, reactions were carried out by slow addition (over 20 minutes) of **2** (0.10 mmol) in CCl_4 (1.0 mL) to a mixture of DIDMH (0.10 mmol), Λ-**1a** (0.01 mmol) and 4 Å MS (100 mg) in CCl_4 (4.0 mL) at -20 °C under an air atmosphere in the absence of light for 72 h. [b] Isolated yield. [c] Determined by HPLC analysis. [d] Values in parentheses are yields and *ee* when DIDMH (0.05 mmol for tryptophols and 0.06 mmol for tryptamines) was employed. [e] CCl_4/toluene (5:1, 5.0 mL) was used as solvent at -30 °C. [f] CCl_4/toluene (20:1, 5.0 mL) was used at -30 °C. [g] DIDMH (0.12 mmol) and CCl_4 (2.0 mL) was used at -20 °C.

Under the optimized reaction conditions, the substrate scope of the asymmetric iodocyclization with respect to the substituted tryptophols and tryptamines **2** was explored (Table 2).[12] The tryptophols **2a**-**2c** with electron-withdrawing protecting groups (Boc, Ts and Alloc) could be converted to the corresponding iodocyclization products with good yields and enantioselectivities (up to 95% *ee*). The substituent on the indole moiety of *N*-Boc-protected tryptophols **2d**-**2m** was then evaluated. In general, the electronic feature of all the substrates did not exert significant effect on the enantioselectivities. Either electron-donating or electron-withdrawing substituents at the different positions of the indole moiety were nicely tolerated to afford the 3-iodofuroindolines **3d**-**3m** in good to excellent yields (up to 97%) and enantioselectivities (up to 96% *ee*).[13] The absolute configuration of **3b** was assigned by X-ray crystallographic diffraction of its enantiopure sample.[14] Furthermore, the *di*-Boc-protected tryptamine **2n** could also undergo the asymmetric iodocyclization,[13] providing the product **3n** with good enantioselectivity. 5-substitutied tryptamines **2o**-**2p** with electron-donating groups could participate in the reaction in good enantioselectivities (up to 89% *ee*) but with moderate yield. In particularly, excellent yield and good enantioselectivity were observed in the case of 7-methyl-

substituted product **3q**. We have also evaluated the iodocyclization when half of DIDMH was employed for a selection of tryptophols and tryptamines (Table 2, values in parentheses). Interestingly, even with 0.50 equiv of DIDMH, 3-iodofuroindolines **3a**, **3c**, **3d** and **3j** were obtained with a slight decrease enantioselectivities. It is indicated that both the N^1- and N^3-iodo groups indeed participate in the anionic chiral Co(III) complex-mediate phase-transfer procedure.

Chiral Co(III)-complex-templated Brønsted acid (Λ-**1a**) was also identified to be a general catalyst for the asymmetric bromocyclization. At the outset of our investigation, different bromine sources including NBS, DBDMH, *N*-bromophthalimide (NBP) and *N*-bromoacetamide (NBA) were studied, and the NBS delivered the best outcome (95% *ee*) (Table 3, entries 1-4). Further screening of other catalysts Λ-**1a**-**1f** didn't give better results (entries 5-9), and lower reaction efficiency was observed when the bromocyclization was performed in CCl_4 with NBS (entry 10). It is noticed that a good enantioselectivity was obtained by premixing Λ-**1a** with NBS (entry 11), while lowering the temperature resulted in a higher enantiomeric excess of 95% (entry 12). As anticipated, the bromocyclization by premixing Λ-**1a** with DBDMH could also proceed smoothly to give the product **4a** in good enantioselectivity (entry 13). Excitingly, the use of CCl_4/toluene co-solvents enabled the reaction in excellent yield with 96% *ee* (entry 14).

Table 3 Optimization of the bromocyclization conditions of **2a**.[a]

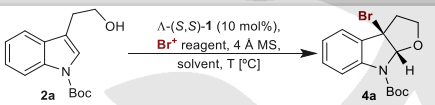

entry	Λ-**1**	Br^+ reagent	solvent	T [°C]	Yield[b] (%)	ee[c] (%)
1	**1a**	NBS	PhMe	-20	93	85
2	**1a**	DBDMH	PhMe	-20	77	78
3	**1a**	NBP	PhMe	-20	74	81
4	**1a**	NBA	PhMe	-20	22	76
5	**1b**	NBS	PhMe	-20	78	84
6	**1c**	NBS	PhMe	-20	77	11
7	**1d**	NBS	PhMe	-20	72	9
8	**1e**	NBS	PhMe	-20	85	85
9	**1f**	NBS	PhMe	-20	52	11
10	**1a**	NBS	CCl_4	-20	81	75
11[d]	**1a**	NBS	PhMe	-20	84	91
12[d]	**1a**	NBS	PhMe	-30	87	95
13[d]	**1a**	DBDMH	PhMe	-30	97	86
14[e]	**1a**	DBDMH	CCl_4/PhMe (20:1)	-30	95	96

[a] Unless otherwise noted, reactions were carried out by addition of solid Br^+ source (0.10 mmol) to a mixture of **2a** (0.1 mmol), Λ-**1** (0.01 mmol) and 4 Å MS (100 mg) in solvent (1.0 mL) under an air atmosphere in the absence of light for 24 h. [b] Isolated yield. [c] Determined by HPLC analysis. [d] A solution of **2a** (0.5 mL) was slowly added to the mixture (0.5 mL) for 48 h. [e] A solution of **2a** (1.0 mL) was slowly added to the mixture (4.0 mL) for 48 h.

To evaluate the efficiency of the chiral anion phase-transfer catalytic procedure, the enantiomeric excesses of the 3-bromofuroindolines **4** of the bromocyclizations were also carried out in the presence of DBDMH (Table 4).[15] All tryptophols bearing carbamate or sulfonate N-protecting groups worked well under these conditions, leading to the formation of the products **4a**-**4c** in up to 96% *ee*. The absolute configuration of **4b** was also assigned by X-ray crystallographic diffraction.[14] The electronic nature of tryptophols **2** has little influence on the reactivity, as products **4d**-**4m** were obtained in 78-97% yield with good to excellent enantioselectivities (82-98% *ee*). This protocol could also be applied for the bromocyclization of tryptamines, providing the products **4n**-**4p** in up to 97% yield and 82% ee. Moreover, 3-bromofuroindolines **4a**, **4c**, **4e**-**4h**, **4k** and **4l** were returned in up to 97% *ee* with 0.50 equiv of DBDMH (Table 4, values in parentheses). In each case both the yields and enantioselectivities nearly match those realized with 1.0 equiv of DBDMH, which suggested that both N^1- and N^3-bromo groups of DBDMH could also be involved in the phase-transfer catalytic bromocyclization.

Table 4 Substrate scope of enantioselective bromocyclization.[a]

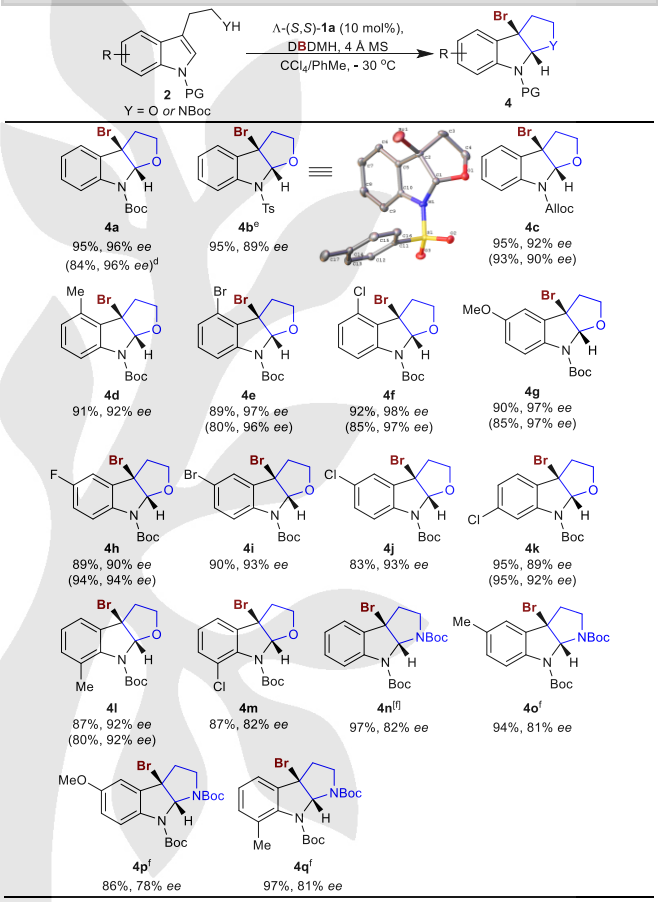

[a] Unless otherwise noted, reactions were carried out by slow addition of the solution of **2** (0.10 mmol) to a mixture of DBDMH (0.10 mmol), Λ-**1a** (0.01 mmol) and 4 Å MS (100.0 mg) at -30 °C under an air atmosphere in the absence of light for 48 h. CCl_4/toluene (20:1, 5.0 mL) was used as solvent. [b] Isolated yield. [c] Determined by HPLC analysis. [d] Values in parentheses are yields and *ee* when 0.50 equiv of DBDMH was employed. [e] CCl_4/toluene (5:1, 5.0 mL) was used as solvent. [f] Solid DBDMH was added in one portion to the reaction mixture.

The asymmetric chlorocyclization reaction of tryptophols **2** with DCDMH in the presence of Brønsted acid (Λ-**1a**) was also successful,[13] delivering the corresponding products in moderate yield with up to 42% *ee* (Scheme 2).

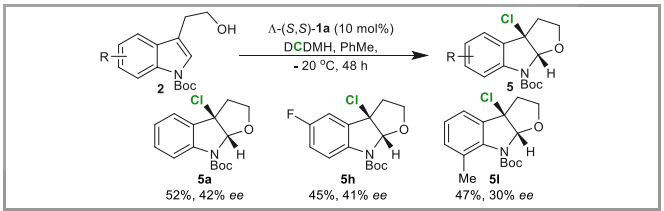

Scheme 2 Asymmetric chlorocyclization reaction with DCDMH.

Interestingly, the enantioselective halocyclization using with 0.50 equiv of DIDMH and DBDMH could be scaled up, even the presence of 2 mol% of Λ-**1a** was sufficient to render a 3 mmol-scale bromocyclization to give **4a** in 87% yield and 89% *ee* (Scheme 3A). To demonstrate the synthetic utility of the halocyclization, silver(I)-mediated both the iodide **3a** and bromide **4a** with acetate[16] could afford the 3-acetoxyfuro-indoline **6**, the core skeleton of (+)-madindoline A,[10c] in 92% and 93% *ee*, respectively (Scheme 3B). Subsequently, a few control experiments were performed to get insight into the mechanism (Scheme 3C). 3-iodofuroindolines **3a** could be obtained in 44% yield with nearly maintained enantioselectivity (93% *ee*) even when 0.30 equiv. of DIDMH was employed. Moreover, the less active 1-ITMH and 3-ITMH were used as iodinating reagents, in which N^1- or N^3-iodo was replaced by a methyl group, affording the product **3a** in high yield but with reduced enantioselectivities. It appeared that the rate of the formation of chiral iodinating species from 1-ITMH or 3-ITMH might be slower than that of DIDMH, leading to a comparable competition between the catalytic and noncatalytic reaction.

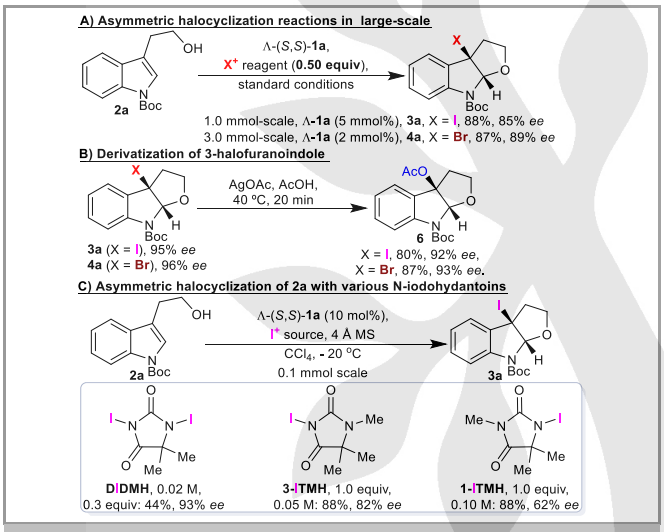

Scheme 3 Synthetic versatility of the catalytic system and preliminary mechanism studies.

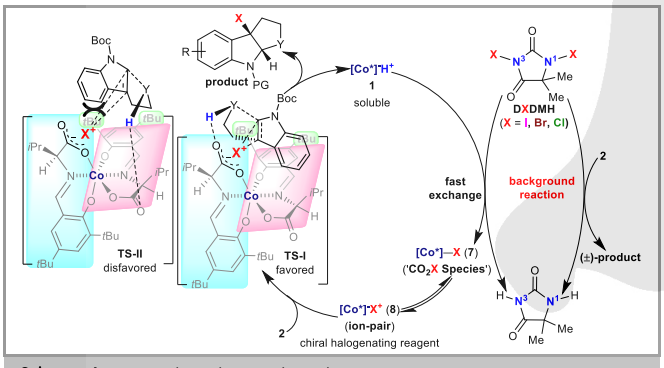

Scheme 4 Proposed catalytic cycle and transition states.

According to these experimental data, we propose a catalytic cycle based on our previous works[7] (Scheme 4). The Brønsted acid of anionic chiral Co(III) complexes Λ-**1** could undergo a fast exchange reaction with DXDMHs to give the covalent 'CO_2X species' **7**[7a] and insoluble hydantoin, and the active species **7** leads to the formation of the chiral ion-pair **8**. The generated chiral halogenating reagent **8** is soluble in the nonpolar solvent (such as CCl_4 and PhMe), thus could render the enantioselective halofunctionalization with indole derivatives **2** to afford the products via the transition states **TS-I** and regenerate the catalyst Λ-**1**. As illustrated in **TS-I** and **TS-II**, the halocyclization could favorably occur on the *Re* face in **TS-I**, as the *Si* face might be disfavored due to the steric repulsion between the indole ring and the *tert*-butyl of the Schiff base (**TS-II**).

In summary, we have developed efficient phase-transfer catalytic halocyclization reactions of indole derivatives (including tryptophols and tryptamines), using DXDMHs that contained two activated halo groups (as little as 0.50 equiv) as atom-economical halogen sources. The employment of Brønsted acid of anionic chiral Co(III) complexes allows the stereoselective formation of 3-halo indolines in excellent yields (up to 98%) with good to excellent enantioselectivities (up to 98% *ee*). The process could also undergo on a large scale even in the presence of 2 mol% catalyst and 0.50 equiv of DXDMHs. Further development of these chiral anion phase-transfer catalysts and application of the halogenation reactions are underway.

Funding Information

We are grateful for financial support from NSFC (Grant 21672002), Anhui Provincial Natural Science Funds for Distinguished Young Scholar (1908085J07), Shennong Scholar Program of Anhui Angricultural University and National Undergraduate Training Program for Innovation and Entrepreneurship (202010364039).

Supporting Information

YES (this text will be updated with links prior to publication)

Primary Data

NO (this text will be deleted prior to publication)

References and Notes

(1) For selected reviews, see: (a) Chen, G.; Ma, S. *Angew. Chem. Int. Ed.* **2010**, *49*, 8306. (b) Castellanos, A.; Fletcher, S. P. *Chem. Eur. J.* **2011**, *17*, 5766. (c) Tan, C. K.; Zhou, L.; Yeung, Y.-Y. *Synlett* **2011**, 1335. (d) Hennecke, U. *Chem.-Asian J.* **2012**, *7*, 456. (e) Denmark, S. E.; Kuester, W. E.; Burk, M. T. *Angew. Chem. Int. Ed*. **2012**, *51*, 10938. (f) Chemler, S. R.; Bovino, M. T. *ACS Catal.* **2013**, *3*, 1076. (g) Chen, J.; Zhou, L. *Synthesis* **2014**, *46*, 586. (h) Cheng, Y. A.; Yu, W. Z.; Yeung, Y.-Y. *Org. Biomol. Chem.* **2014**, *12*, 2333. (i) Zheng, S.; Schienebeck, C. M.; Zhang, W.; Wang, H.-Y.; Tang, W. *Asian J. Org. Chem.* **2014**, *3*, 366. (j) Cresswell, A. J.; Eey, S. T.-C.; Denmark, S. E. *Angew. Chem. Int. Ed.* **2015**, *54*, 15642. (k) Liang, X.-W.; Zheng, C.; You, S.-L. *Chem.-Eur. J.* **2016**, *22*, 11918. (l) Mizar, P.; Wirth, T. *Synthesis* **2017**, *49*, 981. (m) Gieuw, M. H.; Ke, Z.; Yeung, Y.-Y. *Chem. Rec.* **2017**, *17*, 287. (n) Cai, Y.; Liu, X.; Zhou, P.; Feng, X. *J. Org. Chem.* **2019**, *84*, 1.

(2) For selected early examples of asymmetric halofunctionalization, see: (a) Kang, S. H.; Lee, S. B.; Park, C. M. *J. Am. Chem. Soc.* **2003**, *125*, 15748. (b) Haas, J.; Bissmire, S.; Wirth, T. *Chem.-Eur. J.* **2005**, *11*, 5777. (c) Veitch, G. E.; Jacobsen, E. N. *Angew. Chem. Int. Ed.* **2010**, *49*, 7332. (d) Rauniyar, V.; Lackner, A. D.; Hamilton, G. L.; Toste, F. D. *Science* **2011**, *334*, 1681. (e) Hennecke, U.; Mueller, C. H.; Froehlich, R. *Org. Lett.* **2011**, *13*, 860. (f) Huang, D.; Wang, H.; Xue, F.; Guan, H.; Li, L.; Peng, X.; Shi, Y. *Org. Lett.* **2011**, *13*, 6350. (g) Cai, Y.; Liu, X.; Jiang, J.; Chen, W.; Lin, L.; Feng, X. *J. Am. Chem. Soc.* **2011**, *133*, 5636. (h) Zhou, L.; Chen, J.; Tan, C. K.; Yeung, Y.-Y. *J. Am. Chem. Soc.* **2011**, *133*, 9164. (i) Denmark, S. E.; Burk, M. T. *Org. Lett.* **2012**, *14*, 256.

(3) (a) Koval', I. V. *Russ. J. Org. Chem.* **2002**, *38*, 301. (b) Kolvani, E.; Ghorbani-Choghamarani, A.; Salehi, P.; Shirini, F.; Zolfigol, M. A. *J.*

Iran. Chem. Soc. **2007**, *4*, 126. (c) Minakata, S. *Acc. Chem. Res.* **2009**, *42*, 1172. (d) Veisi, H.; Ghorbani-Vaghei, R.; Zolfigol, M. A. *Org. Prep. Proced. Int.* **2011**, *43*, 489. (e) Tan, C. K.; Yeung, Y.-Y. *Chem. Commum.* **2013**, *49*, 7985. (f) Saikia, I.; Borah, A. J.; Phukan, P. *Chem. Rev.* **2016**, *116*, 6837. (g) de Andrade, V. S. C.; de Mattos, M. C. S. *Synthesis* **2019**, *51*, 1841.

(4) For selected examples of asymmetric halogenation involving DCDMH, see: (a) Whitehead, D. C.; Yousefi, R.; Jaganathan, A.; Borhan, B. *J. Am. Chem. Soc.* **2010**, *132*, 3298. (b) Jaganathan, A.; Garzan, A.; Whitehead, D. C.; Staples, R. J.; Borhan, B. *Angew. Chem. Int. Ed.* **2011**, *50*, 2593. (c) Zhang, W.; Liu, N.; Schienebeck, C. M.; Decloux, K.; Zheng, S.; Werness, J. B.; Tang, W. *Chem.-Eur. J.* **2012**, *18*, 7296. (d) Jaganathan, A.; Staples, R. J.; Borhan, B. *J. Am. Chem. Soc.* **2013**, *135*, 14806. (e) Yin, Q.; You, S.-L. *Org. Lett.* **2013**, *15*, 4266. (f) Yin, Q.; You, S.-L. *Org. Lett.* **2014**, *16*, 1810. (g) Yin, Q.; You, S.-L. *Org. Lett.* **2014**, *16*, 2426. (h) Soltanzadeh, B.; Jaganathan, A.; Staples, R. J.; Borhan, B. *Angew. Chem. Int. Ed.* **2015**, *54*, 9517. (i) Yin, Q.; Wang, S.-G.; Liang, X.-W.; Gao, D.-W.; Zheng, J.; You, S.-L. *Chem. Sci.* **2015**, *6*, 4179. (j) Cai, Q.; Luo, J.; Zhao, X. *Angew. Chem. Int. Ed.* **2019**, *58*, 1315. (k) Wedek, V.; Van Lommel, R.; Daniliuc, C. G.; De Proft, F.; Hennecke, U. *Angew. Chem. Int. Ed.* **2019**, *58*, 9239.

(5) For selected examples of asymmetric halogenation involving DBDMH, see: (a) Murai, K.; Matsushita, T.; Nakamura, A.; Fukushima, S.; Shimura, M.; Fujioka, H. *Angew. Chem. Int. Ed.* **2010**, *49*, 9174. (b) Murai, K.; Nakamura, A.; Matsushita, T.; Shimura, M.; Fujioka, H. *Chem.-Eur. J.* **2012**, *18*, 8448. (c) Zhou, L.; Tay, D. W.; Chen, J.; Leung, G. Y. C.; Yeung, Y.-Y. *Chem. Commun.* **2013**, *49*, 4412. (d) Li, Z.; Shi, Y. *Org. Lett.* **2015**, *17*, 5752. (e) Pan, H.; Huang, H.; Liu, W.; Tian, H.; Shi, Y. *Org. Lett.* **2016**, *18*, 896. (f) Guo, S.; Cong, F.; Guo, R.; Wang, L.; Tang, P. *Nat. Chem.* **2017**, *9*, 546. (g) Lu, Y.; Nakatsuji, H.; Okumura, Y.; Yao, L.; Ishihara, K. *J. Am. Chem. Soc.* **2018**, *140*, 6039. (h) Wang, Y.-F.; Shao, J.-J.; Wang, B.; Chu, M.-M.; Qi, S.-S.; Du, X.-H.; Xu, D.-Q. *Adv. Synth. Catal.* **2018**, *360*, 2285.

(6) For an example of asymmetric halogenation involving DIDMH, see: Cai, Y.; Liu, X.; Li, J.; Chen, W.; Wang, W.; Lin, L.; Feng, X. *Chem.-Eur. J.* **2011**, *17*, 14916.

(7) (a) Jiang, H.-J.; Liu, K.; Yu, J.; Zhang, L.; Gong, L.-Z. *Angew. Chem. Int. Ed.* **2017**, *56*, 11931. (b) Liu, K.; Jiang, H.-J.; Li, N.; Wang, J.; Zhang, Z.-Z.; Yu, J. *J. Org. Chem*. **2018**, *83*, 6815. (c) Li, N.; Yu, H.; Wang, R.; Shen, J.; Wu, W.-Q.; Liu, K.; Sun, T.-T.; Zhang, Z.-Z.; Yao, C.-Z.; Yu, J. *Tetrahedron Lett.* **2018**, *59*, 3605. (d) Wang, R.; Wu, W.-Q.; Li, N.; Shen, J.; Liu, K.; Yu, J. *Synlett* **2019**, *30*, 1077.

(8) For selected reviews, see: (a) Lacour, J.; Hebbe-Viton, V. *Chem. Soc. Rev.* **2003**, *32*, 373. (b) Lacour, J.; Moraleda, D. *Chem. Commun.* **2009**, 7073. (c) Zhang, Z.; Schreiner, P. R. *Chem. Soc. Rev.* **2009**, *38*, 1187. (d) Wenzel, M.; Hiscock, J. R.; Gale, P. A. *Chem. Soc. Rev.* **2012**, *41*, 480. (e) Phipps, R. J.; Hamilton, G. L.; Toste, F. D. *Nat. Chem.* **2012**, *4*, 603. (f) Mahlau, M.; List, B. *Angew. Chem. Int. Ed.* **2013**, *52*, 518. (g) Brak, K.; Jacobsen, E. N. *Angew. Chem. Int. Ed.* **2013**, *52*, 534.

(9) For selected examples on chiral anions catalysis, see: (a) Sigman, M. S.; Jacobsen, E. N. *J. Am. Chem. Soc.* **1998**, *120*, 4901. (b) Sigman, M. S.; Vachal, P.; Jacobsen, E. N. *Angew. Chem. Int. Ed.* **2000**, *39*, 1279. (c) Llewellyn, D. B.; Adamson, D.; Arndtsen, B. A. *Org. Lett.* **2000**, *2*, 4165. (d) Carter, C.; Fletcher, S.; Nelson, A. *Tetrahedron: Asymmetry* **2003**, *14*, 1995. (e) Mayer, S.; List, B. *Angew. Chem. Int. Ed.* **2006**, *45*, 4193. (f) Hamilton, G. L.; Kang, E. J.; Mba, M.; Toste, F. D. *Science* **2007**, *317*, 496. (g) Hamilton, G. L.; Kanai, T.; Toste, F. D. *J. Am. Chem. Soc.* **2008**, *130*, 14984. (h) Yu, J.; Jiang, H.-J.; Zhou, Y.; Luo, S.-W.; Gong, L.-Z. *Angew. Chem. Int. Ed.* **2015**, *54*, 11209. (i) Zhang, X.; Zhao, K.; Li, N.; Yu, J.; Gong, L.-Z.; Gu, Z. *Angew. Chem. Int. Ed.* **2020**, *59*, 19899.

(10) For recent reviews, see: (a) Song, J.; Chen, D.-F.; Gong, L.-Z. *Natl. Sci. Rev.* **2017**, *4*, 381. (b) Palmieri, A.; Petrini, M. *Nat. Prod. Rep.* **2019**, *36*, 490. (c) Zheng, C.; You, S.-L. *Nat. Prod. Rep.* **2019**, *36*, 1589.

(11) For selected examples, see: (a) Lozano, O.; Blessley, G.; del Campo, T. M.; Thompson, A. L.; Giuffredi, G. T.; Bettati, M.; Walker, M.; Borman, R.; Gouverneur, V. *Angew. Chem. Int. Ed.* **2011**, *50*, 8105. (b) Xie, W.; Jiang, G.; Liu, H.; Hu, J.; Pan, X.; Zhang, H.; Wan, X.; Lai, Y.; Ma, D. *Angew. Chem. Int. Ed.* **2013**, *52*, 12924. (c) Liu, H.; Jiang, G.; Pan, X.; Wan, X.; Lai, Y.; Ma, D.; Xie, W. *Org. Lett.* **2014**, *16*, 1908. (d) Feng, X.; Jiang, G.; Xia, Z.; Hu, J.; Wan, X.; Gao, J.-M.; Lai, Y.; Xie, W. *Org. Lett.* **2015**, *17*, 4428. (e) Cai, Q.; Yin, Q.; You, S.-L. *Asian J. Org. Chem*. **2014**, *3*, 408. (f) Liang, X.-W.; Liu, C.; Zhang, W.; You, S.-L. *Chem. Commun*. **2017**, *53*, 5531. (g) Liang, X.-W.; Cai, Y.; You, S.-L. *Chin. J. Chem.* **2018**, *36*, 925.

(12) **General experimental procedures for a representative iodocyclization to 3a**

A 10-mL oven-dried vial was charged with DIDMH (0.10 mmol or 0.05 mmol), catalyst Λ-**1a** (7.2 mg, 0.01 mmol), activated 4 Å molecular sieves (100.0 mg) and CCl_4 (4.0 ml) at room temperature in the absence of light. The mixture was cooled to -20 ºC and stirred for 30 min. A precooled solution of the tryptophol **2a** (0.10 mmol) in CCl_4 (1.0 ml) was added dropwise to the mixture over 20 min and the reaction was stirred vigorously until the reaction was complete (monitored by TLC). The reaction was then quenched with pre-cooled NEt_3 (-20 ºC, 1.0 mmol) and saturated aqueous $Na_2S_2O_3$ (0.50 mL). The mixture was purified by flash column chromatography (silica gel, petrol ether/EtOAc = 10/1) to give the enantioenriched product **3a**. yield: for 1.0 equiv DIDMH, 37.9 mg (98%); for 0.5 equiv DIDMH, 32.5 mg (84%); (Flash column chromatography eluent, petroleum ether/ethyl acetate = 10/1); colorless oil; $[\alpha]_D^{20}$ = -82.6 (c 0.38 CH_3OH); ^{1}H-NMR (600 MHz, $CDCl_3$) δ 7.79 (s, 1H), 7.39 (d, *J* = 7.2 Hz, 1H), 7.23 (t, *J* = 7.0 Hz, 1H), 7.05 (t, *J* = 7.4 Hz, 1H), 6.45 – 6.17 (m, 1H), 3.85 – 3.76 (m, 1H), 3.45 – 3.32 (m, 1H), 2.99 – 2.86 (m, 2H), 1.61 (s, 9H); ^{13}C-NMR (151 MHz, $CDCl_3$) δ 151.92, 129.93, 125.17, 123.84, 115.02, 110.12, 103.32, 82.23, 67.81, 67.32, 47.91, 28.46; HRMS (ESI) calculated for $C_{15}H_{18}INNaO_3$ $[M+Na]^+$: 410.0229, found 410.0223; Enantiomeric excess: for 1.0 equiv DIDMH, 95%; for 0.5 equiv DIDMH, 92%; determined by HPLC (Daicel Chirapak IE, hexane / isopropanol = 90/10, flow rate 1.0 mL/min, T = 30 ºC, 254 nm): t_{maj} = 9.20 min, t_{min} = 8.43 min.

(13) See the Supporting Information for details.

(14) CCDC 1938720 (**3b**) and 1938617 (**4b**) contain the supplementary crystallographic data for this paper. These data can be obtained free of charge from The Cambridge Crystallographic Data Centre.

(15) **General experimental procedures for a representative bromocyclization to 4a**

A 10-mL oven-dried vial was charged with DBDMH (0.10 mmol or 0.05 mmol), catalyst Λ-**1a** (7.2 mg, 0.01 mmol), activated 4 Å molecular sieves (100.0 mg) and PhMe/CCl_4 (1:20, 4.0 mL) at room temperature in the absence of light. The mixture was cooled to -30 ºC and stirred for 30 min. A precooled solution of the tryptophol **2a** (0.10 mmol) in PhMe/CCl_4 (1:20, 1.0 mL) was added dropwise to the mixture over 20 min and the reaction was stirred vigorously until the reaction was complete (monitored by TLC). The reaction was then quenched with pre-cooled NEt_3 (-30 ºC, 1.0 mmol) and saturated aqueous $Na_2S_2O_3$ (0.50 mL). The mixture was purified by flash column chromatography (silica gel, petrol ether/EtOAc = 10/1) to give the enantioenriched product **4a**. yield: for 1.0 equiv DBDMH, 32.3 mg (95%); for 0.5 equiv DBDMH, 28.6 mg (84%); (Flash column chromatography eluent, petroleum ether/ethyl acetate = 10/1); colorless oil; $[\alpha]_D^{20}$ = -137.1 (c 0.32 CH_3OH); ^{1}H-NMR (600 MHz, $CDCl_3$) δ 7.84 (s, 1H), 7.41 (d, *J* = 7.5 Hz, 1H), 7.28 (t, *J* = 7.8 Hz, 1H), 7.08 (t, *J* = 7.5 Hz, 1H), 6.34 – 6.12 (m, 1H), 4.00 (t, *J* = 8.0 Hz, 1H), 3.53 – 3.45 (m, 1H), 2.94 – 2.86 (m, 1H), 2.80 (dd, *J* = 12.3, 3.8 Hz, 1H), 1.60 (s, 9H); ^{13}C-NMR (151 MHz, $CDCl_3$) δ 151.86, 141.73, 131.86, 130.50, 124.87, 123.76, 115.00, 100.87, 82.28, 67.79, 61.77, 45.09, 28.43; Enantiomeric excess: for 1.0 equiv DBDMH, 96%; for 0.5 equiv DBDMH, 96%; determined by HPLC (Daicel Chirapak IC, hexane / isopropanol = 70/30, flow rate 1.0 mL/min, T = 30 ºC, 254 nm): t_{maj} = 4.41 min, t_{min} = 4.04 min.

(16) Xu, J.; Tong, R. *Green Chem.* **2017**, *19*, 2952.

Supporting Information for

Enantioselective Halocyclization of Indole Derivatives: Using 1,3-Dihalohydantoins with Anionic Chiral Co(III) Complexes

Ting-Ting Sun, Kun Liu, Shun-Xin Zhang, Chun-Ru Wang, Chuan-Zhi Yao, and Jie Yu*

Department of Applied Chemistry, Anhui Agricultural University, Hefei, Anhui 230036, P. R. China

E-mail: jieyu@ahau.edu.cn

Table of Contents

1. Introduction

1.1. General Data

NMR spectra were recorded on Agilent-600 MHz spectrometer. Melting points were measured on a digital melting point apparatus and the temperature was uncorrected. FT-ICRMS spectra were recorded on P-SIMS-Gly of Bruker Daltonics Inc. HPLC analysis was performed on Waters-Breeze (2487 Dual λ Absorbance Detector and 1525 Binary HPLC Pump, UV detection monitored at 254 nm). Chiralpak IA, IC and IE columns were purchased from Daicel Chemical Industries, Ltd. The absolute configuration of **3b** and **4b** was assigned by the X-ray analysis.

1.2. Materials

Analytic grade solvents for the column chromatography and commercially available reagents were used as received. CCl_4 was dried over CaH_2 and distilled prior to use. Toluene was dried over Na and distilled prior to use. The catalysts (Λ-**1a** to Λ-**1f**) were synthesized according to the literature.[1] Tryptophols **2a**-**2e**, **2g**-**2i**, **2k**-**2m** and tryptamines **2n**-**2q** were prepared according to following procedure and the spectral data were in accordance with the literature.[2] 1-Iodo-3,5,5-trimethylhydantoin (1-ITMH) and 3-iodo-1,5,5-trimethylhydantoin (3-ITMH) were generally synthesized according to the procedure reported.[3]

2. Supplementary Tables

Table S1 Asymmetric Iodocyclization of Tryptophols **2** under Different Solvent and Temperature.[a]

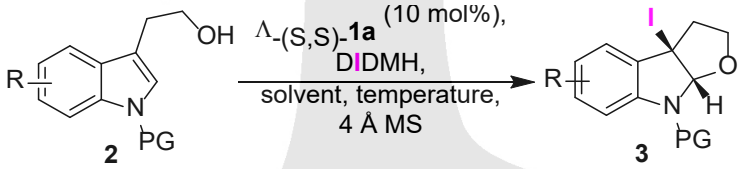

Entry	**3**	R	PG	CCl_4/PhMe (20/1), -30 °C[b]		CCl_4, -20 °C[c]	
				yield (%)[d]	ee (%)[e]	yield (%)[d]	ee (%)[e]
1	**3a**	H	Boc	83	88	98	95
2	**3b**	H	Ts	67[f]	88	22	71
3	**3c**	H	Alloc	84	93	84	85
4	**3d**	4-Me	Boc	97	90	92	87

5	**3e**	4-Br	Boc	95	95	88	91
6	**3f**	4-Cl	Boc	95	96	84	90
7	**3g**	5-OMe	Boc	91	78	92	88
8	**3h**	5-F	Boc	84	92	77	87
9	**3i**	5-Br	Boc	90	77	89	81
10	**3j**	5-Cl	Boc	67	93	86	83
11	**3k**	6-Cl	Boc	72	88	99	74
12	**3l**	7-Me	Boc	97	87	87	80
13	**3m**	7-Cl	Boc	79	89	87	67

[a] Unless otherwise noted, reactions were carried out by slow addition (over 20 minutes) of **2** (0.10 mmol) in solvent (1.0 mL) to a mixture of DIDMH (0.10 mmol), Λ-**1a** (0.01 mmol) and 4 Å MS (100.0 mg) in solvent (4.0 mL) under an air atmosphere in the absence of light for 72 h. [b] CCl_4/toluene (20:1, 5.0 mL) was used at -30 °C. [c] CCl_4 (2.0 mL) was used at -20 °C. [d] Isolated yield. [e] Determined by HPLC analysis. [f] CCl_4/toluene (5:1, 5.0 mL) was used as solvent.

Table S2 Optimization of the Iodocyclization Conditions of Tryptamine **2n**.[a]

Entry	solvent	yield (%)[b]	ee (%)[c]
1	PhMe	16	40
2	PhMe/*n*-hexane (1:1)	48	60
3	PhMe/*n*-hexane (1:3)	10	62
4	CCl_4	36	70
5[d]	CCl_4	53	81
6[d,e]	CCl_4	50	76
7[d,f]	CCl_4	48	76
8[d,g]	CCl_4	55	77

[a] Unless otherwise noted, reactions were carried out by addition of DIDMH (0.12 mmol) in one portion to a mixture of **2n** (0.10 mmol), Λ-**1** (0.01 mmol) and 4 Å MS (100.0 mg) in solvent (2.0 mL) at -20 °C under an air

atmosphere in the absence of light for 48 h. [b] Isolated yield. [c] Determined by HPLC analysis. [d] A solution of **2a** (1.0 mL) was slowly added to the mixture (1.0 mL) for 48 h. [e] DIDMH (0.10 mmol) was used. [f] DIDMH (0.15 mmol) was used. [g] DIDMH (0.30 mmol) was used.

Table S3 Optimization of the Chlorocyclization Conditions of **2a**.[a]

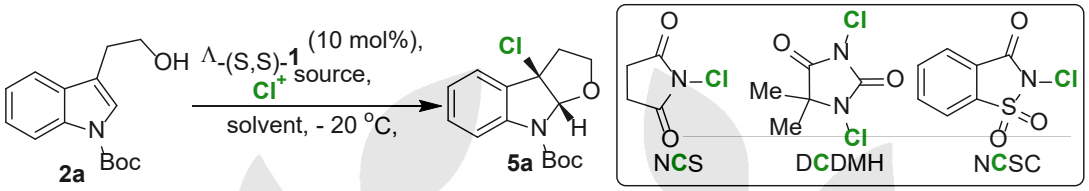

Entry	Λ-**1**	Cl^+ source	solvent	yield (%)[b]	ee (%)[c]
1	**1a**	NCS	PhMe	N.R.	-
2	**1a**	DCDMH	PhMe	52	42
3	**1a**	NCSC	PhMe	N.R.	-
4	**1e**	DCDMH	PhMe	46	35
5[d]	**1a**	DCDMH	PhMe	49	41
6[e]	**1a**	DCDMH	PhMe	21	39
7	**1a**	DCDMH	CCl_4	50	39
8	**1a**	DCDMH	*c*-hexane	53	20
9[f]	**1a**	DCDMH	PhMe	40	24

[a] Unless otherwise noted, reactions were carried out by slow addition (over 20 minutes) of **2a** (0.10 mmol) in solvent (0.50 mL) to a mixture of Cl^+ source (0.20 mmol), Λ-**1** (0.01 mmol) in solvent (0.50 mL) under an air atmosphere in the absence of light for 48 h. [b] Isolated yield. [c] Determined by HPLC analysis. [d] DCDMH (0.30 mmol) was used. [e] The reaction was carried out by addition of DCDMH (0.20 mmol) to a mixture of **2a** (0.10 mmol) and Λ-**1a** (0.01 mmol) in toluene (1.0 mL) at -20 °C. [f] LiCl (0.10 mmol) was used as additive.

3. General Procedure for Preparation of Substrates 2f and 2j

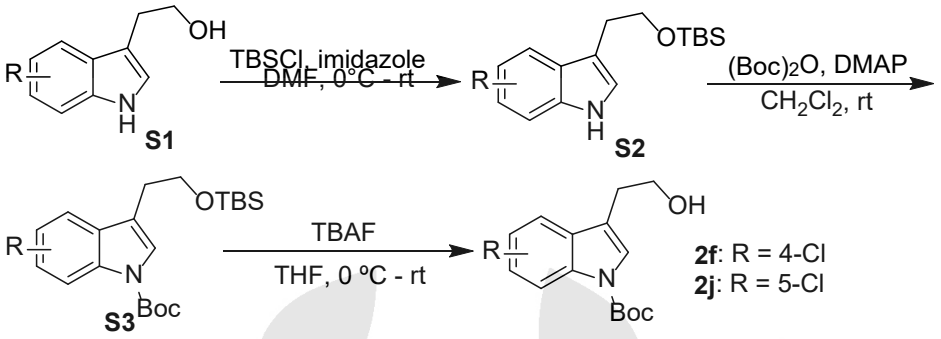

To a solution of tryptophol **S1** (5.0 mmol) and imidazole (11.0 mmol) in DMF (5.0 mL) was added *tert*-butyldimethylsilyl chloride (5.5 mmol) at 0 ºC, the mixture was then allowed to warm to room temperature and stirred for 4.5 h. After the reaction was completed, the reaction mixture was washed with water (2 × 15.0 mL) and extracted with EtOAc (3 × 15.0 mL). The combined organic phases were washed with brine (3 × 10.0 mL), dried over Na_2SO_4, filtered and concentrated. The residue was purified by flash chromatography (petrol ether/EtOAc = 5/1) to afford the intermediate **S2**.

To a solution of **S2** (4.75 mmol) and 4-dimethylaminopyridine (0.48 mmol) in 15.0 mL CH_2Cl_2 was added *di*-tert-butyl dicarbonate (7.125 mmol), the reaction was then stirred at room temperature for 2 h. The reaction was quenched by adding aqueous saturated NH_4Cl (15.0 mL) and extracted with CH_2Cl_2 (3 × 20.0 mL). The organic phases were washed with brine (3 × 20.0 mL), dried over Na_2SO_4, filtered and concentrated. The crude product was purified by flash chromatography (petrol ether/EtOAc = 50/1) to afford the intermediate **S3**.

To a solution of **S3** in THF (20 mL) was added tetrabutylammonium fluoride (1.0 M in THF, 6.6 mL) at 0 ºC, then the ice bath was removed and the reaction was maintained room temperature for 5 h. The reaction was washed with water (10.0 mL) and extracted with EtOAc (10.0 mL). The organic phase was washed with brine (25.0 mL), dried over Na_2SO_4, filtered and concentrated. The residue was purified by flash chromatography (petrol ether/EtOAc = 4/1) gave the substrates **2f** and **2j**.

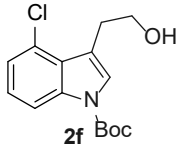

Tert-butyl 4-chloro-3-(2-hydroxyethyl)-1*H*-indole-1-carboxylate 2f: 2-(4-chloro-1H-indol-3-yl)ethanol was used; yield: 1.183 g (80% over 3 steps); **^{1}H-NMR** (600 MHz, $CDCl_3$) δ 8.11 (s, 1H), 7.47 (s, 1H), 7.24 – 7.15 (m, 2H), 3.97 (t, *J* = 6.4 Hz, 2H), 3.21 (t, *J* = 6.4 Hz, 2H), 1.66 (s, 9H); **^{13}C-NMR** (151 MHz, $CDCl_3$) δ 149.14, 137.29, 126.98, 126.30, 125.30, 124.91, 123.69, 116.81, 114.00, 84.09, 62.73, 29.84, 28.15; **HRMS** (ESI) calculated for $C_{15}H_{18}ClNNaO_3$ $[M+Na]^+$: 318.0873, found. 318.0870.

Tert-butyl 5-chloro-3-(2-hydroxyethyl)-1*H*-indole-1-carboxylate 2j: 2-(5-chloro-1H-indol-3-yl)ethanol was used; yield: 1.035 g (70% over 3 steps); **^{1}H-NMR** (600 MHz, $CDCl_3$) δ 8.06 (s, 1H), 7.53 – 7.42 (m, 2H), 7.28 – 7.25 (m, 1H), 3.92 – 3.90 (m, 2H), 2.92 (t, *J* = 6.3 Hz, 2H), 1.66 (s, 9H); **^{13}C-NMR** (151 MHz, $CDCl_3$) δ 149.32, 134.00, 131.74, 128.25, 124.79, 124.57, 118.64, 116.63, 116.34, 83.95, 61.86, 28.29, 28.17; **HRMS** (ESI) calculated for $C_{15}H_{18}ClNNaO_3$ $[M+Na]^+$: 318.0873, found. 318.0875.

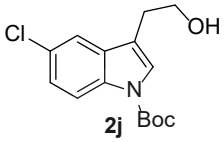

2j

4. Experimental Procedures of Iodocyclization and Characterization Data

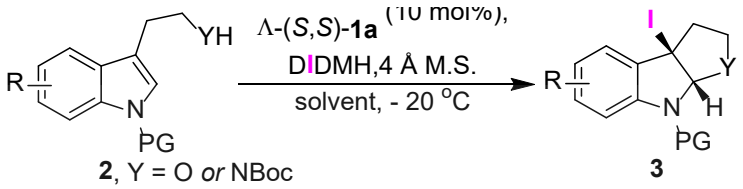

For **3a**, **3g**, **3i**: A 10-mL oven-dried vial was charged with DIDMH (0.10 mmol or 0.05 mmol), catalyst Λ-**1a** (7.2 mg, 0.01 mmol), activated 4 Å molecular sieves (100.0 mg) and CCl_4 (4.0 ml) at room temperature in the absence of light. The mixture was cooled to -20 ºC and stirred for 30 min. A precooled solution of the tryptophol **2** (0.10 mmol) in CCl_4 (1.0 ml) was added dropwise to the mixture over 20 min and the reaction was stirred vigorously until the reaction was complete (monitored by TLC). The reaction was then quenched with pre-cooled NEt_3 (-20 ºC, 1.0 mmol) and saturated aqueous $Na_2S_2O_3$ (0.50 mL). The mixture was purified by flash column chromatography (silica gel, petrol ether/EtOAc = 10/1) to give the enantioenriched indoline derivatives **3**.

For **3b**: A 10-mL oven-dried vial was charged with DIDMH (0.10 mmol), catalyst Λ-**1a** (7.2 mg, 0.01 mmol), activated 4 Å molecular sieves (100.0 mg) and PhMe/CCl_4 (1:5, 4.0 mL) at room temperature. The mixture was cooled to -30 ºC and stirred for 30 min. A precooled solution of the tryptophol **2b** (0.10 mmol) in PhMe/CCl_4 (1:5, 1.0 mL) was added dropwise to the mixture over 20 min and the reaction was stirred vigorously until the reaction was complete (monitored by TLC). The reaction was then quenched with pre-cooled NEt_3 (-30 ºC, 1.0 mmol) and saturated aqueous $Na_2S_2O_3$ (0.50 mL). The mixture was purified by flash column chromatography (silica gel, petrol ether/EtOAc = 5/1) to give the enantioenriched indoline derivative **3b**.

For **3c**-**3f**, **3h**, **3j**-**3m**: A 10-mL oven-dried vial was charged with DIDMH (0.10 mmol or 0.05 mmol), catalyst Λ-**1a** (7.2 mg, 0.01 mmol), activated 4 Å molecular sieves (100.0 mg) and PhMe/CCl_4 (1:20, 4.0 mL) at room temperature. The mixture was cooled to -30 ºC and stirred for 30 min. A precooled solution of the tryptophol **2** (0.10 mmol) in PhMe/CCl_4 (1:20, 1.0 mL) was added dropwise to the mixture over 20 min and the reaction was stirred vigorously until the reaction was complete (monitored by TLC). The reaction was then quenched with pre-cooled NEt_3 (-30 ºC, 1.0 mmol) and saturated aqueous $Na_2S_2O_3$ (0.50 mL). The mixture was purified by flash column chromatography (silica gel, petrol ether/EtOAc = 10/1) to give the enantioenriched indoline derivatives **3**.

For **3n**-**3q**: A 10-mL oven-dried vial was charged with DIDMH (0.12 mmol or 0.06 mmol), catalyst Λ-**1a** (7.2 mg, 0.01 mmol), activated 4 Å molecular sieves (100.0 mg) and CCl_4 (1.0 ml) at room temperature. The mixture was cooled to -20 ºC and stirred for 30 min. A precooled solution of the tryptamine **2** (0.10 mmol) in CCl_4 (1.0 ml) was added dropwise to the mixture over 20 min and the

reaction was stirred vigorously until the reaction was complete (monitored by TLC). The reaction was then quenched with pre-cooled NEt_3 (-20 ºC, 1.0 mmol) and saturated aqueous $Na_2S_2O_3$ (0.50 mL). The mixture was purified by flash column chromatography (silica gel, petrol ether/EtOAc = 10/1) to give the enantioenriched indoline derivatives **3n-3q**.

Tert-butyl (3a*R*,8a*S*)-3a-iodo-2,3,3a,8a-tetrahydro-8*H*-furo[2,3-*b*]indole-8-carboxylate 3a: yield: for 1.0 equiv DIDMH, 37.9 mg (98%); for 0.5 equiv DIDMH, 32.5 mg (84%); (Flash column chromatography eluent, petroleum ether/ethyl acetate = 10/1); colorless oil; **[α]$_D^{20}$** = -82.6 (c 0.38 CH_3OH); ^{1}**H-NMR** (600 MHz, $CDCl_3$) δ 7.79 (s, 1H), 7.39 (d, *J* = 7.2 Hz, 1H), 7.23 (t, *J* = 7.0 Hz, 1H), 7.05 (t, *J* = 7.4 Hz, 1H), 6.45 – 6.17 (m, 1H), 3.85 – 3.76 (m, 1H), 3.45 – 3.32 (m, 1H), 2.99 – 2.86 (m, 2H), 1.61 (s, 9H); ^{13}**C-NMR** (151 MHz, $CDCl_3$) δ 151.92, 129.93, 125.17, 123.84, 115.02, 110.12, 103.32, 82.23, 67.81, 67.32, 47.91, 28.46; **HRMS** (ESI) calculated for $C_{15}H_{18}INNaO_3$ $[M+Na]^+$: 410.0229, found 410.0223; **Enantiomeric excess**: for 1.0 equiv DIDMH, 95%; for 0.5 equiv DIDMH, 92%; determined by HPLC (Daicel Chirapak IE, hexane / isopropanol = 90/10, flow rate 1.0 mL/min, T = 30 ºC, 254 nm): t_{maj} = 9.20 min, t_{min} = 8.43 min.

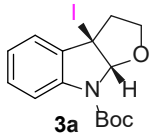

(3a*R*,8a*S*)-3a-Iodo-8-tosyl-3,3a,8,8a-tetrahydro-2*H*-furo[2,3-*b*]indole 3b: yield: 29.6 mg (67%); (Flash column chromatography eluent, petroleum ether/ethyl acetate = 5/1); white solid; m.p. 162.8~164.2 °C; **[α]$_D^{20}$** = -142.4 (c 0.30 CH_3OH); ^{1}**H-NMR** (600 MHz, $CDCl_3$) δ 7.80 (d, *J* = 8.3 Hz, 2H), 7.47 (d, *J* = 8.2 Hz, 1H), 7.34 (d, *J* = 7.7 Hz, 1H), 7.30 – 7.27 (m, 1H), 7.25 (d, *J* = 8.2 Hz, 2H), 7.10 (t, *J* = 7.5 Hz, 1H), 6.24 (s, 1H), 4.03 – 3.99 (m, 1H), 3.44 (ddd, *J* = 11.2, 9.3, 4.7 Hz, 1H), 2.87 – 2.81 (m, 1H), 2.73 (dd, *J* = 12.5, 3.9 Hz, 1H), 2.37 (s, 3H); ^{13}**C-NMR** (151 MHz, $CDCl_3$) δ 144.51, 140.65, 135.61, 132.51, 130.73, 129.80, 127.51, 125.32, 124.90, 114.32, 103.34, 68.07, 61.48, 44.80, 21.67; **HRMS** (ESI) calculated for $C_{17}H_{16}INNaO_3S$ $[M+Na]^+$: 463.9793, found 463.9788; **Enantiomeric excess**: 88%; determined by HPLC (Daicel Chirapak IC, hexane / isopropanol = 70/30, flow rate 1.0 mL/min, T = 30 ºC, 254 nm): t_{maj} = 47.95 min, t_{min} = 32.74 min.

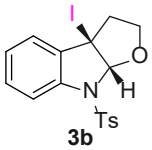

Allyl (3a*R*,8a*S*)-3a-iodo-2,3,3a,8a-tetrahydro-8*H*-furo[2,3-*b*]indole-8-carboxylate 3c: yield: for 1.0 equiv DIDMH, 31.4 mg (84%); for 0.5 equiv DIDMH, 26.7 mg (72%); (Flash column chromatography eluent, petroleum ether/ethyl acetate = 10/1); colorless oil; **[α]$_D^{20}$** = -104.4 (c 0.31 CH_3OH); ^{1}**H-NMR** (600 MHz, $CDCl_3$) δ 7.81 (s, 1H), 7.41 (d, *J* = 7.5 Hz, 1H), 7.26 (d, *J* = 7.8 Hz, 1H), 7.09 (t, *J* = 7.4 Hz, 1H), 6.38 (s, 1H), 6.04 (s, 1H), 5.44 (d, *J* = 17.1 Hz, 1H), 5.31 (d, *J* = 9.9 Hz, 1H), 4.81 (s, 2H), 3.83 (t, *J* = 7.8 Hz, 1H), 3.41 (td, *J* = 10.0, 5.1 Hz, 1H), 2.99 – 2.87 (m, 2H); ^{13}**C-NMR** (151 MHz, $CDCl_3$) 152.33, 140.22, 132.15, 130.06, 125.18, 124.32, 118.48, 117.06, 103.24, 67.52, 66.71, 47.86; **HRMS** (ESI) calculated for $C_{14}H_{14}INNaO_3$ $[M+Na]^+$: 393.9916, found 393.9919; **Enantiomeric excess**: for 1.0 equiv DIDMH, 93%; for 0.5 equiv DIDMH, 90%;

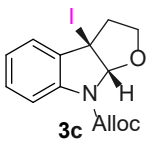

determined by HPLC (Daicel Chirapak IA, hexane / isopropanol = 70/30, flow rate 1.0 mL/min, T = 30 ºC, 254 nm): t_{maj} = 5.99 min, t_{min} = 4.90 min.

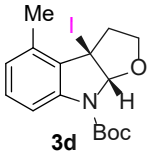

3d

Tert-butyl (3a*R*,8a*S*)-3a-iodo-4-methyl-2,3,3a,8a-tetrahydro-8*H*-furo[2,3-*b*]indole-8-carboxylate 3d: yield: for 1.0 equiv DIDMH, 39.9 mg (97%); for 0.5 equiv DIDMH, 29.3 mg (73%); (Flash column chromatography eluent, petroleum ether/ethyl acetate = 10/1); colorless oil; **[α]$_D^{20}$** = -74.2 (c 0.39 CH_3OH); ^{1}**H-NMR** (600 MHz, $CDCl_3$) δ 7.67 (s, 1H), 7.17 (t, *J* = 7.8 Hz, 1H), 6.81 (d, *J* = 7.6 Hz, 1H), 6.38 (s, 1H), 3.81 (t, *J* = 6.6 Hz, 1H), 3.50 (s, 1H), 3.01 – 2.94 (m, 1H), 2.91 – 2.84 (m, 1H), 2.42 (s, 3H), 1.61 (s, 9H); ^{13}**C-NMR** (151 MHz, $CDCl_3$) δ 148.47, 138.45, 134.74, 130.07, 126.06, 112.87, 104.29, 82.48, 66.80, 62.14, 45.37, 28.46, 19.17; **HRMS** (ESI) calculated for $C_{16}H_{20}INNaO_3$ $[M+Na]^+$: 424.0386, found 424.0389; **Enantiomeric excess**: for 1.0 equiv DIDMH, 90%; for 0.5 equiv DIDMH, 90%; determined by HPLC (Daicel Chirapak IC, hexane / isopropanol = 70/30, flow rate 1.0 mL/min, T = 30 ºC, 254 nm): t_{maj} = 4.63 min, t_{min} = 4.29 min.

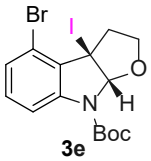

3e

Tert-butyl (3a*R*,8a*S*)-4-bromo-3a-iodo-2,3,3a,8a-tetrahydro-8*H*-furo[2,3-*b*]indole-8-carboxylate 3e: yield: for 1.0 equiv DIDMH, 44.3 mg (95%); for 0.5 equiv DIDMH, 31.2 mg (67%); (Flash column chromatography eluent, petroleum ether/ethyl acetate = 10/1); colorless oil; **[α]$_D^{20}$** = -83.0 (c 0.44 CH_3OH); ^{1}**H-NMR** (600 MHz, $CDCl_3$) δ 7.84 (s, 1H), 7.19 (d, *J* = 8.0 Hz, 1H), 7.12 (t, *J* = 8.0 Hz, 1H), 6.37 (s, 1H), 3.82 (t, *J* = 7.3 Hz, 1H), 3.49 (s, 1H), 3.38 (d, *J* = 12.5 Hz, 1H), 2.86 – 2.75 (m, 1H), 1.59 (d, *J* = 15.7 Hz, 9H); ^{13}**C-NMR** (151 MHz, $CDCl_3$) δ 151.58, 142.44, 131.21, 127.94, 120.49, 114.28, 104.31, 82.79, 67.52, 66.98, 44.38, 28.40; **HRMS** (ESI) calculated for $C_{15}H_{17}BrINNaO_3$ $[M+Na]^+$: 487.9334, found 487.9334; **Enantiomeric excess**: for 1.0 equiv DIDMH, 95%; for 0.5 equiv DIDMH, 84%; determined by HPLC (Daicel Chirapak IC, hexane / isopropanol = 97/3, flow rate 1.0 mL/min, T = 30 ºC, 254 nm): t_{maj} = 6.17 min, t_{min} = 5.55 min.

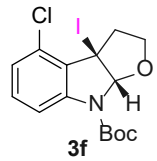

3f

Tert-butyl (3a*R*,8a*S*)-4-chloro-3a-iodo-2,3,3a,8a-tetrahydro-8*H*-furo[2,3-*b*]indole-8-carboxylate 3f: yield: for 1.0 equiv DIDMH, 40.0 mg (95%); for 0.5 equiv DIDMH, 29.1 mg (69%); (Flash column chromatography eluent, petroleum ether/ethyl acetate = 10/1); colorless oil; **[α]$_D^{20}$** = -83.2 (c 0.40 CH_3OH); ^{1}**H-NMR** (600 MHz, $CDCl_3$) δ 7.78 (s, 1H), 7.21 (t, *J* = 8.1 Hz, 1H), 7.00 (d, *J* = 8.1 Hz, 1H), 6.35 (s, 1H), 3.82 (t, *J* = 7.8 Hz, 1H), 3.48 (s, 1H), 3.32 (d, *J* = 12.4 Hz, 1H), 2.83 (dd, *J* = 20.0, 10.8 Hz, 1H), 1.61 (s, 9H); ^{13}**C-NMR** (151 MHz, $CDCl_3$) δ 151.62, 142.43, 131.42, 131.11, 124.65, 113.64, 104.25, 82.80, 67.49, 67.22, 44.43, 28.40; **HRMS** (ESI) calculated for $C_{15}H_{17}ClINNaO_3$ $[M+Na]^+$: 443.9839, found 443.9839; **Enantiomeric excess**: for 1.0 equiv DIDMH, 96%; for 0.5 equiv DIDMH, 88%; determined by HPLC (Daicel Chirapak IC, hexane / isopropanol = 97/3, flow rate 1.0 mL/min, T = 30 ºC, 254 nm): t_{maj} = 5.79 min, t_{min} = 5.29 min.

Tert-butyl (3a*R*,8a*S*)-3a-iodo-5-methoxy-2,3,3a,8a-tetrahydro-8*H*-furo[2,3-*b*]indole-8-carboxylate

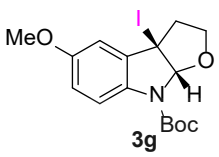

3g

3g: yield: 38.4 mg (92%); (Flash column chromatography eluent, petroleum ether/ethyl acetate = 10/1); colorless oil; **[α]$_D^{20}$** = -107.6 (c 0.38 CH_3OH); ^{1}**H-NMR** (600 MHz, $CDCl_3$) δ 7.69 (s, 1H), 6.90 (s, 1H), 6.79 (d, *J* = 7.6 Hz, 1H), 6.25 (s, 1H), 3.80 (s, 4H), 3.41 (s, 1H), 2.96 – 2.89 (m, 1H), 2.89 – 2.83 (m, 1H), 1.60 (s, 9H); ^{13}**C-NMR** (151 MHz, $CDCl_3$) δ 156.51, 151.98, 129.99, 115.88, 115.72, 110.34, 103.52, 81.89, 67.31, 57.28, 55.87, 47.78, 28.48; **HRMS** (ESI) calculated for $C_{16}H_{20}INNaO_4$ $[M+Na]^+$: 440.0335, found 440.0329; **Enantiomeric excess**: 90%, determined by HPLC (Daicel Chirapak IC, hexane / isopropanol = 70/30, flow rate 1.0 mL/min, T = 30 ºC, 254 nm): t_{maj} = 5.73 min, t_{min} = 5.16 min.

Tert-butyl (3a*R*,8a*S*)-5-fluoro-3a-iodo-2,3,3a,8a-tetrahydro-8*H*-furo[2,3-*b*]indole-8-carboxylate 3h:

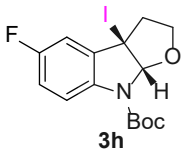

3h

yield: for 1.0 equiv DIDMH, 34.0 mg (84%); for 0.5 equiv DIDMH, 25.9 mg (64%); (Flash column chromatography eluent, petroleum ether/ethyl acetate = 10/1); colorless oil; **[α]$_D^{20}$** = -114.7 (c 0.34 CH_3OH); ^{1}**H-NMR** (600 MHz, $CDCl_3$) δ 7.76 (s, 1H), 7.13 – 7.02 (m, 1H), 6.93 (t, *J* = 7.8 Hz, 1H), 6.26 (s, 1H), 3.82 (t, *J* = 8.0 Hz, 1H), 3.45 – 3.37 (m, 1H), 2.95 – 2.88 (m, 1H), 2.84 (dd, *J* = 12.5, 4.2 Hz, 1H), 1.60 (s, 9H); ^{13}**C-NMR** (151 MHz, $CDCl_3$) δ 160.13, 158.52, 151.80, 136.70, 116.73 (d, *J* = 23.4 Hz), 116.09 (d, *J* = 8.0 Hz), 111.94 (d, *J* = 24.7 Hz), 103.70, 82.47, 67.31, 47.69, 28.43; **HRMS** (ESI) calculated for $C_{15}H_{17}FINNaO_3$ $[M+Na]^+$: 428.0135, found 428.0134; **Enantiomeric excess**: for 1.0 equiv DIDMH, 92%; for 0.5 equiv DIDMH, 67%; determined by HPLC (Daicel Chirapak IC, hexane / isopropanol = 80/20, flow rate 1.0 mL/min, T = 30 ºC, 254 nm): t_{maj} = 4.57 min, t_{min} = 4.31 min.

Tert-butyl (3a*R*,8a*S*)-5-bromo-3a-iodo-2,3,3a,8a-tetrahydro-8*H*-furo[2,3-*b*]indole-8-carboxylate 3i:

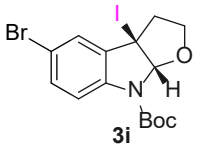

3i

yield: 41.5 mg (89%); (Flash column chromatography eluent, petroleum ether/ethyl acetate = 10/1); colorless oil; **[α]$_D^{20}$** = -93.0 (c 0.41 CH_3OH); ^{1}**H-NMR** (600 MHz, $CDCl_3$) δ 7.68 (s, 1H), 7.49 (s, 1H), 7.33 (d, *J* = 8.0 Hz, 1H), 6.24 (s, 1H), 3.82 (t, *J* = 7.5 Hz, 1H), 3.44 – 3.36 (m, 1H), 2.95 – 2.88 (m, 1H), 2.87 – 2.82 (m, 1H), 1.60 (s, 9H); ^{13}**C-NMR** (151 MHz, $CDCl_3$) δ 151.64, 132.84, 128.14, 123.83, 116.51, 115.94, 115.02, 103.59, 82.47, 67.35, 67.32, 47.71, 28.41; **HRMS** (ESI) calculated for $C_{15}H_{17}BrINNaO_3$ $[M+Na]^+$: 487.9334, found 487.9333; **Enantiomeric excess**: 81%, determined by HPLC (Daicel Chirapak IC, hexane / isopropanol = 80/20, flow rate 1.0 mL/min, T = 30 ºC, 254 nm): t_{maj} = 6.83 min, t_{min} = 5.57 min.

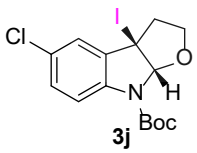

3j

Tert-butyl (3a*R*,8a*S*)-5-chloro-3a-iodo-2,3,3a,8a-tetrahydro-8*H*-furo[2,3-*b*]indole-8-carboxylate 3j: yield: for 1.0 equiv DIDMH, 28.3 mg (67%); for 0.5 equiv DIDMH, 21.9 mg (52%); (Flash column chromatography eluent, petroleum ether/ethyl acetate = 10/1); colorless oil; **[α]$_D^{20}$** = -141.8 (c 0.28 CH_3OH); ^{1}**H-NMR** (600 MHz, $CDCl_3$) δ 7.73 (s, 1H), 7.35

(s, 1H), 7.19 (d, J = 7.6 Hz, 1H), 6.24 (s, 1H), 3.82 (t, J = 7.6 Hz, 1H), 3.46 – 3.33 (m, 1H), 2.98 – 2.88 (m, 1H), 2.88 – 2.80 (m, 1H), 1.60 (s, 9H); **^{13}C-NMR** (151 MHz, $CDCl_3$) δ 151.67, 139.17, 136.43, 129.97, 128.69, 125.22, 116.09, 103.65, 82.69, 67.34, 47.69, 28.41; **HRMS** (ESI) calculated for $C_{15}H_{17}ClINNaO_3$ $[M+Na]^+$: 443.9839, found 443.9839; **Enantiomeric excess**: for 1.0 equiv DIDMH, 93%; for 0.5 equiv DIDMH, 88%; determined by HPLC (Daicel Chirapak IC, hexane / isopropanol = 97/3, flow rate 1.0 mL/min, T = 30 ºC, 254 nm): t_{maj} = 6.52 min, t_{min} = 5.64 min.

Tert-butyl (3a*R*,8a*S*)-6-chloro-3a-iodo-2,3,3a,8a-tetrahydro-8*H*-furo[2,3-*b*]indole-8-carboxylate

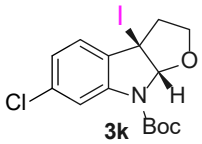

3k: yield: 30.6 mg (72%); (Flash column chromatography eluent, petroleum ether/ethyl acetate = 10/1); colorless oil; **[α]$_D^{20}$** = -134.7 (c 0.32 CH_3OH); **^{1}H-NMR** (600 MHz, $CDCl_3$) δ 7.86 (s, 1H), 7.30 (d, J = 8.1 Hz, 1H), 7.03 (dd, J = 8.2, 1.8 Hz, 1H), 6.26 (s, 1H), 3.81 (t, J = 7.5 Hz, 1H), 3.43 – 3.35 (m, 1H), 2.96 – 2.88 (m, 1H), 2.85 (dd, J = 12.4, 4.1 Hz, 1H), 1.60 (s, 9H); **^{13}C-NMR** (151 MHz, $CDCl_3$) δ 151.59, 141.63, 135.78, 133.23, 125.93, 123.95, 115.42, 103.84, 82.76, 67.85, 67.36, 47.83, 28.38; **HRMS** (ESI) calculated for $C_{15}H_{17}ClINNaO_3$ $[M+Na]^+$: 443.9839, found 443.9847; **Enantiomeric excess**: 88%, determined by HPLC (Daicel Chirapak IC, hexane / isopropanol = 90/10, flow rate 1.0 mL/min, T = 30 ºC, 254 nm): t_{maj} = 4.83 min, t_{min} = 4.50 min.

Tert-butyl (3a*R*,8a*S*)-3a-iodo-7-methyl-2,3,3a,8a-tetrahydro-8*H*-furo[2,3-*b*]indole-8-carboxylate 3l:

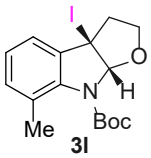

yield: 38.9 mg (97%); (Flash column chromatography eluent, petroleum ether/ethyl acetate = 10/1); colorless oil; **[α]$_D^{20}$** = -120.6 (c 0.39 CH_3OH); **^{1}H-NMR** (600 MHz, $CDCl_3$) δ 7.25 – 7.22 (m, 1H), 7.10 – 7.07 (m, 2H), 6.30 (s, 1H), 3.80 – 3.77 (m, 1H), 3.36 – 3.31 (m, 1H), 2.91 – 2.87 (m, 2H), 2.31 (s, 3H), 1.59 (s, 9H); **^{13}C-NMR** (151 MHz, $CDCl_3$) δ 152.65, 139.46, 137.50, 132.35, 128.67, 125.82, 121.60, 105.57, 82.23, 67.58, 46.16, 36.62, 28.30, 20.04; **HRMS** (ESI) calculated for $C_{16}H_{20}INNaO_3$ $[M+Na]^+$: 424.0386, found 424.0380; **Enantiomeric excess**: 87%, determined by HPLC (Daicel Chirapak IA, hexane / isopropanol = 97/3, flow rate 1.0 mL/min, T = 30 ºC, 254 nm): t_{maj} = 7.15 min, t_{min} = 6.79 min.

Tert-butyl (3a*R*,8a*S*)-7-chloro-3a-iodo-2,3,3a,8a-tetrahydro-8*H*-furo[2,3-*b*]indole-8-carboxylate

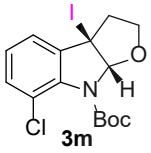

3m: yield: 33.3 mg (79%); (Flash column chromatography eluent, petroleum ether/ethyl acetate = 10/1); colorless oil; **[α]$_D^{20}$** = -150.5 (c 0.33 CH_3OH); **^{1}H-NMR** (600 MHz, $CDCl_3$) δ 7.31 (dd, J = 7.6, 1.0 Hz, 1H), 7.28 (dd, J = 8.0, 1.0 Hz, 1H), 7.11 (t, J = 7.8 Hz, 1H), 6.27 (s, 1H), 3.84 – 3.79 (m, 1H), 3.37 (ddd, J = 10.2, 8.8, 5.5 Hz, 1H), 2.94 – 2.88 (m, 1H), 2.88 – 2.83 (m, 1H), 1.59 (s, 9H); **^{13}C-NMR** (151 MHz, $CDCl_3$) δ 151.84, 140.09, 138.13, 131.39, 126.57, 124.24, 122.67, 106.07, 82.94, 67.57, 45.96, 35.01, 28.17; **HRMS** (ESI) calculated for $C_{15}H_{17}ClINNaO_3$ $[M+Na]^+$: 443.9839, found 443.9839; **Enantiomeric excess**: 89%, determined by

HPLC (Daicel Chirapak IA, hexane / isopropanol = 70/30, flow rate 1.0 mL/min, T = 30 ºC, 254 nm): t_{maj} = 4.99 min, t_{min} = 4.61 min.

Di-*tert*-butyl (3a*R*,8a*R*)-3a-iodo-2,3,3a,8a-tetrahydropyrrolo[2,3-*b*]indole-1,8-dicarboxylate 3n:

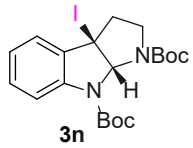

3n

yield: for 1.2 equiv DIDMH, 25.8 mg (53%); for 0.6 equiv DIDMH, 19.0 mg (39%); (Flash column chromatography eluent, petroleum ether/ethyl acetate = 10/1); colorless oil; **[α]$_D^{20}$** = -143.5 (c 0.21 CH_3OH); **^{1}H-NMR** (600 MHz, $CDCl_3$) δ 7.44 (s, 1H), 7.28 (d, *J* = 7.4 Hz, 1H), 7.20 – 7.15 (m, 1H), 7.05 – 6.97 (m, 1H), 6.38 (s, 1H), 3.49 – 3.40 (m, 1H), 2.87 – 2.78 (m, 1H), 2.77 – 2.67 (m, 2H), 1.52 (s, 9H), 1.41 (s, 9H); **^{13}C-NMR** (151 MHz, $CDCl_3$) δ 153.27, 152.30, 141.13, 135.83, 129.75, 124.28, 123.79, 117.84, 86.31, 82.14, 80.83, 64.26, 46.11, 37.14, 28.53, 28.40; **HRMS** (ESI) calculated for $C_{20}H_{27}IN_2NaO_4$ $[M+Na]^+$: 509.0913, found 509.0916; **Enantiomeric excess**: for 1.2 equiv DIDMH, 81%; for 0.6 equiv DIDMH, 74%; determined by HPLC (Daicel Chirapak IC, hexane / isopropanol = 80/20, flow rate 1.0 mL/min, T = 30 ºC, 254 nm): t_{maj} = 6.52 min, t_{min} = 6.18 min.

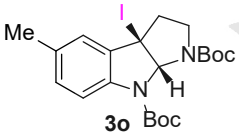

3o

Di-*tert*-butyl(3a*R*,8a*R*)-3a-iodo-5-methyl-2,3,3a,8a-tetrahydropyrrolo[2,3-*b*]indole-1,8-dicarboxylate 3o: yield: 22.0 mg (44%); (Flash column chromatography eluent, petroleum ether/ethyl acetate = 10/1); colorless oil; **[α]$_D^{20}$** = -156.7 (c 0.17 CH_3OH); **^{1}H-NMR** (600 MHz, $CDCl_3$) δ 7.37 (s, 1H), 7.14 (s, 1H), 7.04 (d, *J* = 8.1 Hz, 1H), 6.44 (s, 1H), 3.50 (s, 1H), 2.94 – 2.85 (m, 1H), 2.83 – 2.71 (m, 2H), 2.31 (s, 3H), 1.58 (s, 9H), 1.48 (s, 9H); **^{13}C-NMR** (151 MHz, $CDCl_3$) δ 153.29, 152.40, 138.90, 134.01, 131.19, 130.57, 124.01, 117.65, 86.38, 81.92, 80.82, 63.58, 46.05, 37.59, 28.53, 28.40, 21.09; **HRMS** (ESI) calculated for $C_{21}H_{29}IN_2NaO_4$ $[M+Na]^+$: 523.1070, found 523.1071; **Enantiomeric excess**: 89%, determined by HPLC (Daicel Chirapak IC, hexane / isopropanol = 90/10, flow rate 1.0 mL/min, T = 30 ºC, 254 nm): t_{maj} = 6.35 min, t_{min} = 5.86 min.

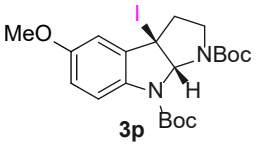

3p

Di-*tert*-butyl (3a*R*,8a*R*)-3a-iodo-5-methoxy-2,3,3a,8a-tetrahydropyrrolo[2,3-*b*]indole-1,8-dicarboxylate 3p: yield: 20.7 mg (40%); (Flash column chromatography eluent, petroleum ether/ethyl acetate = 10/1); colorless oil; **[α]$_D^{20}$** = -157.0 (c 0.16 CH_3OH); **^{1}H-NMR** (600 MHz, $CDCl_3$) δ 7.40 (s, 1H), 6.89 – 6.84 (m, 1H), 6.80 (dd, *J* = 8.8, 2.2 Hz, 1H), 6.43 (s, 1H), 3.79 (s, 3H), 3.56 – 3.45 (m, 1H), 2.91 – 2.83 (m, 1H), 2.83 – 2.72 (m, 2H), 1.58 (s, 9H), 1.48 (s, 9H); **^{13}C-NMR** (151 MHz, $CDCl_3$) δ 156.83, 153.26, 152.50, 136.96, 134.77, 118.95, 115.65, 108.60, 86.50, 81.85, 80.85, 55.85, 45.98, 43.86, 28.53, 28.39; **HRMS** (ESI) calculated for $C_{21}H_{29}IN_2NaO_5$ $[M+Na]^+$: 539.1019, found 539.1020; **Enantiomeric excess**: 85%, determined by HPLC (Daicel Chirapak IC, hexane / isopropanol = 90/10, flow rate 1.0 mL/min, T = 30 ºC, 254 nm): t_{maj} = 6.58 min, t_{min} = 5.94 min.

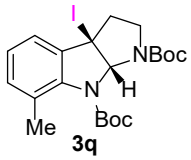

3q

Di-*tert*-butyl (3a*R*,8a*R*)-3a-iodo-7-methyl-2,3,3a,8a-tetrahydropyrrolo[2,3-*b*]indole-1,8-dicarboxylate 3q: yield: for 1.2 equiv DIDMH, 47.5 mg (95%); for 0.6 equiv DIDMH, 39.5 mg (79%); (Flash column chromatography eluent, petroleum ether/ethyl acetate = 10/1); colorless oil; **[α]$_D^{20}$** = -91.3 (c 0.35 CH_3OH); **^{1}H-NMR** (600 MHz, $CDCl_3$) ^{1}H NMR (400 MHz, $CDCl_3$) δ 7.17 (d, *J* = 6.5 Hz, 1H), 7.13 – 7.03 (m, 2H), 6.29 (s, 1H), 3.41 – 3.30 (m, 1H), 2.89 (d, *J* = 7.5 Hz, 1H), 2.78 – 2.67 (m, 2H), 2.27 (s, 3H), 1.55 (s, 9H), 1.49 (s, 9H);**^{13}C-NMR** (151 MHz, CDCl3) δ 153.59, 153.35, 140.62, 138.10, 131.78, 131.04, 126.21, 120.09, 88.22, 82.04, 80.66, 60.43, 45.58, 38.01, 28.69, 28.32, 19.30; **HRMS** (ESI) calculated for $C_{21}H_{29}IN_2NaO_5$ $[M+Na]^+$: 523.1070, found 523.1071; **Enantiomeric excess**: for 1.2 equiv DIDMH, 88%; for 0.6 equiv DIDMH, 78%; determined by HPLC (Daicel Chirapak IC, hexane / isopropanol = 90/10, flow rate 1.0 mL/min, T = 30 ºC, 254 nm): t_{maj} = 6.73 min, t_{min} = 6.07 min.

5. Experimental Procedures of Bromocyclization and Characterization Data

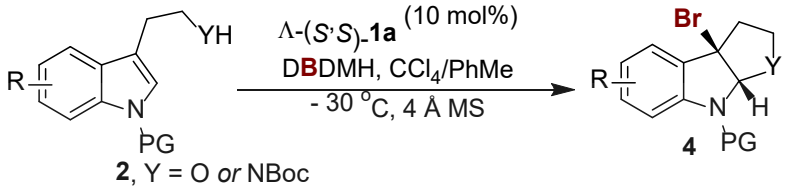

For **4a, 4c-4m**: A 10-mL oven-dried vial was charged with DBDMH (0.10 mmol or 0.05 mmol), catalyst Λ-**1a** (7.2 mg, 0.01 mmol), activated 4 Å molecular sieves (100.0 mg) and PhMe/CCl_4 (1:20, 4.0 mL) at room temperature in the absence of light. The mixture was cooled to -30 ºC and stirred for 30 min. A precooled solution of the tryptophol **2** (0.10 mmol) in PhMe/CCl_4 (1:20, 1.0 mL) was added dropwise to the mixture over 20 min and the reaction was stirred vigorously until the reaction was complete (monitored by TLC). The reaction was then quenched with pre-cooled NEt_3 (-30 ºC, 1.0 mmol) and saturated aqueous $Na_2S_2O_3$ (0.50 mL). The mixture was purified by flash column chromatography (silica gel, petrol ether/EtOAc = 10/1) to give the enantioenriched indoline derivatives **4**.

For **4b**: A 10-mL oven-dried vial was charged with DBDMH (0.10 mmol), catalyst Λ-**1a** (7.2 mg, 0.01 mmol), activated 4 Å molecular sieves (100.0 mg) and PhMe/CCl_4 (1:5, 4.0 mL) at room temperature in the absence of light. The mixture was cooled to -30 ºC and stirred for 30 min. A precooled solution of the tryptophol **2b** (0.10 mmol) in PhMe/CCl_4 (1:5, 1.0 mL) was added dropwise to the mixture over 20 min and the reaction was stirred vigorously until the reaction was complete (monitored by TLC). The reaction was then quenched with pre-cooled NEt_3 (-30 ºC, 1.0 mmol) and saturated aqueous $Na_2S_2O_3$ (0.50 mL). The mixture was purified by flash column chromatography (silica gel, petrol ether/EtOAc = 5/1) to give the enantioenriched indoline derivative **4b**.

For **4n-4q**: A 10-mL oven-dried vial was charged with the tryptamine **2** (0.10 mmol), catalyst Λ-**1a** (7.2 mg, 0.01 mmol), activated 4 Å molecular sieves (100.0 mg) and PhMe/CCl_4 (1:20, 5.0 mL) at room temperature in the absence of light. The mixture was cooled to -30 ºC and stirred for 30 min. DBDMH (0.10 mmol) was added in one portion to the mixture and the reaction was stirred vigorously until the reaction was complete (monitored by TLC). The reaction was then quenched with pre-cooled NEt_3 (-30 ºC, 1.0 mmol) and saturated aqueous $Na_2S_2O_3$ (0.50 mL). The mixture was purified by flash column chromatography (silica gel, petrol ether/EtOAc = 10/1) to give the enantioenriched indoline derivatives **4n-4q**.

Tert-butyl (3a*R*,8a*S*)-3a-bromo-2,3,3a,8a-tetrahydro-8*H*-furo[2,3-*b*]indole-8-carboxylate 4a: yield:

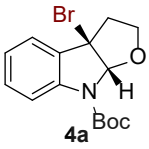

4a

for 1.0 equiv DBDMH, 32.3 mg (95%); for 0.5 equiv DBDMH, 28.6 mg (84%); (Flash column chromatography eluent, petroleum ether/ethyl acetate = 10/1); colorless oil; **[α]$_D^{20}$** = -137.1 (c 0.32 CH_3OH); ^{1}**H-NMR** (600 MHz, $CDCl_3$) δ 7.84 (s, 1H), 7.41 (d, *J* = 7.5 Hz, 1H), 7.28 (t, *J* = 7.8 Hz, 1H), 7.08 (t, *J* = 7.5 Hz, 1H), 6.34 – 6.12 (m, 1H), 4.00 (t, *J* = 8.0 Hz, 1H), 3.53 – 3.45 (m, 1H), 2.94 – 2.86 (m, 1H), 2.80 (dd, *J* = 12.3, 3.8 Hz, 1H), 1.60 (s, 9H); ^{13}**C-NMR** (151 MHz, $CDCl_3$) δ 151.86, 141.73, 131.86, 130.50, 124.87, 123.76, 115.00, 100.87, 82.28, 67.79, 61.77, 45.09, 28.43; **Enantiomeric excess**: for 1.0 equiv DBDMH, 96%; for 0.5 equiv DBDMH, 96%; determined by HPLC (Daicel Chirapak IC, hexane / isopropanol = 70/30, flow rate 1.0 mL/min, T = 30 ºC, 254 nm): t_{maj} = 4.41 min, t_{min} = 4.04 min.

(3a*R*,8a*S*)-3a-Bromo-8-tosyl-3,3a,8,8a-tetrahydro-2*H*-furo[2,3-*b*]indole 4b: yield: 37.4 mg (95%);

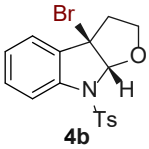

4b

(Flash column chromatography eluent, petroleum ether/ethyl acetate = 5/1); white solid; m.p. 180.4~181.1 °C; **[α]$_D^{20}$** = -63.2 (c 0.36 CH_3OH); ^{1}**H-NMR** (600 MHz, $CDCl_3$) δ 7.80 (d, *J* = 8.3 Hz, 2H), 7.47 (d, *J* = 8.2 Hz, 1H), 7.34 (d, *J* = 7.7 Hz, 1H), 7.28 (d, *J* = 7.5 Hz, 1H), 7.25 (d, *J* = 8.2 Hz, 2H), 7.10 (t, *J* = 7.5 Hz, 1H), 6.24 (s, 1H), 4.01 (t, *J* = 8.3 Hz, 1H), 3.44 (ddd, *J* = 11.2, 9.3, 4.7 Hz, 1H), 2.87 – 2.81 (m, 1H), 2.73 (dd, *J* = 12.5, 3.9 Hz, 1H), 2.37 (s, 3H); ^{13}**C-NMR** (151 MHz, $CDCl_3$) δ 144.49, 140.65, 135.65, 132.53, 130.73, 129.80, 127.51, 125.32, 124.90, 114.32, 103.34, 68.07, 61.48, 44.80, 21.67; **Enantiomeric excess**: 89%, determined by HPLC (Daicel Chirapak IC, hexane / isopropanol = 70/30, flow rate 1.0 mL/min, T = 30 ºC, 254 nm): t_{maj} = 43.03 min, t_{min} = 31.23 min.

Allyl (3a*R*,8a*S*)-3a-bromo-2,3,3a,8a-tetrahydro-8*H*-furo[2,3-*b*]indole-8-carboxylate 4c: yield: for

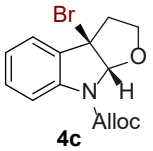

4c

1.0 equiv DBDMH, 30.8 mg (95%); for 0.5 equiv DBDMH, 30.1 mg (93%); (Flash column chromatography eluent, petroleum ether/ethyl acetate = 10/1); colorless oil; **[α]$_D^{20}$** = -183.9 (c 0.31 CH_3OH); ^{1}**H-NMR** (600 MHz, $CDCl_3$) δ 7.86 (s, 1H), 7.43 (d, *J* = 7.6 Hz, 1H), 7.31 (t, *J* = 7.4 Hz, 1H), 7.12 (t, *J* = 7.5 Hz, 1H), 6.28 (s, 1H), 6.03 (s, 1H), 5.44 (d, *J* = 17.2 Hz, 1H), 5.30 (d, *J* = 10.2 Hz, 1H), 4.81 (s, 2H), 4.02 (t, *J* = 8.2 Hz, 1H), 3.54 – 3.48 (m, 1H), 2.91 (td, *J* = 11.7, 7.9 Hz, 1H), 2.82 (dd, *J* = 12.4, 4.3 Hz, 1H); ^{13}**C-NMR** (151 MHz, $CDCl_3$) δ 152.33, 141.46, 132.09, 131.84, 130.64, 124.89, 124.24, 118.47, 115.04, 100.77, 67.99, 66.71, 61.70, 45.04; **Enantiomeric excess**: for 1.0 equiv DBDMH, 92%; for 0.5 equiv DBDMH, 90%; determined by HPLC (Daicel Chirapak IC, hexane / isopropanol = 90/10, flow rate 1.0 mL/min, T = 30 ºC, 254 nm): t_{maj} = 7.19 min, t_{min} = 6.61 min.

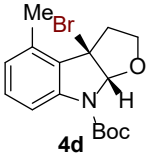

4d

Tert-butyl (3a*R*,8a*S*)-3a-bromo-4-methyl-2,3,3a,8a-tetrahydro-8*H*-furo[2,3-*b*]indole-8-carboxylate 4d: yield: 32.2 mg (91%); (Flash column chromatography eluent,

petroleum ether/ethyl acetate = 10/1); colorless oil; **[α]$_D^{20}$** = -117.8 (c 0.32 CH_3OH); ^{1}**H-NMR** (600 MHz, $CDCl_3$) δ 7.71 (s, 1H), 7.20 (t, *J* = 7.9 Hz, 1H), 6.85 (d, *J* = 7.6 Hz, 1H), 6.22 (s, 1H), 4.02 – 3.96 (m, 1H), 3.65 – 3.55 (m, 1H), 2.92 – 2.82 (m, 2H), 2.49 (s, 3H), 1.60 (s, 9H); ^{13}**C-NMR** (151 MHz, $CDCl_3$) 151.85, 141.90, 135.56, 130.60, 125.83, 112.78, 101.63, 82.30, 67.29, 62.90, 43.22, 28.43, 18.48; **Enantiomeric excess**: 92%, determined by HPLC (Daicel Chirapak IC, hexane / isopropanol = 70/30, flow rate 1.0 mL/min, T = 30 ºC, 254 nm): t_{maj} = 4.57 min, t_{min} = 4.17 min.

Tert-butyl (3a*R*,8a*S*)-3a,4-dibromo-2,3,3a,8a-tetrahydro-8*H*-furo[2,3-*b*]indole-8-carboxylate 4e:

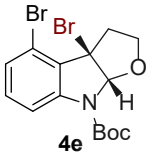

4e

yield: for 1.0 equiv DBDMH, 37.3 mg (89%); for 0.5 equiv DBDMH, 33.5 mg (80%); (Flash column chromatography eluent, petroleum ether/ethyl acetate = 10/1); colorless oil; **[α]$_D^{20}$** = -93.0 (c 0.37 CH_3OH); ^{1}**H-NMR** (600 MHz, $CDCl_3$) δ 7.87 (s, 1H), 7.22 (d, *J* = 8.0 Hz, 1H), 7.15 (t, *J* = 8.0 Hz, 1H), 6.20 (s, 1H), 4.04 – 3.97 (m, 1H), 3.63 – 3.54 (m, 1H), 3.27 (d, *J* = 12.6 Hz, 1H), 2.86 – 2.77 (m, 1H), 1.60 (s, 9H); ^{13}**C-NMR** (151 MHz, $CDCl_3$) δ 151.53, 143.69, 131.79, 127.83, 120.30, 114.26, 101.61, 82.77, 67.52, 62.19, 42.22, 28.39; **Enantiomeric excess**: for 1.0 equiv DBDMH, 97%; for 0.5 equiv DBDMH, 96%; determined by HPLC (Daicel Chirapak IC, hexane / isopropanol = 97/3, flow rate 1.0 mL/min, T = 30 ºC, 254 nm): t_{maj} = 5.92 min, t_{min} = 5.15 min.

Tert-butyl (3a*R*,8a*S*)-3a-bromo-4-chloro-2,3,3a,8a-tetrahydro-8*H*-furo[2,3-*b*]indole-8-carboxylate

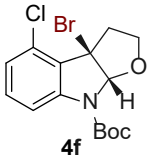

4f

4f: yield: for 1.0 equiv DBDMH, 34.4 mg (92%); for 0.5 equiv DBDMH, 31.8 mg (85%); (Flash column chromatography eluent, petroleum ether/ethyl acetate = 10/1); colorless oil; **[α]$_D^{20}$** = -77.8 (c 0.34 CH_3OH); ^{1}**H-NMR** (600 MHz, $CDCl_3$) δ 7.81 (s, 1H), 7.24 (t, *J* = 8.1 Hz, 1H), 7.03 (d, *J* = 8.0 Hz, 1H), 6.19 (s, 1H), 4.01 (t, *J* = 7.3 Hz, 1H), 3.62 – 3.54 (m, 1H), 3.22 (d, *J* = 11.9 Hz, 1H), 2.86 – 2.79 (m, 1H), 1.60 (s, 9H); ^{13}**C-NMR** (151 MHz, $CDCl_3$) δ 151.57, 143.41, 131.72, 124.53, 113.63, 101.56, 82.78, 67.74, 61.05, 42.18, 28.39; **HRMS** (ESI) calculated for $C_{15}H_{17}BrClNNaO_3$ $[M+Na]^+$: 395.9978, found 395.9977. **Enantiomeric excess**: for 1.0 equiv DBDMH, 98%; for 0.5 equiv DBDMH, 97%; determined by HPLC (Daicel Chirapak IC, hexane / isopropanol = 97/3, flow rate 1.0 mL/min, T = 30 ºC, 254 nm): t_{maj} = 10.49 min, t_{min} = 9.62 min.

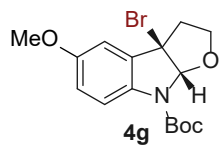

4g

Tert-butyl (3a*R*,8a*S*)-3a-bromo-5-methoxy-2,3,3a,8a-tetrahydro-8*H*-furo[2,3-*b*]indole-8-carboxylate 4g: yield: for 1.0 equiv DBDMH, 33.3 mg (90%); for 0.5 equiv DBDMH, 31.5 mg (85%); (Flash column chromatography eluent, petroleum ether/ethyl acetate = 10/1); colorless oil; **[α]$_D^{20}$** = -93.8 (c 0.33 CH_3OH); ^{1}**H-NMR** (600 MHz, $CDCl_3$) δ 7.74 (s, 1H), 6.92 (d, *J* = 2.3 Hz, 1H), 6.87 – 6.79 (m, 1H), 6.15 (s, 1H), 4.00 (t, *J* = 8.0 Hz, 1H), 3.80 (s, 3H), 3.55 – 3.46 (m, 1H), 2.92 – 2.82 (m, 1H), 2.78 (dd, *J* = 12.4, 3.7 Hz, 1H), 1.59 (s, 9H); ^{13}**C-NMR** (151 MHz, $CDCl_3$) δ 156.47, 151.89, 135.55, 132.77, 116.36, 115.86, 109.92, 101.07, 81.94, 67.73, 62.02, 55.85, 44.99, 28.44; **Enantiomeric excess**: for 1.0 equiv DBDMH, 97%; for 0.5 equiv DBDMH,

97%; determined by HPLC (Daicel Chirapak IC, hexane / isopropanol = 70/30, flow rate 1.0 mL/min, T = 30 ºC, 254 nm): t_{maj} = 5.08 min, t_{min} = 4.57 min.

Tert-butyl (3a*R*,8a*S*)-3a-bromo-5-fluoro-2,3,3a,8a-tetrahydro-8*H*-furo[2,3-*b*]indole-8-carboxylate

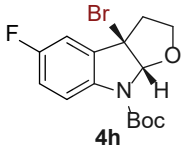

4h

4h: yield: for 1.0 equiv DBDMH, 31.9 mg (89%); for 0.5 equiv DBDMH, 33.7 mg (94%); (Flash column chromatography eluent, petroleum ether/ethyl acetate = 10/1); colorless oil; **[α]$_D^{20}$** = -150.1 (c 0.32 CH_3OH); ^{1}**H-NMR** (600 MHz, $CDCl_3$) δ 7.80 (s, 1H), 7.09 (dd, *J* = 7.7, 2.3 Hz, 1H), 6.98 (td, *J* = 8.7, 1.9 Hz, 1H), 6.18 (s, 1H), 4.01 (t, *J* = 8.0 Hz, 1H), 3.55 – 3.45 (m, 1H), 2.94 – 2.84 (m, 1H), 2.75 (dd, *J* = 12.6, 3.6 Hz, 1H), 1.59 (s, 9H); ^{13}**C-NMR** (151 MHz, $CDCl_3$) δ 160.12, 158.51, 151.77, 137.96, 117.33 (d, *J* = 23.2 Hz), 116.12 (d, *J* = 7.9 Hz), 111.69 (d, *J* = 21.9 Hz) 101.26, 82.33, 67.74, 60.84, 44.97, 28.42; **Enantiomeric excess**: for 1.0 equiv DBDMH, 90%; for 0.5 equiv DBDMH, 94%; determined by HPLC (Daicel Chirapak IC, hexane / isopropanol = 90/10, flow rate 1.0 mL/min, T = 30 ºC, 254 nm): t_{maj} = 5.54 min, t_{min} = 5.10 min.

Tert-butyl (3a*R*,8a*S*)-3a,5-dibromo-2,3,3a,8a-tetrahydro-8*H*-furo[2,3-*b*]indole-8-carboxylate 4i:

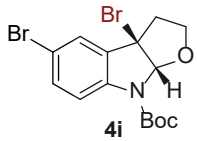

4i

yield: 37.7 mg (90%); (Flash column chromatography eluent, petroleum ether/ethyl acetate = 10/1); colorless oil; **[α]$_D^{20}$** = -34.0 (c 0.38 CH_3OH); ^{1}**H-NMR** (600 MHz, $CDCl_3$) δ 7.73 (s, 1H), 7.51 (s, 1H), 7.38 (d, *J* = 8.5 Hz, 1H), 6.15 (s, 1H), 4.01 (t, *J* = 8.0 Hz, 1H), 3.53 – 3.46 (m, 1H), 2.91 – 2.84 (m, 1H), 2.77 (dd, *J* = 12.5, 3.0 Hz, 1H), 1.59 (s, 9H); ^{13}**C-NMR** (151 MHz, $CDCl_3$) δ 151.58, 140.91, 133.40, 127.90, 116.53, 115.86, 101.10, 82.60, 67.77, 60.47, 44.95, 28.38; **Enantiomeric excess**: 93%, determined by HPLC (Daicel Chirapak IC, hexane / isopropanol = 97/3, flow rate 1.0 mL/min, T = 30 ºC, 254 nm): t_{maj} = 6.25 min, t_{min} = 5.48 min.

Tert-butyl (3a*R*,8a*S*)-3a-bromo-5-chloro-2,3,3a,8a-tetrahydro-8*H*-furo[2,3-*b*]indole-8-carboxylate

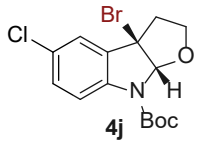

4j

4j: yield: 31.1 mg (83%); (Flash column chromatography eluent, petroleum ether/ethyl acetate = 10/1); colorless oil; **[α]$_D^{20}$** = -67.0 (c 0.31 CH_3OH); ^{1}**H-NMR** (600 MHz, $CDCl_3$) δ 7.78 (s, 1H), 7.37 (s, 1H), 7.24 (d, *J* = 8.4 Hz, 1H), 6.15 (s, 1H), 4.02 (t, *J* = 8.0 Hz, 1H), 3.54 – 3.46 (m, 1H), 2.93 – 2.83 (m, 1H), 2.77 (dd, *J* = 12.5, 3.9 Hz, 1H), 1.59 (s, 9H); ^{13}**C-NMR** (151 MHz, $CDCl_3$) δ 151.66, 130.56, 128.67, 124.98, 116.12, 110.12, 101.18, 82.77, 67.80, 60.69, 44.97, 28.40; **HRMS** (ESI) calculated for $C_{15}H_{17}BrClNNaO_3$ $[M+Na]^+$: 395.9978, found 395.9977; **Enantiomeric excess**: 93%, determined by HPLC (Daicel Chirapak IC, hexane / isopropanol = 97/3, flow rate 1.0 mL/min, T = 30 ºC, 254 nm): t_{maj} = 10.62 min, t_{min} = 9.52 min.

Tert-butyl (3a*R*,8a*S*)-3a-bromo-6-chloro-2,3,3a,8a-tetrahydro-8*H*-furo[2,3-*b*]indole-8-carboxylate

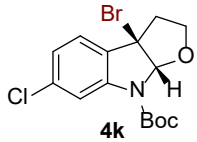

4k

4k: yield: for 1.0 equiv DBDMH, 35.6 mg (95%); for 0.5 equiv DBDMH, 35.6 mg (95%); (Flash column chromatography eluent, petroleum ether/ethyl acetate = 10/1);

colorless oil; **[α]$_D^{20}$** = -156.5 (c 0.35 CH_3OH); **^{1}H-NMR** (600 MHz, $CDCl_3$) δ 7.90 (s, 1H), 7.31 (d, *J* = 8.1 Hz, 1H), 7.05 (dd, *J* = 8.1, 1.6 Hz, 1H), 6.17 (s, 1H), 4.01 (t, *J* = 8.1 Hz, 1H), 3.52 – 3.46 (m, 1H), 2.92 – 2.85 (m, 1H), 2.76 (dd, *J* = 12.4, 4.3 Hz, 1H), 1.60 (s, 9H); **^{13}C-NMR** (151 MHz, $CDCl_3$) δ 151.52, 142.77, 136.45, 130.39, 125.67, 123.89, 115.42, 101.36, 82.76, 67.82, 60.87, 45.02, 28.35; **Enantiomeric excess**: for 1.0 equiv DBDMH, 89%; for 0.5 equiv DBDMH, 92%; determined by HPLC (Daicel Chirapak IC, hexane / isopropanol = 90/10, flow rate 1.0 mL/min, T = 30 ºC, 254 nm): t_{maj} = 5.45 min, t_{min} = 5.04 min.

Tert-butyl (3a*R*,8a*S*)-3a-bromo-7-methyl-2,3,3a,8a-tetrahydro-8*H*-furo[2,3-*b*]indole-8-carboxylate

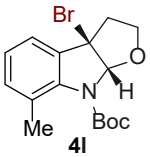

4l

4l: yield: for 1.0 equiv DBDMH, 30.8 mg (87%); for 0.5 equiv DBDMH, 28.3 mg (80%); (Flash column chromatography eluent, petroleum ether/ethyl acetate = 10/1); colorless oil; **[α]$_D^{20}$** = -174.5 (c 0.31 CH_3OH); **^{1}H-NMR** (600 MHz, $CDCl_3$) δ 7.25 (d, *J* = 7.2 Hz, 1H), 7.16 – 7.08 (m, 2H), 6.18 (s, 1H), 3.98 – 3.94 (m, 1H), 3.42 (ddd, *J* = 10.4, 8.9, 5.1 Hz, 1H), 2.90 – 2.84 (m, 1H), 2.81 – 2.76 (m, 1H), 2.32 (s, 3H), 1.57 (s, 9H); **^{13}C-NMR** (151 MHz, $CDCl_3$) δ 152.64, 140.59, 134.63, 133.00, 128.49, 125.72, 121.61, 102.98, 82.27, 68.00, 61.67, 43.57, 28.30, 20.18; **Enantiomeric excess**: for 1.0 equiv DBDMH, 92%; for 0.5 equiv DBDMH, 92%; determined by HPLC (Daicel Chirapak IC, hexane / isopropanol = 97/3, flow rate 1.0 mL/min, T = 30 ºC, 254 nm): t_{maj} = 7.28 min, t_{min} = 6.25 min.

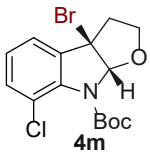

4m

Tert-butyl (3a*R*,8a*S*)-3a-bromo-7-chloro-2,3,3a,8a-tetrahydro-8*H*-furo[2,3-*b*]indole-8-carboxylate 4m: yield: 32.6 mg (87%); (Flash column chromatography eluent, petroleum ether/ethyl acetate = 10/1); colorless oil; **[α]$_D^{20}$** = -150.3 (c 0.33 CH_3OH); **^{1}H-NMR** (600 MHz, $CDCl_3$) δ 7.33 (d, *J* = 7.8 Hz, 2H), 7.13 (t, *J* = 7.8 Hz, 1H), 6.16 (s, 1H), 4.01 – 3.97 (m, 1H), 3.48 – 3.43 (m, 1H), 2.90 – 2.85 (m, 1H), 2.77 (ddd, *J* = 12.7, 4.9, 1.7 Hz, 1H), 1.58 (s, 9H); **^{13}C-NMR** (151 MHz, $CDCl_3$) δ 151.84, 139.25, 137.18, 132.09, 126.48, 122.73, 103.41, 83.03, 67.96, 60.79, 43.44, 28.17; **HRMS** (ESI) calculated for $C_{15}H_{17}ClINNaO_3$ $[M+Na]^+$: 443.9839, found 443.9834; **Enantiomeric excess**: 82%, determined by HPLC (Daicel Chirapak IC, hexane / isopropanol = 70/30, flow rate 1.0 mL/min, T = 30 ºC, 254 nm): t_{maj} = 5.69 min, t_{min} = 4.76 min.

Di-tert-butyl (3a*R*,8a*R*)-3a-bromo-2,3,3a,8a-tetrahydropyrrolo[2,3-*b*]indole-1,8-dicarboxylate 4n:

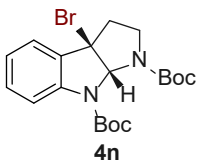

4n

yield: 42.6 mg (97%); (Flash column chromatography eluent, petroleum ether/ethyl acetate = 10/1); colorless oil; **[α]$_D^{20}$** = -132.7 (c 0.27 CH_3OH); **^{1}H-NMR** (600 MHz, $CDCl_3$) δ 7.65-7.51 (m, 1H), 7.40-7.34 (m, 1H), 7.31-7.27 (m, 1H), 7.09 (t, *J* = 7.3 Hz, 1H), 6.44 (s, 1H), 3.76-3.70 (m, 1H), 2.85-2.77 (m, 2H), 2.75-2.68 (m, 1H), 1.58 (s, 9H), 1.49 (s, 9H); **^{13}C-NMR** (151 MHz, $CDCl_3$) δ 153.52, 152.23, 142.19, 132.75, 130.37, 124.12, 123.85, 117.48, 84.01, 82.18, 80.83, 62.33, 46.26, 41.67, 28.48, 28.38; **Enantiomeric excess**: 82%,

determined by HPLC (Daicel Chirapak IC, hexane / isopropanol = 90/10, flow rate 1.0 mL/min, T = 30 ºC, 254 nm): t_{maj} = 5.27 min, t_{min} = 6.24 min.

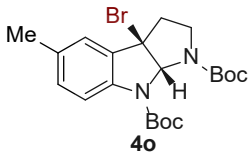

4o

Di-tert-butyl (3a*R*,8a*R*)-3a-bromo-5-methyl-2,3,3a,8a-tetrahydropyrrolo[2,3-*b*]indole-1,8-dicarboxylate 4o: yield: 42.6 mg (94%); (Flash column chromatography eluent, petroleum ether/ethyl acetate = 10/1); colorless oil; **[α]$_D^{20}$** = -123.7 (c 0.37 CH_3OH); ^{1}**H-NMR** (600 MHz, $CDCl_3$) δ 7.51-7.37 (m, 1H), 7.17-7.13 (m, 1H), 7.12-7.06 (m, 1H), 6.41 (s, 1H), 3.75-3.68 (m, 1H), 2.85-2.75 (m, 2H), 2.74-2.65 (m, 1H), 2.33 (s, 3H), 1.57 (s, 9H), 1.48 (s, 9H); ^{13}**C-NMR** (151 MHz, $CDCl_3$) δ 153.49, 152.27, 139.89, 133.83, 131.12, 124.01, 117.32, 84.01, 81.90, 80.75, 62.50, 46.14, 28.42, 28.31, 20.97; **Enantiomeric excess**: 81%, determined by HPLC (Daicel Chirapak IC, hexane / isopropanol = 90/10, flow rate 1.0 mL/min, T = 30 ºC, 254 nm): t_{maj} = 5.50 min, t_{min} = 6.78 min.

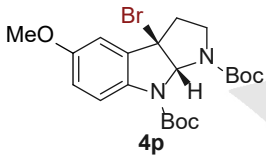

4p

Di-tert-butyl (3a*R*,8a*R*)-3a-bromo-5-methoxy-2,3,3a,8a-tetrahydropyrrolo[2,3-*b*]indole-1,8-dicarboxylate 4p: yield: 40.4 mg (86%); (Flash column chromatography eluent, petroleum ether/ethyl acetate = 10/1); colorless oil; **[α]$_D^{20}$** = -113.2 (c 0.36 CH_3OH); ^{1}**H-NMR** (600 MHz, $CDCl_3$) δ 7.58-7.40 (m, 1H), 6.93-6.81 (m, 2H), 6.44-6.30 (m, 1H), 3.81 (s, 3H), 3.76-3.68 (m, 1H), 2.88-2.80 (m, 1H), 2.78 – 2.67 (m, 1H), 2.66-2.55 (m, 1H), 1.57 (s, 9H), 1.49 (s, 9H); ^{13}**C-NMR** (151 MHz, $CDCl_3$) δ 155.67, 152.43, 151.35, 134.75, 132.77, 115.25, 107.52, 83.11, 80.81, 79.77, 61.36, 54.76, 45.03, 30.22, 27.40, 27.29; **Enantiomeric excess**: 78%, determined by HPLC (Daicel Chirapak IC, hexane / isopropanol = 90/10, flow rate 1.0 mL/min, T = 30 ºC, 254 nm): t_{maj} = 5.98 min, t_{min} = 7.41 min.

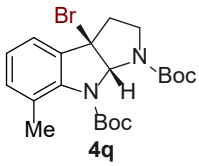

4q

Di-tert-butyl (3a*R*,8a*R*)-3a-bromo-7-methyl-2,3,3a,8a-tetrahydropyrrolo[2,3-*b*]indole-1,8-dicarboxylate 4q: yield: 44.0 mg (97%); (Flash column chromatography eluent, petroleum ether/ethyl acetate = 10/1); colorless oil; **[α]$_D^{20}$** = -96.8 (c 0.37 CH_3OH); ^{1}**H-NMR** (600 MHz, $CDCl_3$) δ 7.22-7.16 (m, 1H), 7.16-7.07 (m, 2H), 6.31-6.18 (m, 1H), 3.58-3.48 (m, 1H), 2.86-2.78 (m, 1H), 2.77-2.63 (m, 2H), 2.30 (s, 3H), 1.54 (s, 9H), 1.50 (s, 9H); ^{13}**C-NMR** (151 MHz, $CDCl_3$) δ 153.73, 141.76, 135.24, 132.41, 131.06, 126.19, 120.30, 86.12, 82.04, 80.69, 62.24, 45.66, 28.68, 28.31, 19.33; **Enantiomeric excess**: 81%, determined by HPLC (Daicel Chirapak IC, hexane / isopropanol = 90/10, flow rate 1.0 mL/min, T = 30 ºC, 254 nm): t_{maj} = 9.51 min, t_{min} = 11.96 min.

6. Experimental Procedures of Chlorocyclization and Characterization Data

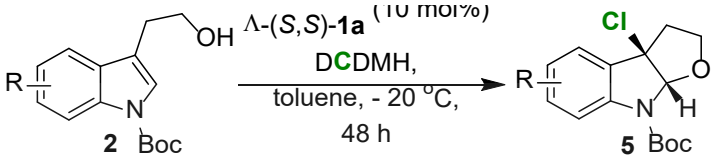

A 10-mL oven-dried vial was charged with DCDMH (0.20 mmol), catalyst Λ-**1a** (7.2 mg, 0.01 mmol) and PhMe (0.50 mL) at room temperature in the absence of light. The mixture was cooled to -20 ºC and stirred for 30 min. A precooled solution of the tryptophols **2** (0.10 mmol) in PhMe (0.50 mL) was added dropwise to the mixture over 20 min and the reaction was stirred vigorously until the reaction was complete (monitored by TLC). The reaction was then quenched with pre-cooled NEt_3 (-20 ºC, 1.0 mmol) and saturated aqueous $Na_2S_2O_3$ (0.50 mL). The mixture was purified by flash column chromatography (silica gel, petrol ether/EtOAc = 10/1) to give the enantioenriched indoline derivatives **5**.

Tert-butyl (3a*R*,8a*S*)-3a-chloro-2,3,3a,8a-tetrahydro-8*H*-furo[2,3-*b*]indole-8-carboxylate 5a: yield:

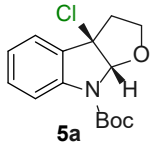

5a

15.4 mg (52%); (Flash column chromatography eluent, petroleum ether/ethyl acetate = 10/1); colorless oil; **[α]$_D^{20}$** = -138.8 (c 0.15 CH_3OH); ^{1}**H-NMR** (600 MHz, $CDCl_3$) δ 7.81 (s, 1H), 7.43 – 7.35 (m, 1H), 7.33 – 7.26 (m, 1H), 7.08 (t, *J* = 7.4 Hz, 1H), 6.07 (s, 1H), 4.12 – 4.05 (m, 1H), 3.59 – 3.51 (m, 1H), 2.83 – 2.75 (m, 1H), 2.72 – 2.64 (m, 1H), 1.60 (d, *J* = 4.5 Hz, 9H); ^{13}**C-NMR** (151 MHz, $CDCl_3$) δ 151.63, 130.70, 128.64, 123.71, 116.12, 115.02, 110.11, 100.44, 80.95, 67.92, 59.69, 44.15, 28.44; **HRMS** (ESI) calculated for $C_{15}H_{18}ClNNaO_3$ $[M+Na]^+$: 318.0873, found 318.0879; **Enantiomeric excess**: 42%, determined by HPLC (Daicel Chirapak IC, hexane / isopropanol = 80/20, flow rate 1.0 mL/min, T = 30 ºC, 254 nm): t_{maj} = 7.50 min, t_{min} = 6.81 min.

Tert-butyl (3a*R*,8a*S*)-3a-chloro-5-fluoro-2,3,3a,8a-tetrahydro-8*H*-furo[2,3-*b*]indole-8-carboxylate

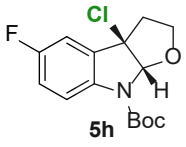

5h

5h: yield: 14.1 mg (45%); (Flash column chromatography eluent, petroleum ether/ethyl acetate = 10/1); colorless oil; **[α]$_D^{20}$** = -132.6 (c 0.14 CH_3OH); ^{1}**H-NMR** (600 MHz, $CDCl_3$) δ 7.82 (s, 1H), 7.14 – 7.05 (m, 1H), 7.01 (t, *J* = 7.9 Hz, 1H), 6.06 (s, 1H), 4.10 (t, *J* = 8.1 Hz, 1H), 3.56 (s, 1H), 2.82 – 2.74 (m, 1H), 2.66 (dd, *J* = 12.4, 3.5 Hz, 1H), 1.59 (s, 9H); ^{13}**C-NMR** (151 MHz, $CDCl_3$) δ 160.12, 158.51, 151.78, 138.71, 117.44 (d, *J* = 23.2 Hz), 116.11 (d, *J* = 8.0 Hz), 110.11, 100.53, 93.45, 67.85, 60.32, 44.05, 28.41; **HRMS** (ESI) calculated for $C_{15}H_{17}FClNNaO_3$ $[M+Na]^+$: 336.0779, found 336.0781; **Enantiomeric excess**: 41%, determined by HPLC (Daicel Chirapak IC, hexane / isopropanol = 80/20, flow rate 1.0 mL/min, T = 30 ºC, 254 nm): t_{maj} = 6.83 min, t_{min} = 6.41 min.

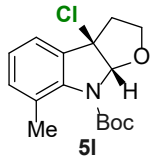

5l

Tert-butyl (3a*R*,8a*S*)-3a-chloro-7-methyl-2,3,3a,8a-tetrahydro-8*H*-furo[2,3-*b*]indole-8-carboxylate 5l: yield: 14.6 mg (47%); (Flash column chromatography eluent, petroleum ether/ethyl acetate = 10/1); colorless oil; $[\alpha]_D^{20}$ = -162.3 (c 0.15 CH_3OH); ^{1}**H-NMR** (600 MHz, $CDCl_3$) δ 7.25 (d, *J* = 7.2 Hz, 1H), 7.19 – 7.06 (m, 2H), 6.18 (s, 1H), 3.99 – 3.93 (m, 1H), 3.42 (ddd, *J* = 10.4, 8.9, 5.1 Hz, 1H), 2.91 – 2.83 (m, 1H), 2.81 – 2.76 (m, 1H), 2.32 (s, 3H), 1.57 (s, 9H); ^{13}**C-NMR** (151 MHz, $CDCl_3$) δ 152.64, 140.59, 134.63, 133.00, 128.49, 125.72, 121.61, 102.98, 82.27, 68.00, 61.67, 43.57, 28.30, 20.18; **HRMS** (ESI) calculated for $C_{16}H_{20}ClNNaO_3$ $[M+Na]^+$: 332.1029, found 332.1031; **Enantiomeric excess**: 30%, determined by HPLC (Daicel Chirapak IC, hexane / isopropanol = 80/20, flow rate 1.0 mL/min, T = 30 ºC, 254 nm): t_{maj} = 7.00 min, t_{min} = 6.64 min.

7. Scale-up of the halocyclization process

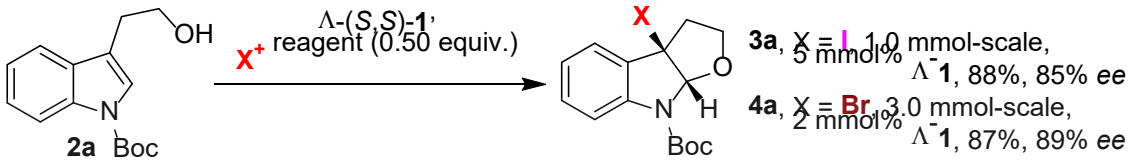

For iodocyclization of 2a: A 50 mL oven-dried round-bottomed flask was charged with DIDMH (0.50 mmol), catalyst Λ-**1a** (36.0 mg, 0.05 mmol), activated 4 Å molecular sieves (500.0 mg) and CCl_4 (7.0 ml) at room temperature in the absence of light. The mixture was cooled to -20 ºC and stirred for 30 min. A precooled solution of the tryptophol **2** (1.0 mmol, 261.3 mg) in CCl_4 (3.0 ml) was added dropwise to the mixture over 30 min and the reaction was stirred vigorously until the reaction was complete (monitored by TLC, about 72 h). The reaction was then quenched with pre-cooled NEt_3 (-20 ºC, 5.0 mmol) and saturated aqueous $Na_2S_2O_3$ (5.0 mL). The mixture was purified by flash column chromatography (silica gel, petrol ether/EtOAc = 10/1) to give the enantioenriched indoline derivative **3** (334.0 mg, 88% yield, 85% *ee*).

For bromocyclization of 2a: A 50 mL oven-dried round-bottomed flask was charged with DBDMH (1.50 mmol), catalyst Λ-**1a** (43.2 mg, 0.06 mmol), activated 4 Å molecular sieves (1.00 g) and PhMe/CCl_4 (1:20, 12.0 mL) at room temperature in the absence of light. The mixture was cooled to -30 ºC and stirred for 30 min. A precooled solution of the tryptophol **2** (3.0 mmol, 784.0 mg) in PhMe/CCl_4 (1:20, 3.0 mL) was added dropwise to the mixture over 30 min and the reaction was stirred vigorously until the reaction was complete (monitored by TLC, about 36 h). The reaction was then quenched with pre-cooled NEt_3 (-30 ºC, 5.0 mmol) and saturated aqueous $Na_2S_2O_3$ (5.0 mL). The mixture was purified by flash column chromatography (silica gel, petrol ether/EtOAc = 10/1) to give the enantioenriched indoline derivative **4** (885.0 mg, 87% yield, 89% *ee*).

8. The Derivation of 3-Halofuranoindolines 3a and 4a

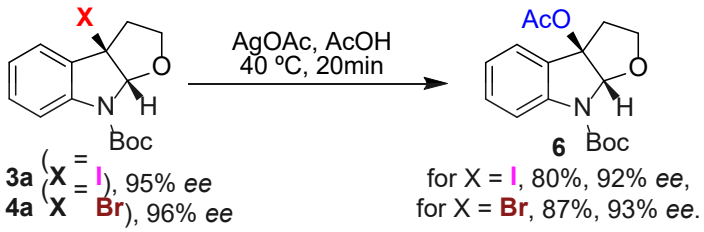

To a solution of **3a** (0.10 mmol) or **4a** (0.10 mmol) in AcOH (1.0 mL) was added silver(I) acetate (0.11 mmol), and the reaction mixture was stirred at 40 ºC in the absence of light for 20 min. After the mixture was cooled to room temperature, Et_2O was added. The mixture was filtered and washed with Et_2O. The organic volatile solvents were removed under reduced pressure, and the residue was purified by column chromatography on silica gel to afford the product **6**.

Tert-butyl (3a*R*,8a*S*)-3a-acetoxy-2,3,3a,8a-tetrahydro-8*H*-furo[2,3-*b*]indole-8-carboxylate 6: yield: 27.8 mg (87%); (Flash column chromatography eluent, dichloromethane / methanol = 20/1); colorless oil; $[\alpha]_D^{20}$ = -164.1 (c 0.28 CH_3OH); ^{1}**H-NMR** (600 MHz, $CDCl_3$) δ 7.86 (s, 1H), 7.51 (d, *J* = 6.8 Hz, 1H), 7.35 – 7.27 (m, 1H), 7.08 – 6.96 (m, 1H), 6.09 (s, 1H), 4.09 (t, *J* = 7.5 Hz, 1H), 3.55 (s, 1H), 2.74 – 2.67 (m, 1H), 2.66 – 2.58 (m, 1H), 2.03 (s, 3H), 1.59 (s, 9H); ^{13}**C-NMR** (151 MHz, $CDCl_3$) δ 169.81, 152.18, 141.27, 135.86, 130.73, 125.37, 123.16, 114.92, 96.76, 96.58, 82.89, 67.23, 39.74, 28.47, 21.43; **HRMS** (ESI) calculated for $C_{17}H_{21}NNaO_5$ $[M+Na]^+$: 342.1317, found 342.1312; **Enantiomeric excess**: 93%, determined by HPLC (Daicel Chirapak IC, hexane / isopropanol = 90/10, flow rate 1.0 mL/min, T = 30 ºC, 254 nm): t_{maj} = 8.01 min, t_{min} = 7.37 min.

9. General Procedure for Mechanistic Studies

General Procedure for Asymmetric Halocyclization with Various N-halohydantoins

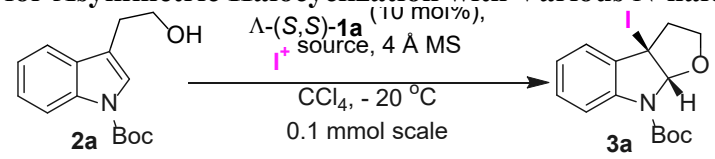

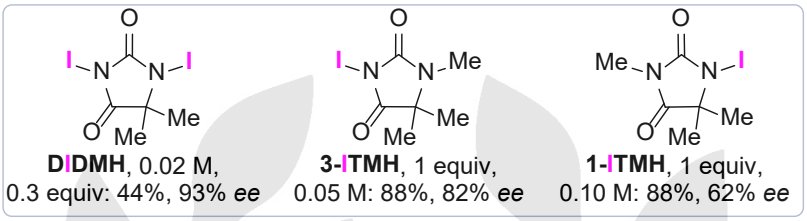

For DIDMH: A 10-mL oven-dried vial was charged with DIDMH (0.03 mmol), Λ-**1a** (0.01 mmol), activated 4 Å molecular sieves (100 mg) and CCl_4 (4.0 ml) at room temperature. The mixture was cooled to -20 ºC and stirred for 30 min. A precooled solution of the tryptophol **2a** (0.10 mmol) in CCl_4 (1.0 ml) was added dropwise to the mixture over 20 min and the reaction was stirred vigorously until the reaction was complete (monitored by TLC). The reaction was then quenched with pre-cooled NEt_3 (-20 ºC, 1.0 mmol) and saturated aqueous $Na_2S_2O_3$ (0.5 mL). The mixture was purified by flash column chromatography (silica gel, petrol ether/EtOAc = 10/1) to give the product **3a**.

For 3-ITMH: A 10-mL oven-dried vial was charged with 3-ITMH (0.10 mmol), Λ-**1a** (0.01 mmol), activated 4 Å molecular sieves (100 mg) and CCl_4 (1.0 mL) at room temperature. The mixture was cooled to -20 ºC and stirred for 30 min. A precooled solution of the tryptophol **2a** (0.10 mmol) in CCl_4 (1.0 ml) was added dropwise to the mixture over 20 min and the reaction was stirred vigorously until the reaction was complete (monitored by TLC). The reaction was then quenched with pre-cooled NEt_3 (-20 ºC, 1.0 mmol) and saturated aqueous $Na_2S_2O_3$ (0.5 mL). The mixture was purified by flash column chromatography (silica gel, petrol ether/EtOAc = 10/1) to give the product **3a**.

For 1-ITMH: A 10-mL oven-dried vial was charged with 1-ITMH (0.10 mmol), Λ-**1a** (0.01 mmol), activated 4 Å molecular sieves (100 mg) and CCl_4 (0.5 mL) at room temperature. The mixture was cooled to -20 ºC and stirred for 30 min. A precooled solution of the tryptophol **2a** (0.10 mmol) in CCl_4 (0.5 mL) was added dropwise to the mixture over 20 min and the reaction was stirred vigorously until the reaction was complete (monitored by TLC). The reaction was then quenched with pre-cooled NEt_3 (-20 ºC, 1.0 mmol) and saturated aqueous $Na_2S_2O_3$ (0.5 mL). The mixture was purified by flash column chromatography (silica gel, petrol ether/EtOAc = 10/1) to give the product **3a**.

10. X-Ray diffraction Data

10.1. X-ray single crystal data for 3b

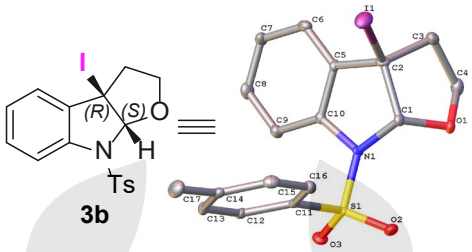

Table S4. Crystal data and structure refinement for **3b** (CCDC 1938720)

Empirical formula	$C_{17}H_{16}INO_3S$
Formula weight	441.27
Temperature/K	170.03
Crystal system	monoclinic
Space group	$P12_11$
a/Å	11.8476(2)
b/Å	11.4035(2)
c/Å	12.3660(2)
α/°	90
β/°	97.8570
γ/°	90
Volume/Å^3	1655.01(5)
Z	4
ρ_{calc}g/cm^3	1.771
μ/mm^{-1}	11.033
F(000)	872
Crystal size/mm^3	0.11 × 0.08 × 0.05
Radiation	CuKα (λ = 1.34139)
2Θ range for data collection/°	3.139 to 54.942
Index ranges	$-14 \le h \le 14$, $-13 \le k \le 13$, $-15 \le l \le 13$
Reflections collected	17379
Independent reflections	6047 [$R_{(int)}$ = 0.0451]
Data/restraints/parameters	6047/1/417
Goodness-of-fit on F^2	1.054
Final R indexes [I>=2σ (I)]	R_1 = 0.0316, wR_2 = 0.0683
Final R indexes [all data]	R_1 = 0.0339, wR_2 = 0.0699
Largest diff. peak/hole / e Å^{-3}	0.389/-1.083
Flack parameter	0.061(5)

10.2. X-ray single crystal data for 4b

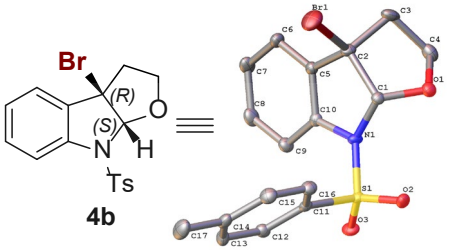

Table S5. Crystal data and structure refinement for **4b** (CCDC 1938617)

Empirical formula	$C_{17}H_{16}BrNO_3S$
Formula weight	394.28
Temperature/K	173
Crystal system	monoclinic
Space group	$P12_11$
a/Å	11.9542(4)
b/Å	11.4519(4)
c/Å	12.0091(4)
α/°	90
β/°	98.268
γ/°	90
Volume/Å^3	1626.94(10)
Z	4
ρ_{calc}g/cm^3	1.610
μ/mm^{-1}	3.238
F(000)	800
Crystal size/mm^3	0.1 × 0.08 × 0.05
Radiation	CuKα (λ = 1.34139)
2Θ range for data collection/°	3.235 to 55.237
Index ranges	$-14 \le h \le 14$, $-12 \le k \le 14$, $-14 \le l \le 14$
Reflections collected	17784
Independent reflections	6015 [$R_{(int)}$ = 0.0448]
Data/restraints/parameters	6015/1/417
Goodness-of-fit on F^2	1.136
Final R indexes [I>=2σ (I)]	R_1 = 0.0316, wR_2 = 0.0871
Final R indexes [all data]	R_1 = 0.0382, wR_2 = 0.0887
Largest diff. peak/hole / e Å^{-3}	0.592/-0.718
Flack parameter	0.054(10)

11. References

(1) (a) J. Yu, H.-J. Jiang, Y. Zhou, S.-W. Luo, L.-Z. Gong, *Angew. Chem., Int. Ed.* **2015**, *54*, 11209. (b) H.-J. Jiang, K. Liu, J. Yu, L. Zhang, L.-Z. Gong, *Angew. Chem., Int. Ed.* **2017**, *56*, 11931. (c) H.-J. Jiang, X.-M. Zhong, J. Y, Y. Zhang, X. Zhang, Y.-D. Wu, L.-Z. Gong, *Angew. Chem., Int. Ed.* **2019**, *58*, 1803.

(2) (a) W. Xie, G. Jiang, H. Liu, J. Hu, X. Pan, H. Zhang, X. Wan, Y. Lai, D. Ma, *Angew. Chem., Int. Ed.* **2013**, *52*, 12924. (b) H. Liu, G. Jiang, X. Pan, X. Wan, Y. Lai, D. Ma, W. Xie, *Org. Lett.* **2014**, *16*, 1908. (c) K. Liu, H.-J. Jiang, N. Li, H. Li, J. Wang, Z.-Z. Zhang, J. Yu, *J. Org. Chem*. **2018**, *83*, 6815.

(3) A. Artaryan, A. Mardyukov, K. Kulbitski, I. Avigdori, G. A. Nisnevich, P. R. Schreiner, M. Gandelman, *J. Org. Chem.* **2017**, *82*, 7093.

12. Selected NMR and HPLC

12.1. NMR of the substrates 2f and 2j

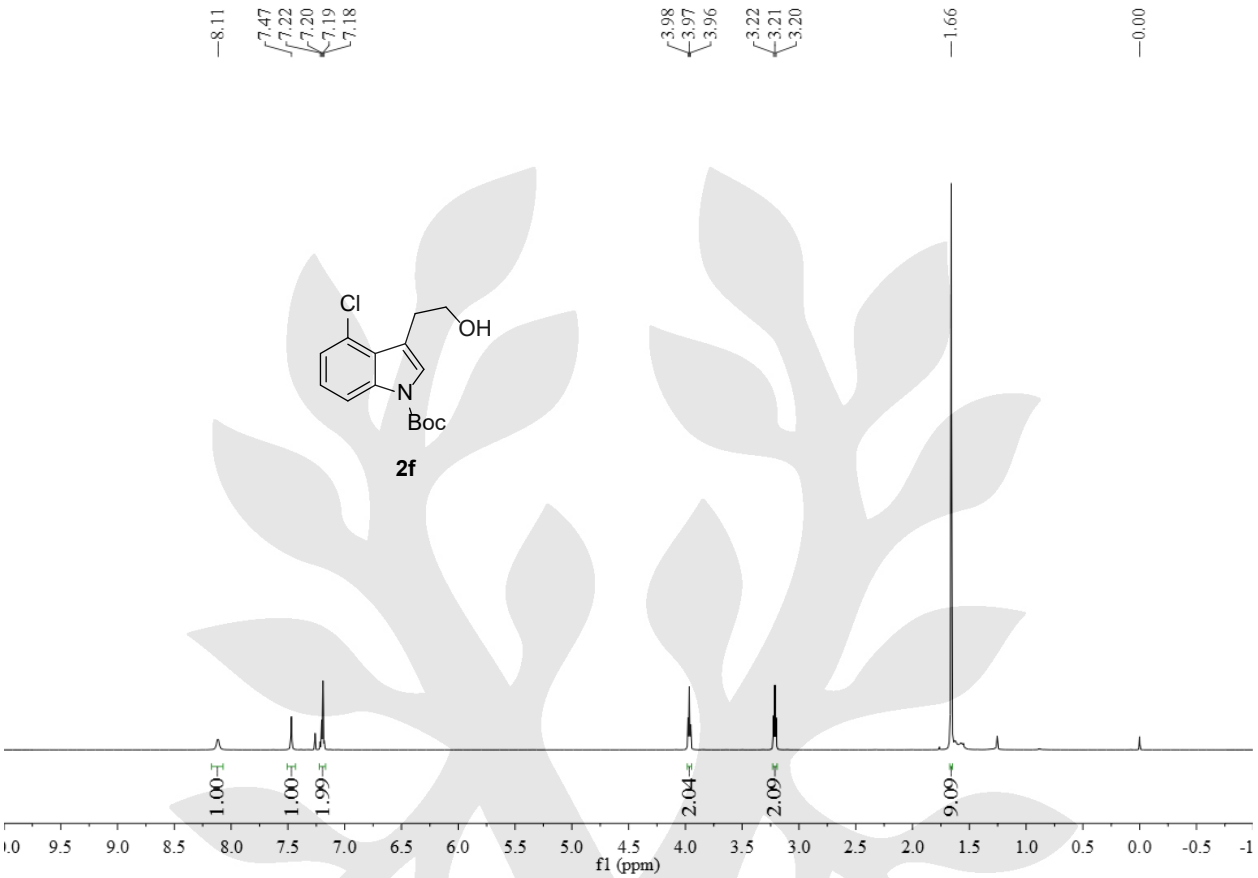

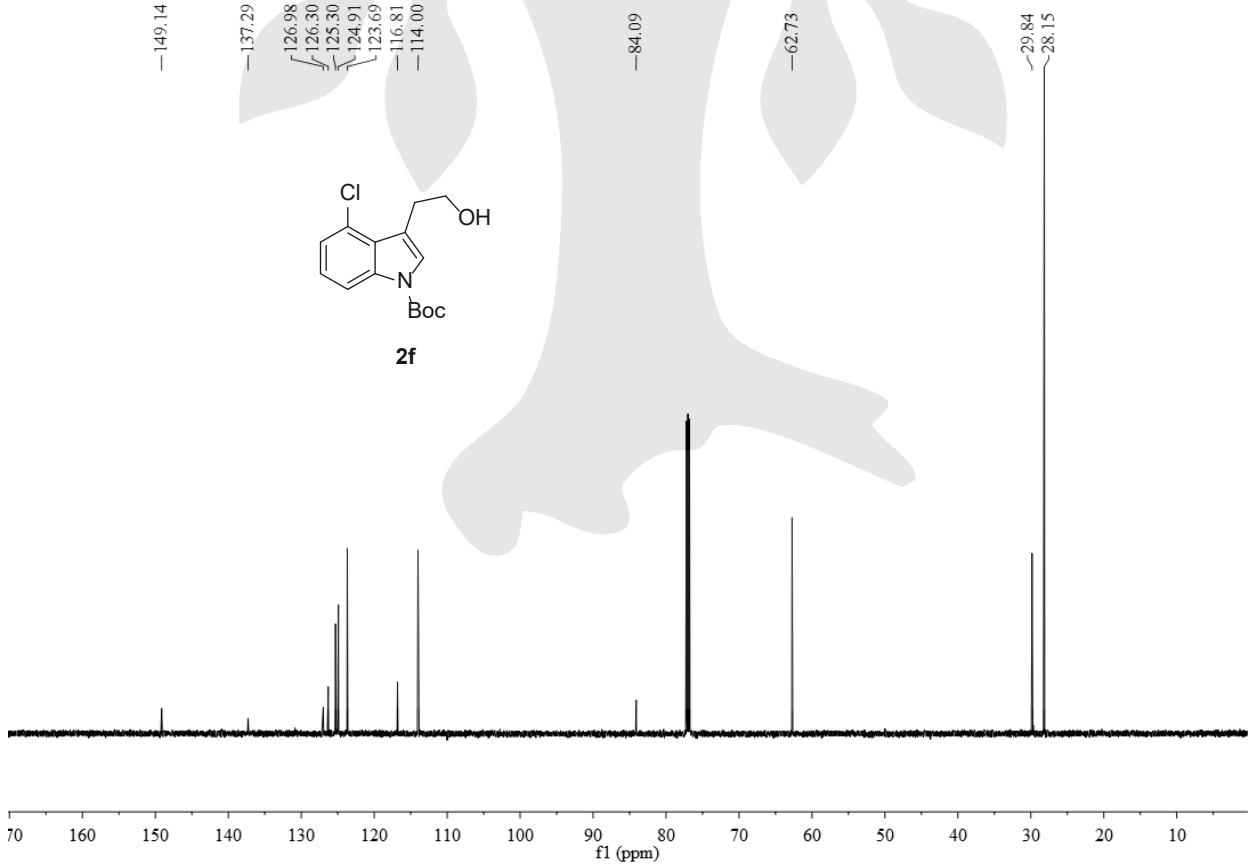

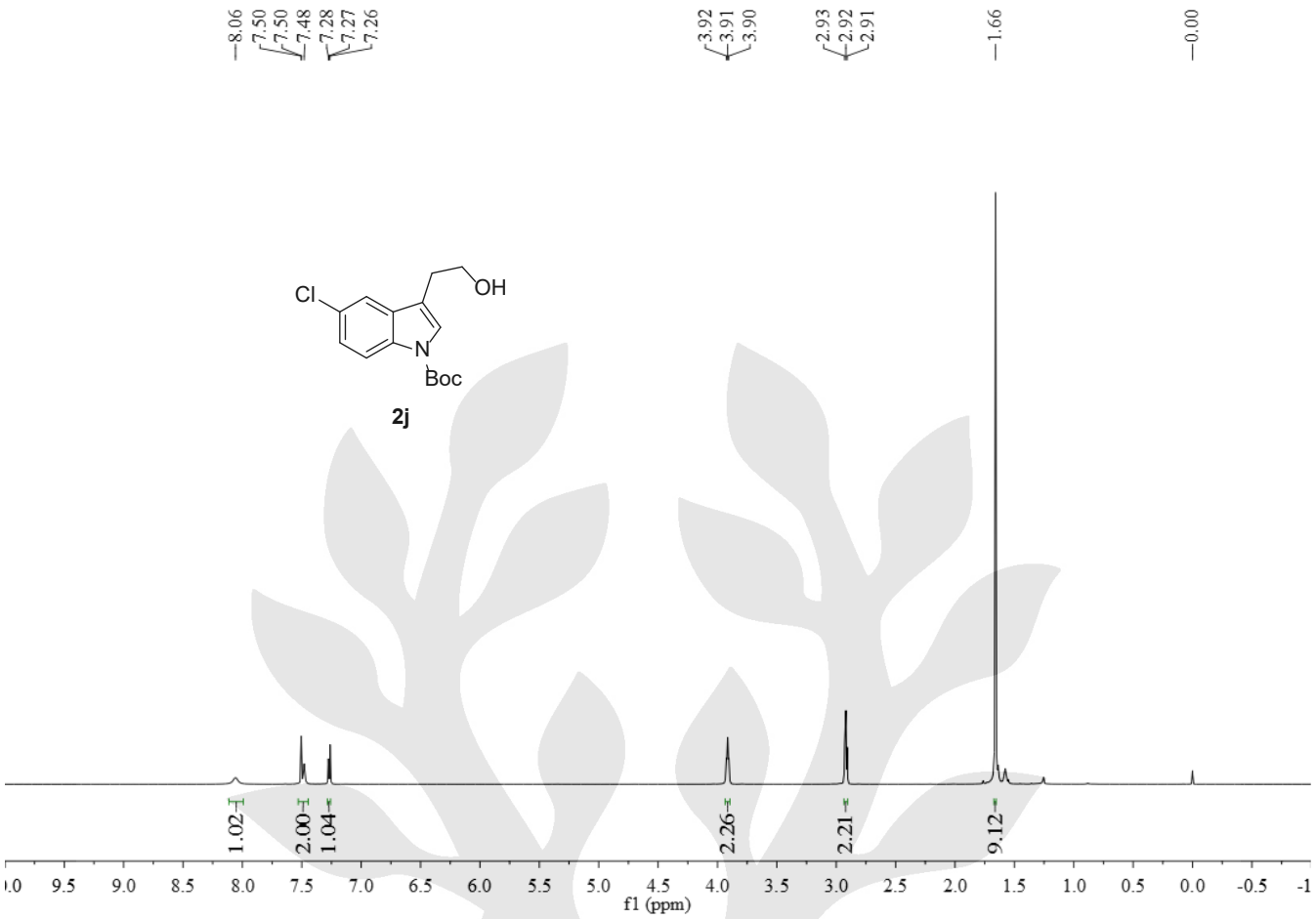

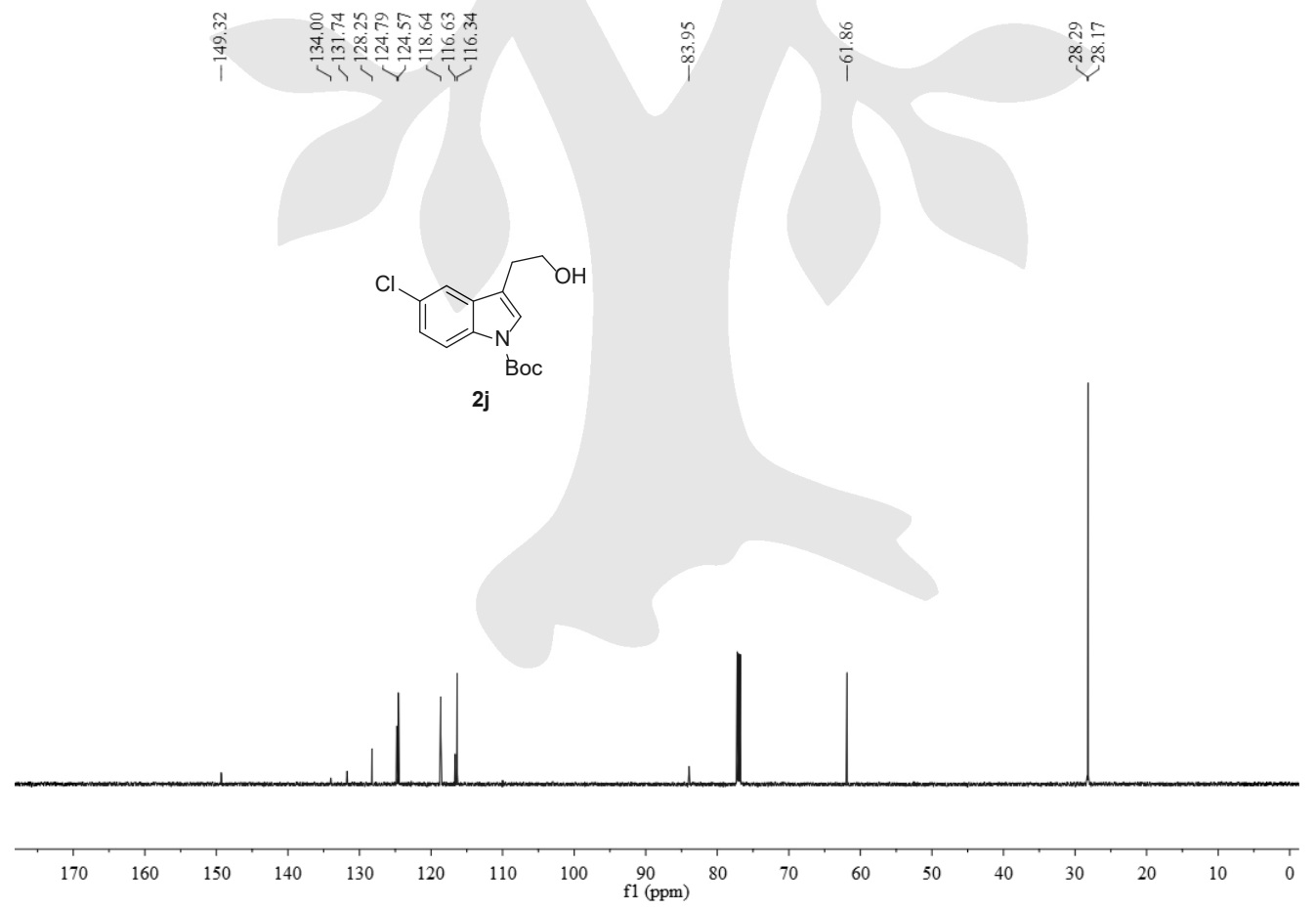

12.2. NMR and HPLC of the products 3-6

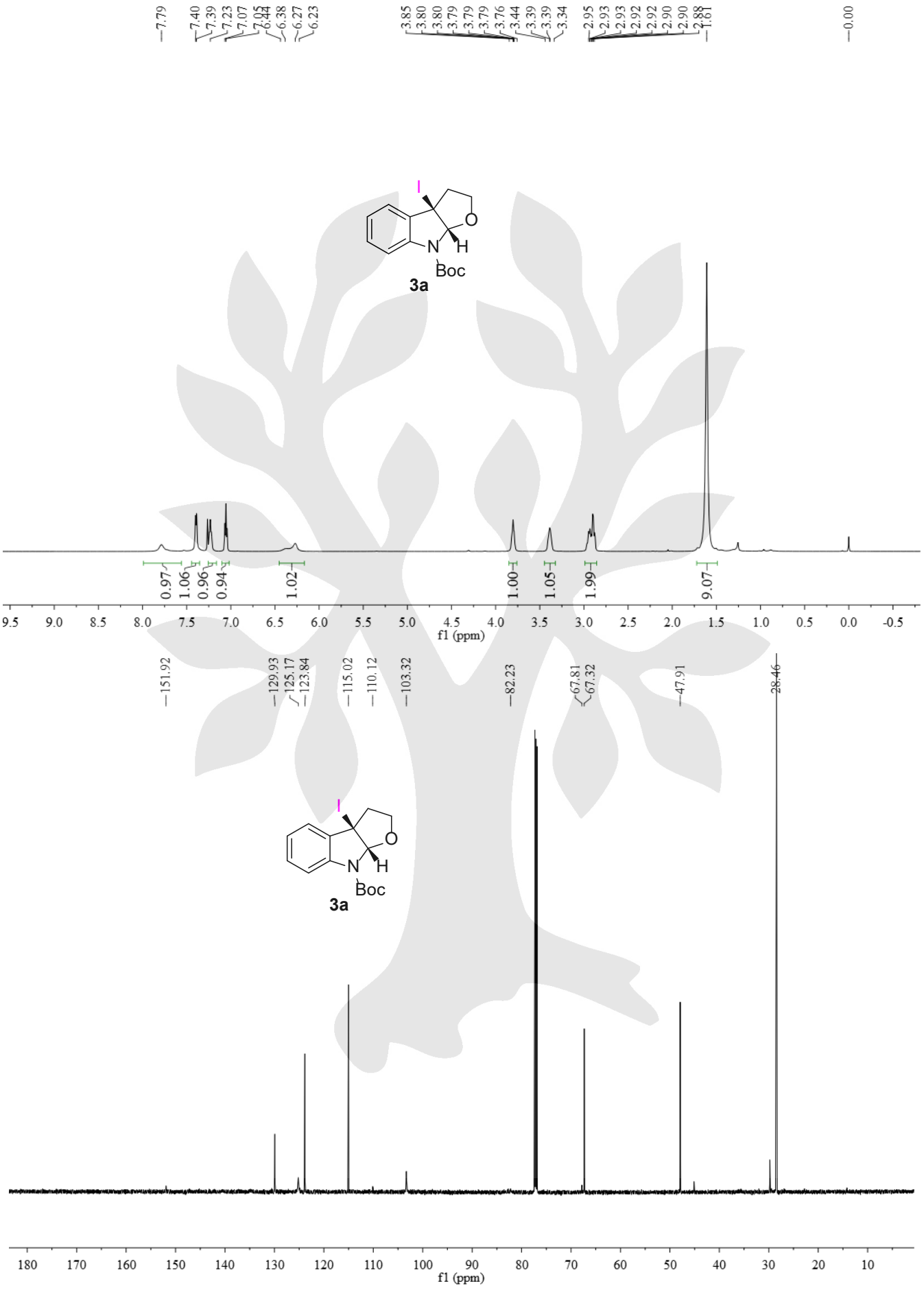

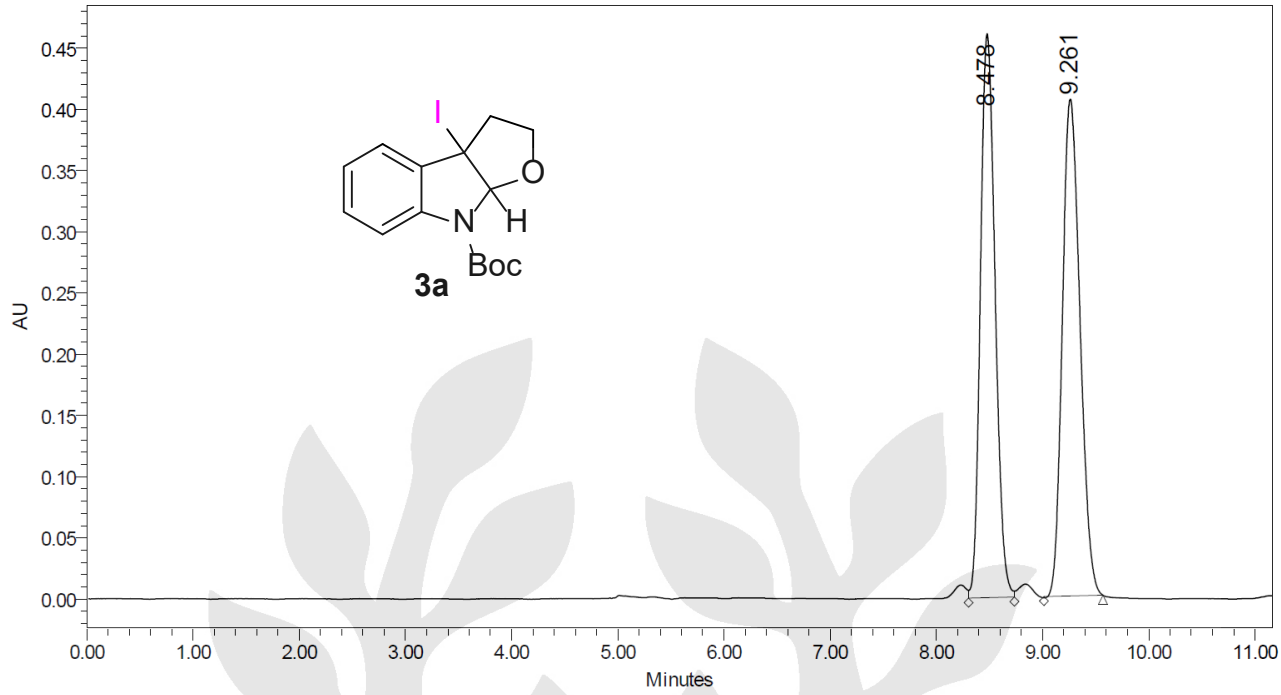

	RT (min)	Peak Type	Area (µV*sec)	% Area	Height (µV)	% Height	Integration Type	Points Across Peak	Start Time (min)	End Time (min)
1	8.478	Unknown	4426269	48.58	460709	53.16	VV	259	8.303	8.735
2	9.261	Unknown	4685751	51.42	405864	46.84	Vb	334	9.013	9.570

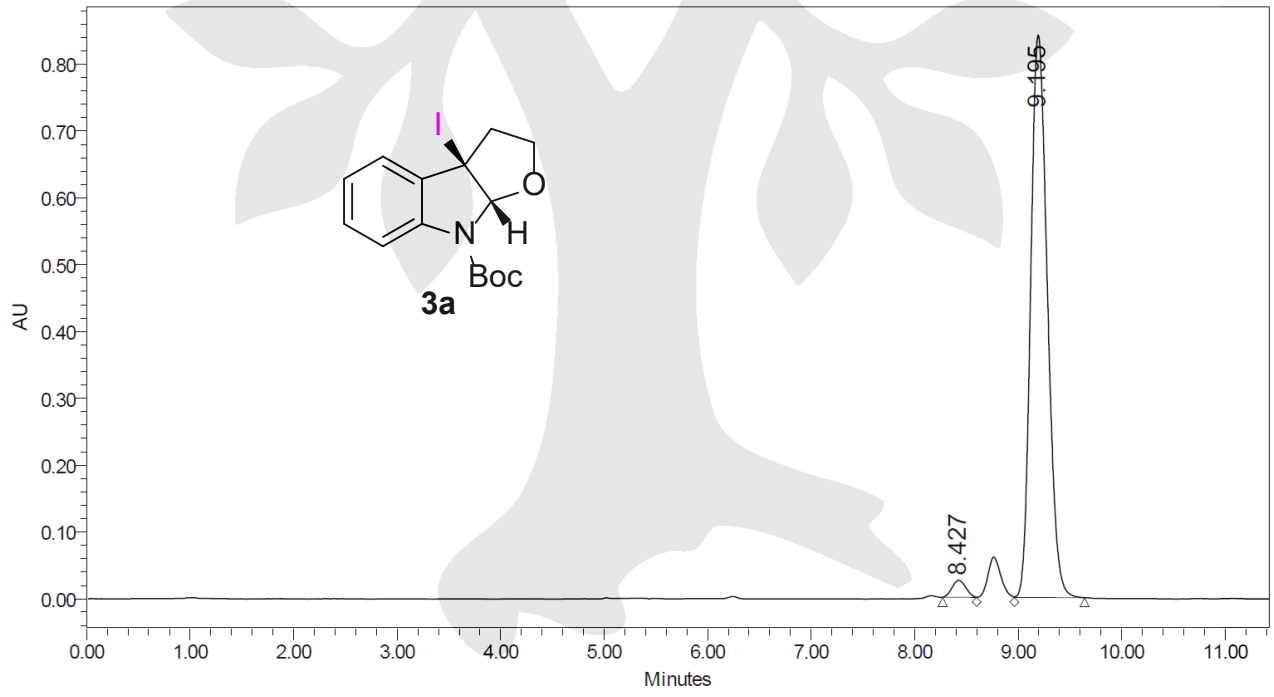

	RT (min)	Peak Type	Area (µV*sec)	% Area	Height (µV)	% Height	Integration Type	Points Across Peak	Start Time (min)	End Time (min)
1	8.427	Unknown	232587	2.41	25377	2.93	bV	197	8.272	8.600
2	9.195	Unknown	9406494	97.59	841933	97.07	Vb	407	8.963	9.642

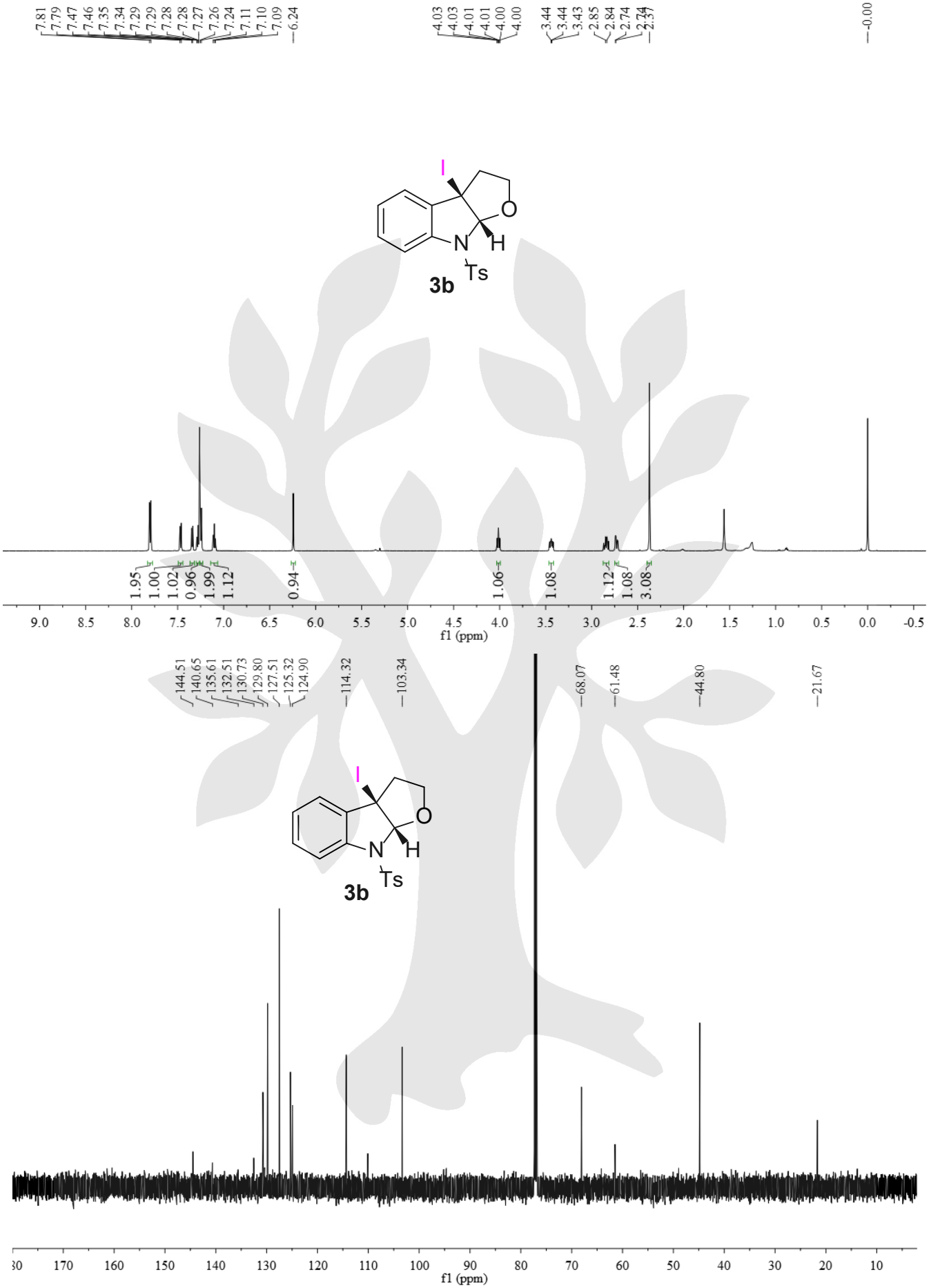

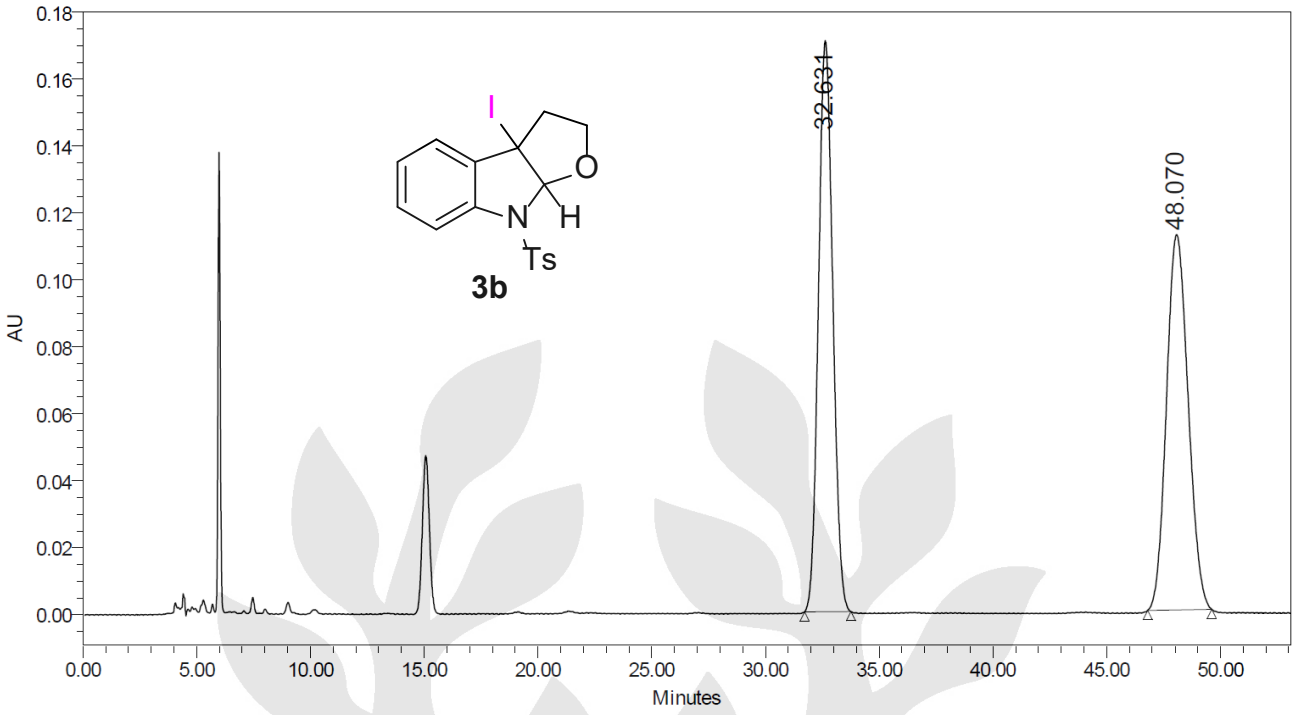

	RT (min)	Peak Type	Area (μV*sec)	% Area	Height (μV)	% Height	Integration Type	Points Across Peak	Start Time (min)	End Time (min)
1	32.631	Unknown	7476313	50.18	170717	60.35	BB	1222	31.722	33.758
2	48.070	Unknown	7422630	49.82	112173	39.65	BB	1689	46.803	49.618

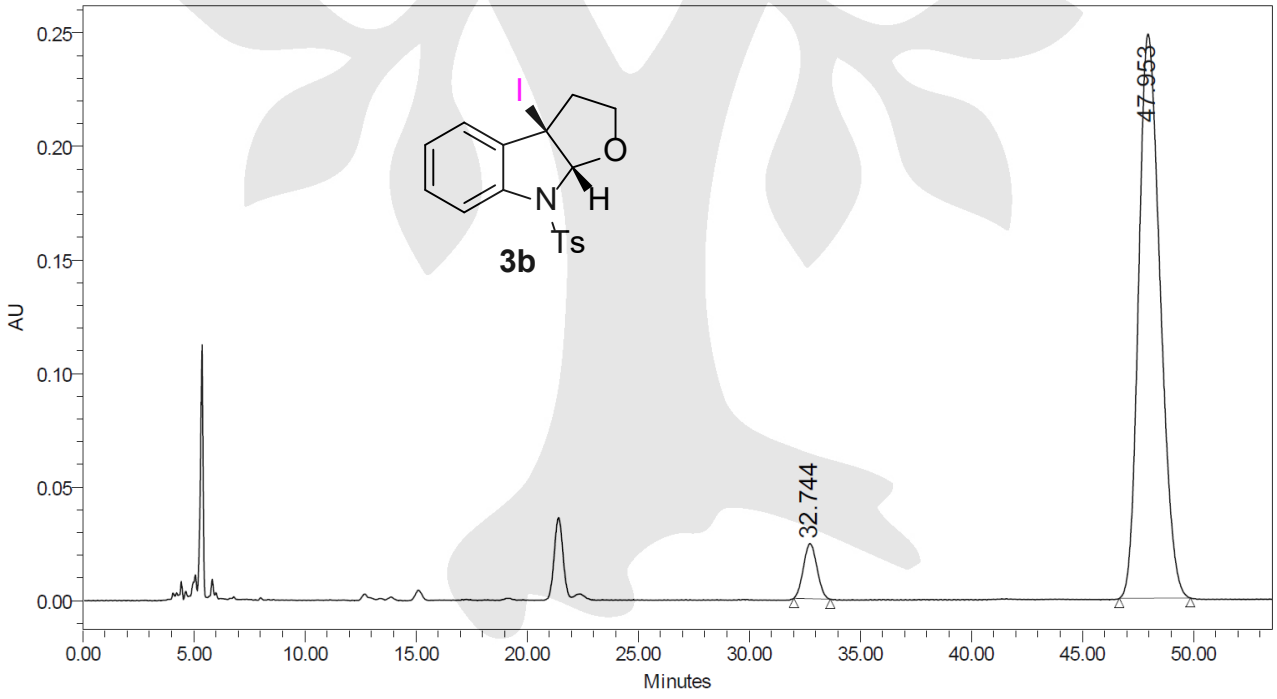

	RT (min)	Peak Type	Area (μV*sec)	% Area	Height (μV)	% Height	Integration Type	Points Across Peak	Start Time (min)	End Time (min)
1	32.744	Unknown	1025785	5.77	24243	8.89	BB	987	32.017	33.662
2	47.953	Unknown	16744256	94.23	248332	91.11	BB	1916	46.670	49.863

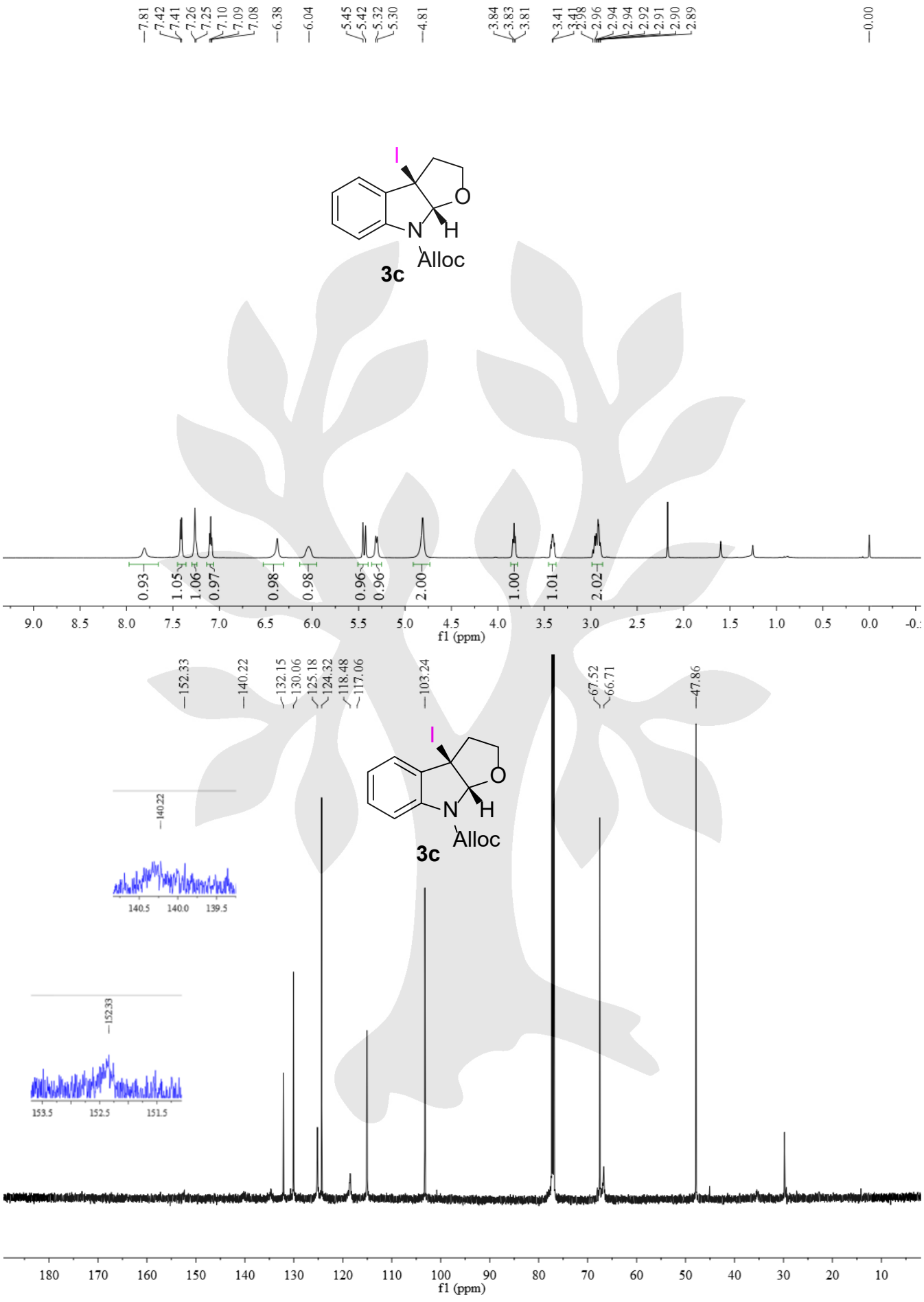

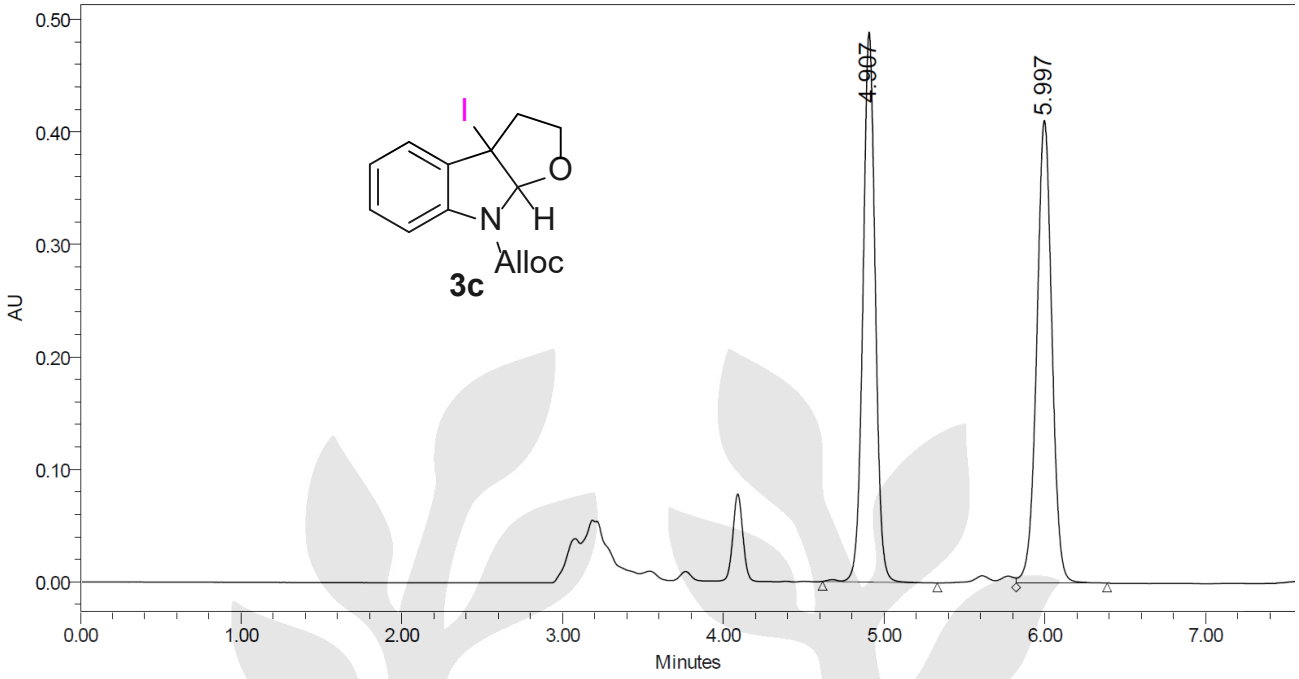

	RT (min)	Area (μV*sec)	% Area	Height (μV)	% Height
1	4.907	2612040	49.10	489003	54.32
2	5.997	2708085	50.90	411148	45.68

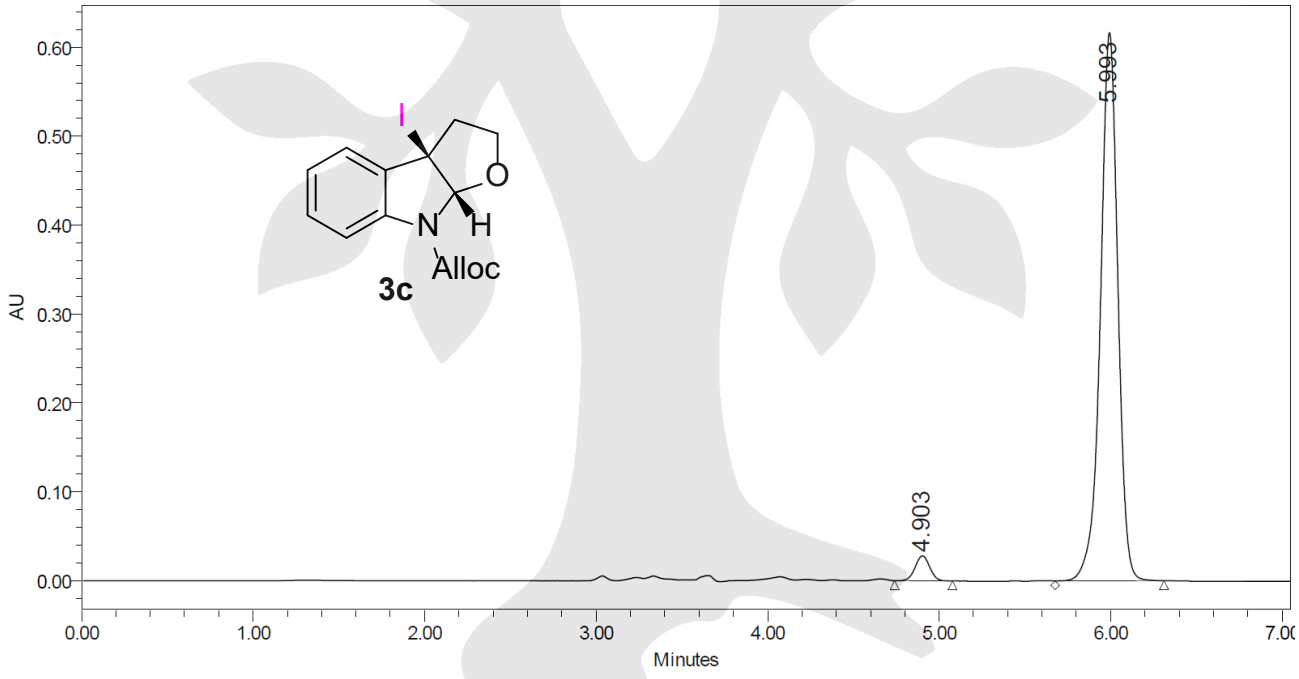

	RT (min)	Area (μV*sec)	% Area	Height (μV)	% Height
1	4.903	164613	3.65	28068	4.35
2	5.993	4350312	96.35	616621	95.65

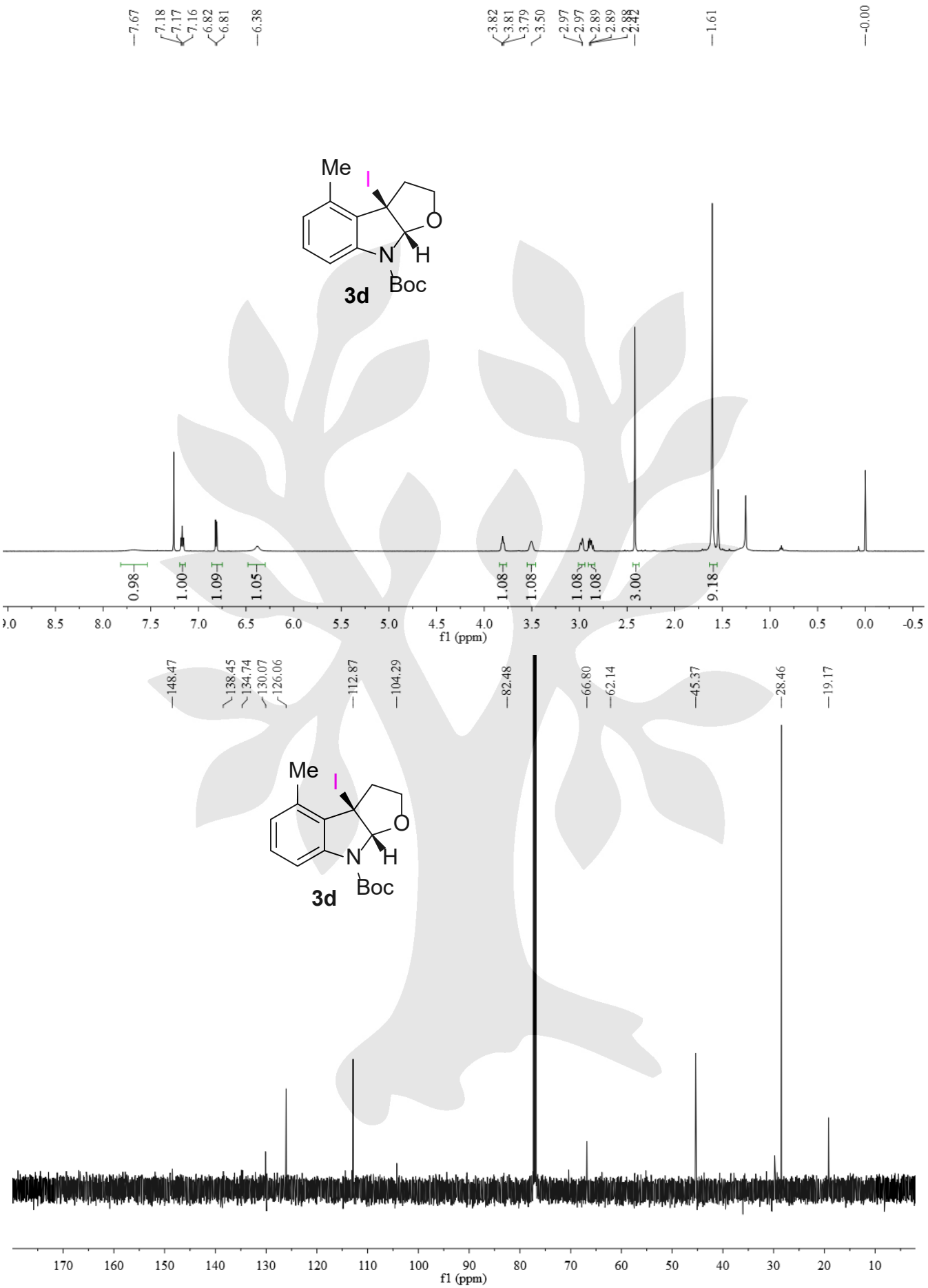

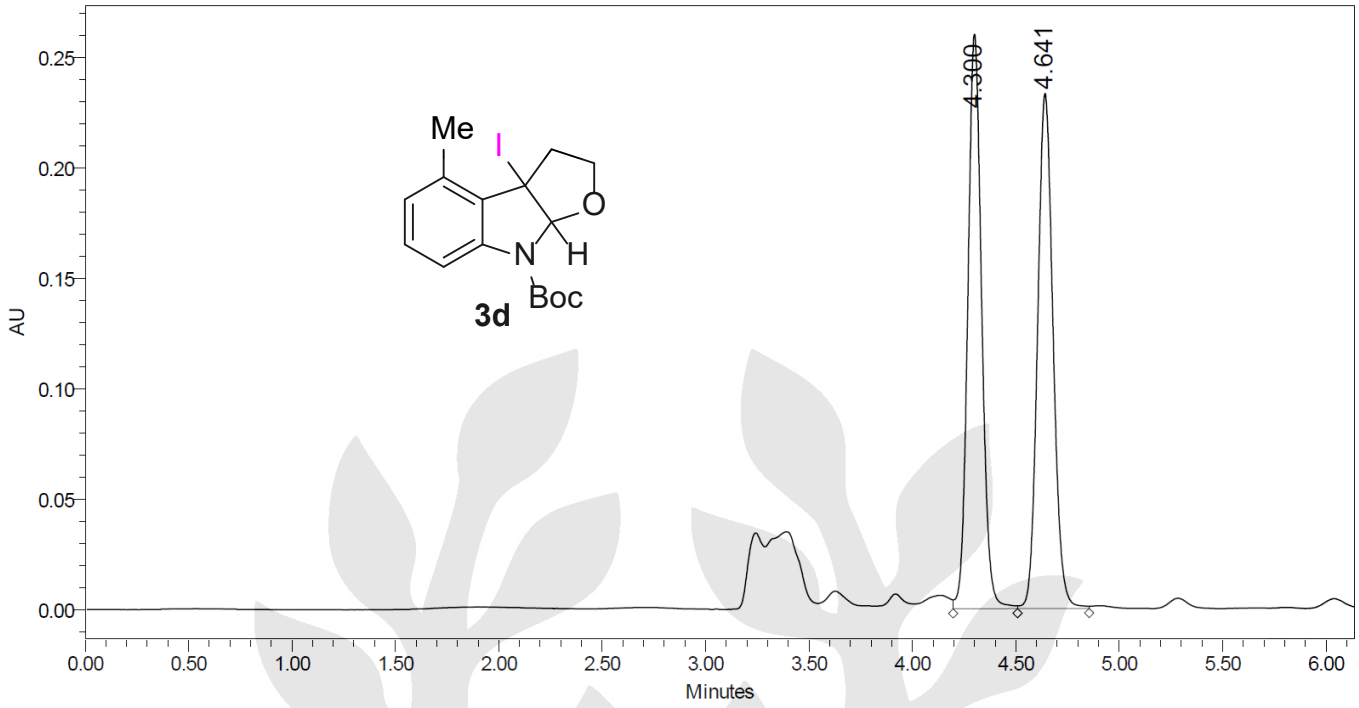

	RT (min)	Area (μV*sec)	% Area	Height (μV)	% Height
1	4.300	1214150	49.96	260169	52.73
2	4.641	1215943	50.04	233256	47.27

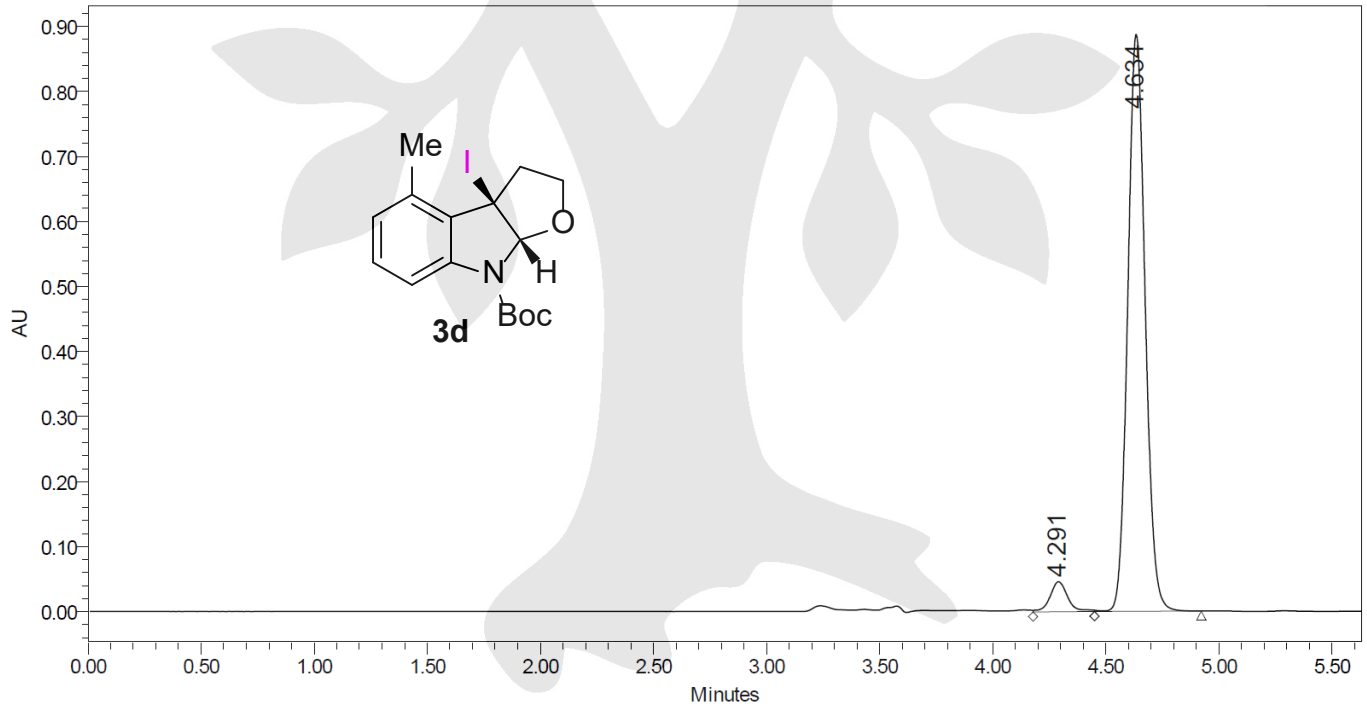

	RT (min)	Area (μV*sec)	% Area	Height (μV)	% Height
1	4.291	249495	5.00	46073	4.94
2	4.634	4736890	95.00	887358	95.06

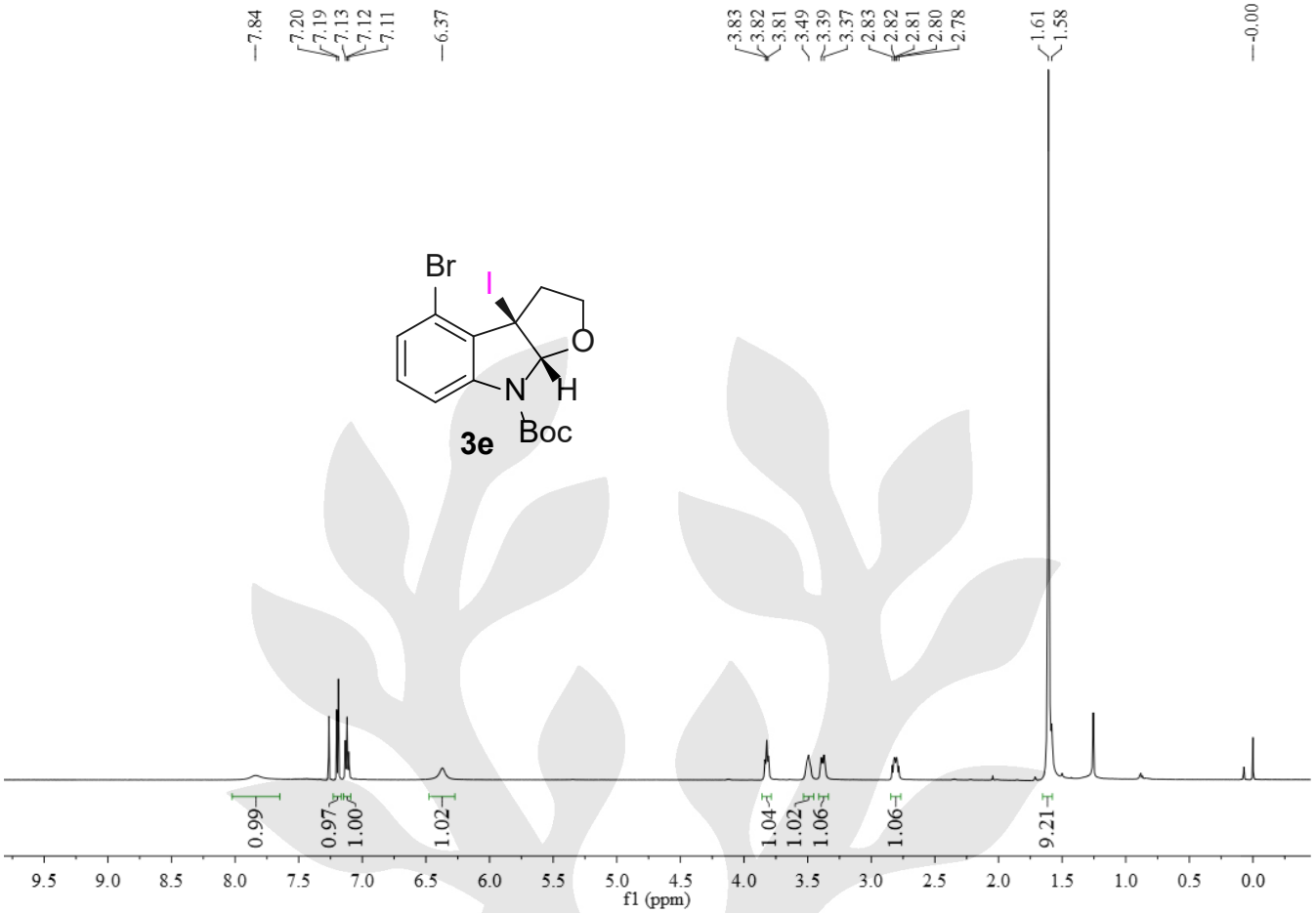

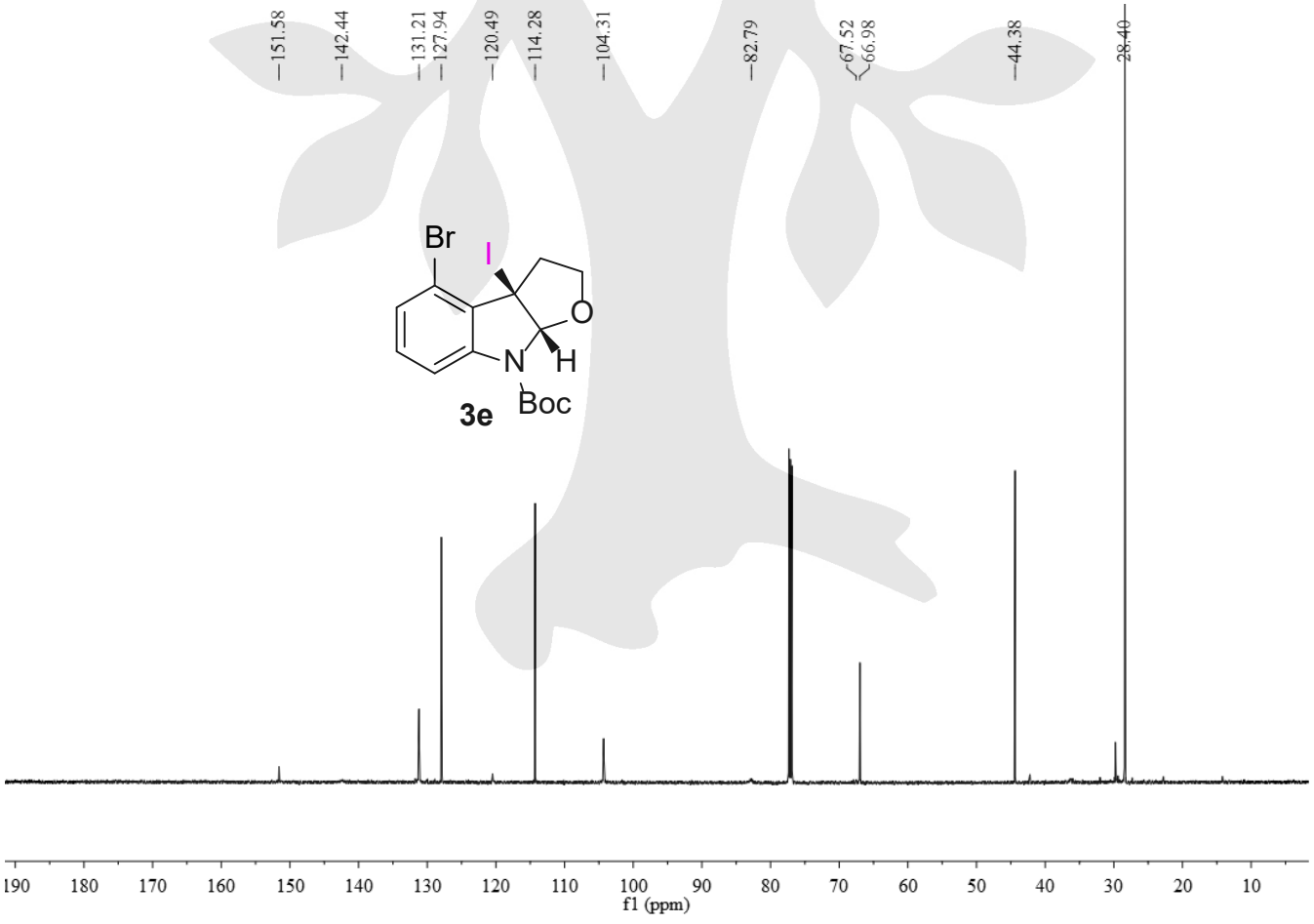

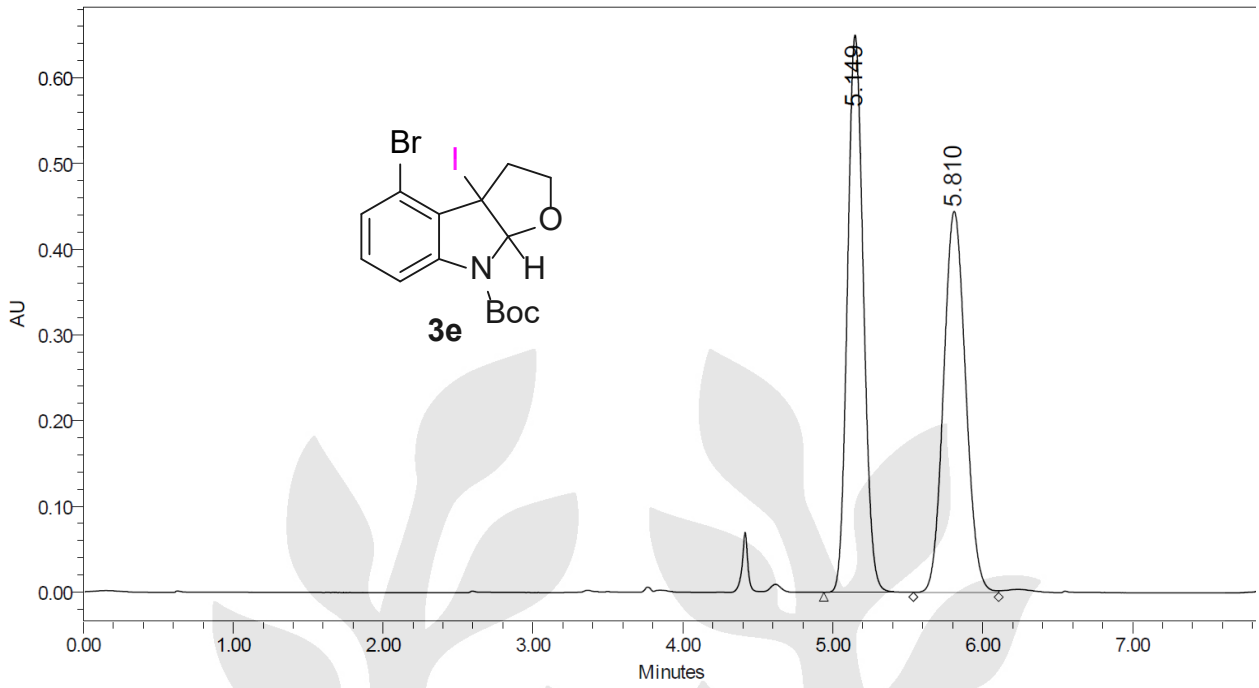

	RT (min)	Peak Type	Area (μV*sec)	% Area	Height (μV)	% Height	Integration Type	Points Across Peak	Start Time (min)	End Time (min)
1	5.149	Unknown	4815828	51.42	650607	59.39	BV	358	4.940	5.537
2	5.810	Unknown	4550155	48.58	444915	40.61	VV	342	5.537	6.107

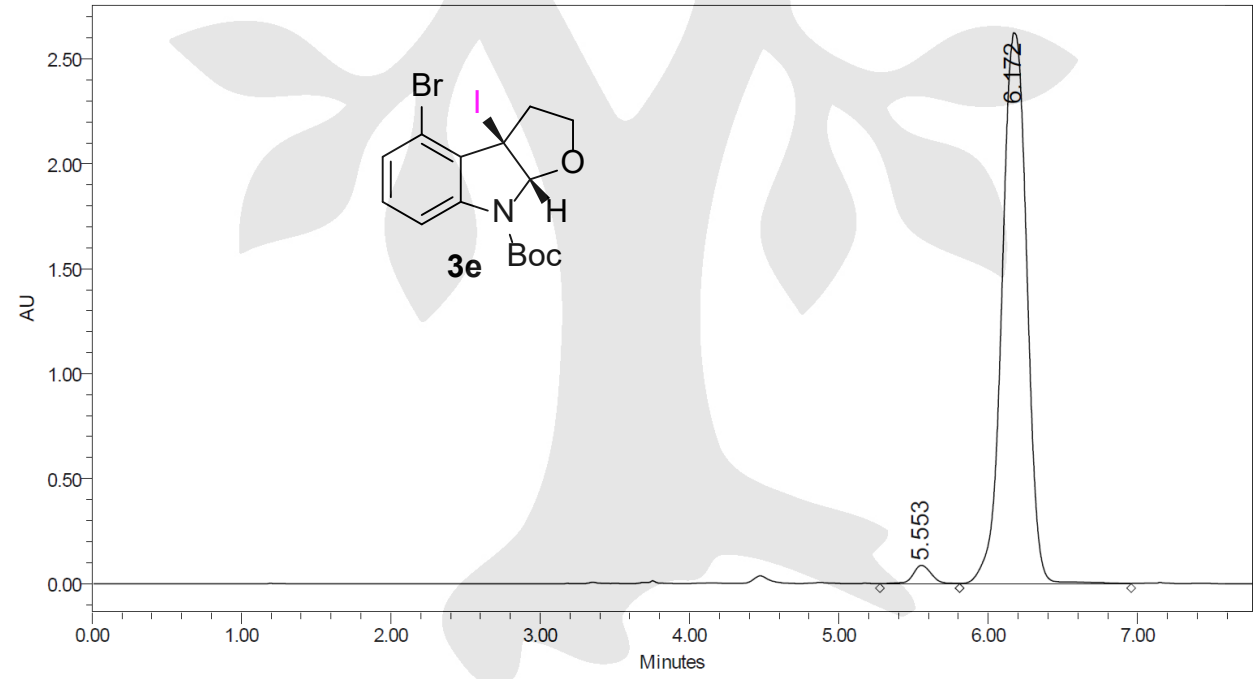

	RT (min)	Peak Type	Area (μV*sec)	% Area	Height (μV)	% Height	Integration Type	Points Across Peak	Start Time (min)	End Time (min)
1	5.553	Unknown	758686	2.43	87844	3.24	VV	320	5.275	5.808
2	6.172	Unknown	30408286	97.57	2624896	96.76	VV	689	5.808	6.957

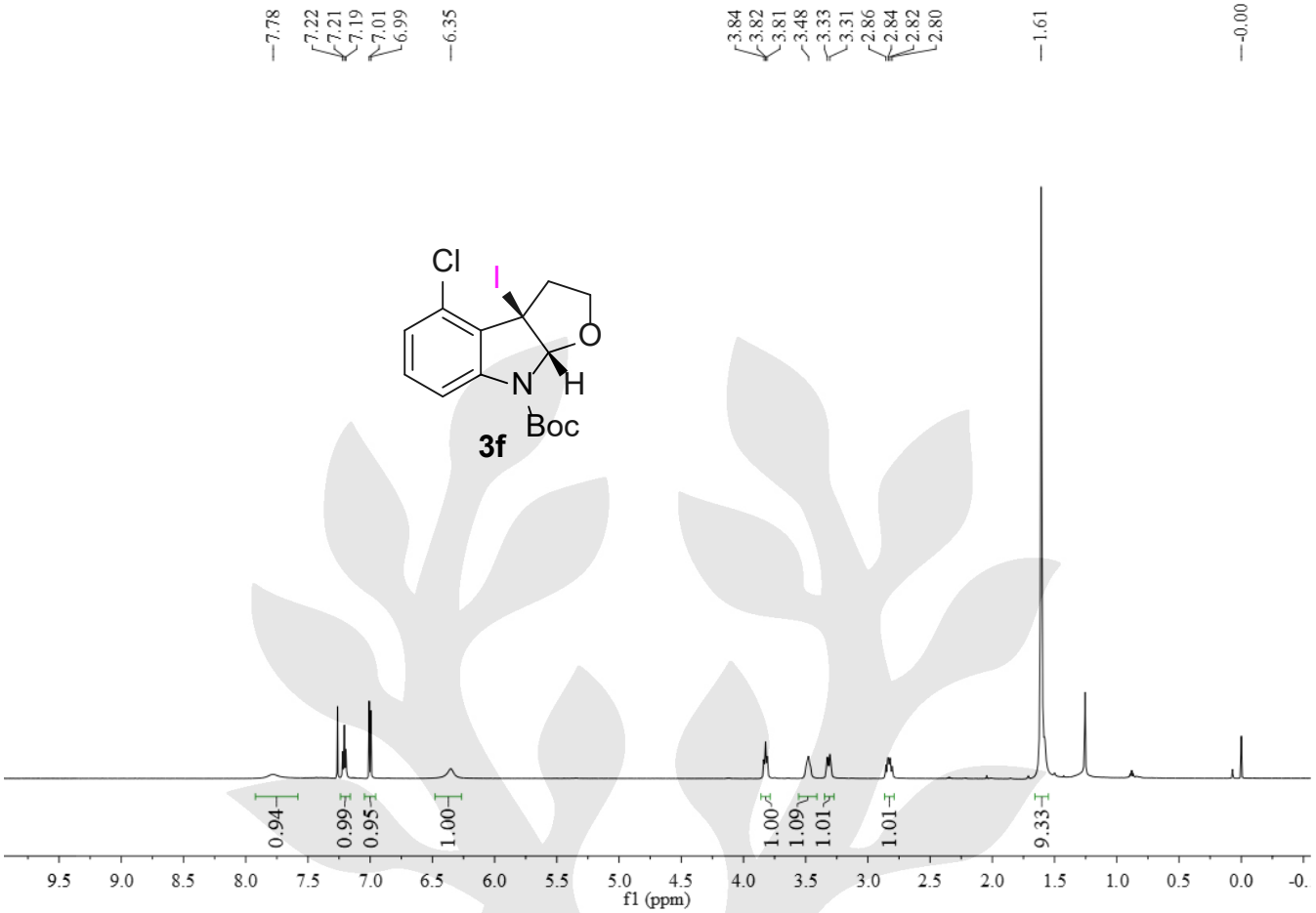

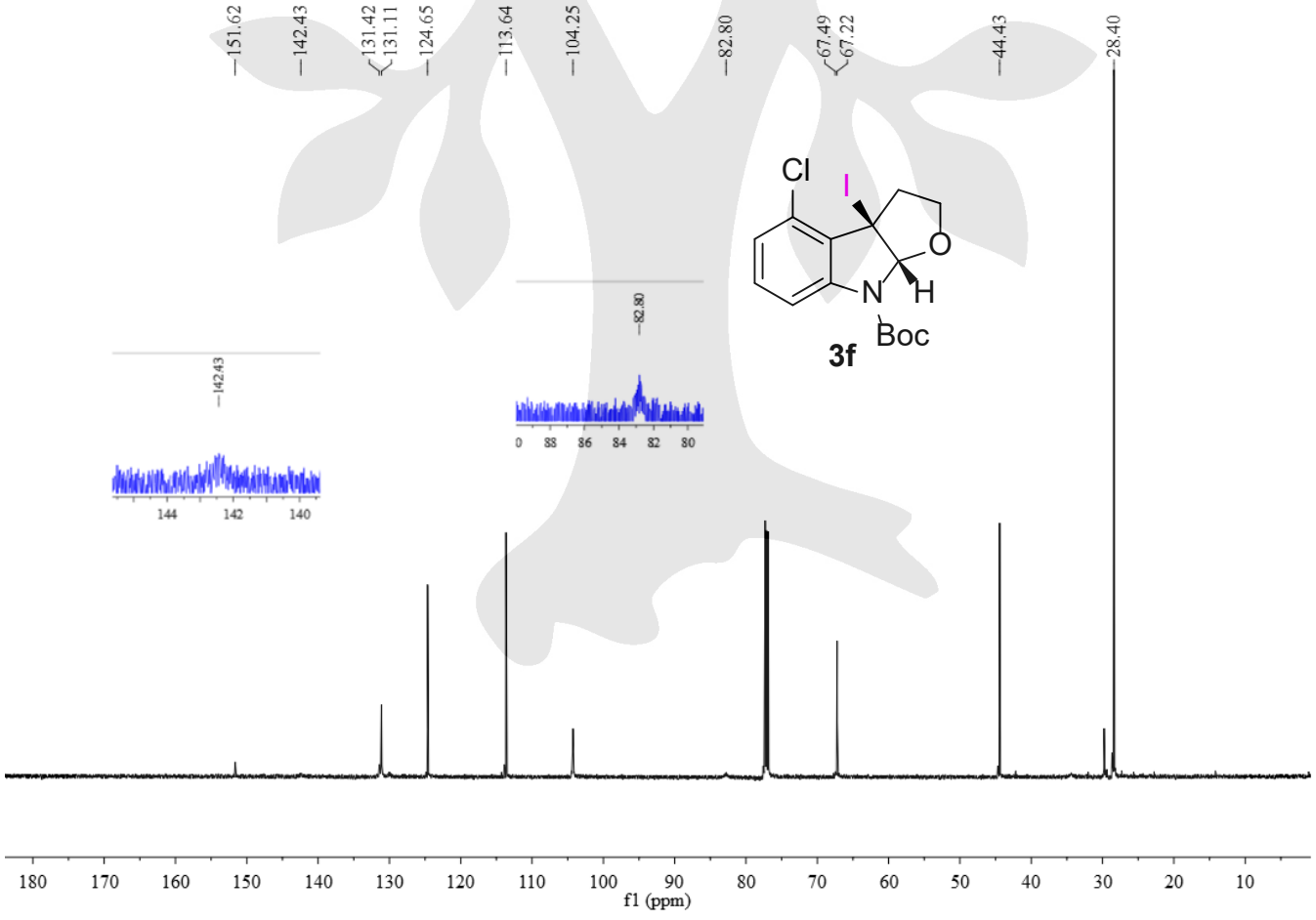

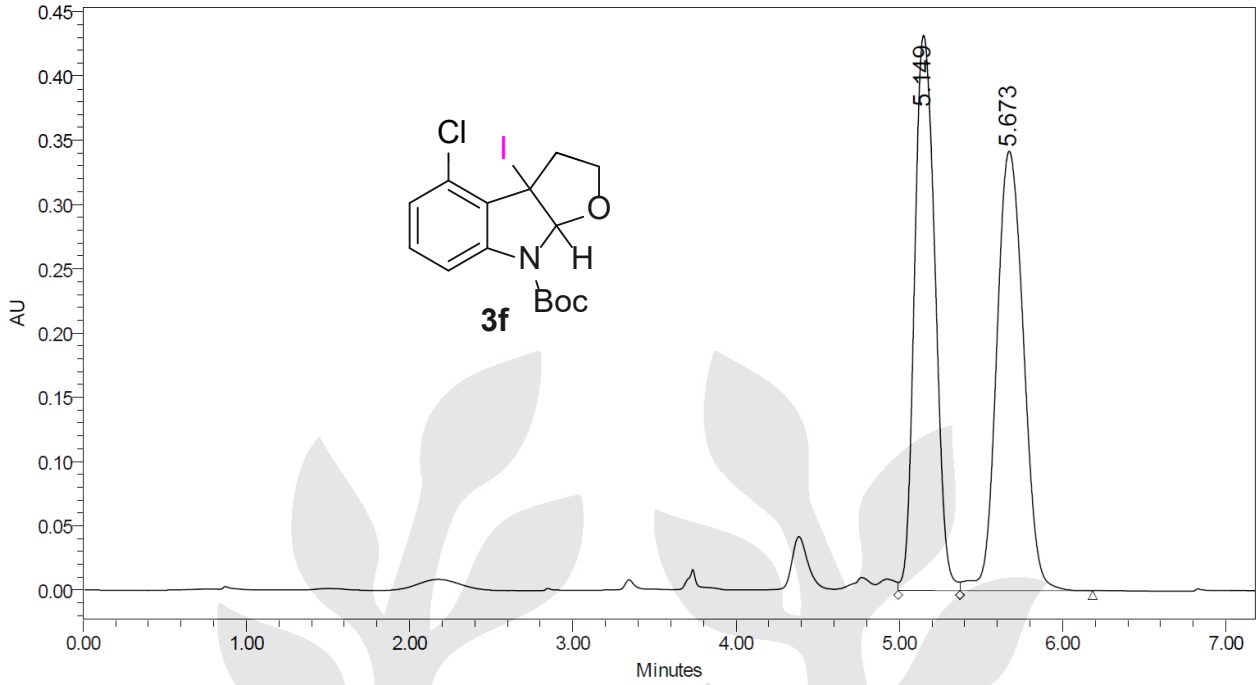

	RT (min)	Peak Type	Area (μV*sec)	% Area	Height (μV)	% Height	Integration Type	Points Across Peak	Start Time (min)	End Time (min)
1	5.149	Unknown	3770049	49.09	432054	55.83	VV	227	4.993	5.372
2	5.673	Unknown	3910452	50.91	341865	44.17	VB	488	5.372	6.185

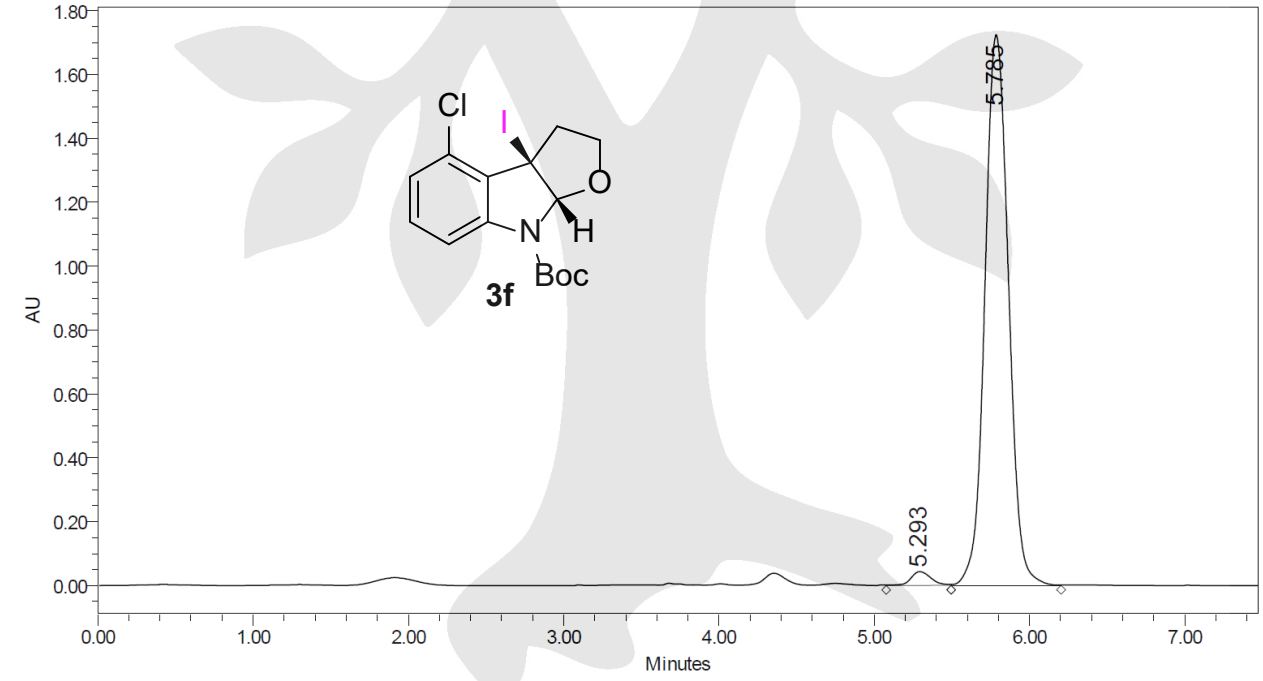

	RT (min)	Peak Type	Area (μV*sec)	% Area	Height (μV)	% Height	Integration Type	Points Across Peak	Start Time (min)	End Time (min)
1	5.293	Unknown	394579	2.13	43308	2.45	VV	251	5.077	5.495
2	5.785	Unknown	18147286	97.87	1725046	97.55	VV	425	5.495	6.203

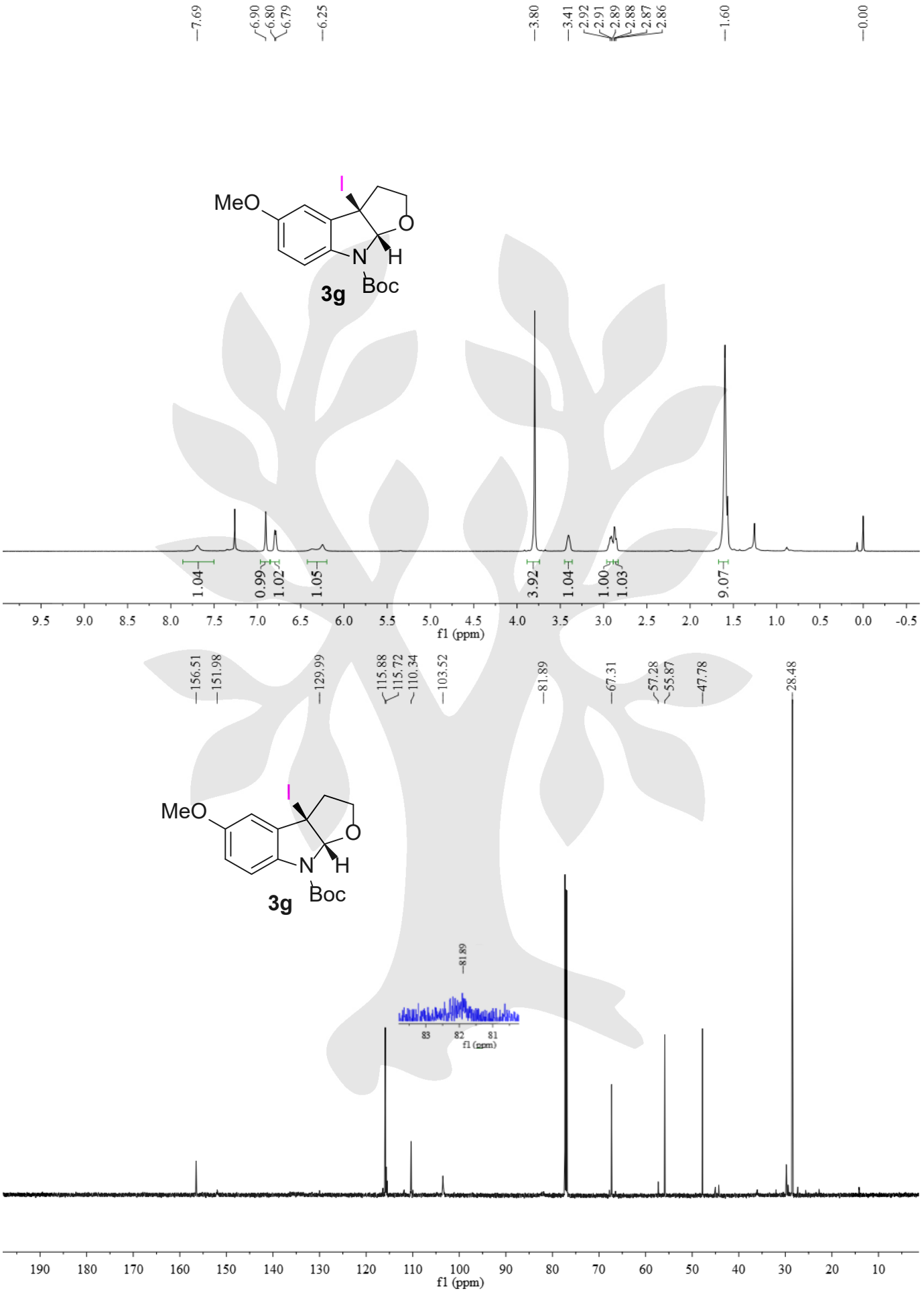

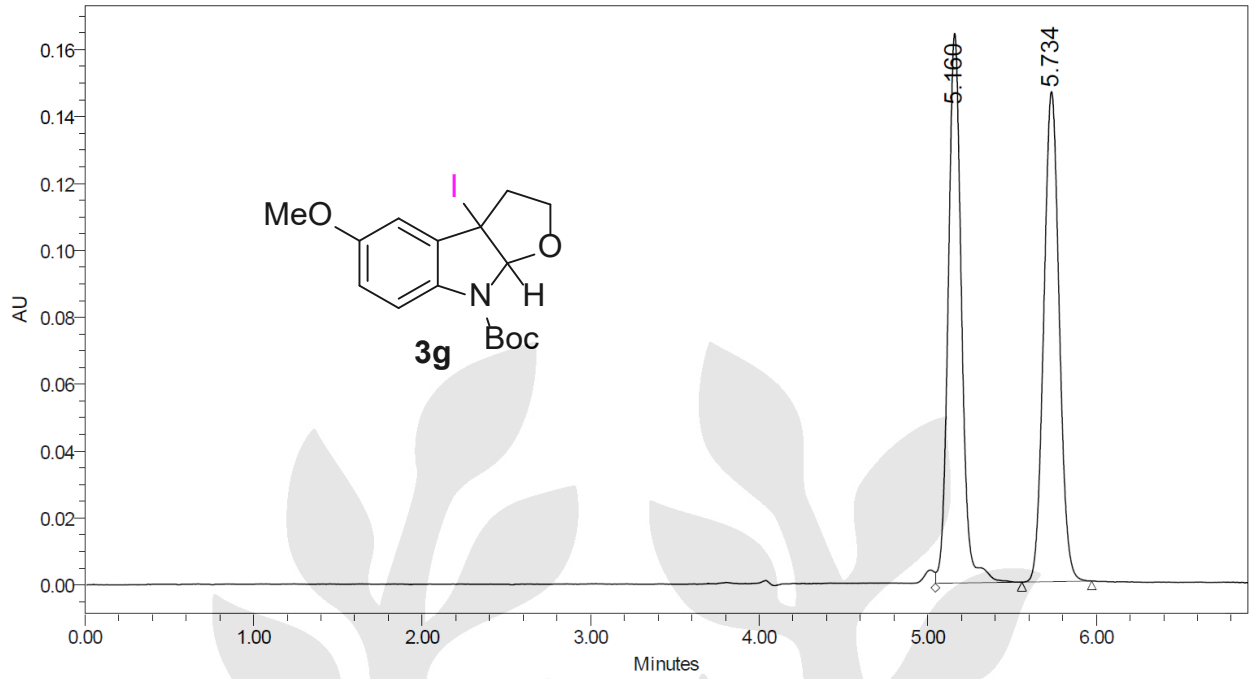

	RT (min)	Peak Type	Area (μV*sec)	% Area	Height (μV)	% Height	Integration Type	Points Across Peak	Start Time (min)	End Time (min)
1	5.160	Unknown	902060	49.15	164375	52.87	VB	308	5.045	5.558
2	5.734	Unknown	933435	50.85	146537	47.13	BB	249	5.558	5.973

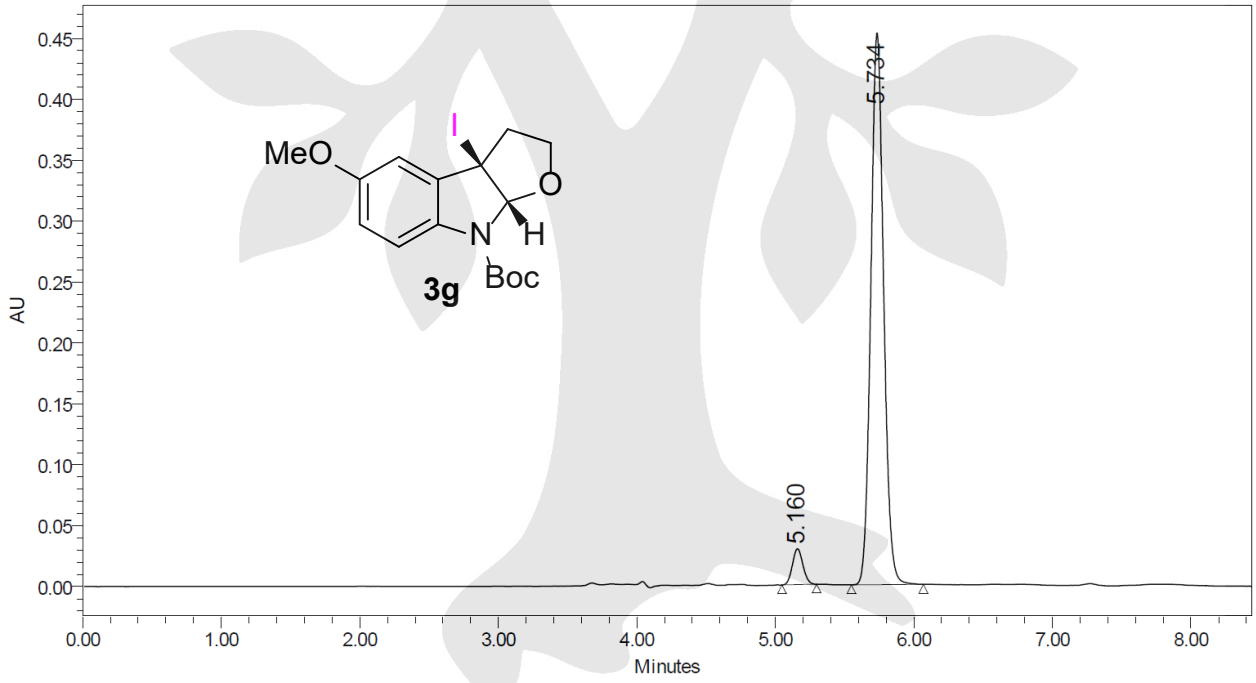

	RT (min)	Peak Type	Area (μV*sec)	% Area	Height (μV)	% Height	Integration Type	Points Across Peak	Start Time (min)	End Time (min)
1	5.160	Unknown	154248	5.04	29377	6.09	bb	150	5.048	5.298
2	5.734	Unknown	2903993	94.96	452933	93.91	BB	312	5.548	6.068

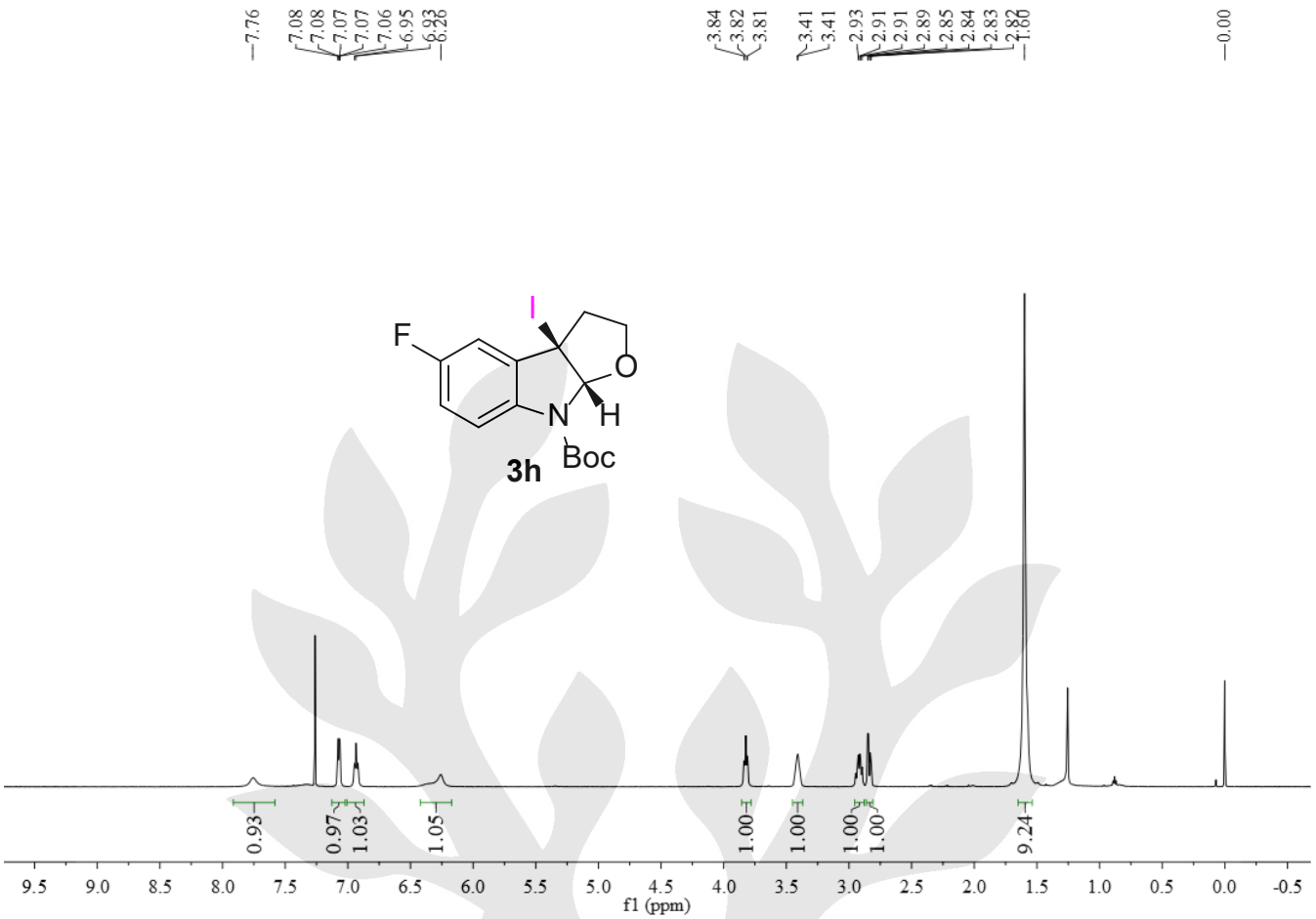

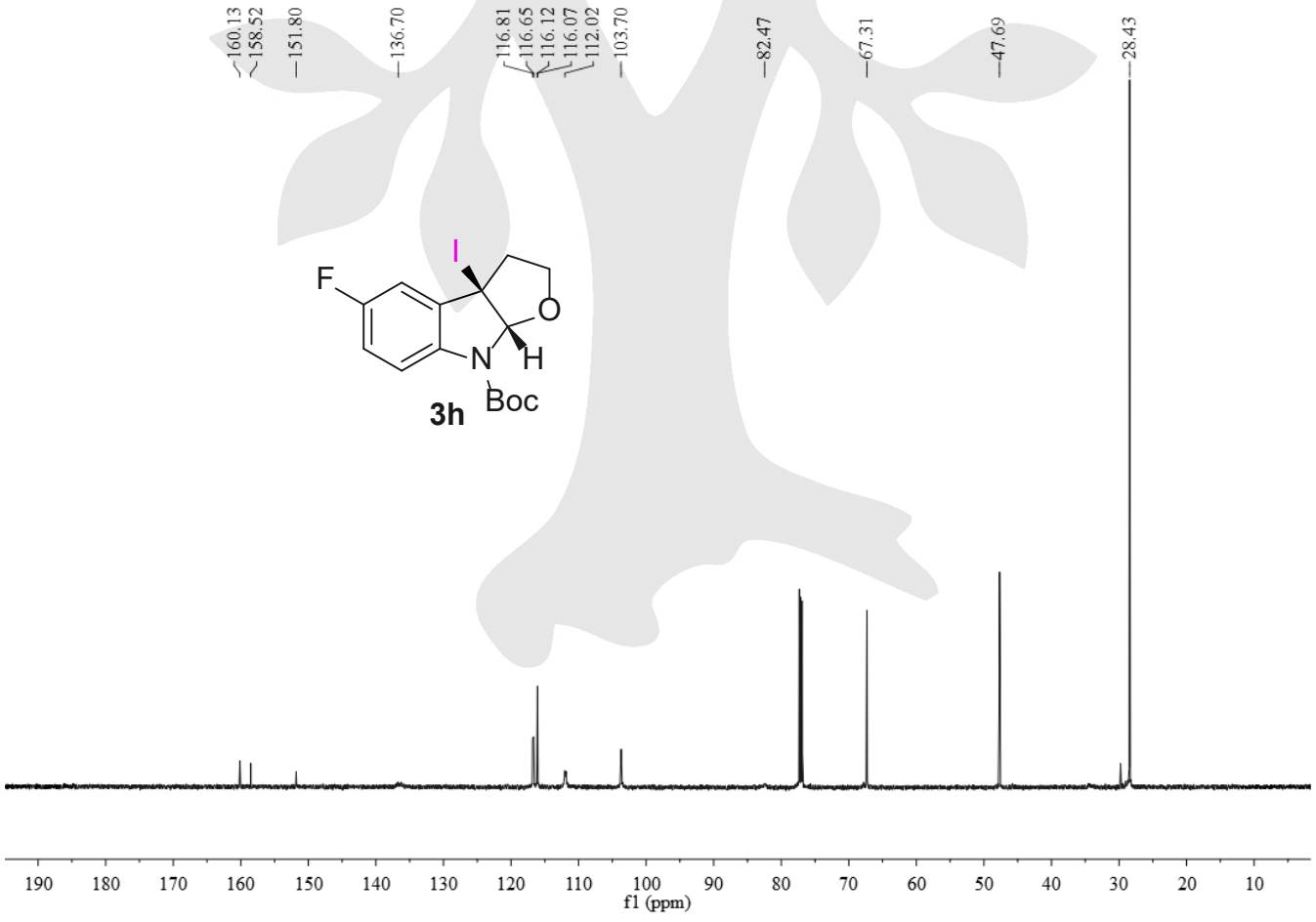

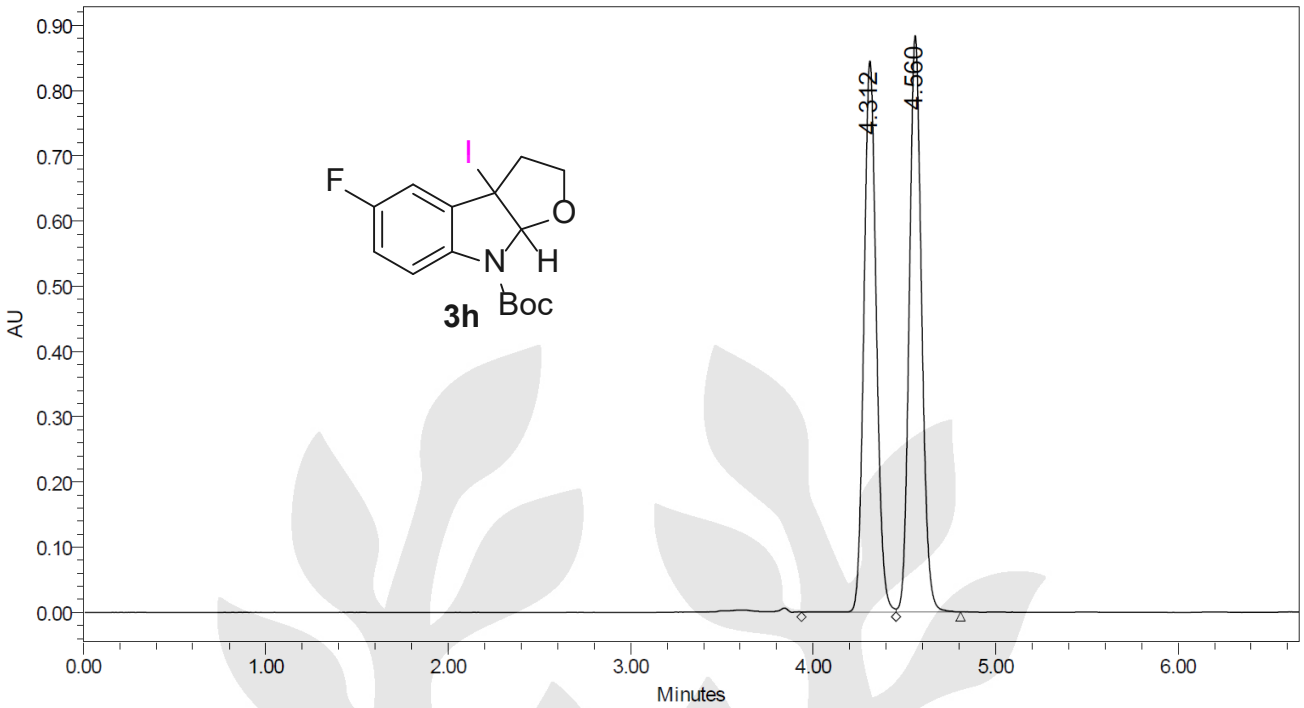

	RT (min)	Peak Type	Area (μV*sec)	% Area	Height (μV)	% Height	Integration Type	Points Across Peak	Start Time (min)	End Time (min)
1	4.312	Unknown	3990537	49.04	844680	48.88	VV	311	3.937	4.455
2	4.560	Unknown	4146361	50.96	883520	51.12	VB	212	4.455	4.808

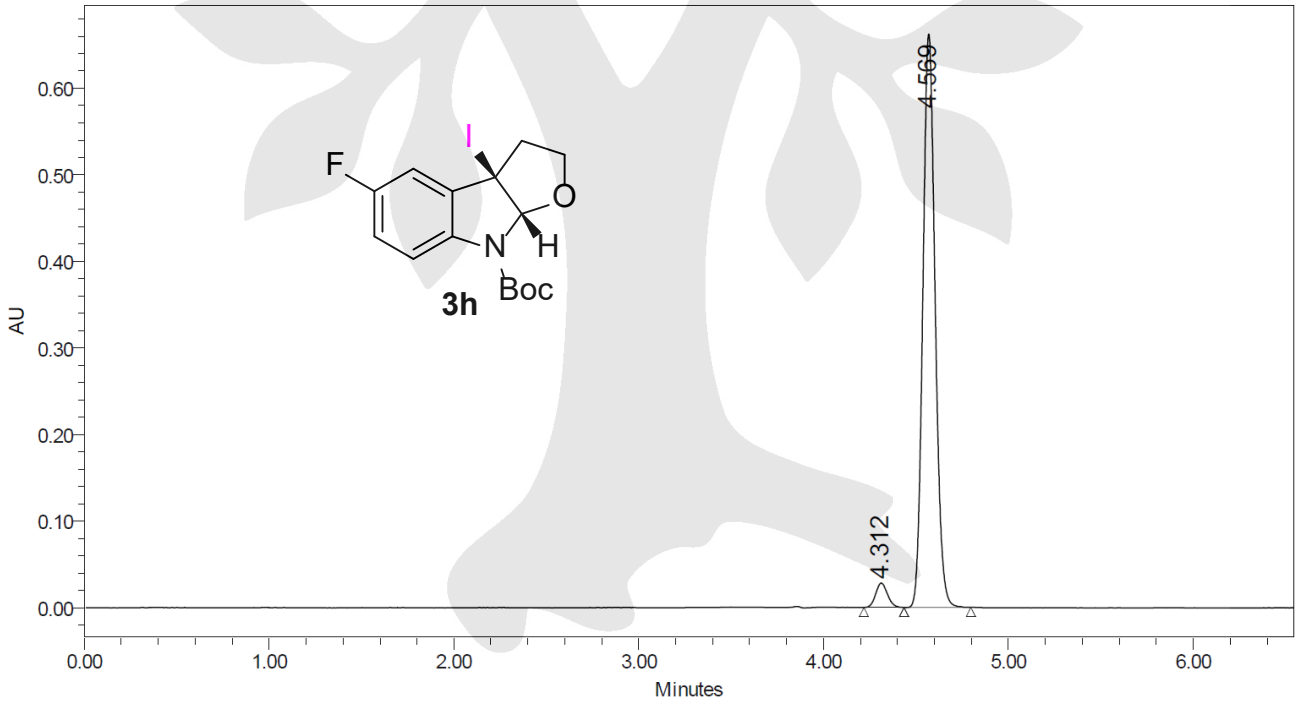

	RT (min)	Peak Type	Area (μV*sec)	% Area	Height (μV)	% Height	Integration Type	Points Across Peak	Start Time (min)	End Time (min)
1	4.312	Unknown	125622	3.96	28179	4.08	BB	130	4.218	4.435
2	4.569	Unknown	3047402	96.04	662450	95.92	BB	217	4.435	4.797

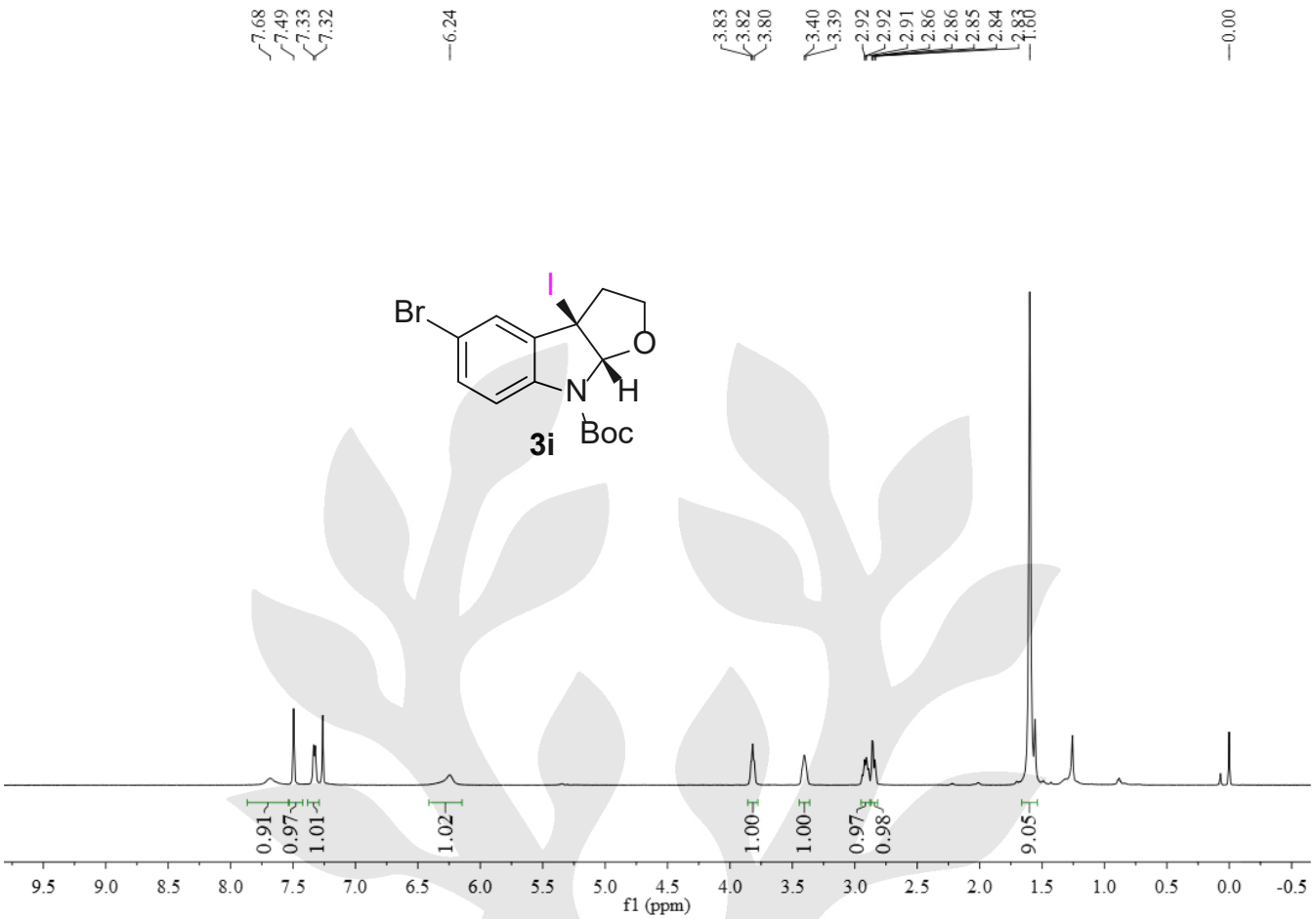

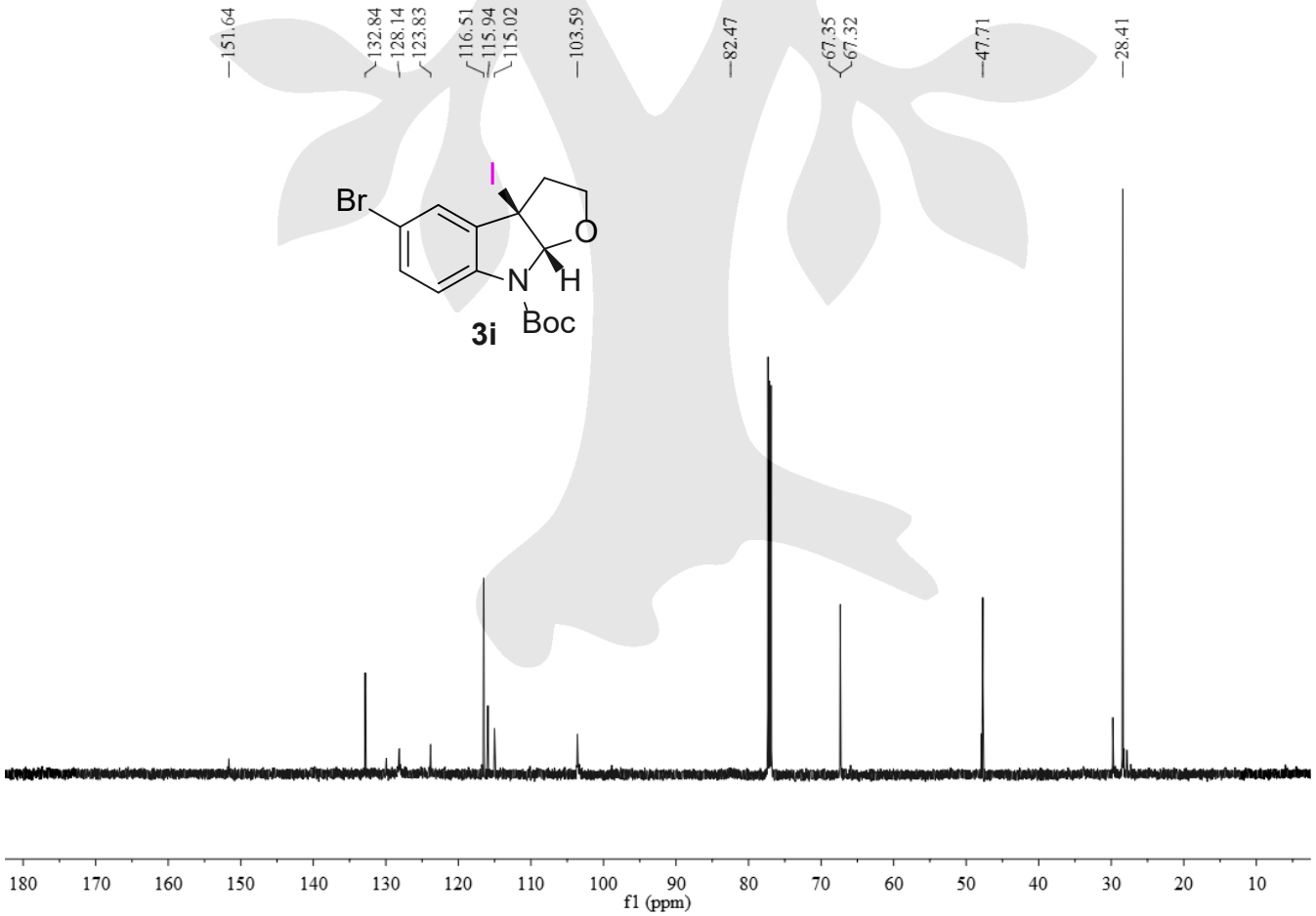

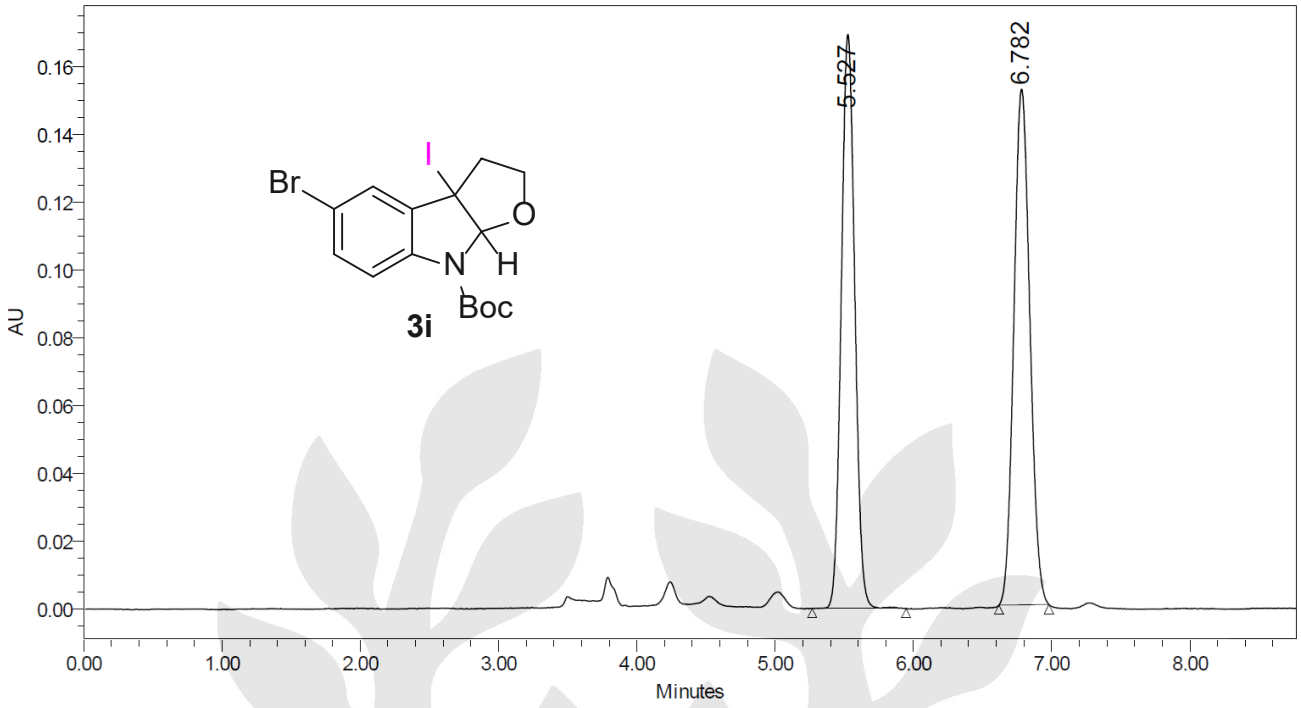

	RT (min)	Peak Type	Area (μV*sec)	% Area	Height (μV)	% Height	Integration Type	Points Across Peak	Start Time (min)	End Time (min)
1	5.527	Unknown	1151420	48.46	169448	52.68	bb	407	5.268	5.947
2	6.782	Unknown	1224449	51.54	152213	47.32	bb	217	6.618	6.980

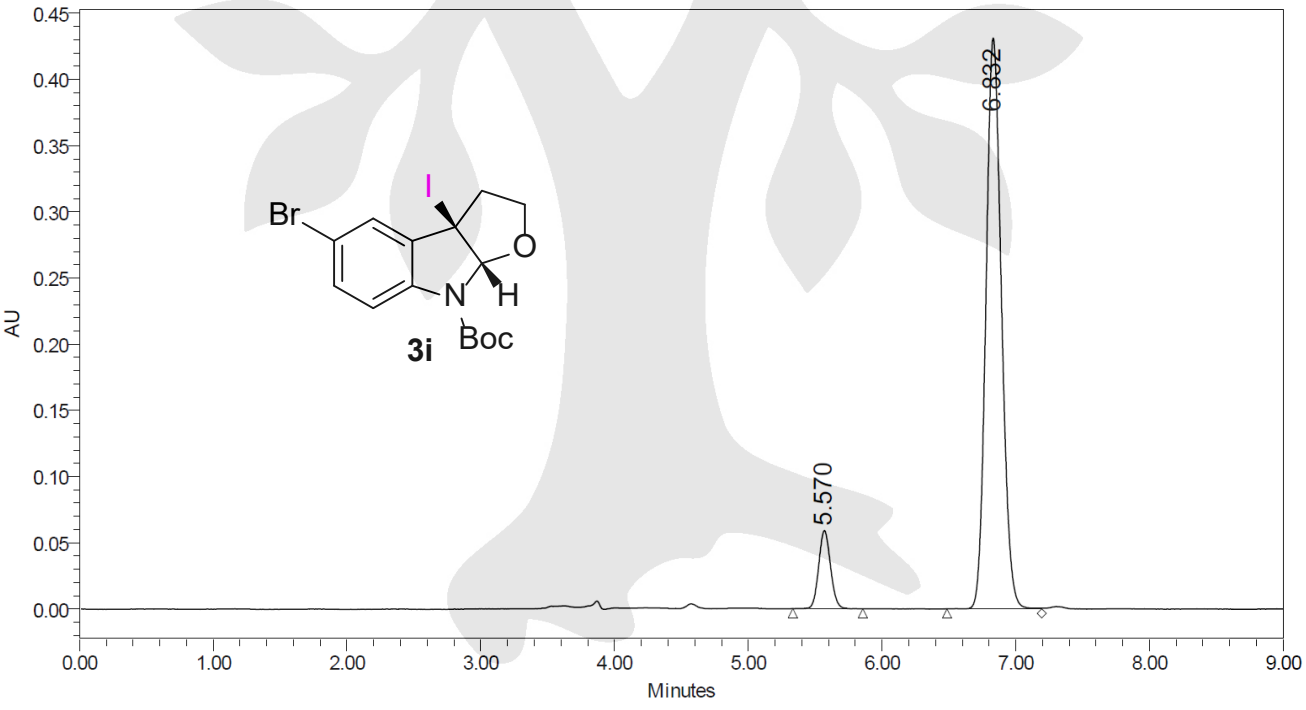

	RT (min)	Peak Type	Area (μV*sec)	% Area	Height (μV)	% Height	Integration Type	Points Across Peak	Start Time (min)	End Time (min)
1	5.570	Unknown	361330	9.43	58976	12.03	bb	314	5.333	5.857
2	6.832	Unknown	3471246	90.57	431225	87.97	bV	425	6.487	7.195

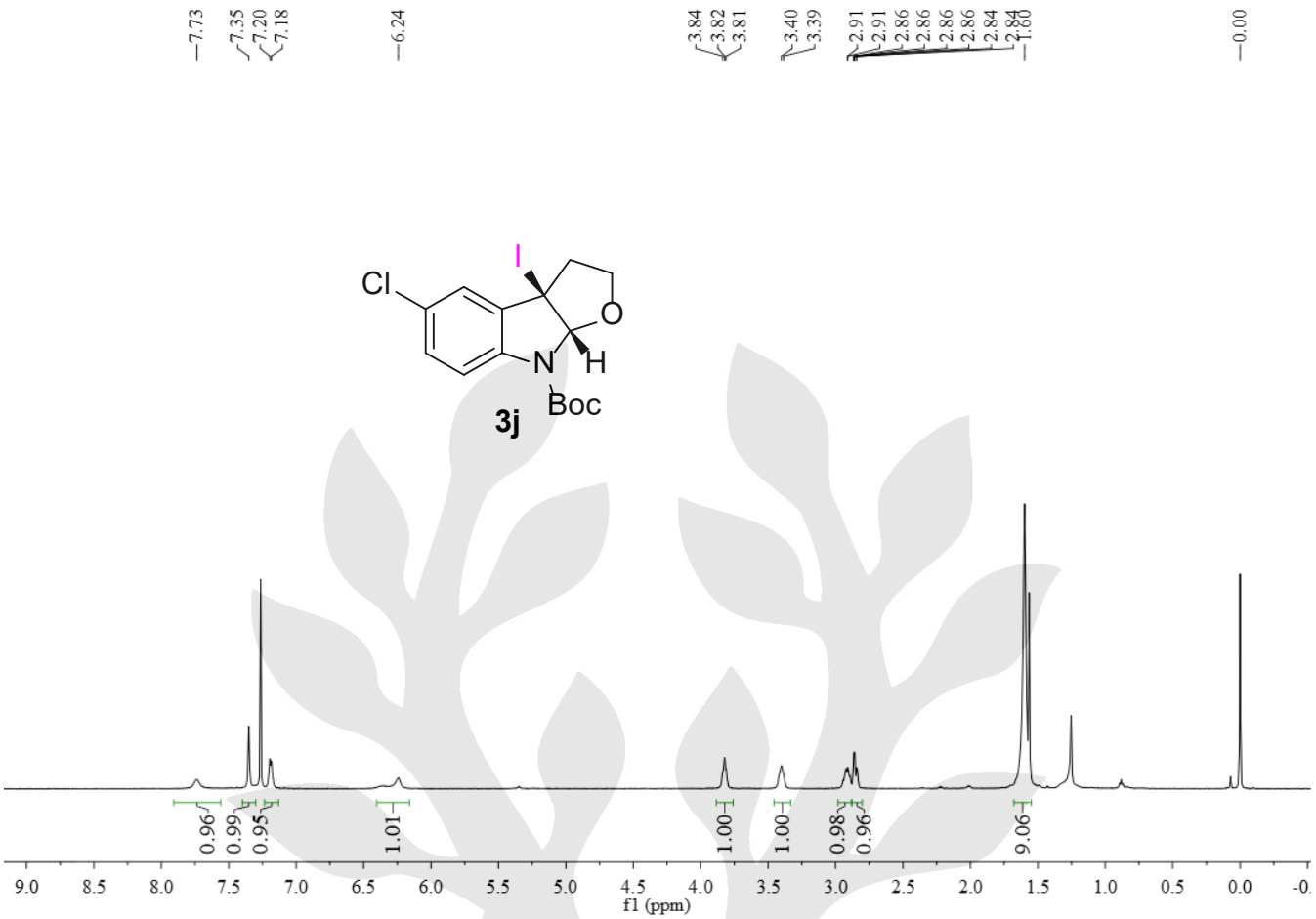

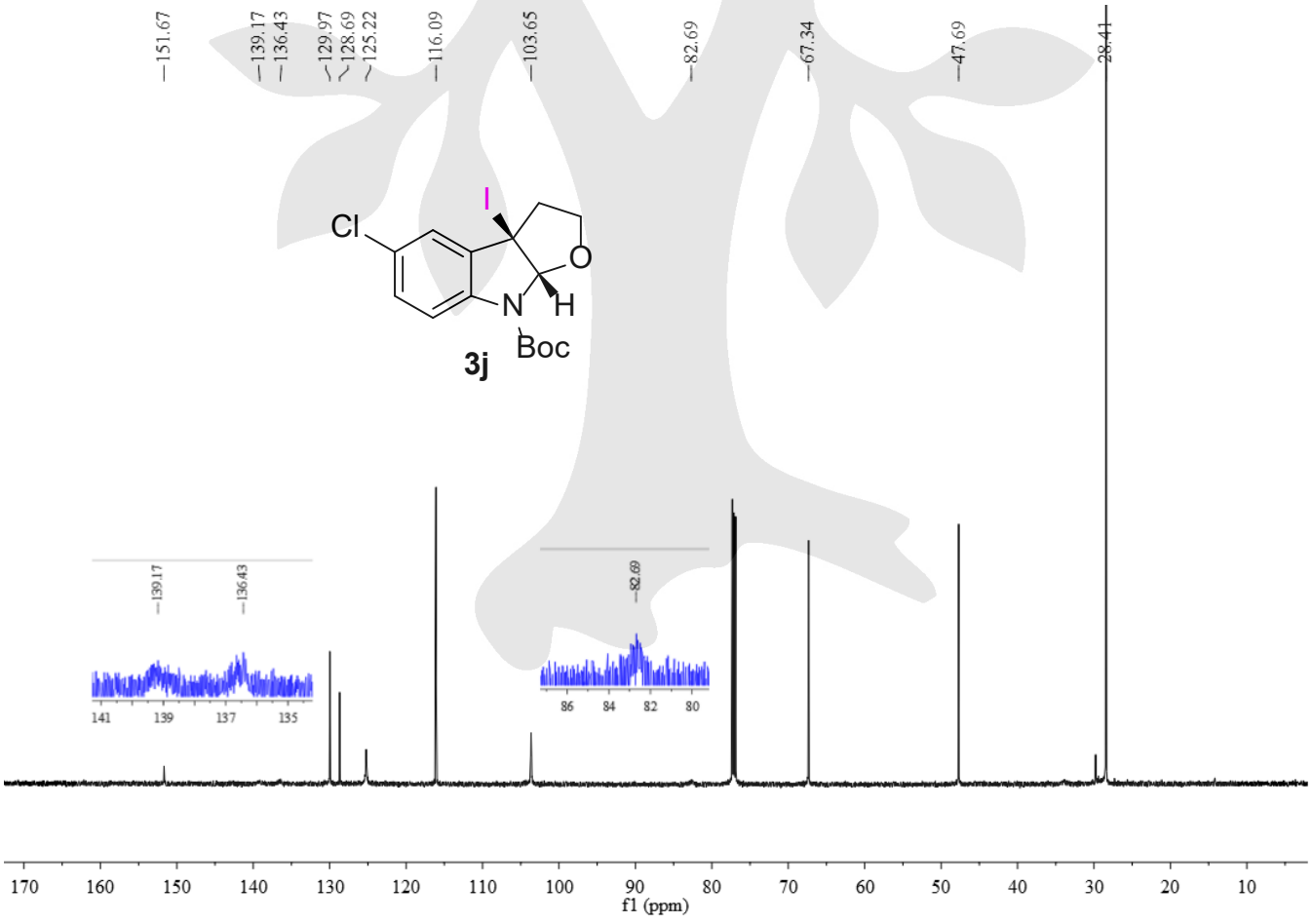

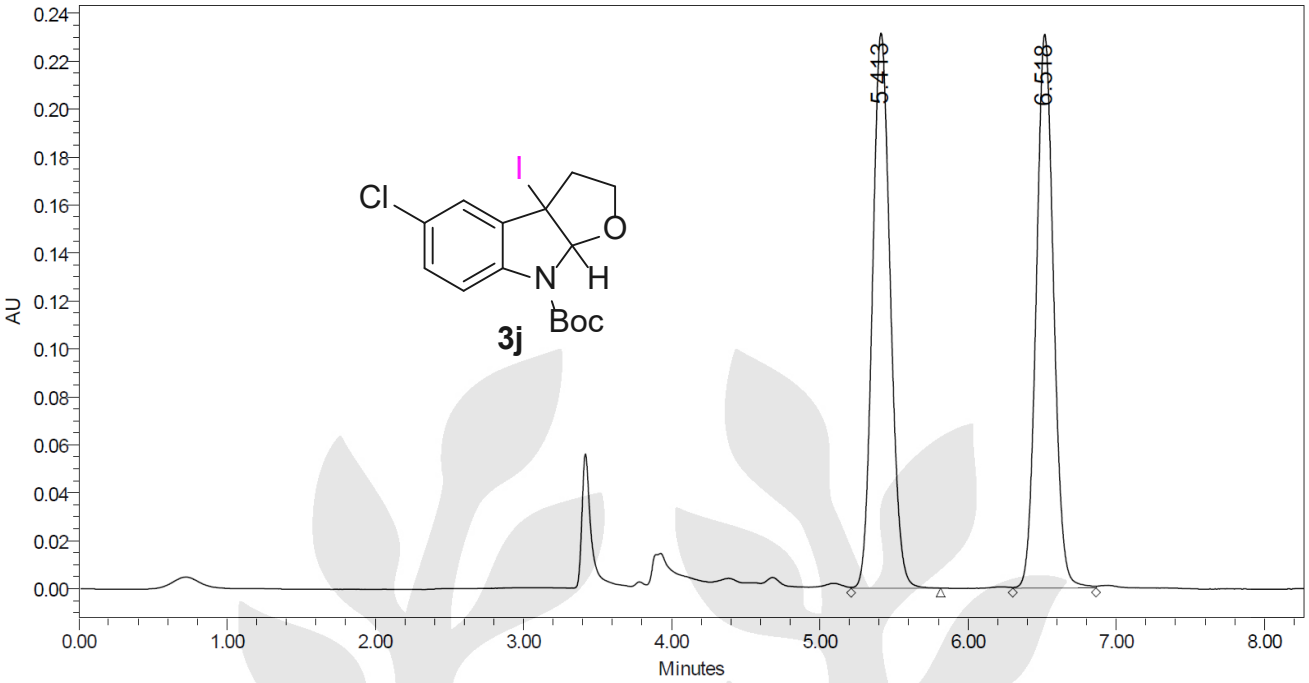

	RT (min)	Area (μV*sec)	% Area	Height (μV)	% Height
1	5.413	1931858	50.74	231488	50.06
2	6.518	1875335	49.26	230907	49.94

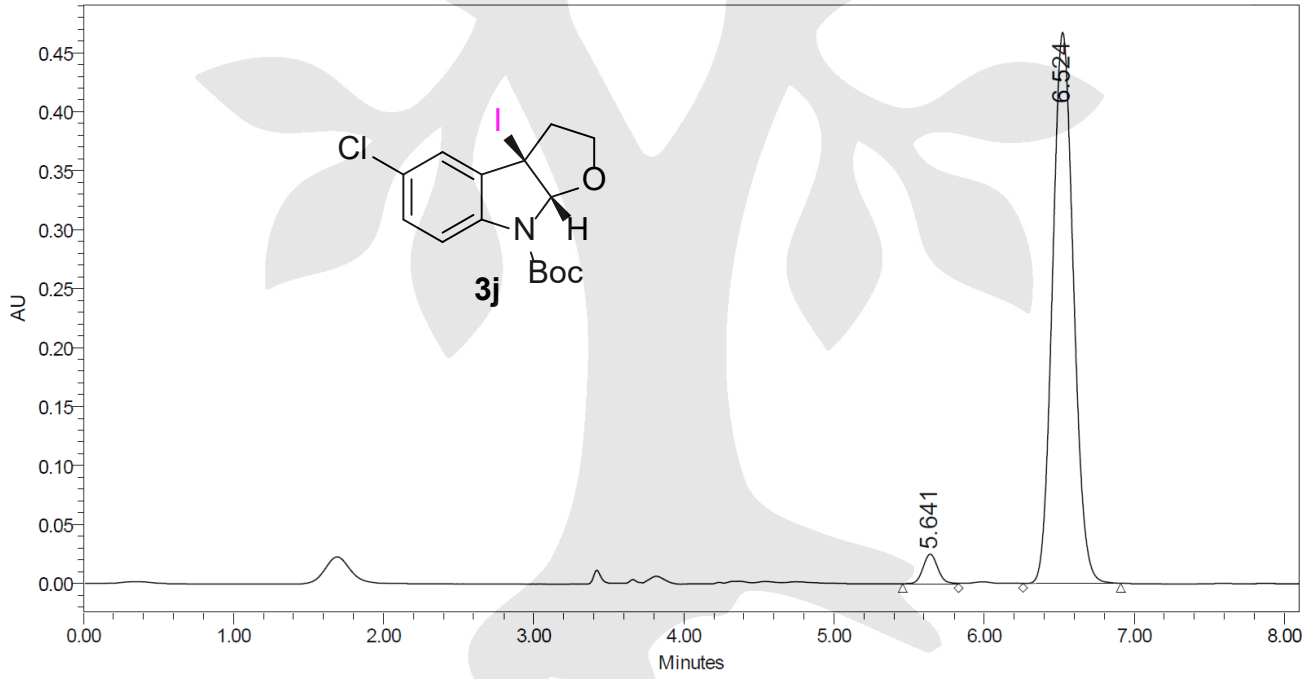

	RT (min)	Area (μV*sec)	% Area	Height (μV)	% Height
1	5.641	168393	3.58	24942	5.07
2	6.524	4540878	96.42	467188	94.93

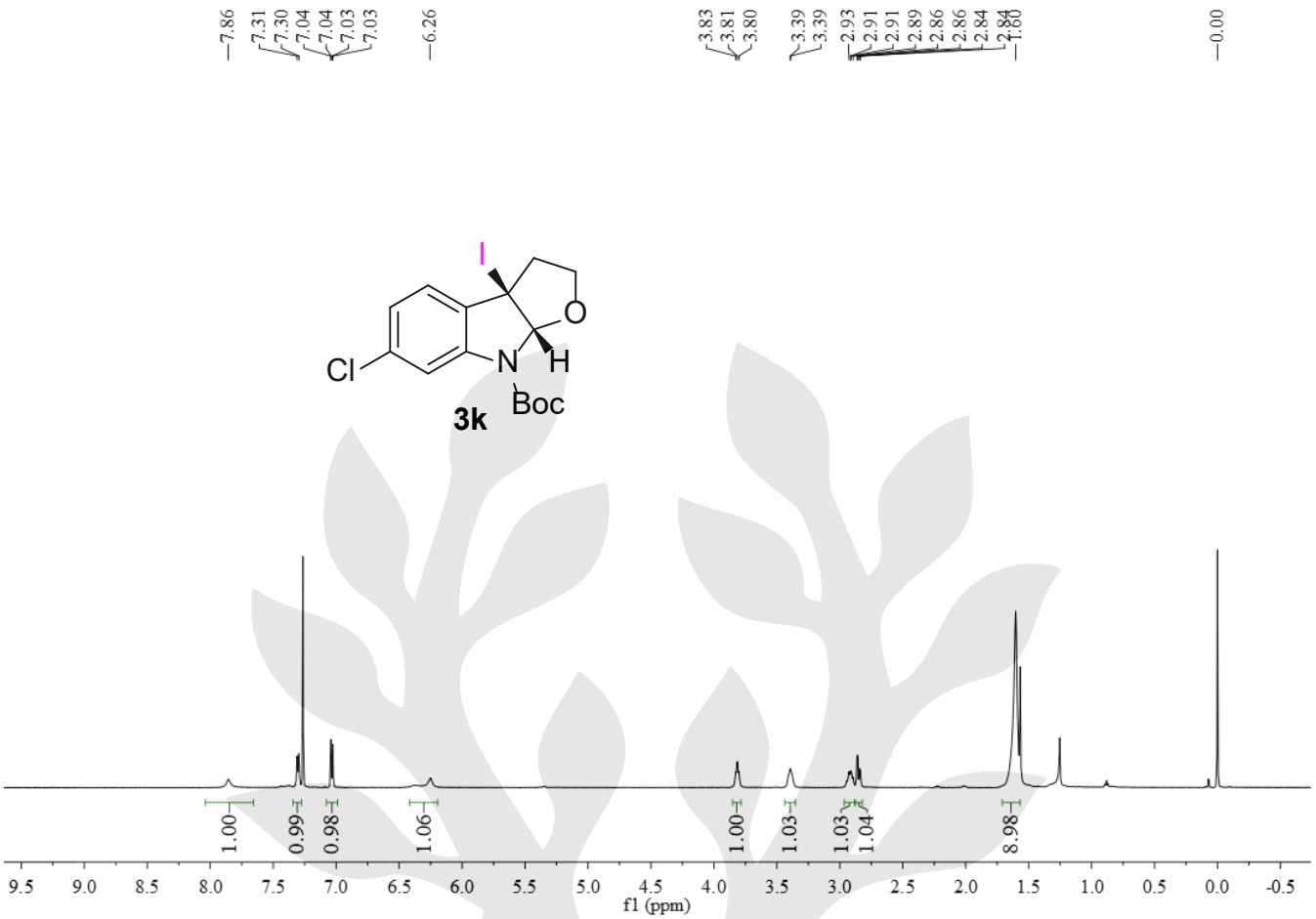

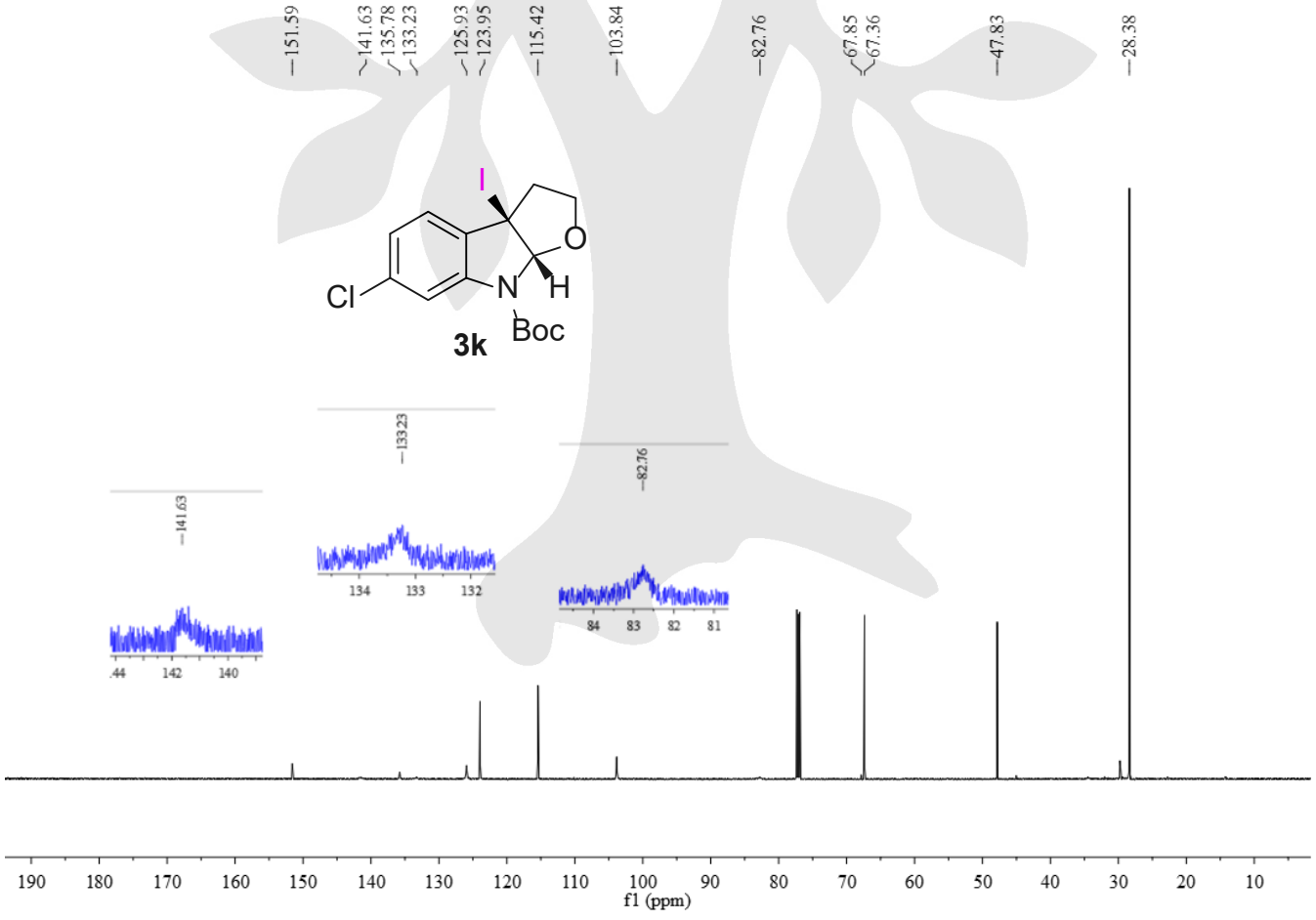

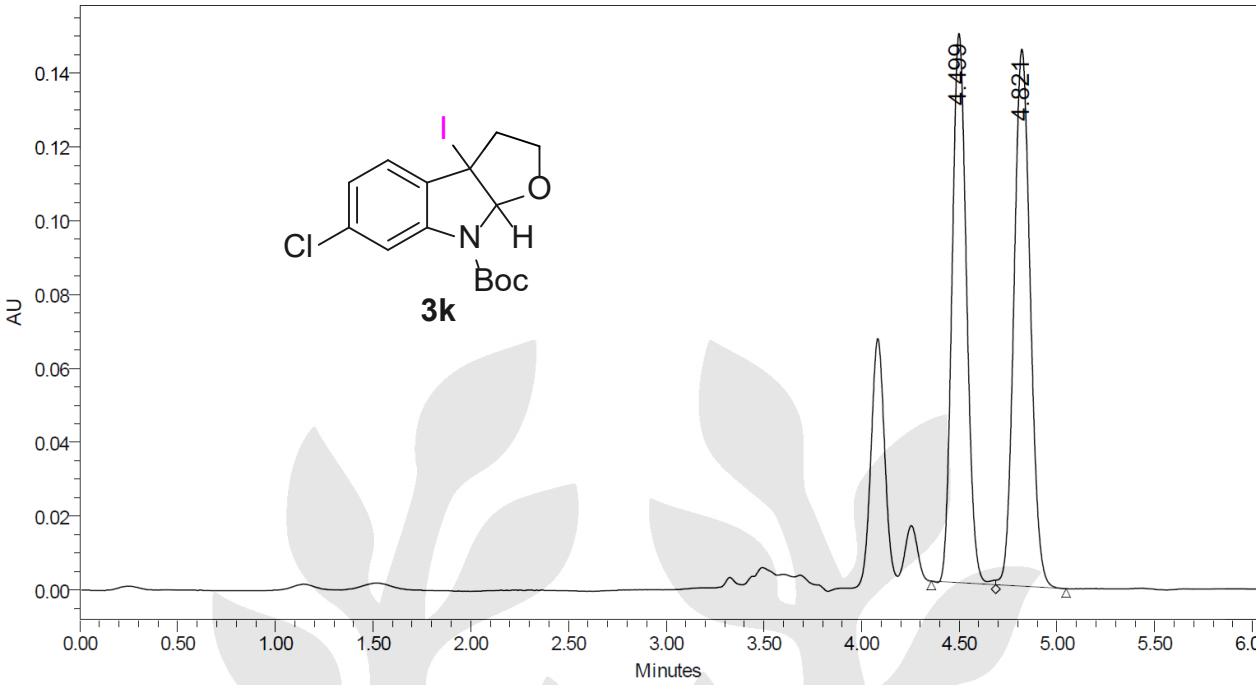

	RT (min)	Peak Type	Area (μV*sec)	% Area	Height (μV)	% Height	Integration Type	Points Across Peak	Start Time (min)	End Time (min)
1	4.499	Unknown	766591	47.60	148797	50.56	bv	198	4.357	4.687
2	4.821	Unknown	844030	52.40	145482	49.44	vB	216	4.687	5.047

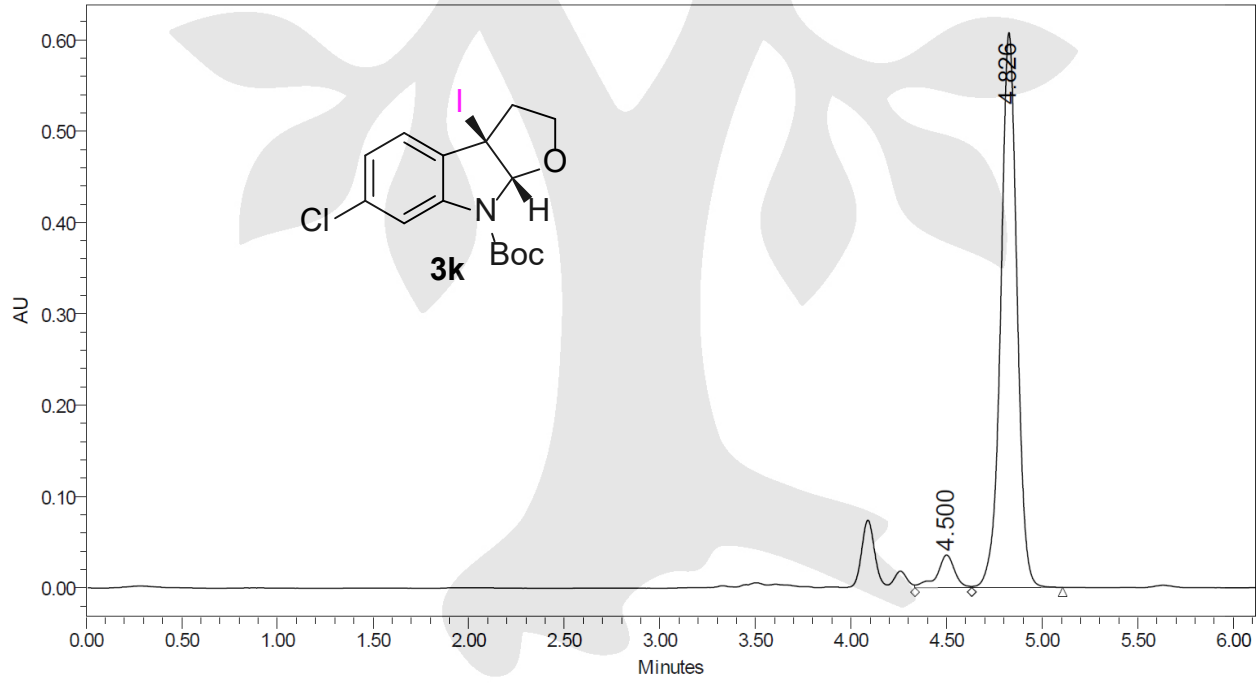

	RT (min)	Peak Type	Area (μV*sec)	% Area	Height (μV)	% Height	Integration Type	Points Across Peak	Start Time (min)	End Time (min)
1	4.500	Unknown	228731	6.00	35636	5.54	VV	178	4.335	4.632
2	4.826	Unknown	3585836	94.00	607798	94.46	VB	285	4.632	5.107

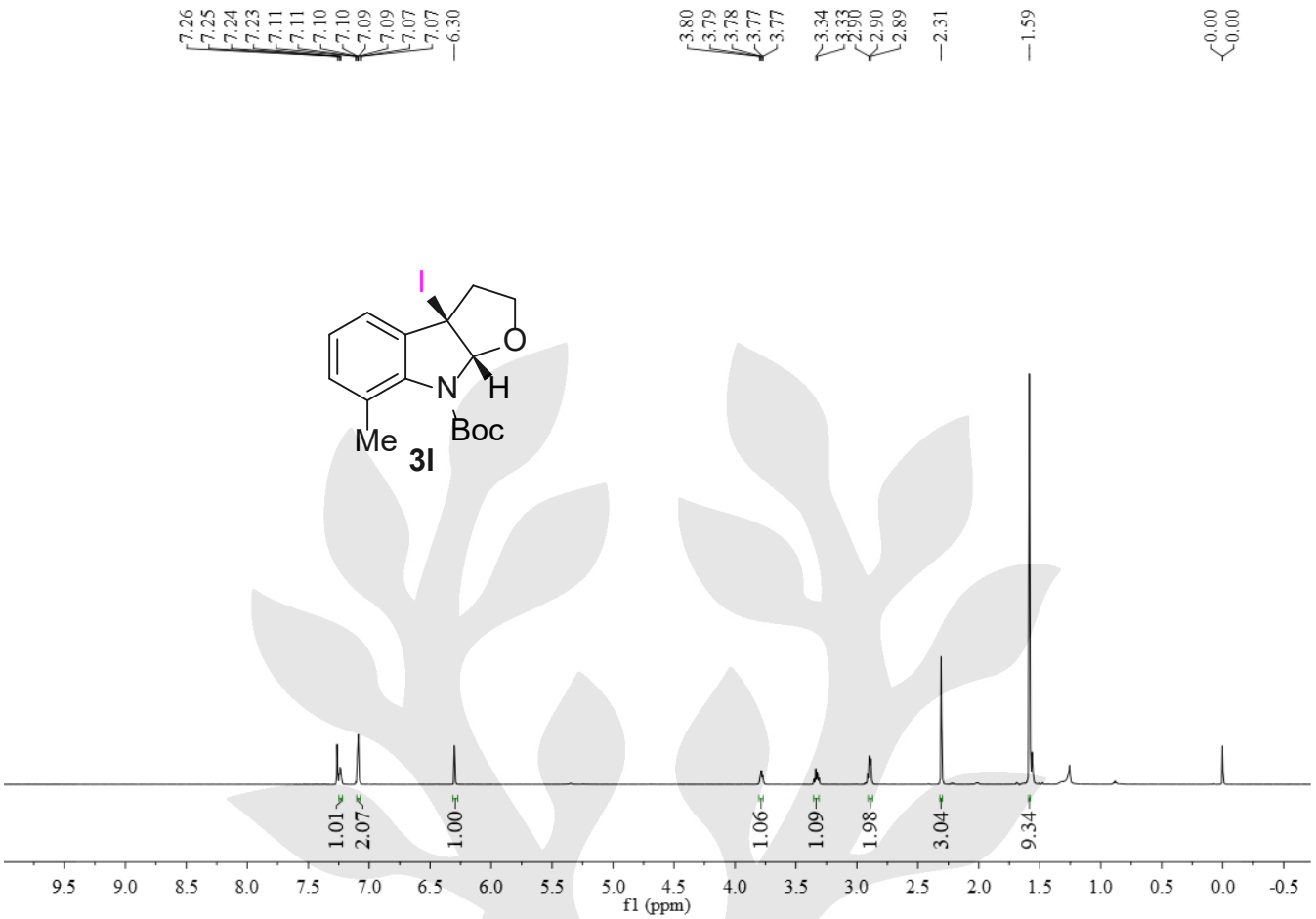

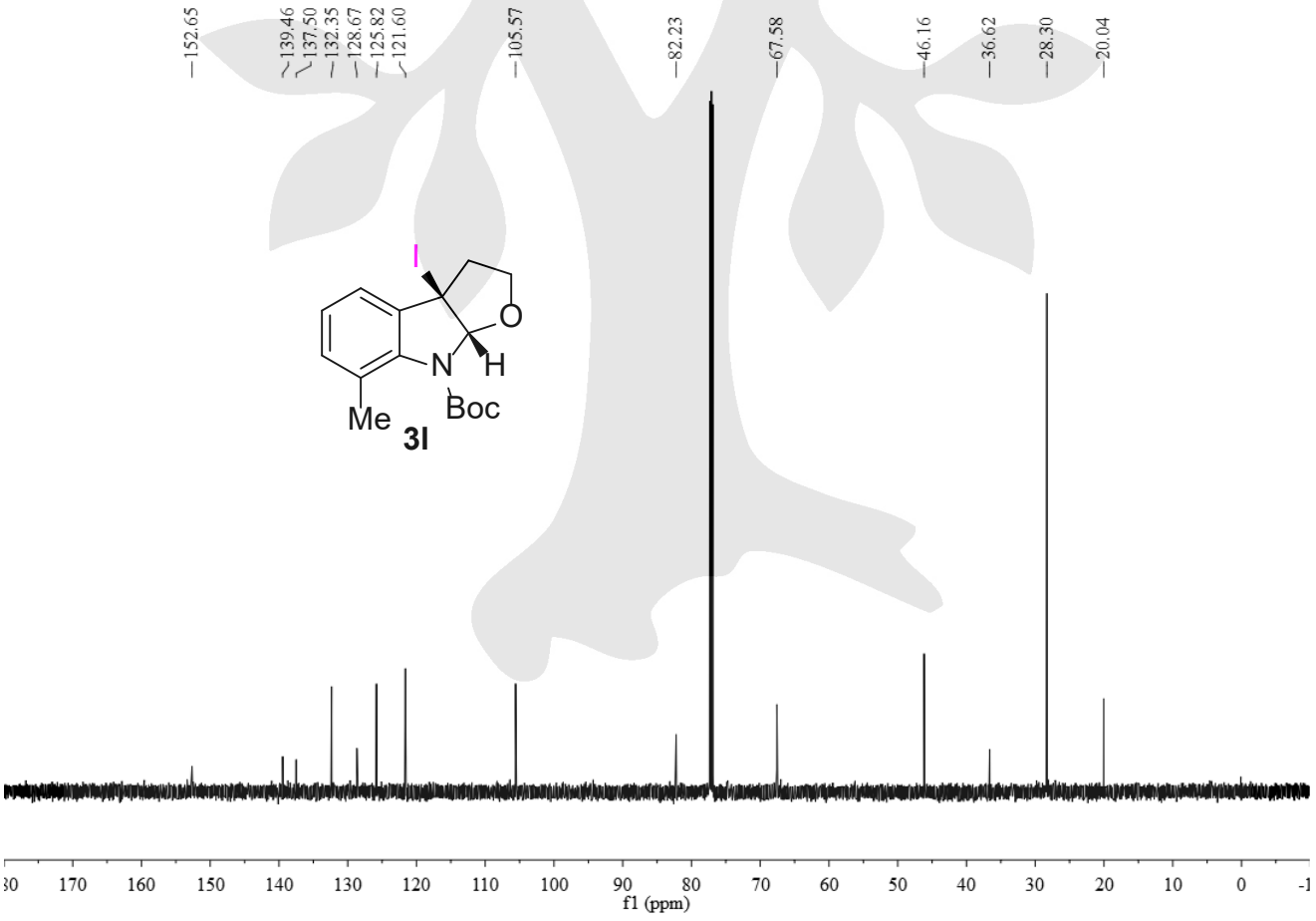

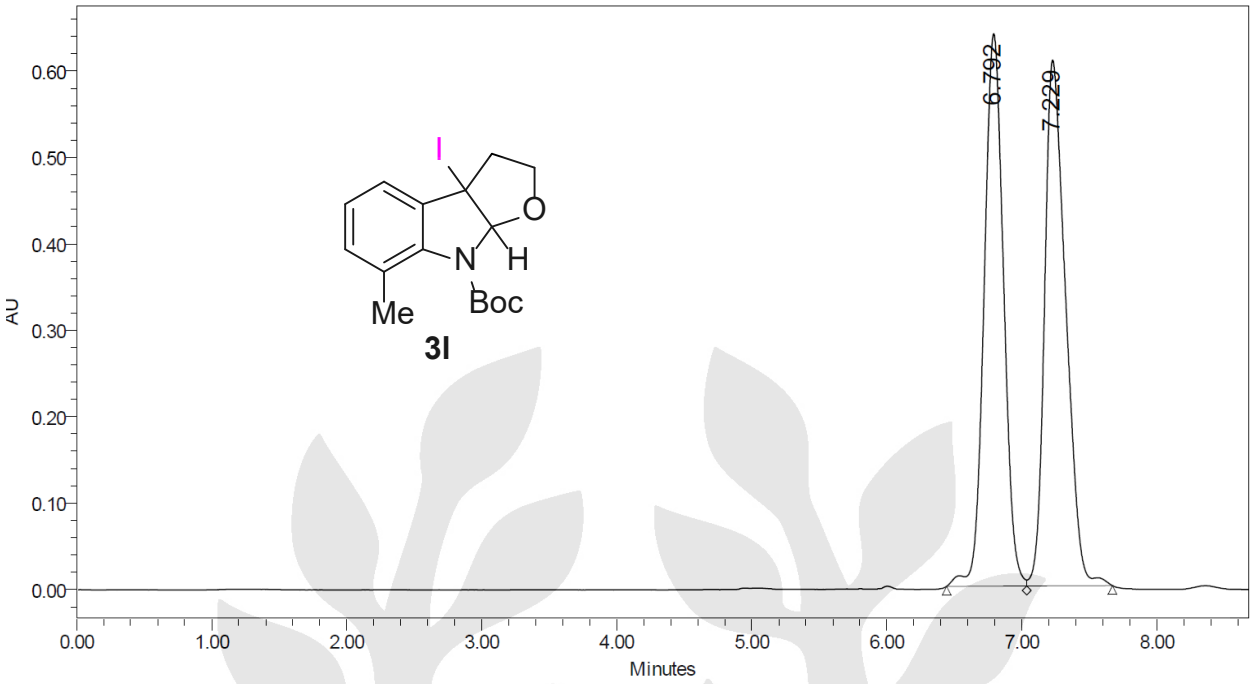

	RT (min)	Peak Type	Area (μV*sec)	% Area	Height (μV)	% Height	Integration Type	Points Across Peak	Start Time (min)	End Time (min)
1	6.792	Unknown	6410187	49.20	639122	51.24	bV	356	6.443	7.037
2	7.229	Unknown	6619148	50.80	608267	48.76	Vb	381	7.037	7.672

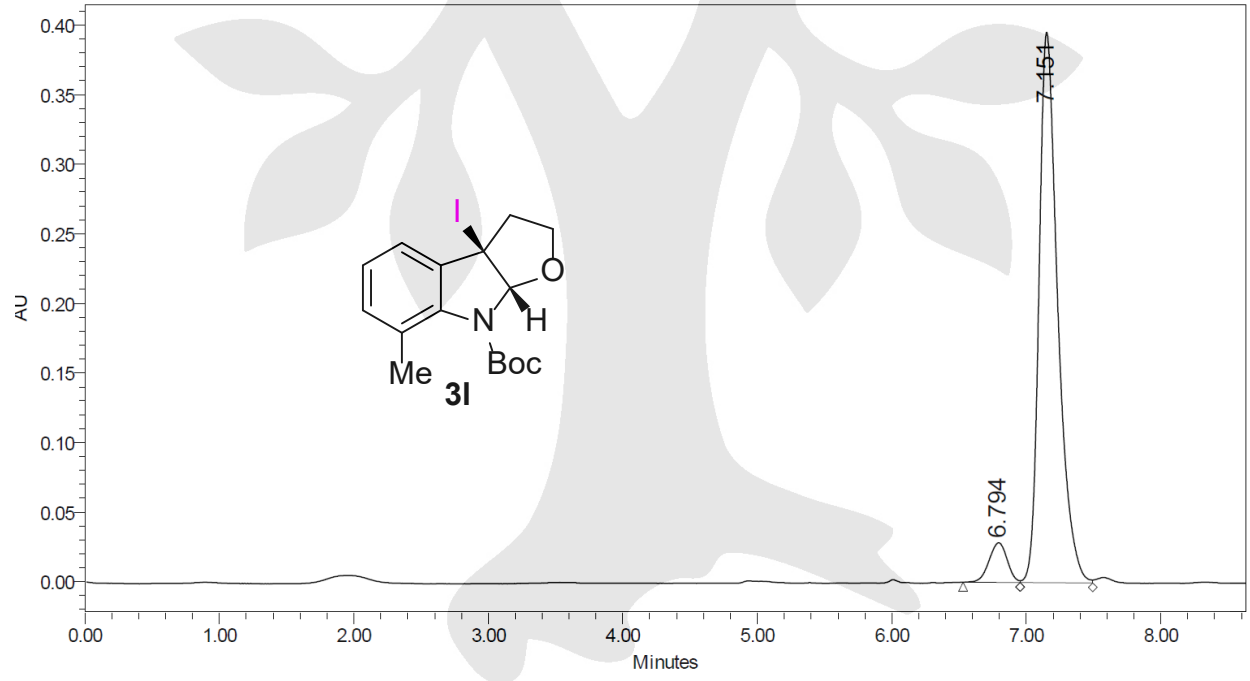

	RT (min)	Peak Type	Area (μV*sec)	% Area	Height (μV)	% Height	Integration Type	Points Across Peak	Start Time (min)	End Time (min)
1	6.794	Unknown	266482	6.49	28460	6.71	bV	254	6.530	6.953
2	7.151	Unknown	3836815	93.51	395508	93.29	VV	324	6.953	7.493

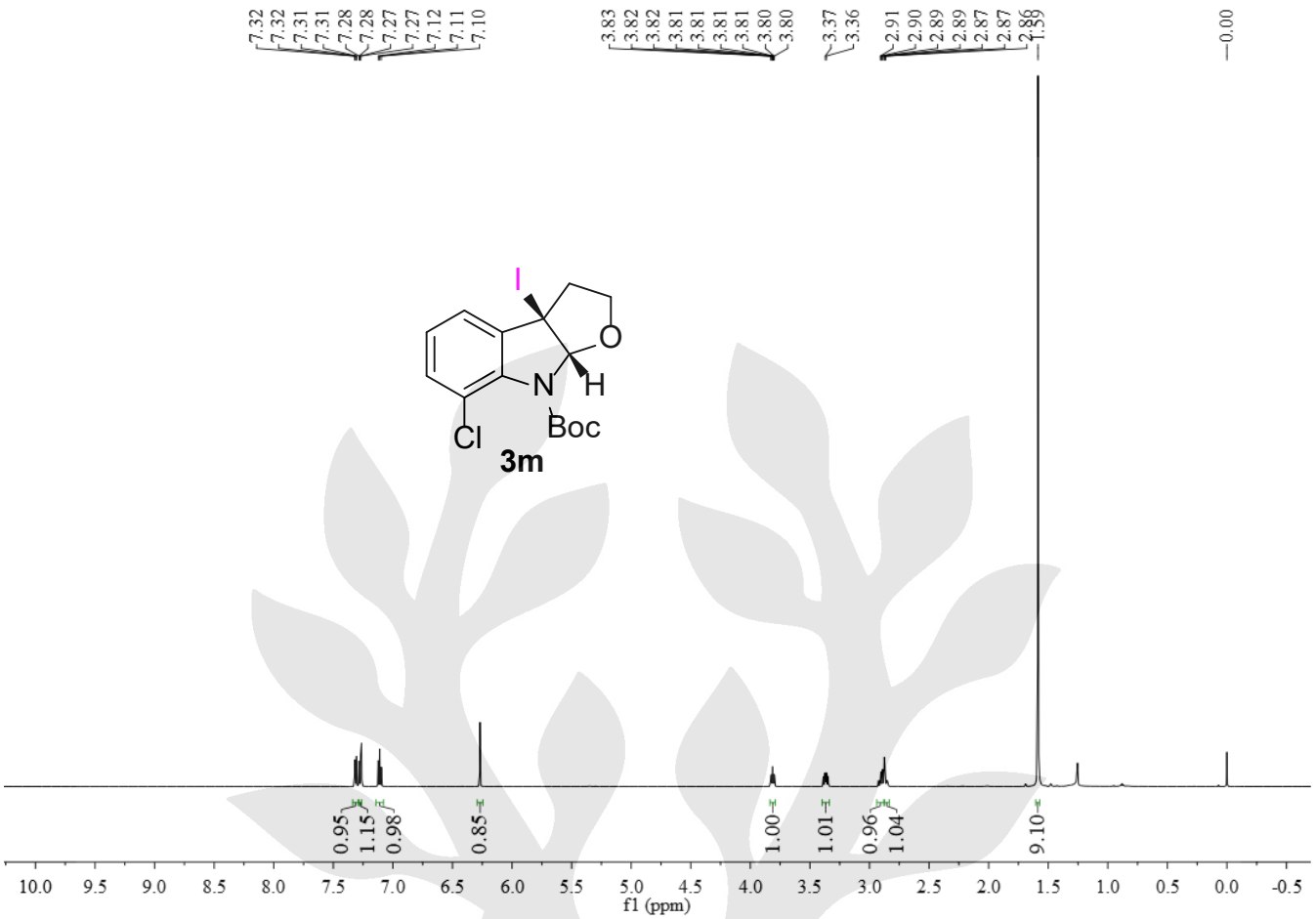

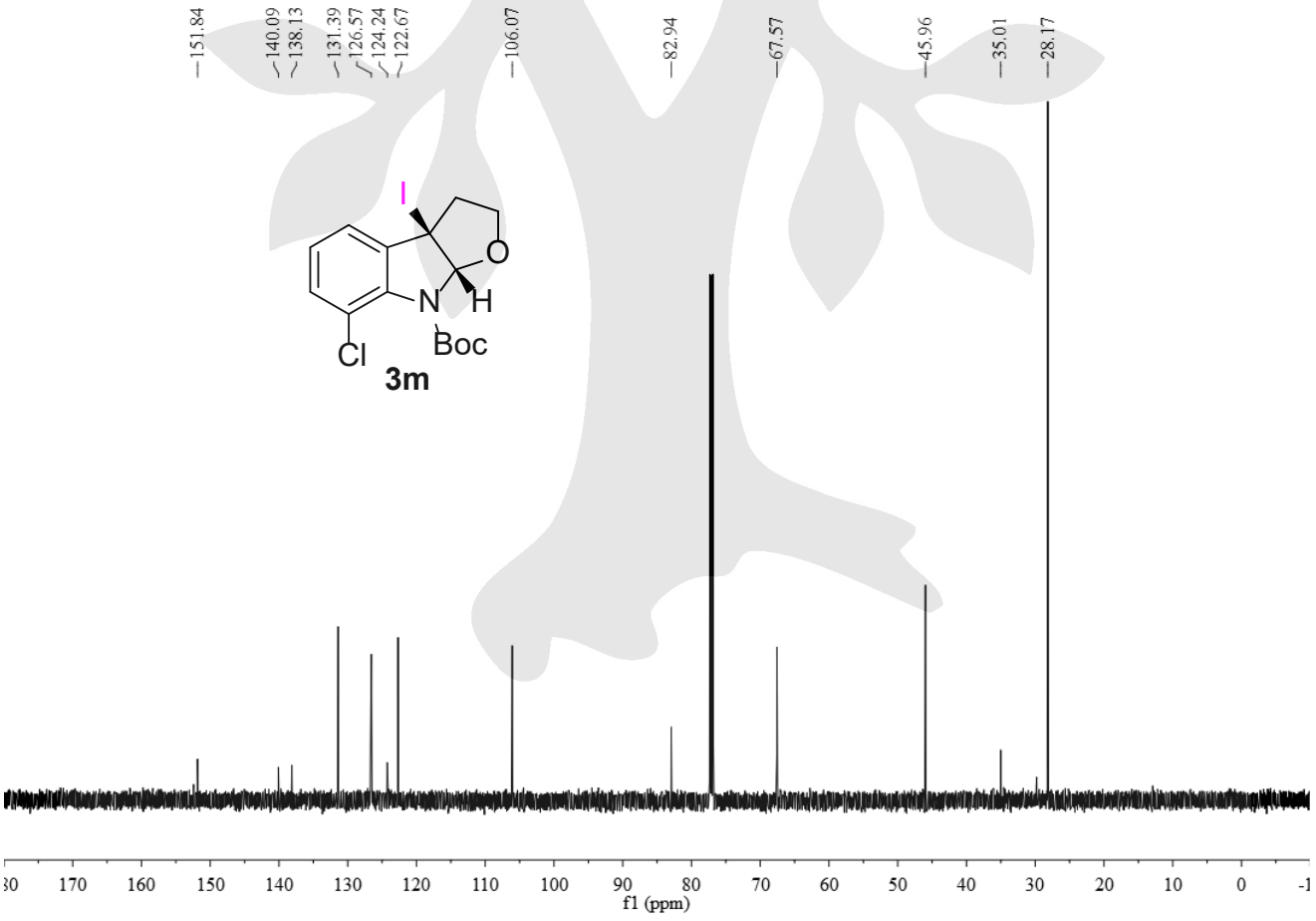

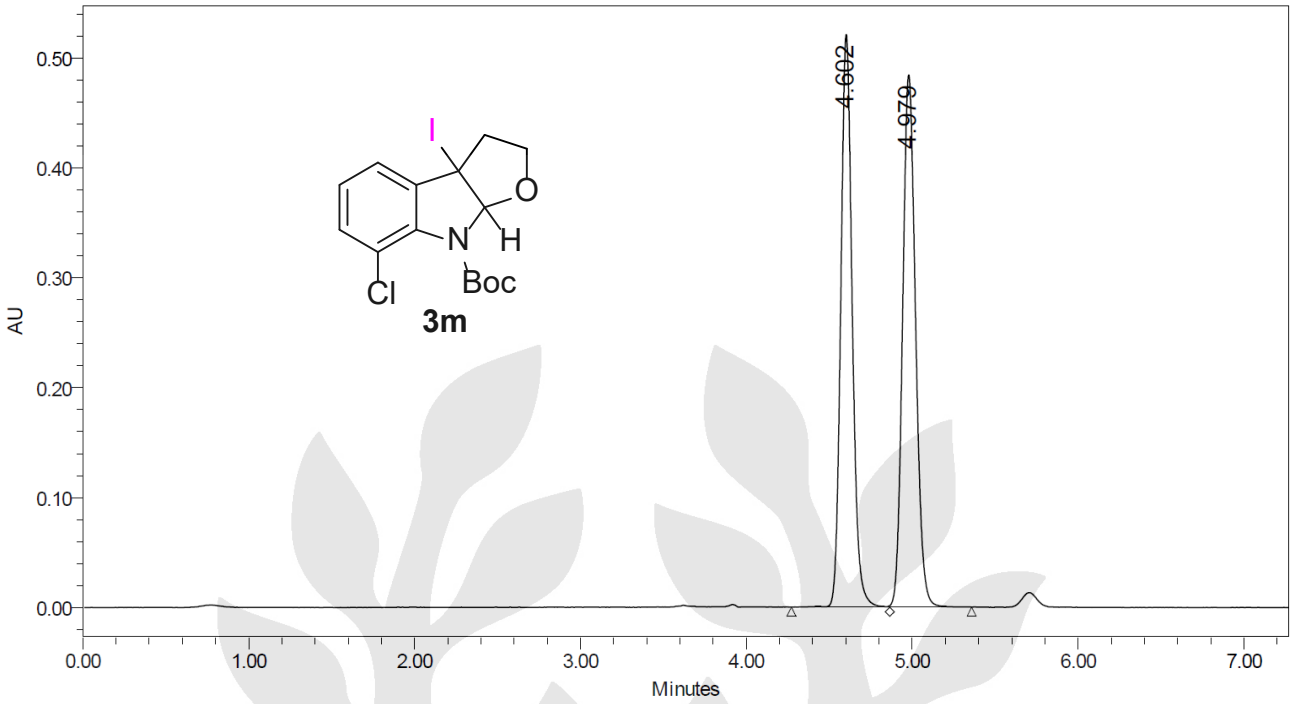

	RT (min)	Peak Type	Area (μV*sec)	% Area	Height (μV)	% Height	Integration Type	Points Across Peak	Start Time (min)	End Time (min)
1	4.602	Unknown	2507444	48.87	521220	51.84	Bv	356	4.272	4.865
2	4.979	Unknown	2623273	51.13	484237	48.16	vb	296	4.865	5.358

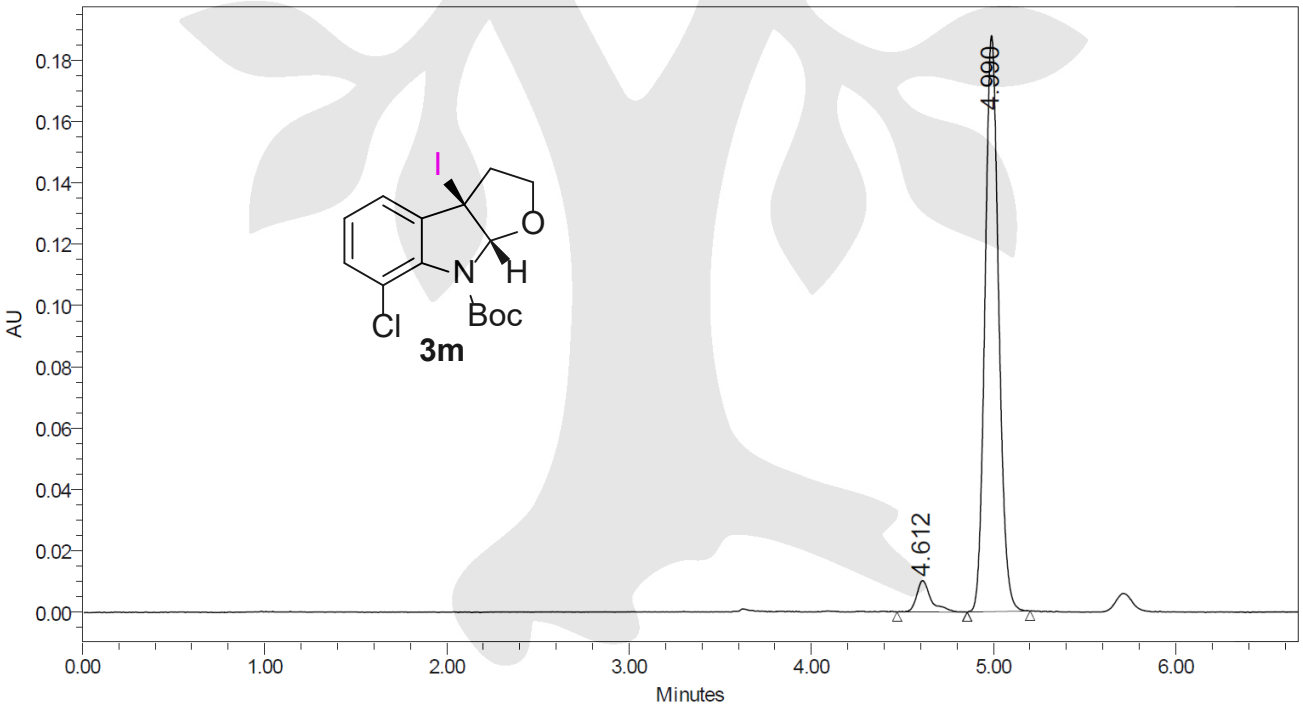

	RT (min)	Peak Type	Area (μV*sec)	% Area	Height (μV)	% Height	Integration Type	Points Across Peak	Start Time (min)	End Time (min)
1	4.612	Unknown	56139	5.40	10163	5.13	BB	230	4.472	4.855
2	4.990	Unknown	983247	94.60	187758	94.87	BB	207	4.857	5.202

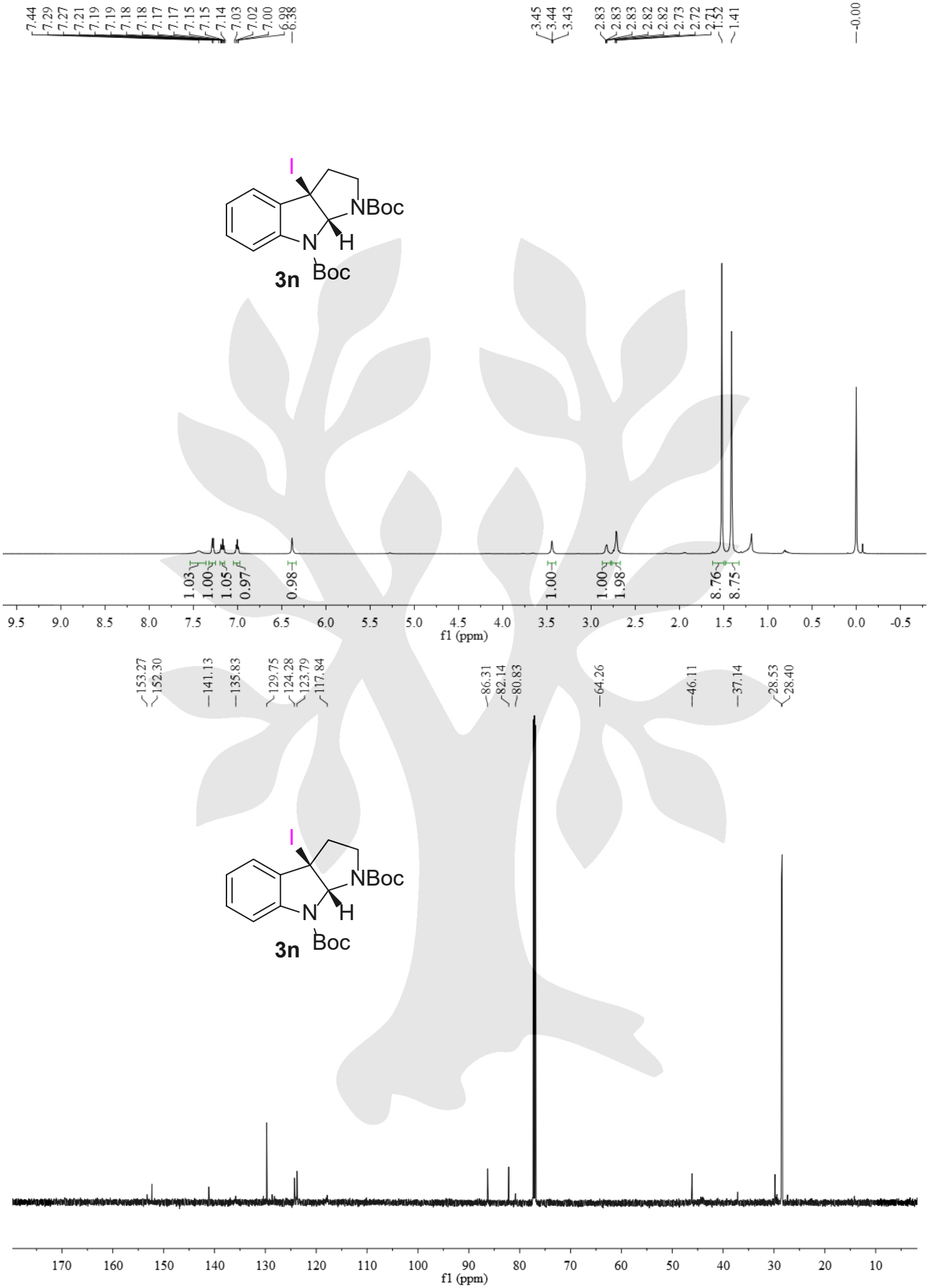

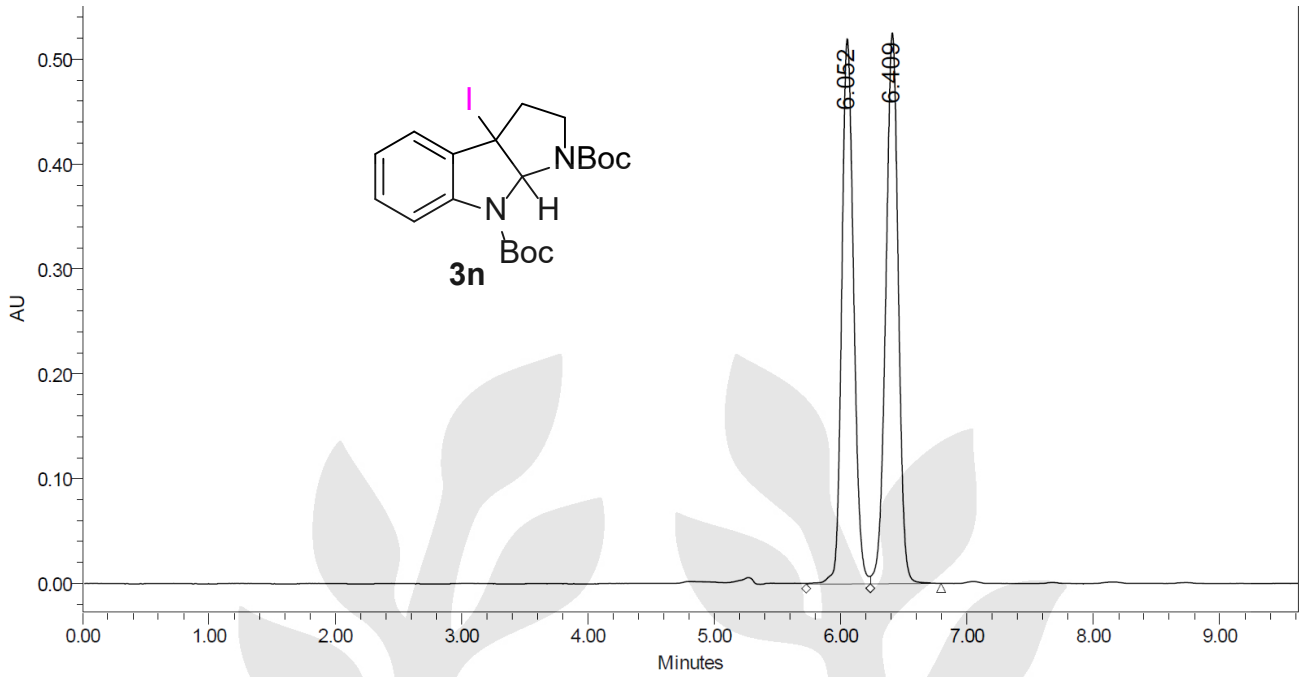

	RT (min)	Area (μV*sec)	% Area	Height (μV)	% Height
1	6.052	3406533	48.54	519888	49.74
2	6.409	3611119	51.46	525265	50.26

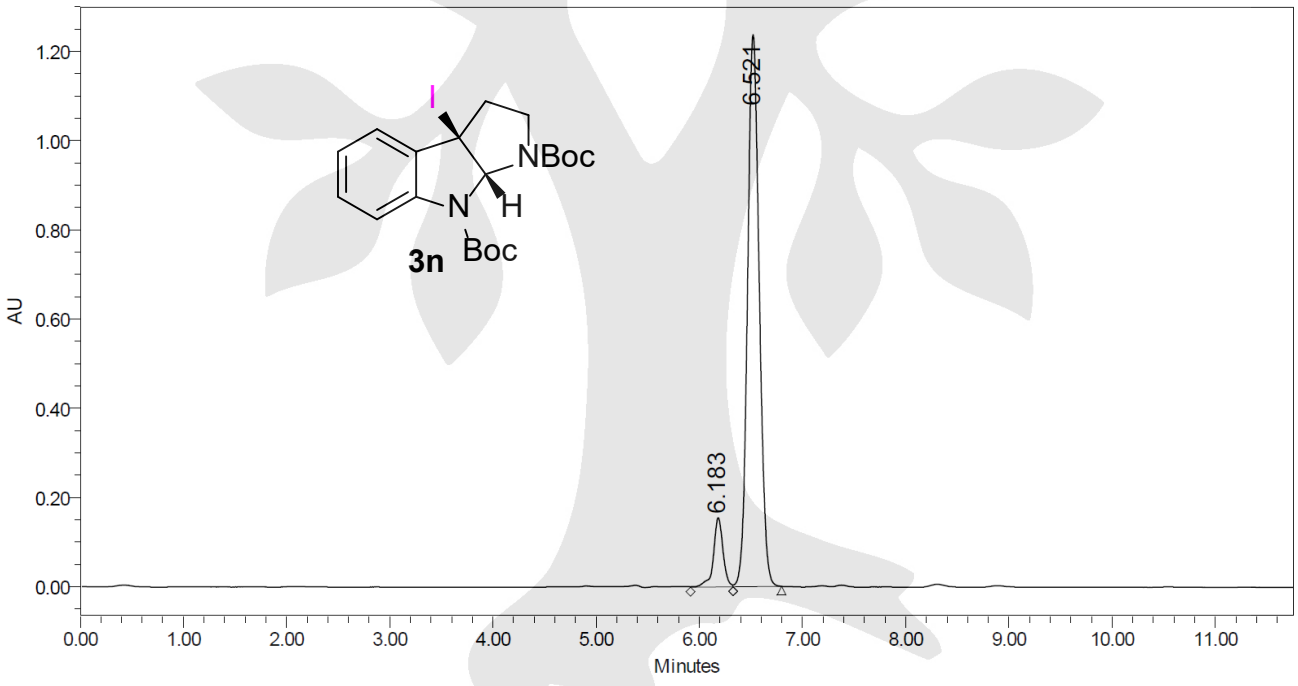

	RT (min)	Area (μV*sec)	% Area	Height (μV)	% Height
1	6.183	1002251	9.32	155121	11.14
2	6.521	9750644	90.68	1237444	88.86

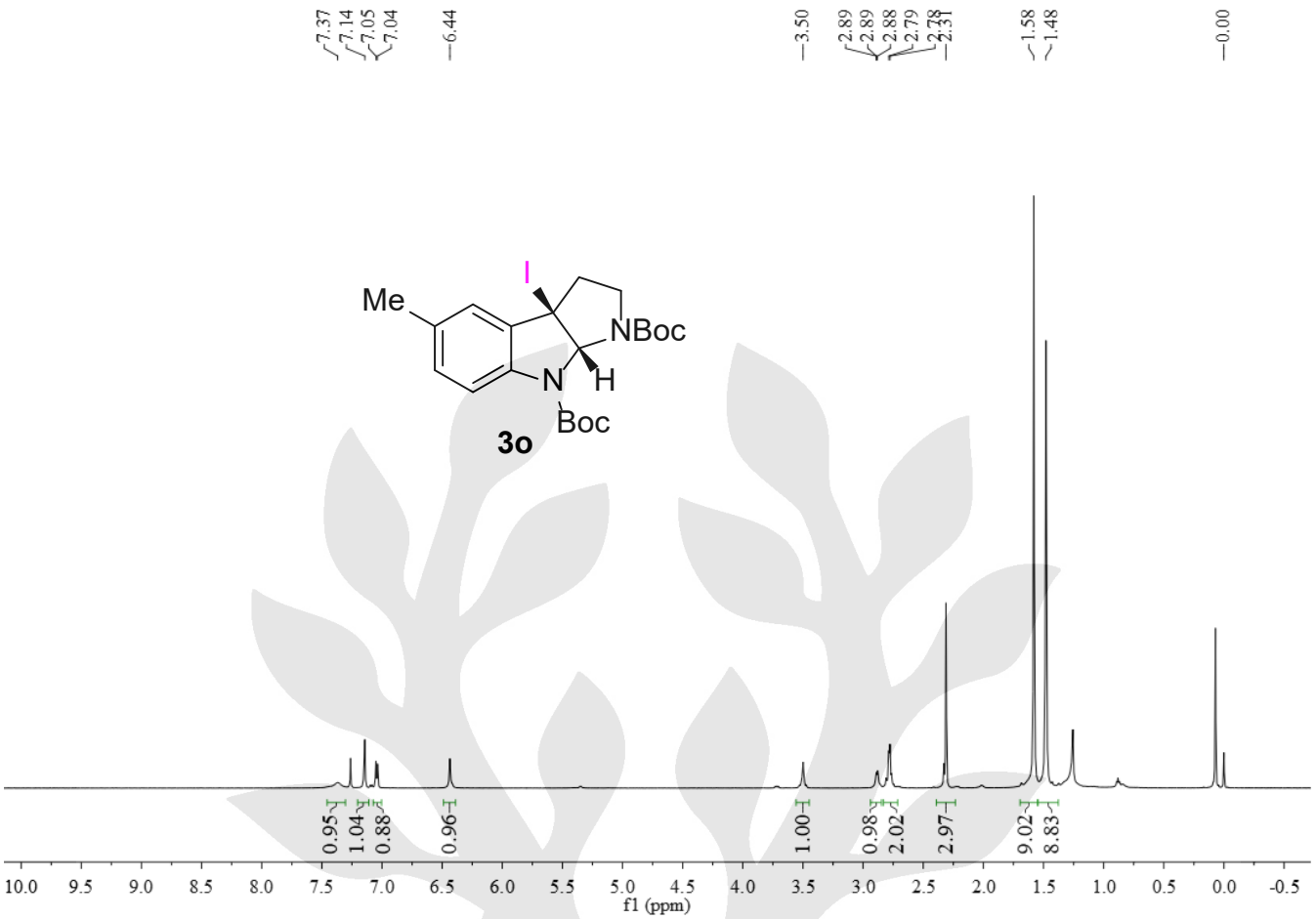

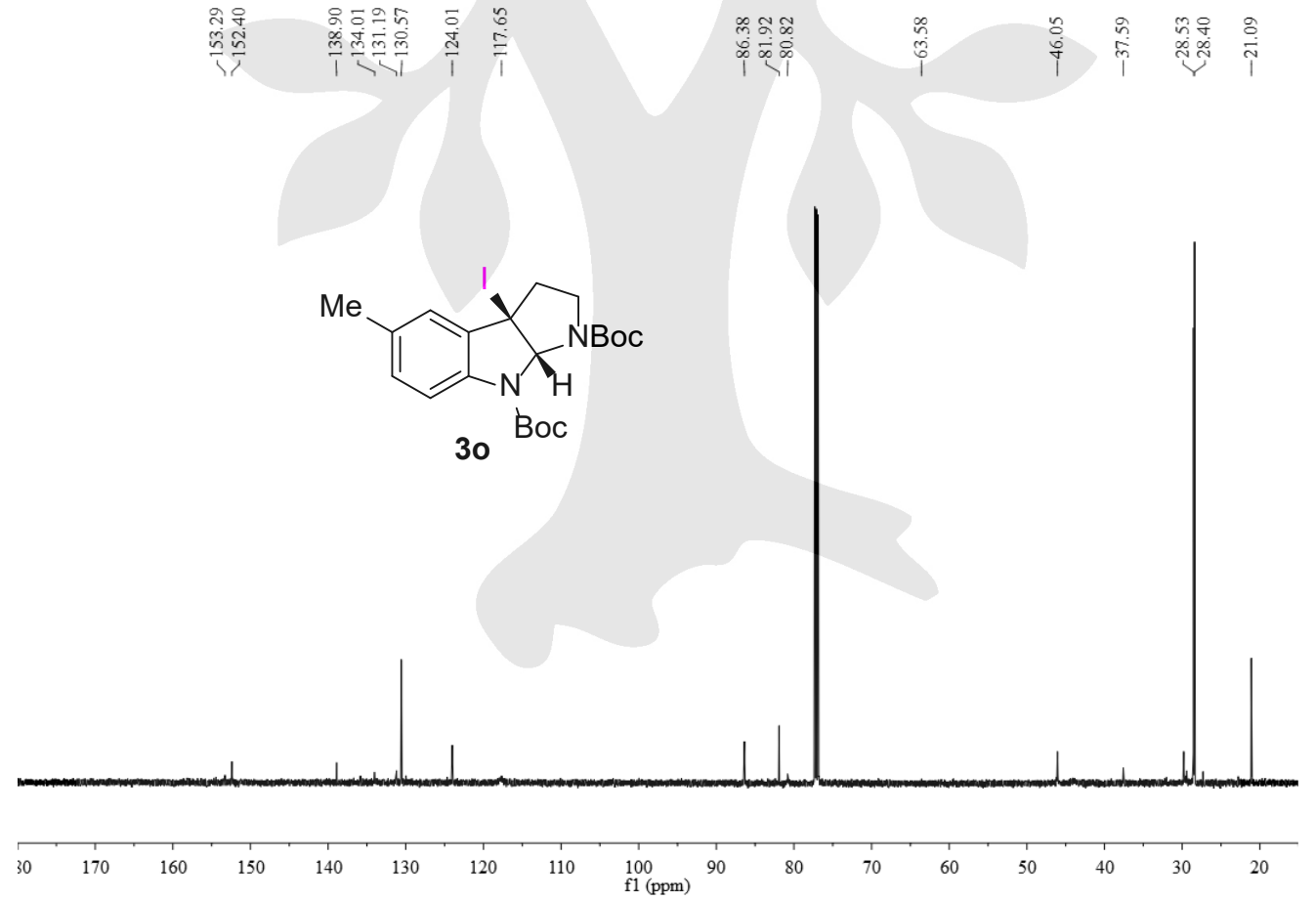

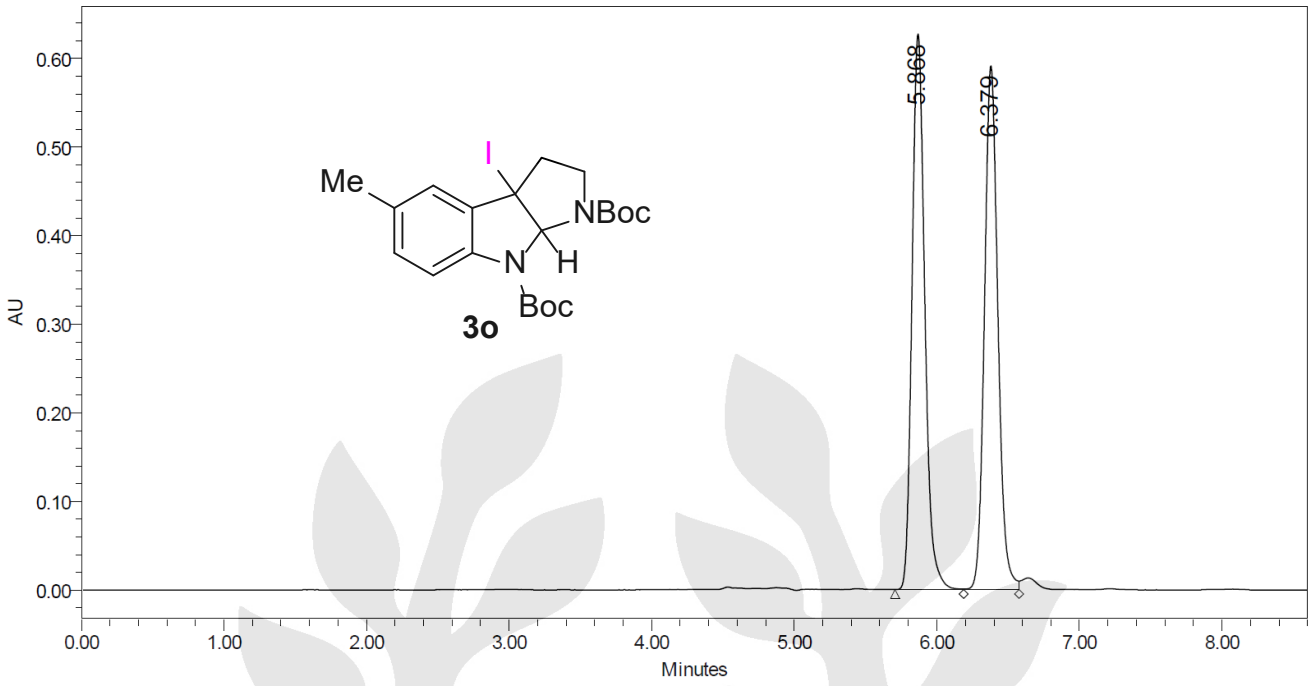

	RT (min)	Area (μV*sec)	% Area	Height (μV)	% Height
1	5.868	3897067	50.24	626996	51.47
2	6.379	3859584	49.76	591080	48.53

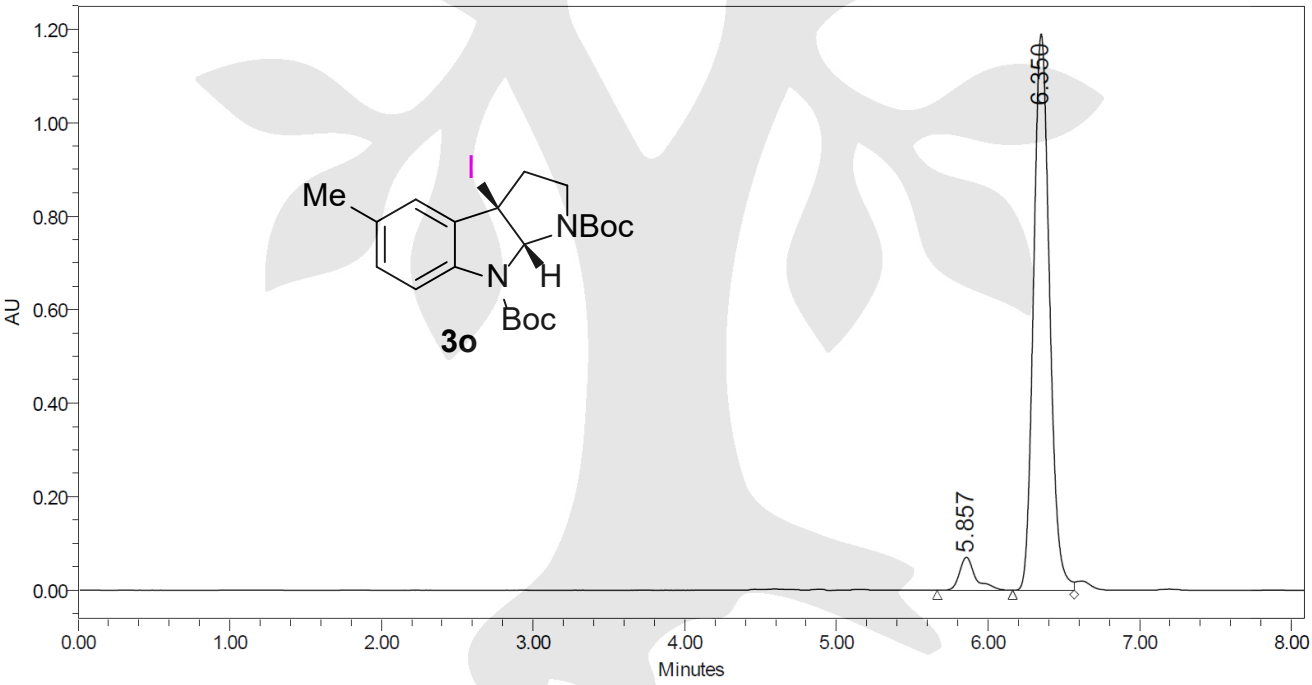

	RT (min)	Area (μV*sec)	% Area	Height (μV)	% Height
1	5.857	516273	5.58	70391	5.58
2	6.350	8737426	94.42	1190062	94.42

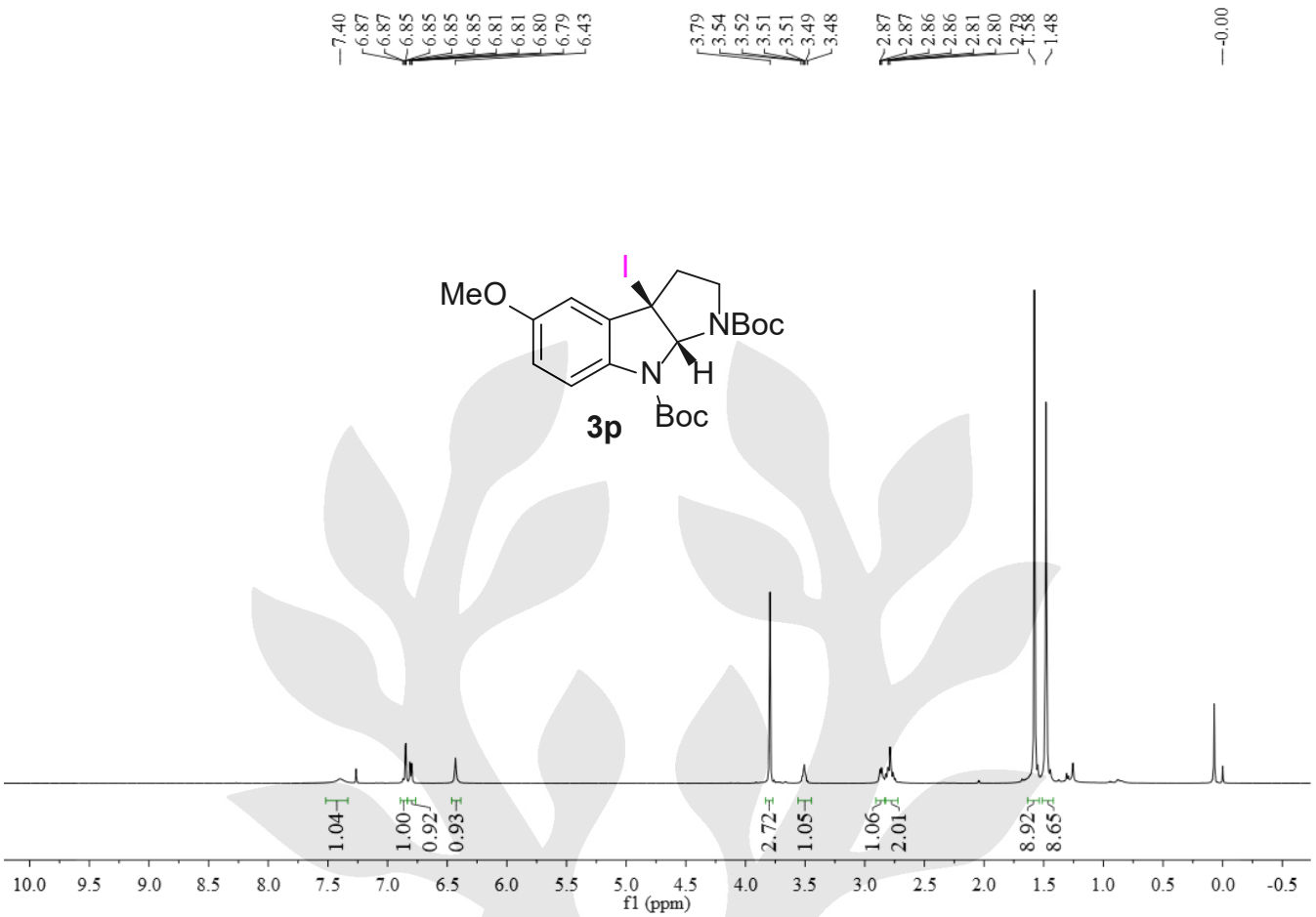

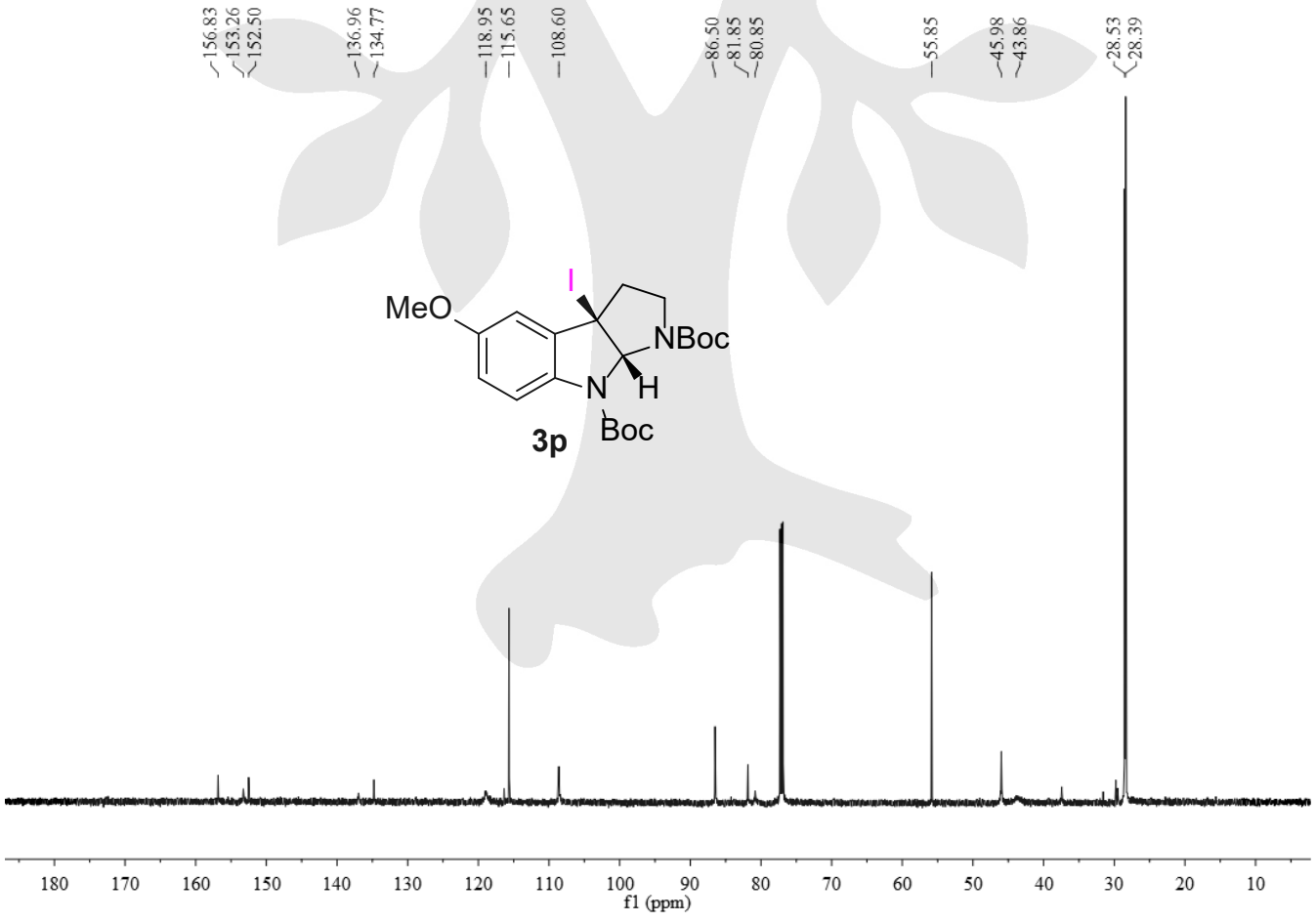

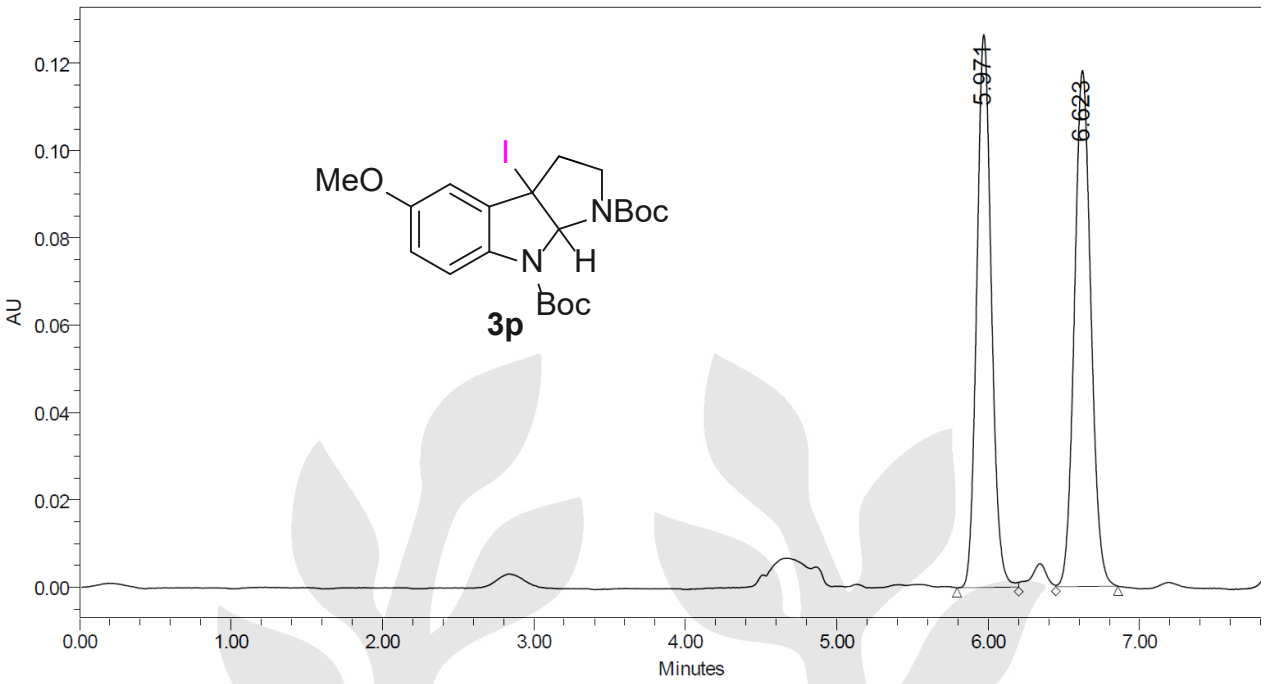

	RT (min)	Area (μV*sec)	% Area	Height (μV)	% Height
1	5.971	848927	48.70	126601	51.72
2	6.623	894390	51.30	118157	48.28

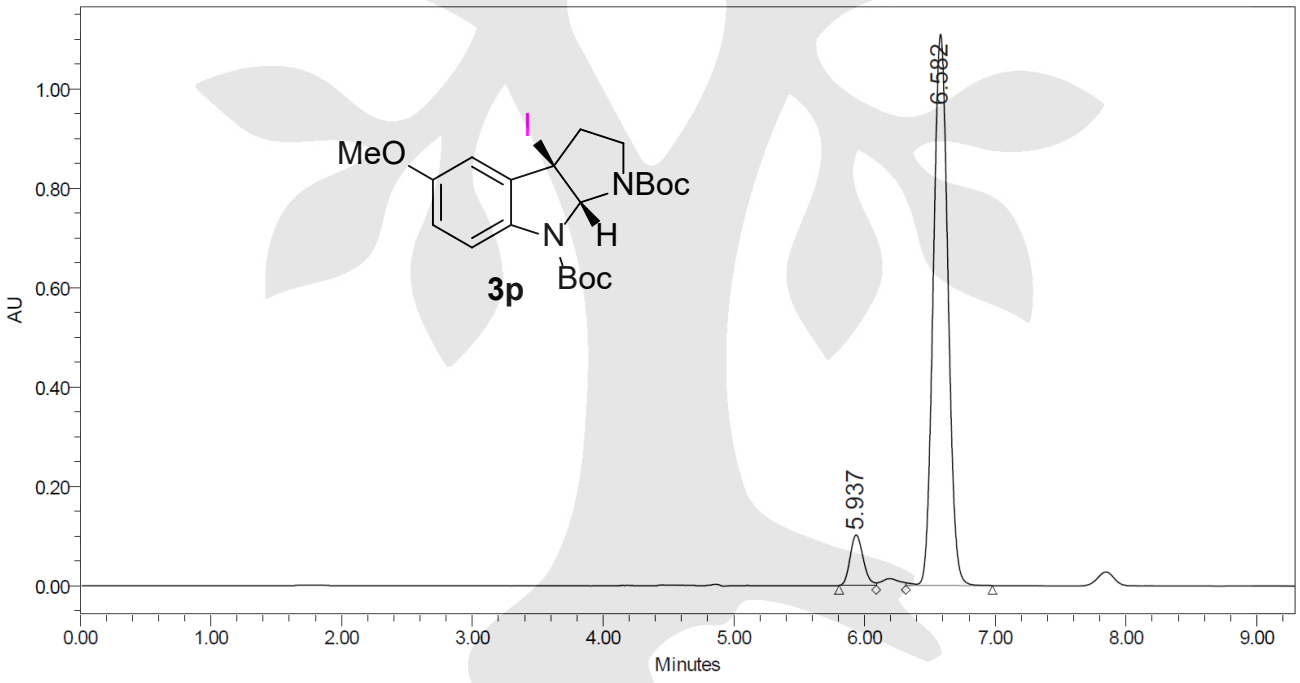

	RT (min)	Area (μV*sec)	% Area	Height (μV)	% Height
1	5.937	702518	7.49	101654	8.39
2	6.582	8680294	92.51	1109901	91.61

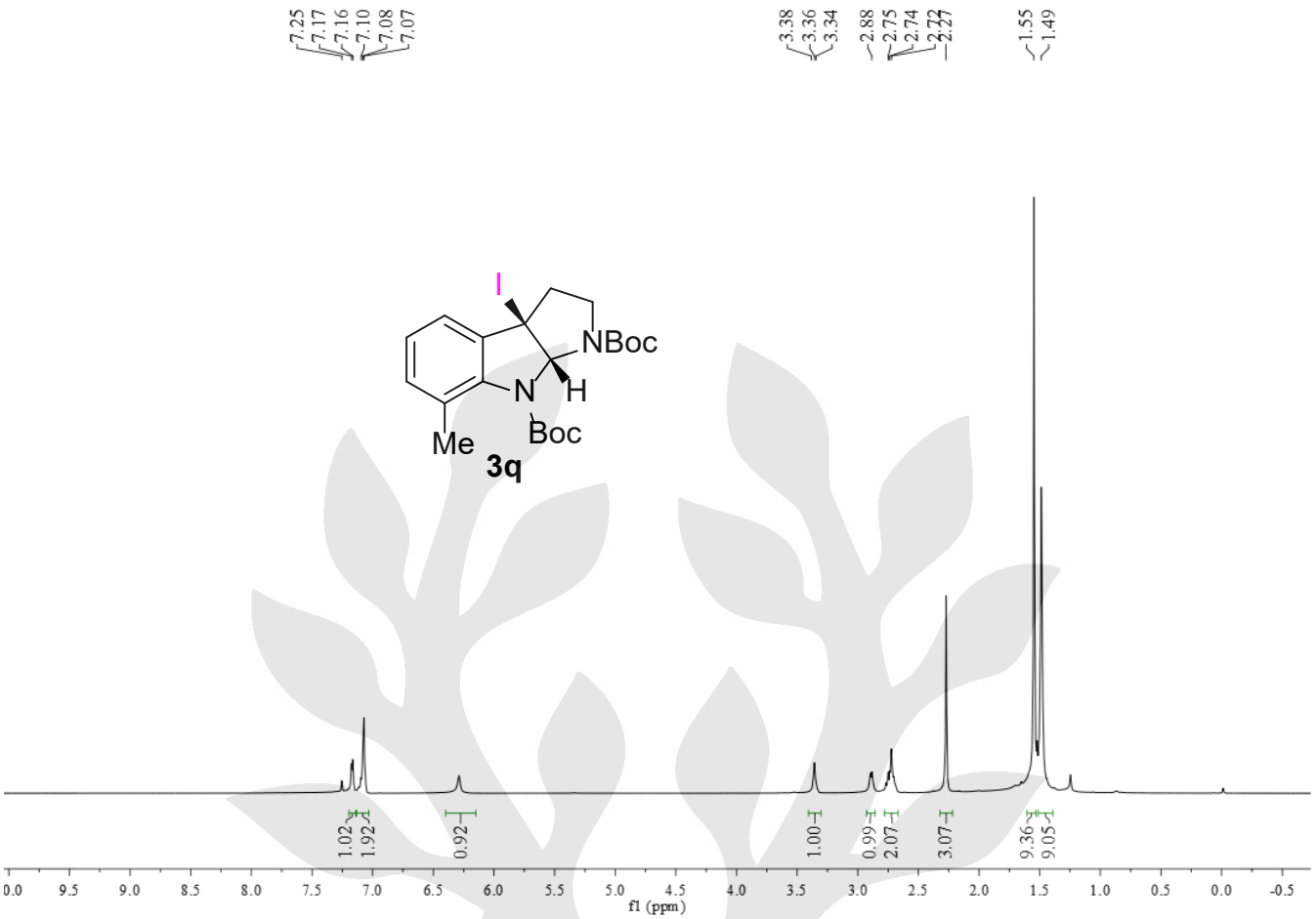

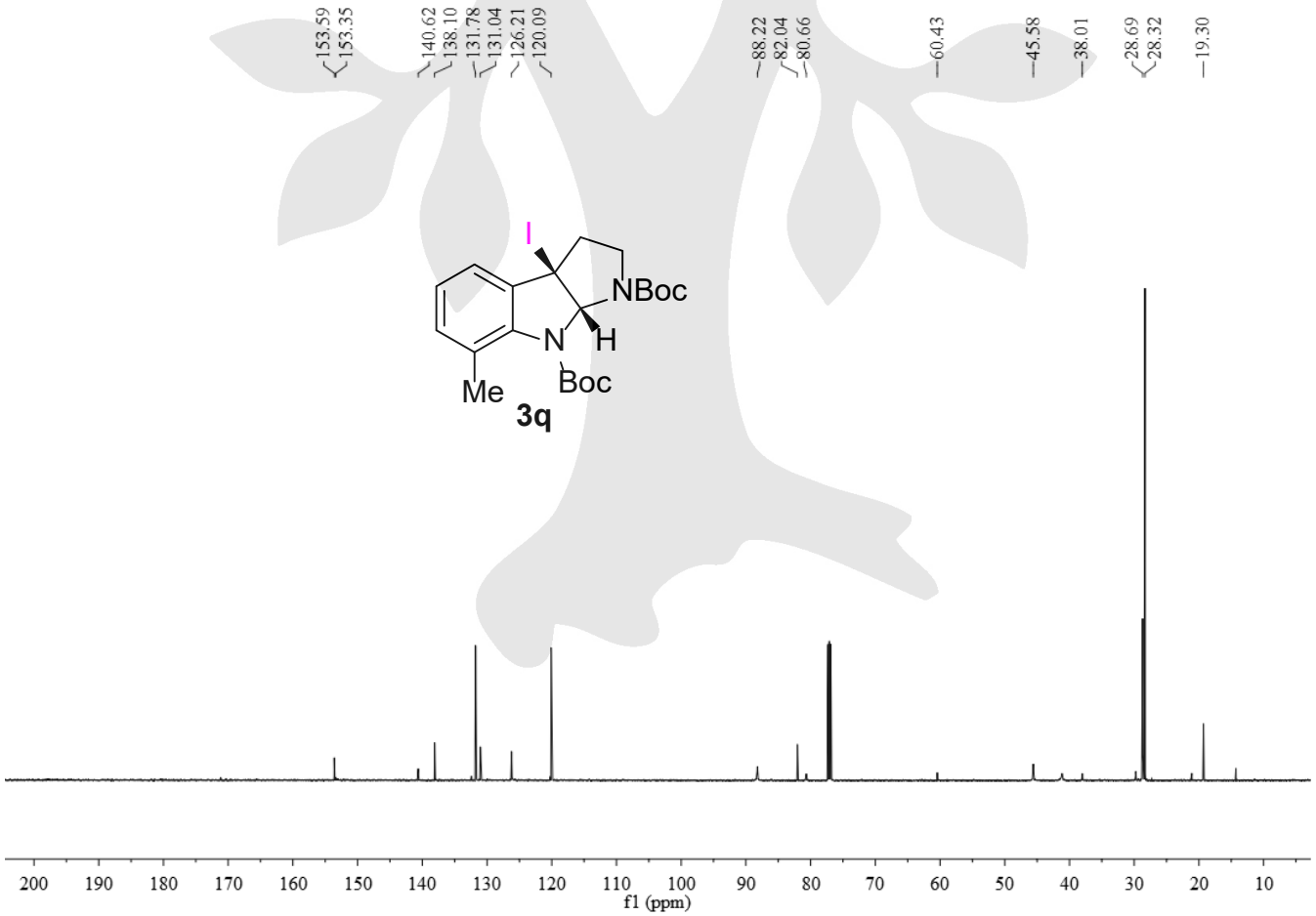

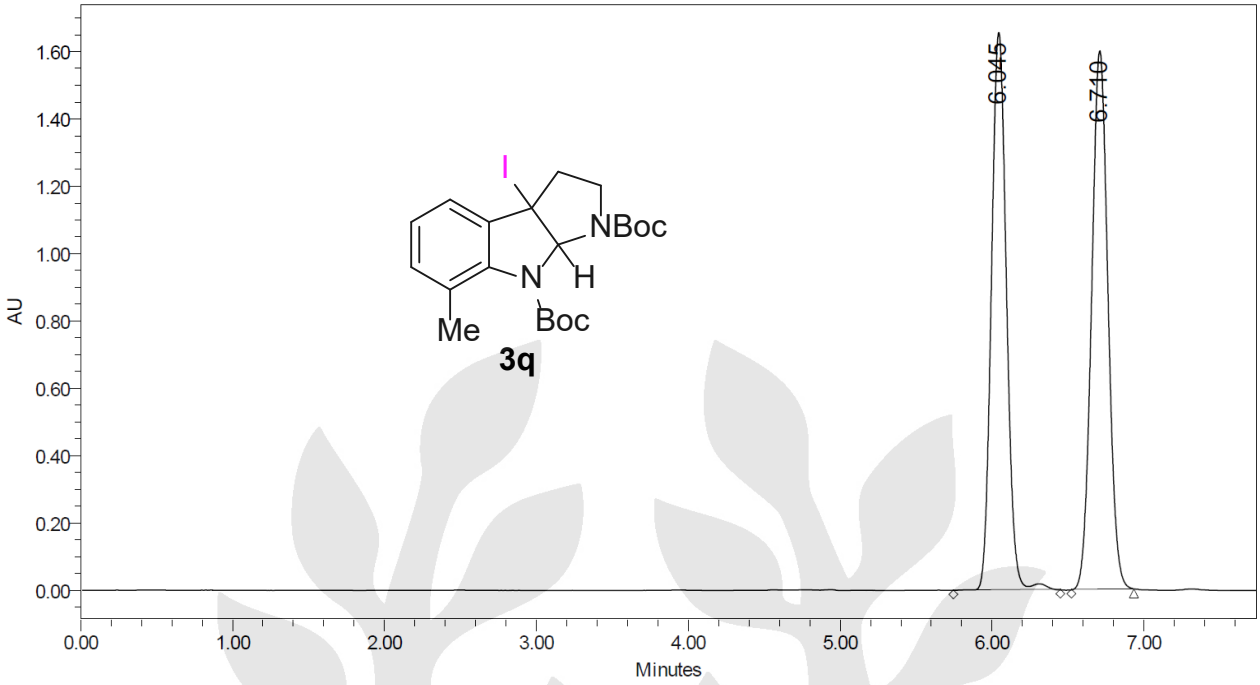

	RT (min)	Peak Type	Area (μV*sec)	% Area	Height (μV)	% Height	Integration Type	Points Across Peak	Start Time (min)	End Time (min)
1	6.045	Unknown	11385720	48.76	1654881	50.86	Vv	423	5.745	6.450
2	6.710	Unknown	11964365	51.24	1598837	49.14	vb	246	6.523	6.933

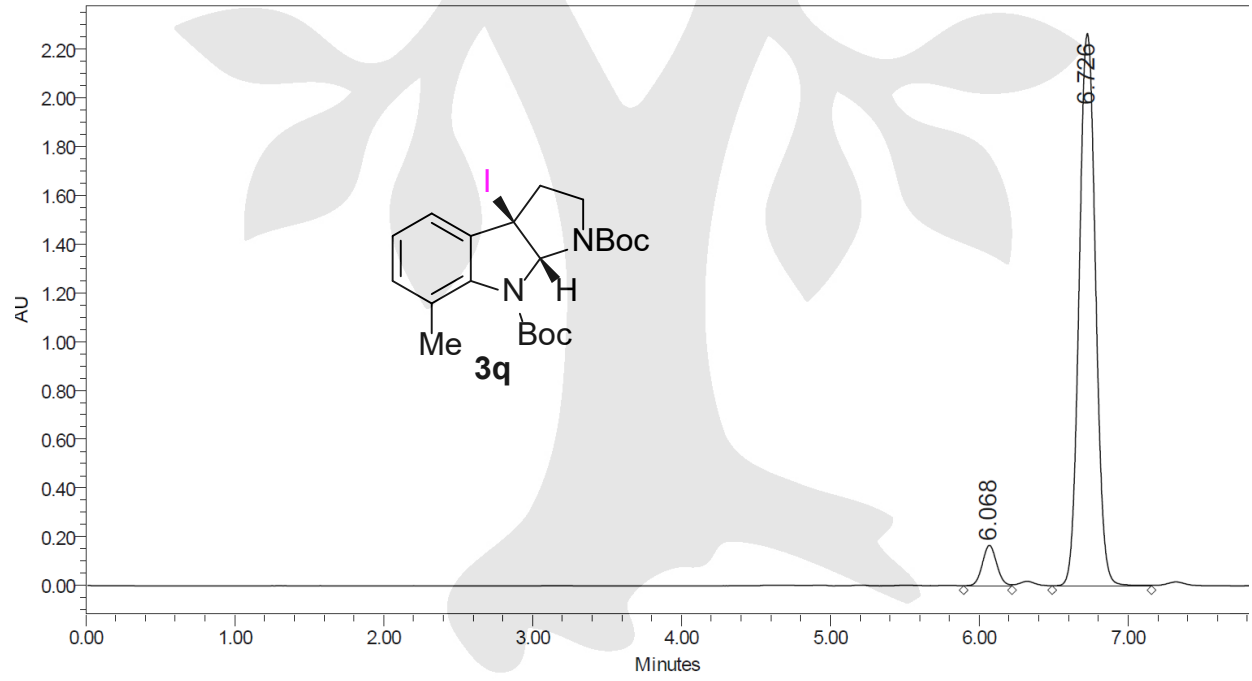

	RT (min)	Peak Type	Area (μV*sec)	% Area	Height (μV)	% Height	Integration Type	Points Across Peak	Start Time (min)	End Time (min)
1	6.068	Unknown	1106610	5.99	165828	6.82	VV	195	5.895	6.220
2	6.726	Unknown	17355780	94.01	2266720	93.18	VV	400	6.490	7.157

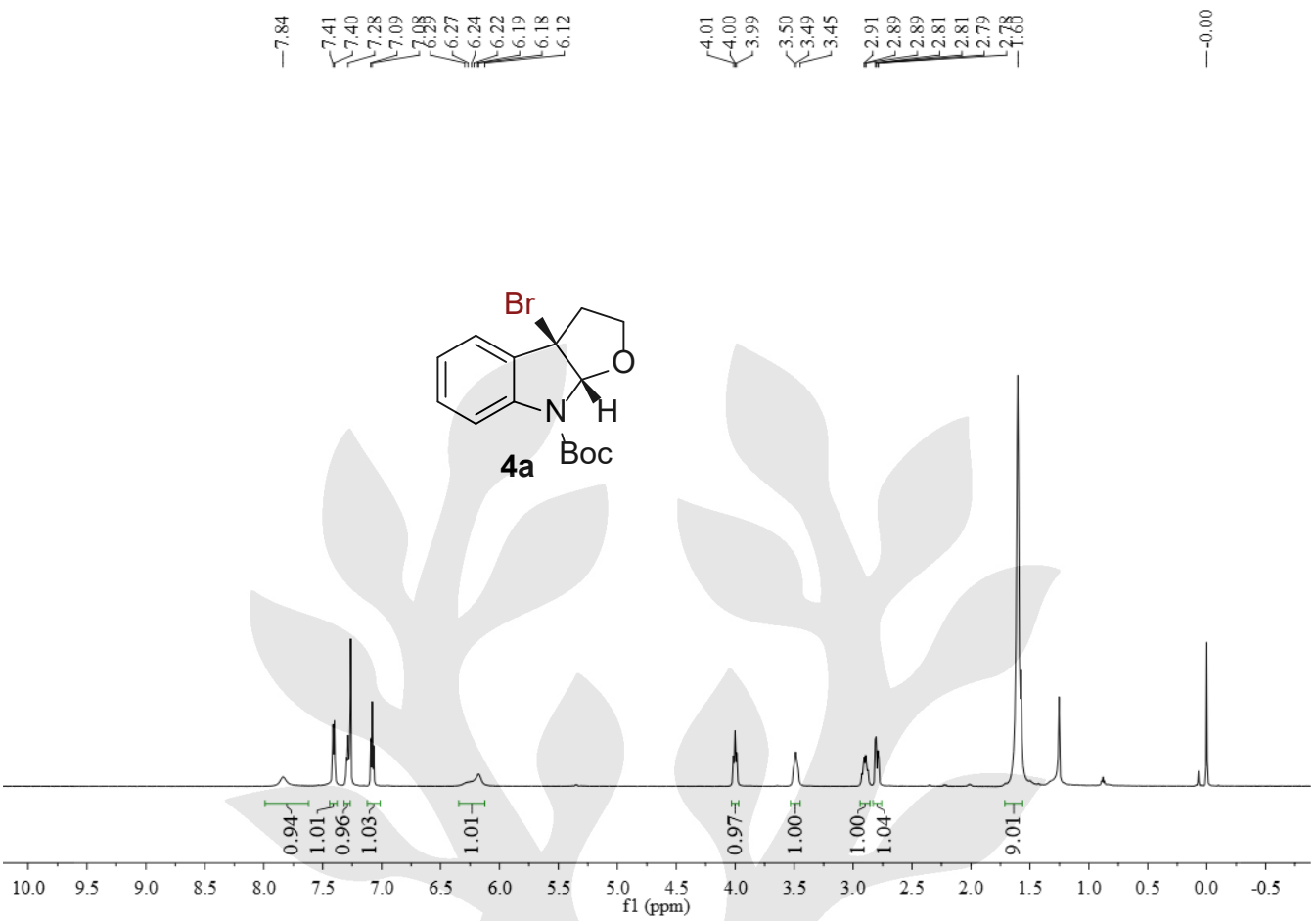

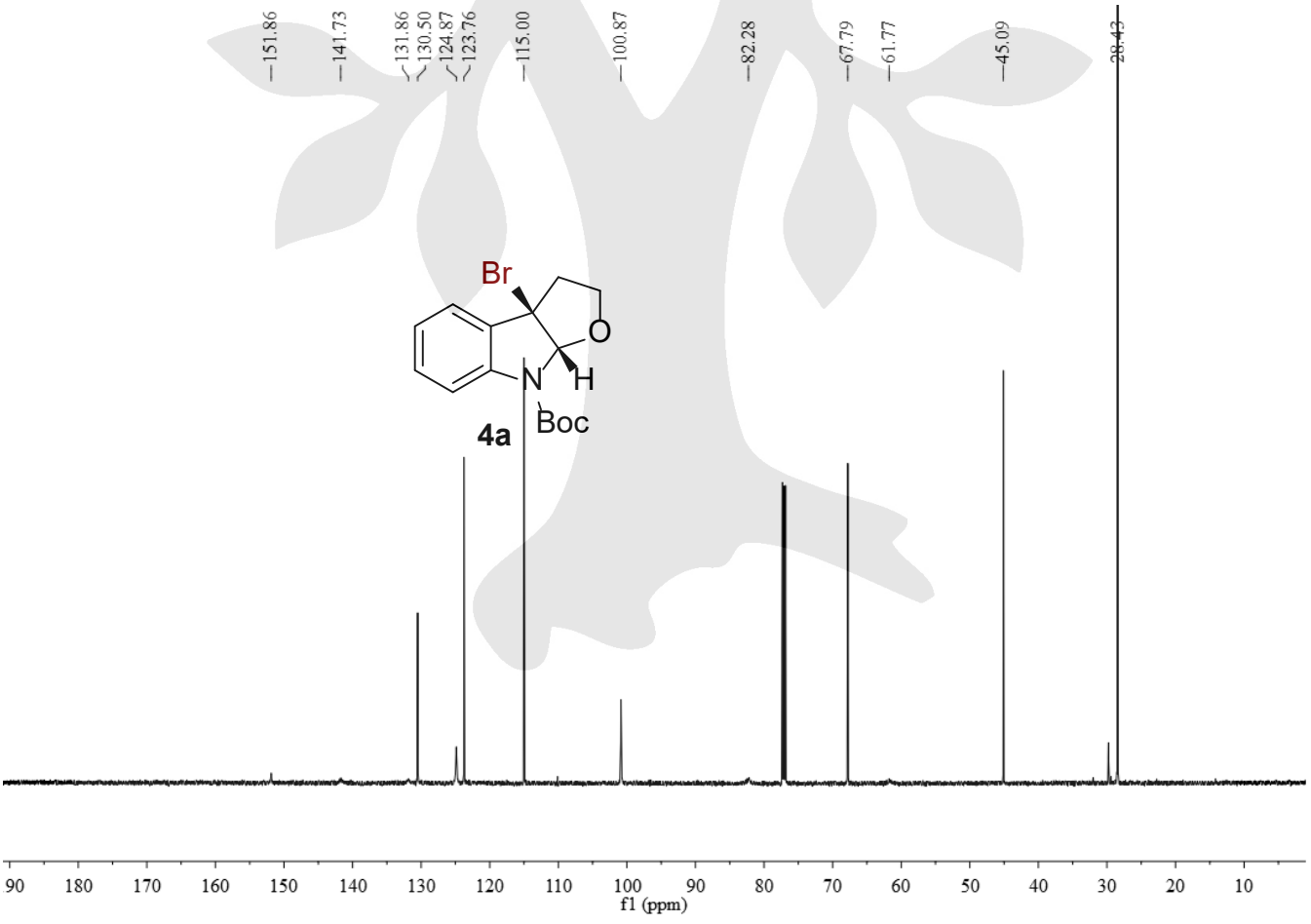

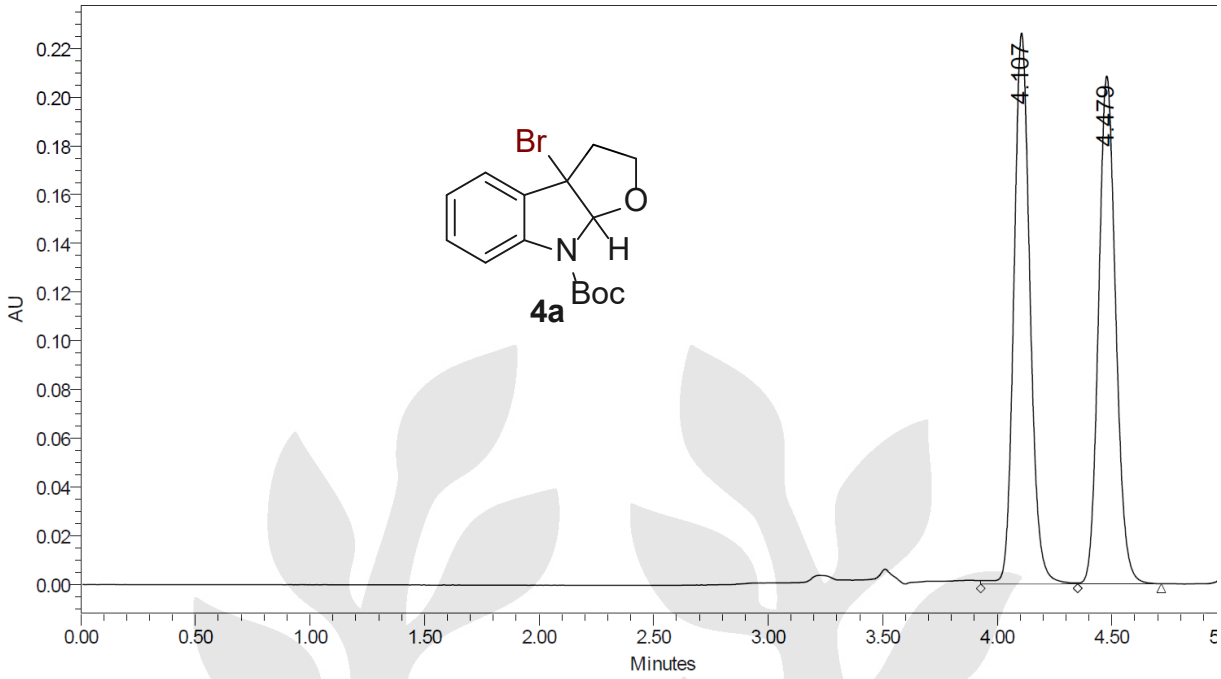

	RT (min)	Peak Type	Area (μV*sec)	% Area	Height (μV)	% Height	Integration Type	Points Across Peak	Start Time (min)	End Time (min)
1	4.107	Unknown	1111075	50.58	226151	52.03	VV	254	3.928	4.352
2	4.479	Unknown	1085763	49.42	208476	47.97	VB	219	4.352	4.717

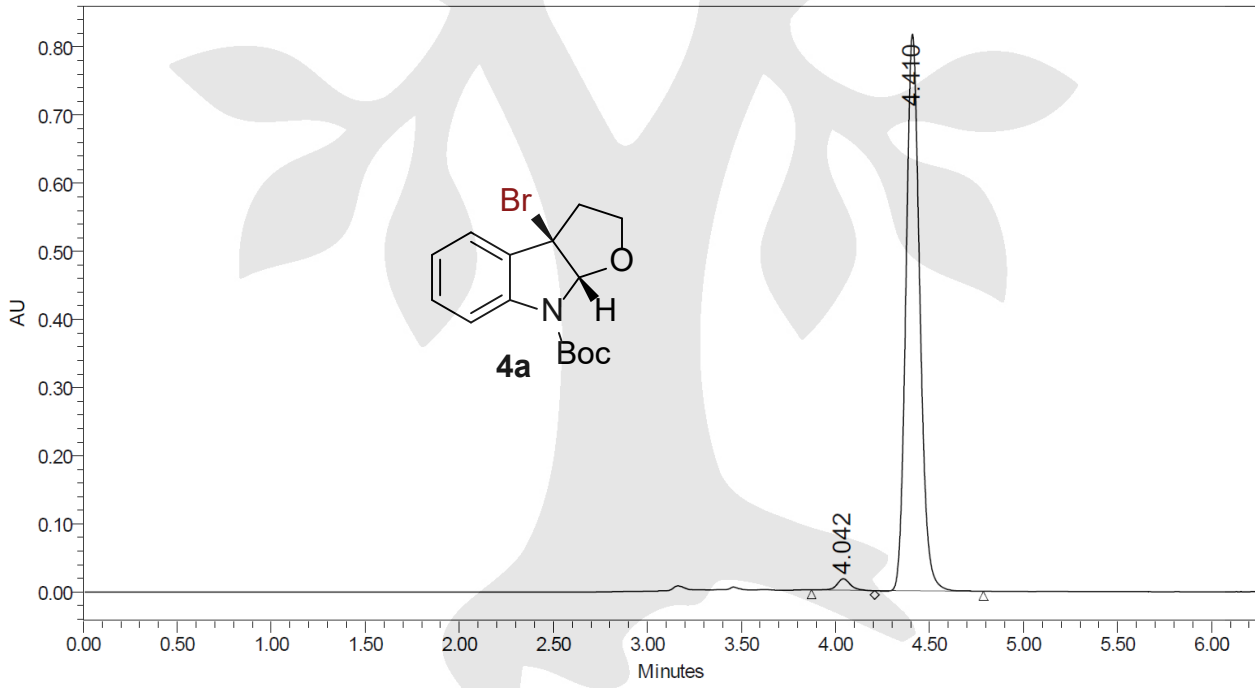

	RT (min)	Peak Type	Area (μV*sec)	% Area	Height (μV)	% Height	Integration Type	Points Across Peak	Start Time (min)	End Time (min)
1	4.042	Unknown	82401	1.92	16608	1.99	bv	201	3.873	4.208
2	4.410	Unknown	4199721	98.08	816936	98.01	vB	347	4.208	4.787

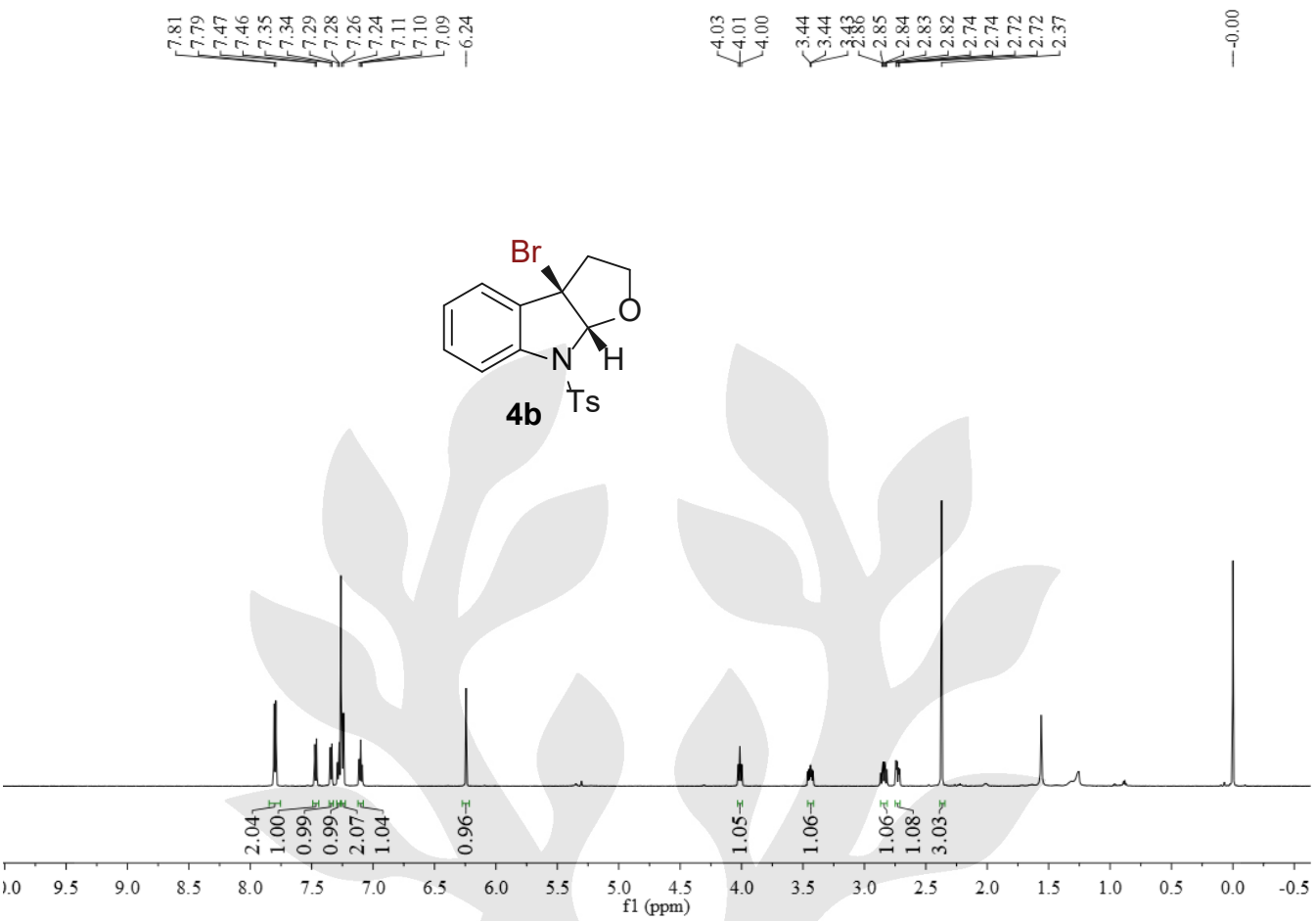

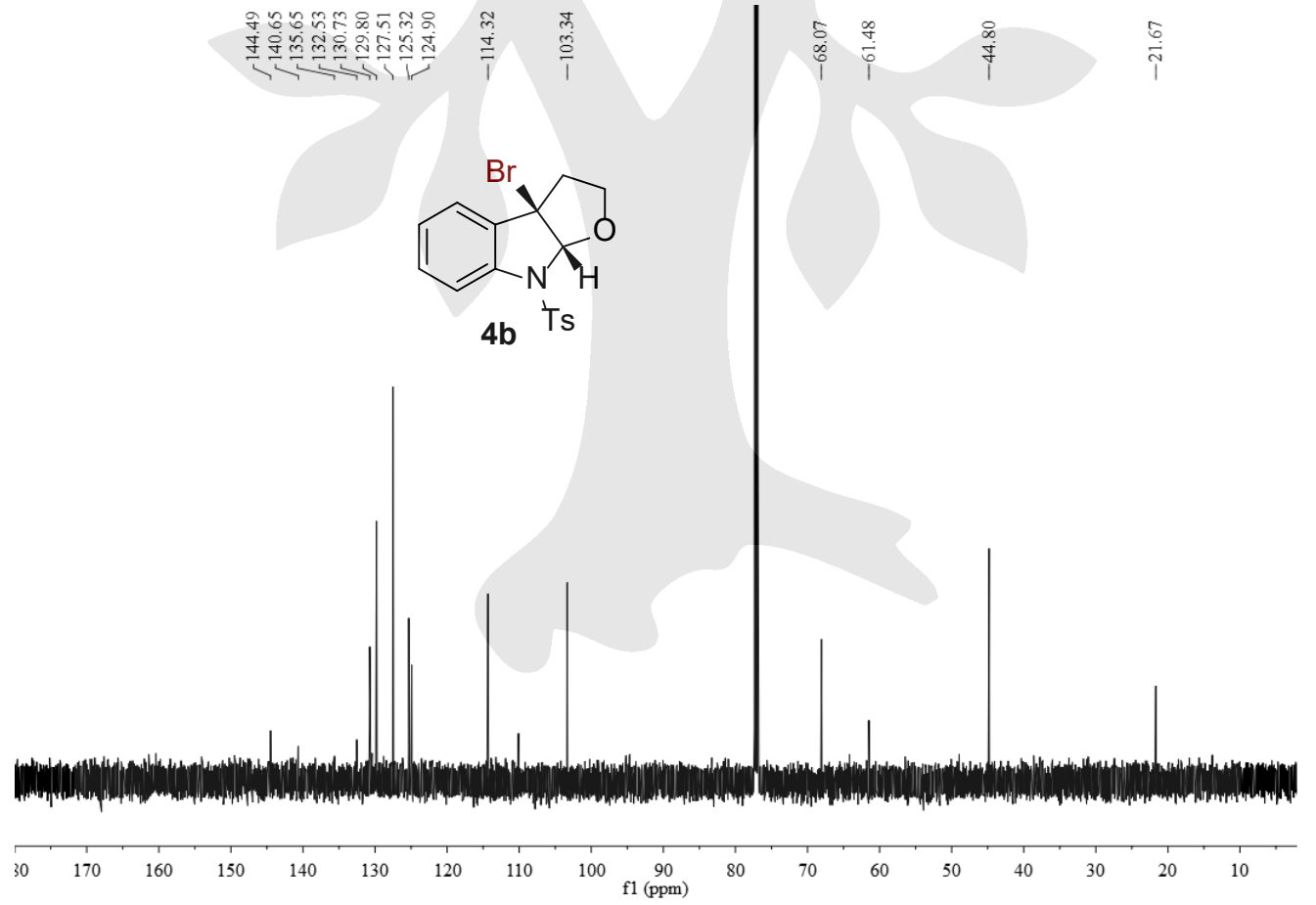

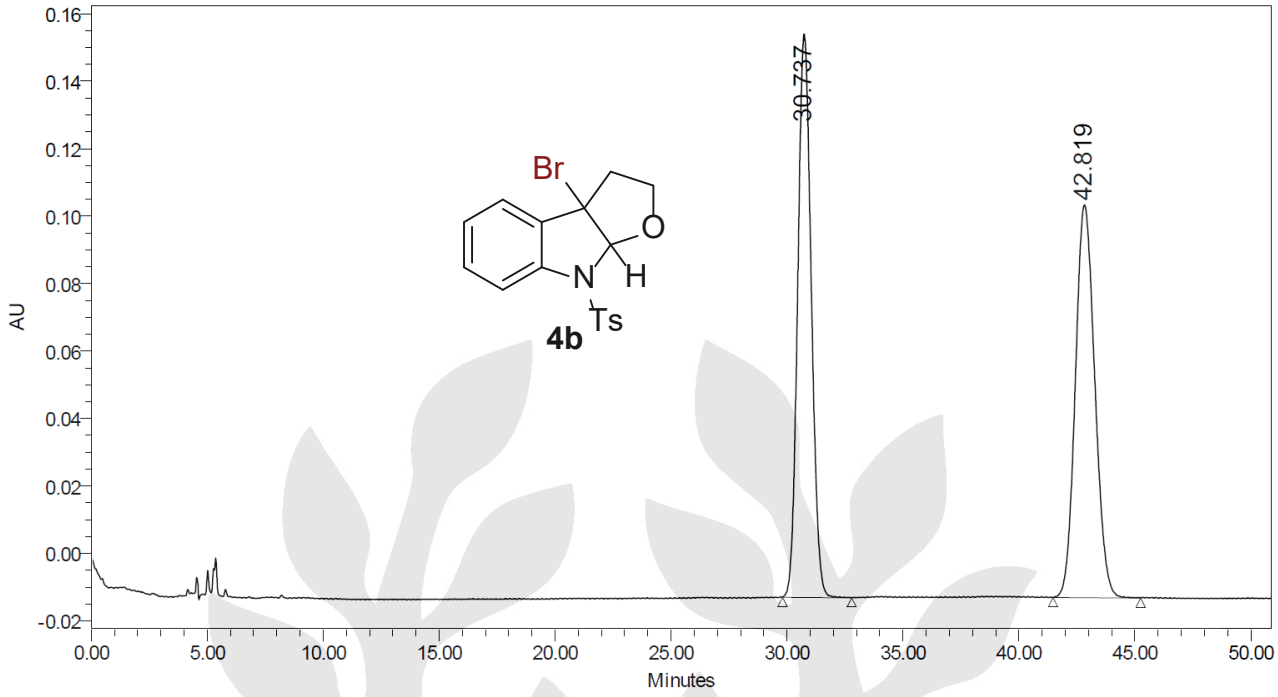

	RT (min)	Peak Type	Area (μV*sec)	% Area	Height (μV)	% Height	Integration Type	Points Across Peak	Start Time (min)	End Time (min)
1	30.737	Unknown	6784575	49.98	167084	58.92	BB	1792	29.800	32.787
2	42.819	Unknown	6790164	50.02	116474	41.08	BB	2266	41.470	45.247

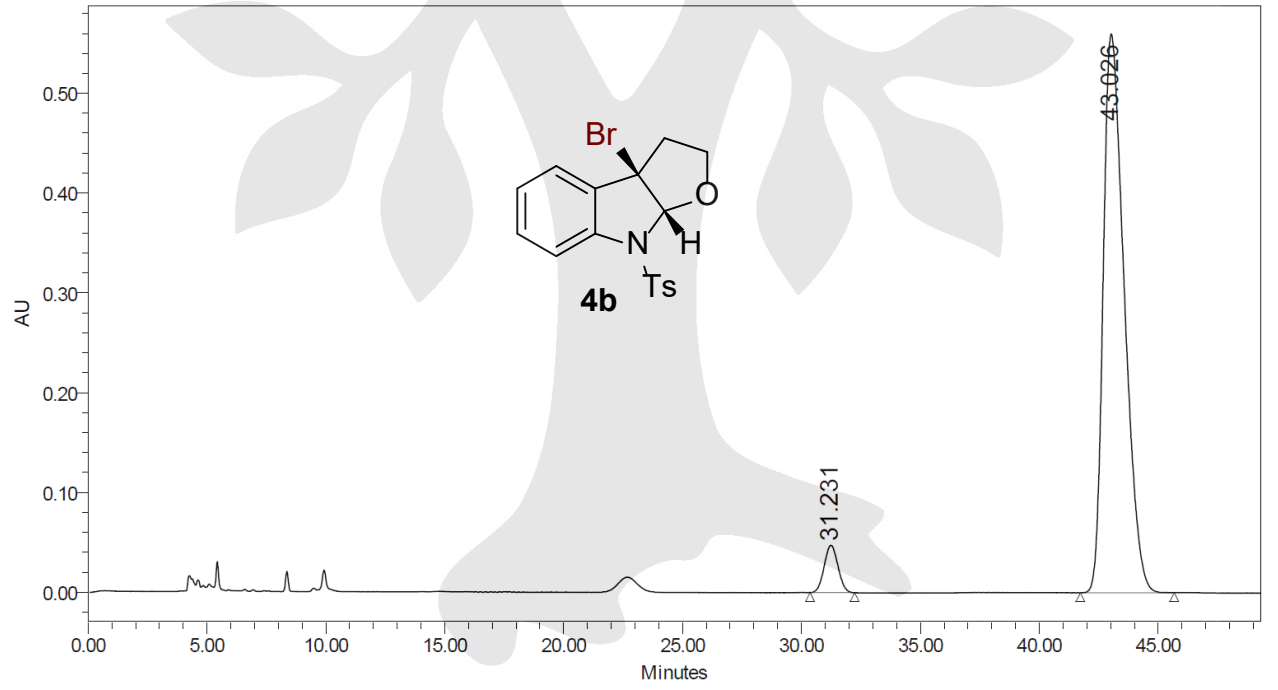

	RT (min)	Peak Type	Area (μV*sec)	% Area	Height (μV)	% Height	Integration Type	Points Across Peak	Start Time (min)	End Time (min)
1	31.231	Unknown	1913799	5.28	47445	7.81	bb	1127	30.358	32.237
2	43.026	Unknown	34348909	94.72	560339	92.19	BB	2369	41.730	45.678

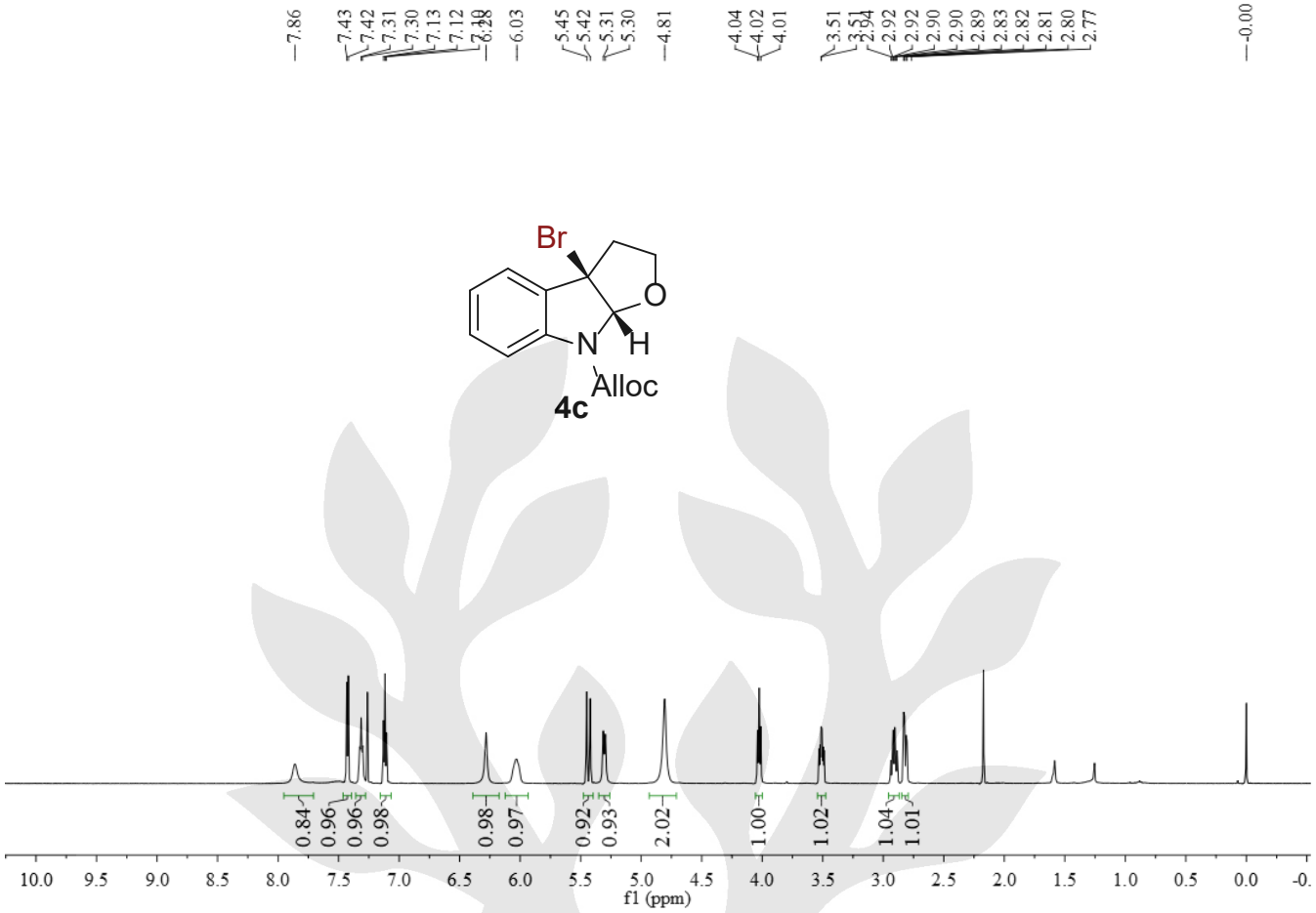

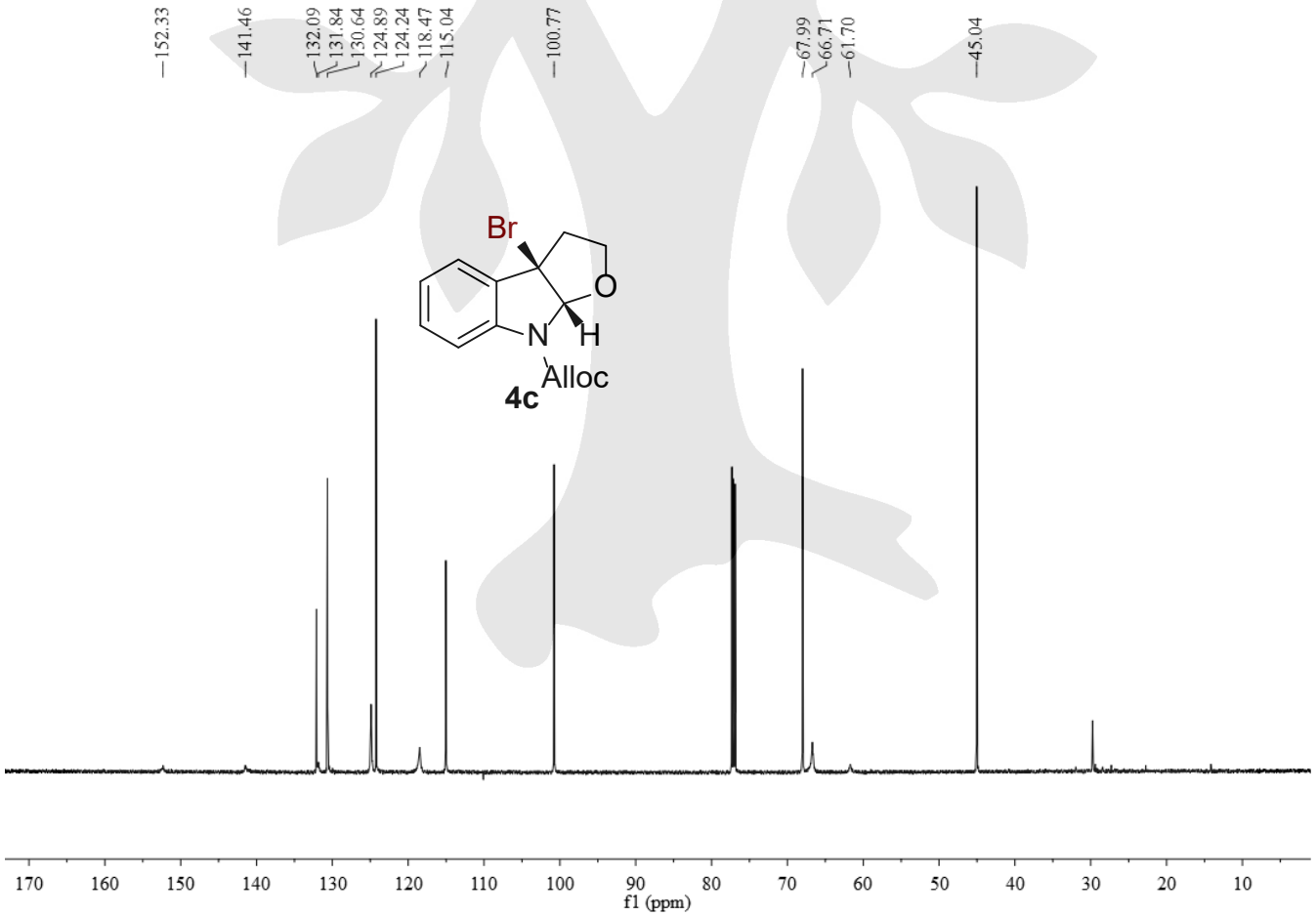

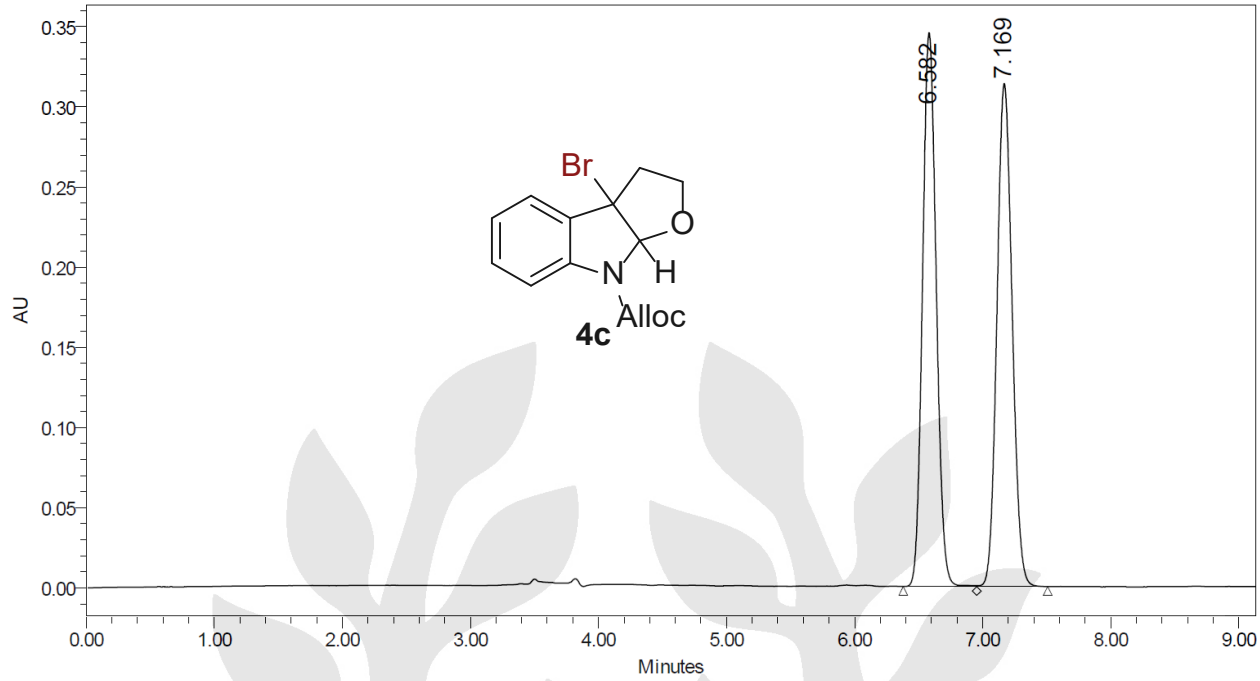

	RT (min)	Peak Type	Area (μV*sec)	% Area	Height (μV)	% Height	Integration Type	Points Across Peak	Start Time (min)	End Time (min)
1	6.582	Unknown	2569261	49.81	345350	52.40	BV	344	6.380	6.953
2	7.169	Unknown	2589358	50.19	313709	47.60	VB	333	6.953	7.508

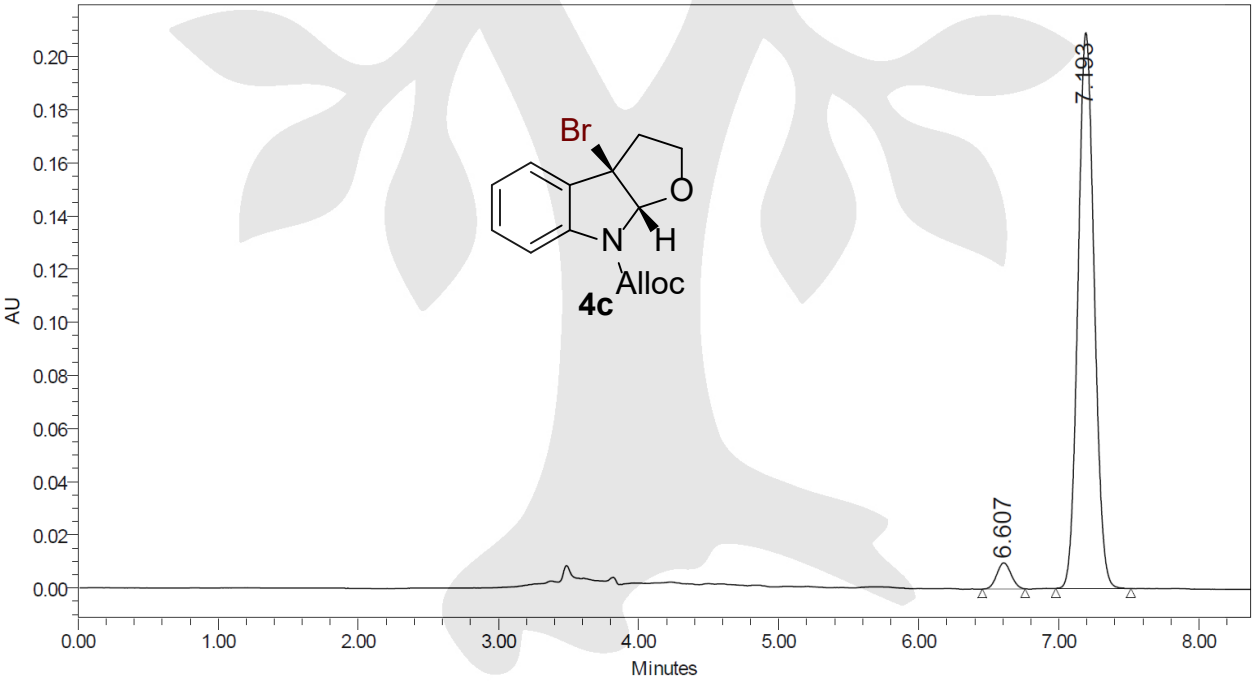

	RT (min)	Peak Type	Area (μV*sec)	% Area	Height (μV)	% Height	Integration Type	Points Across Peak	Start Time (min)	End Time (min)
1	6.607	Unknown	69803	3.99	9820	4.48	Bb	184	6.453	6.760
2	7.193	Unknown	1681438	96.01	209203	95.52	BB	322	6.978	7.515

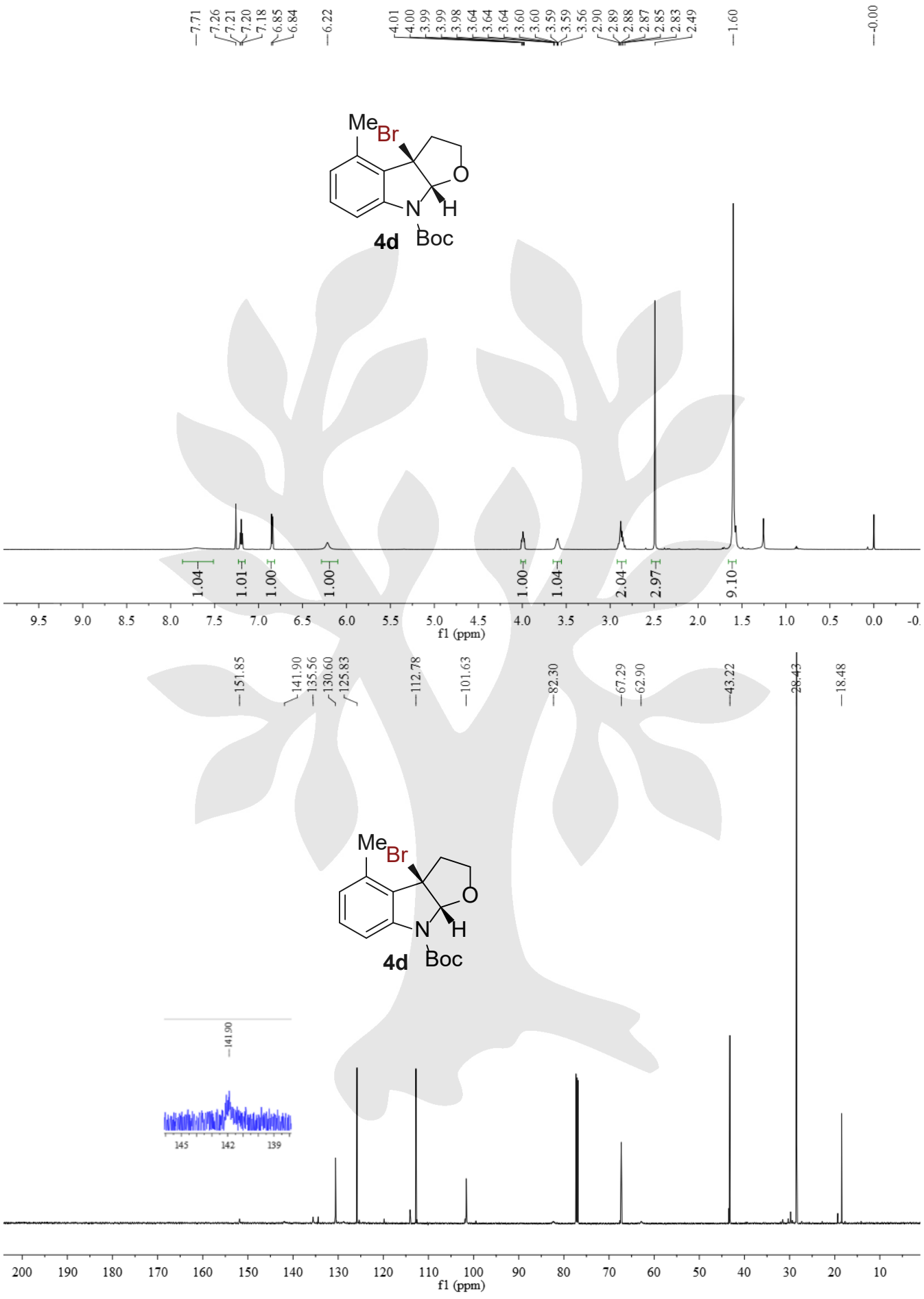

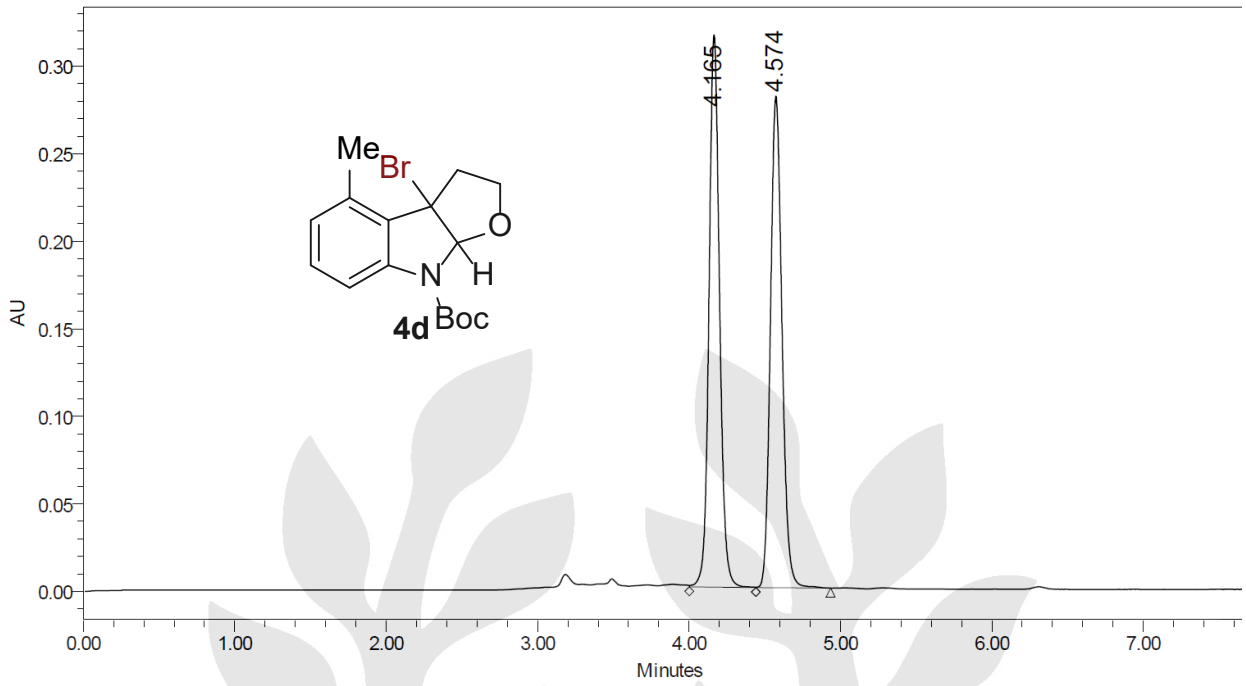

	RT (min)	Peak Type	Area (μV*sec)	% Area	Height (μV)	% Height	Integration Type	Points Across Peak	Start Time (min)	End Time (min)
1	4.165	Unknown	1526367	50.65	315447	52.91	VV	264	4.002	4.442
2	4.574	Unknown	1487260	49.35	280741	47.09	VB	296	4.442	4.935

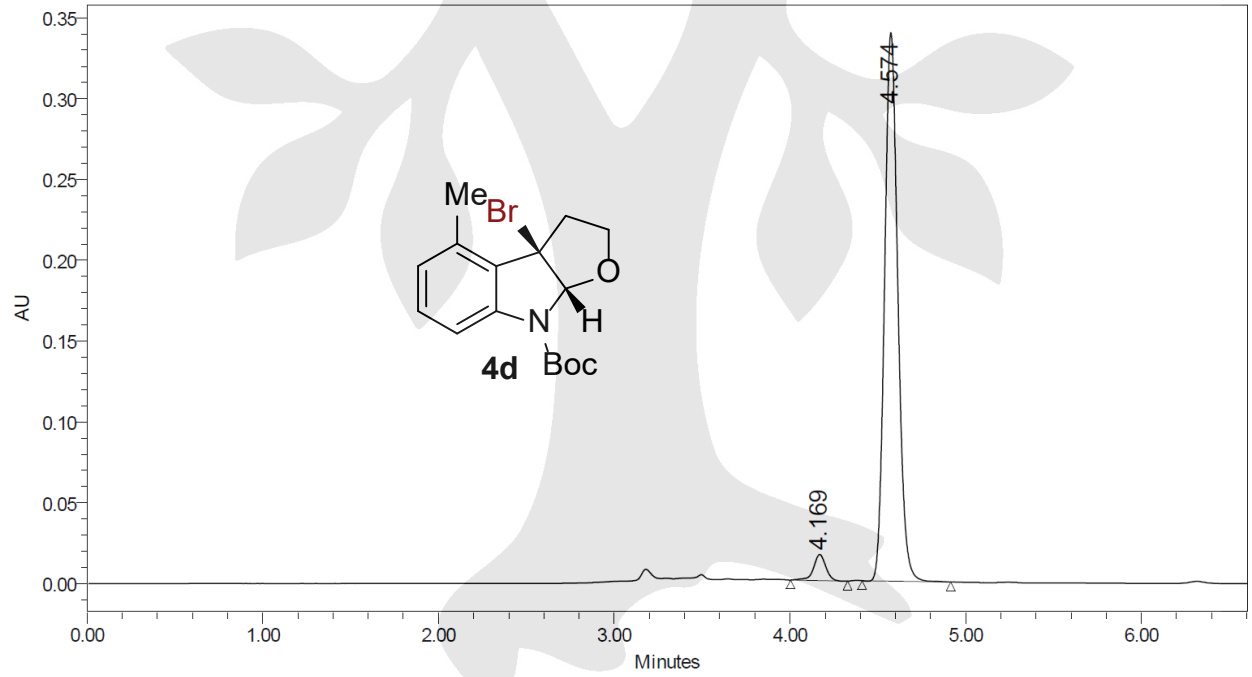

	RT (min)	Peak Type	Area (μV*sec)	% Area	Height (μV)	% Height	Integration Type	Points Across Peak	Start Time (min)	End Time (min)
1	4.169	Unknown	77727	4.19	16067	4.52	bb	195	4.003	4.328
2	4.574	Unknown	1775609	95.81	339410	95.48	bB	303	4.410	4.915

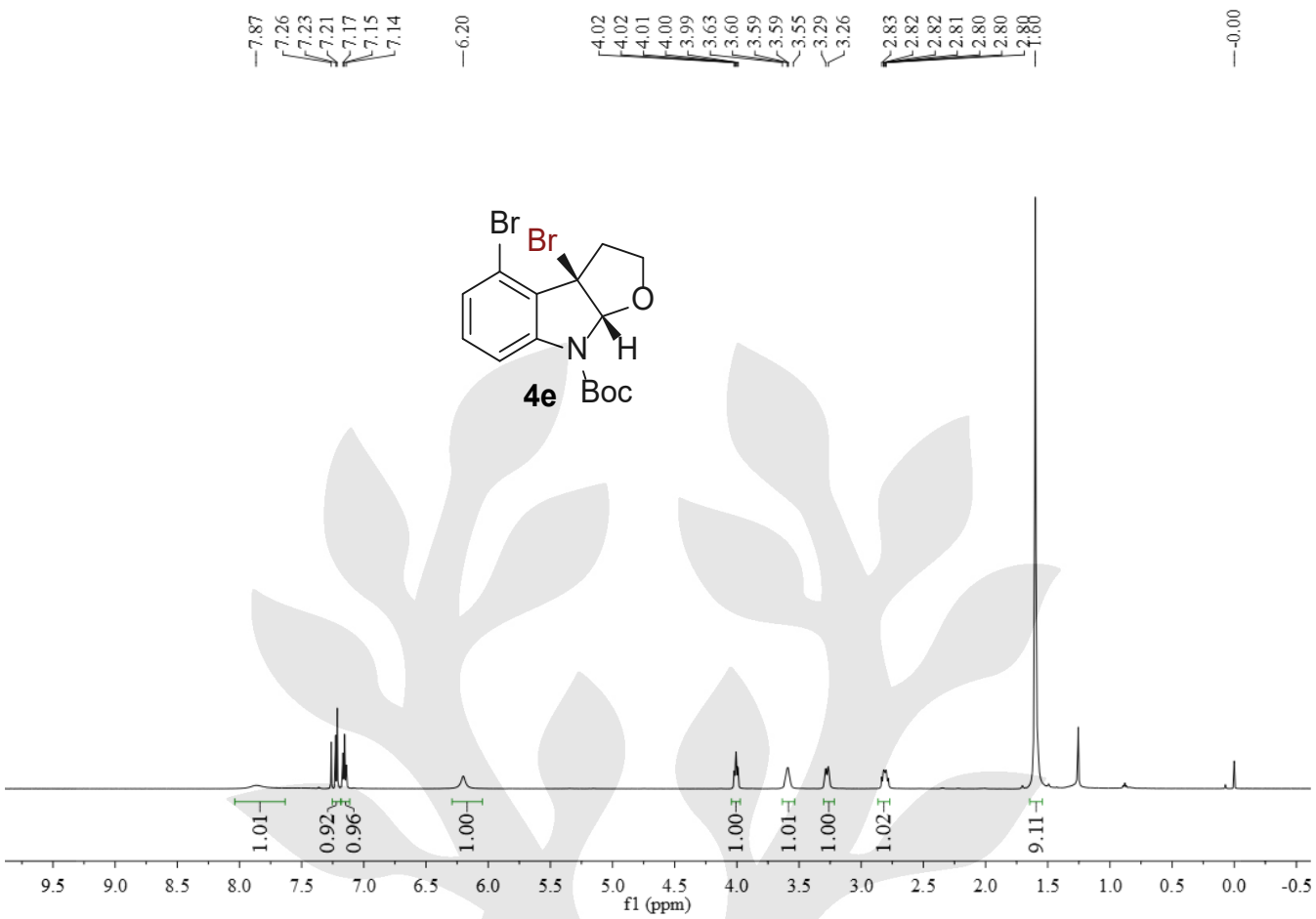

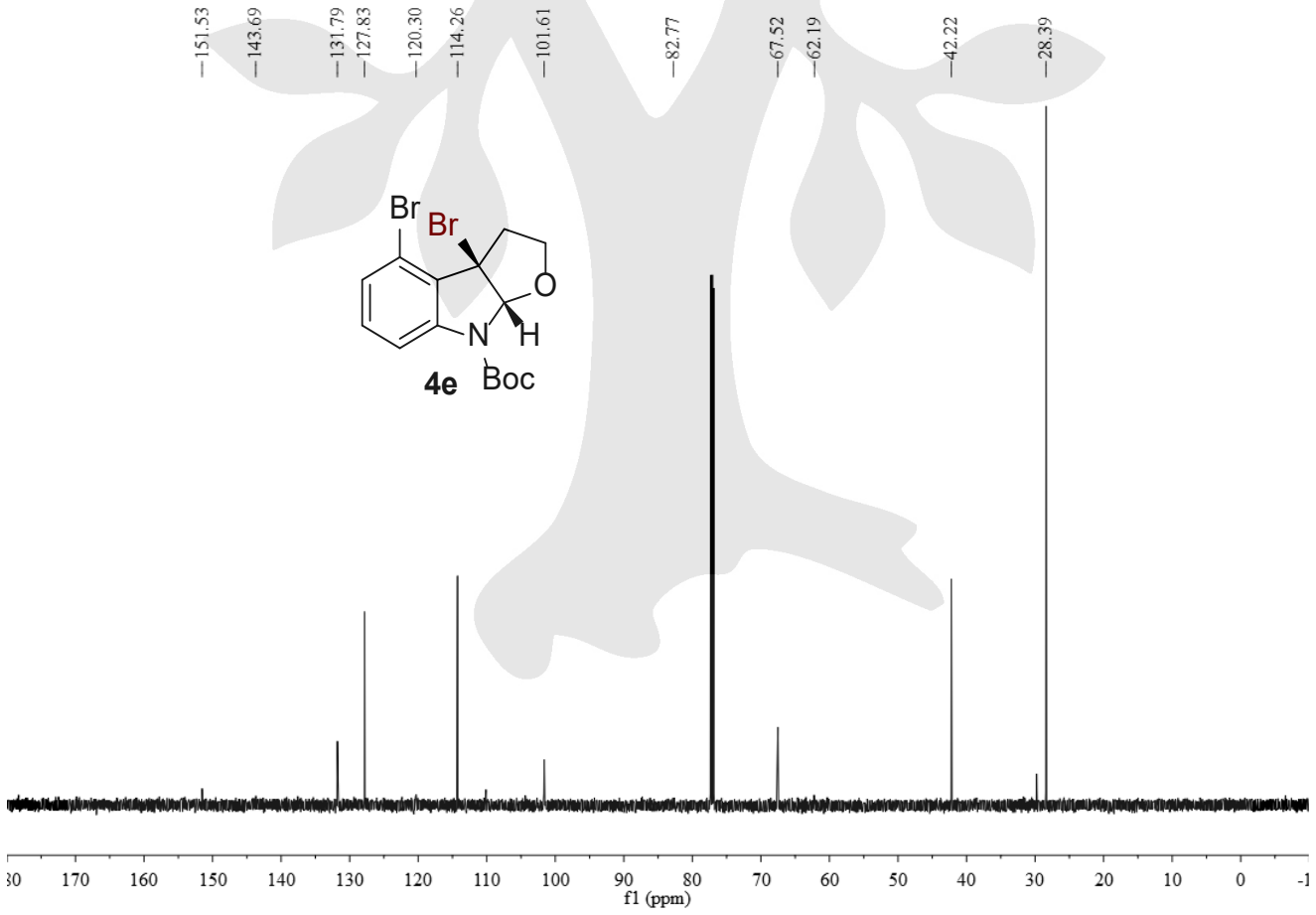

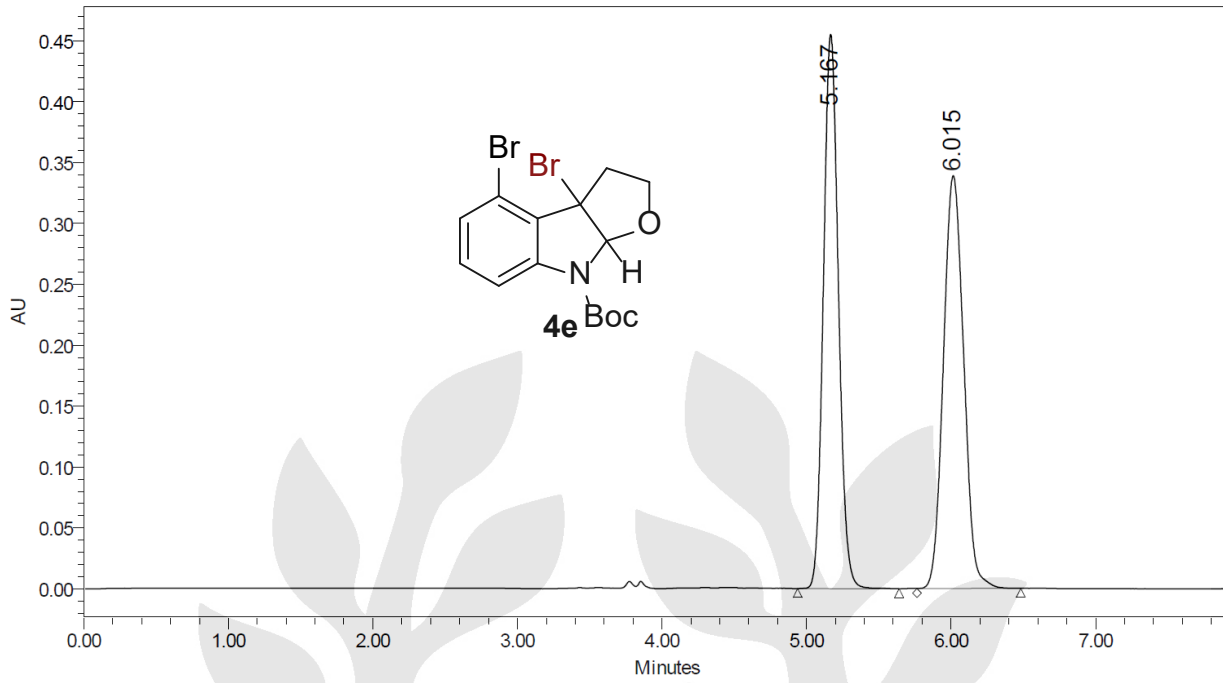

	RT (min)	Peak Type	Area (μV*sec)	% Area	Height (μV)	% Height	Integration Type	Points Across Peak	Start Time (min)	End Time (min)
1	5.167	Unknown	3291300	49.90	455259	57.31	BB	421	4.938	5.640
2	6.015	Unknown	3305087	50.10	339110	42.69	VB	430	5.765	6.482

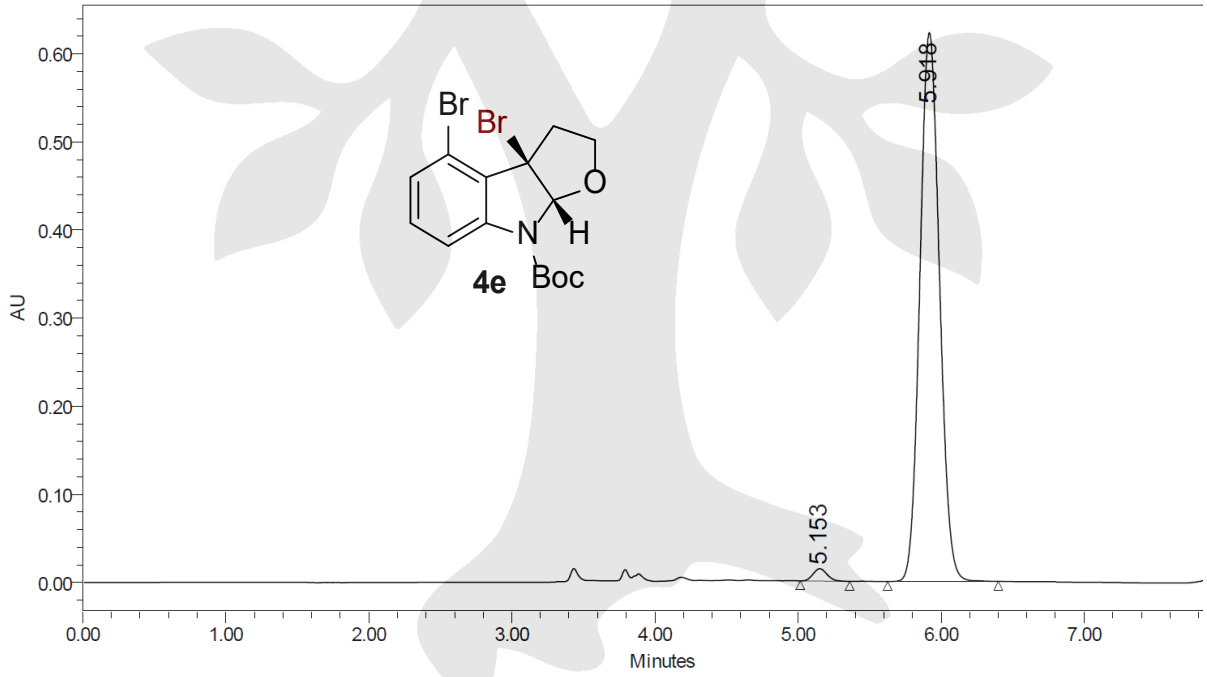

	RT (min)	Peak Type	Area (μV*sec)	% Area	Height (μV)	% Height	Integration Type	Points Across Peak	Start Time (min)	End Time (min)
1	5.153	Unknown	96149	1.60	14060	2.21	BB	207	5.017	5.362
2	5.918	Unknown	5929514	98.40	622921	97.79	BB	464	5.627	6.400

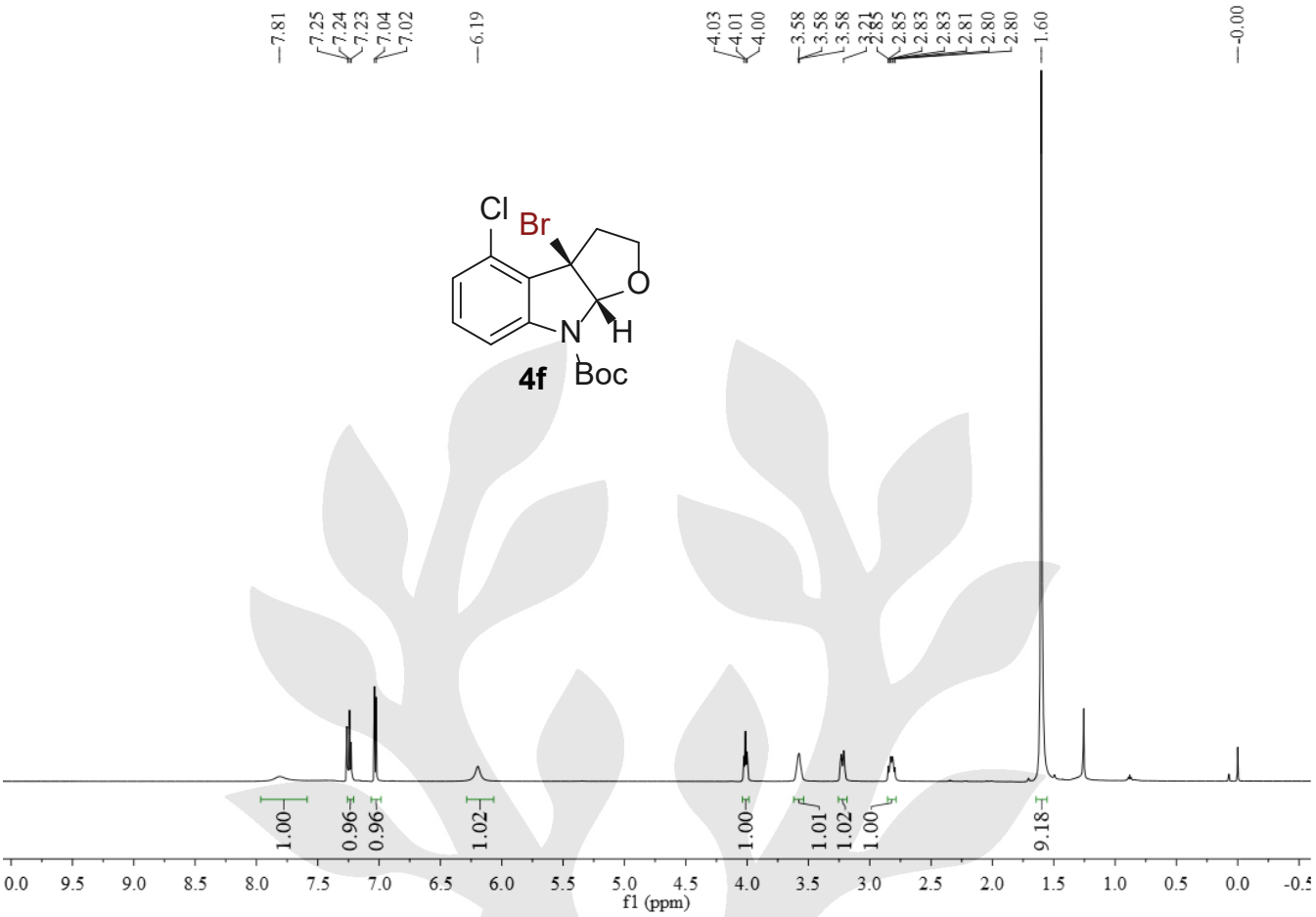

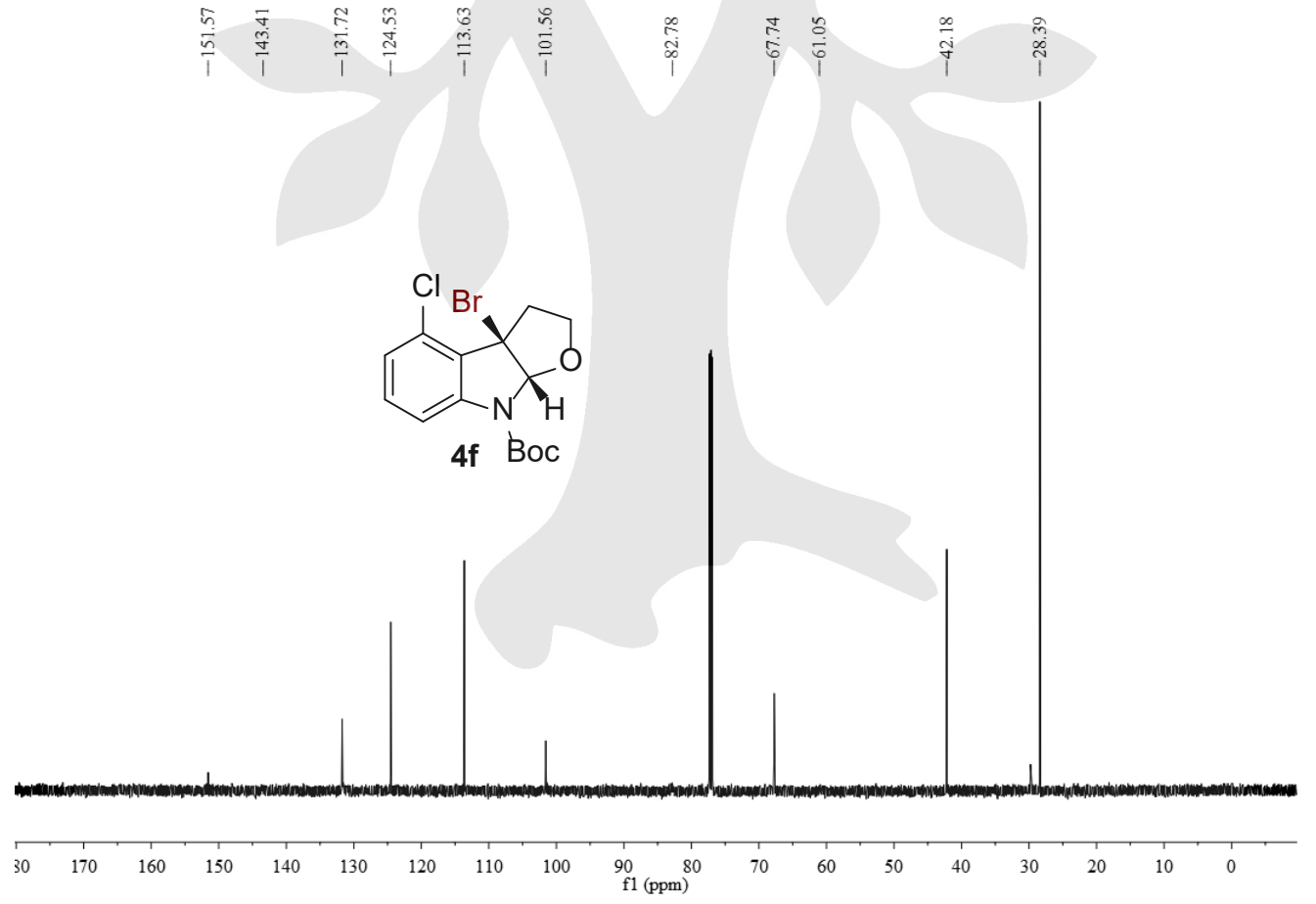

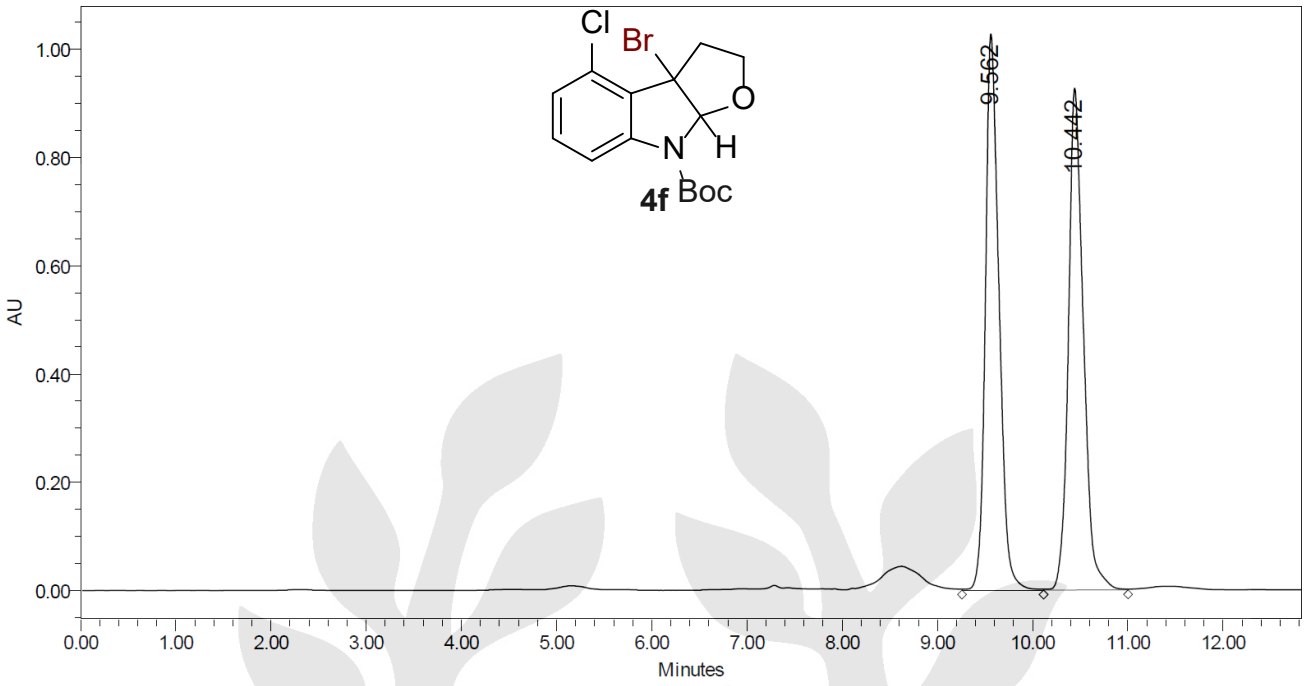

	RT (min)	Area (μV*sec)	% Area	Height (μV)	% Height
1	9.562	10184322	50.17	1027605	52.56
2	10.442	10117325	49.83	927386	47.44

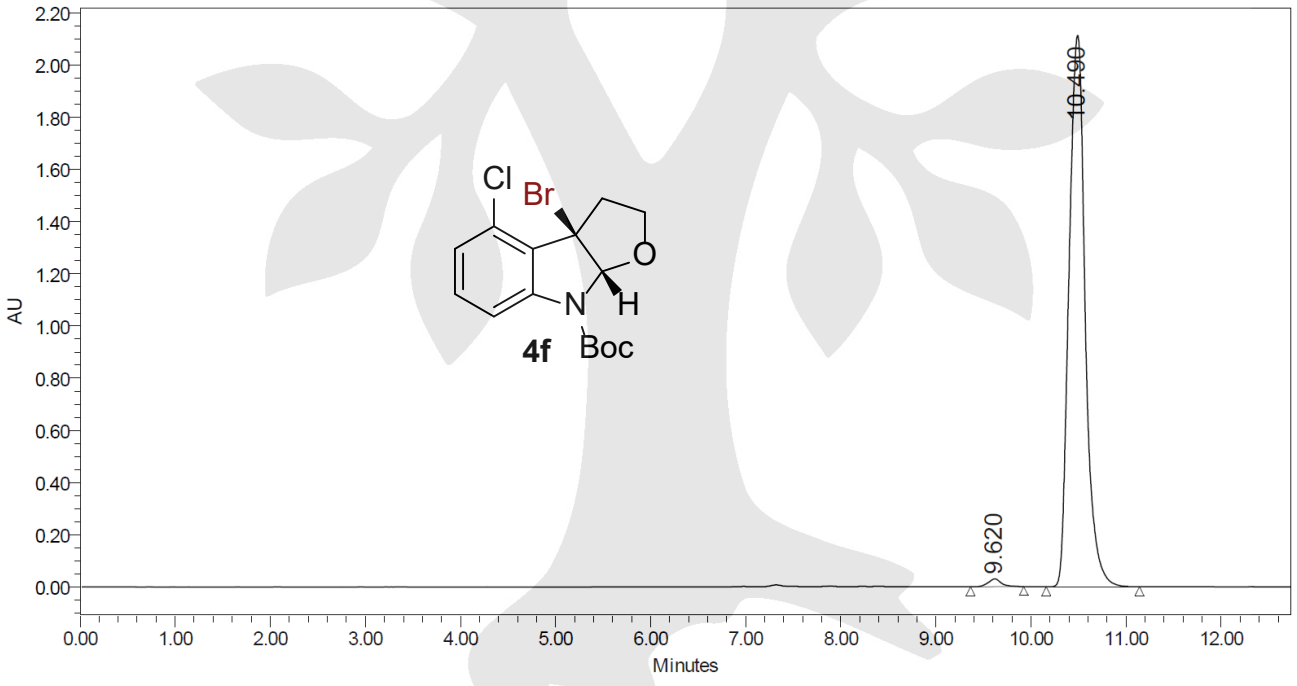

	RT (min)	Area (μV*sec)	% Area	Height (μV)	% Height
1	9.620	281908	1.12	29872	1.39
2	10.490	24975599	98.88	2113438	98.61

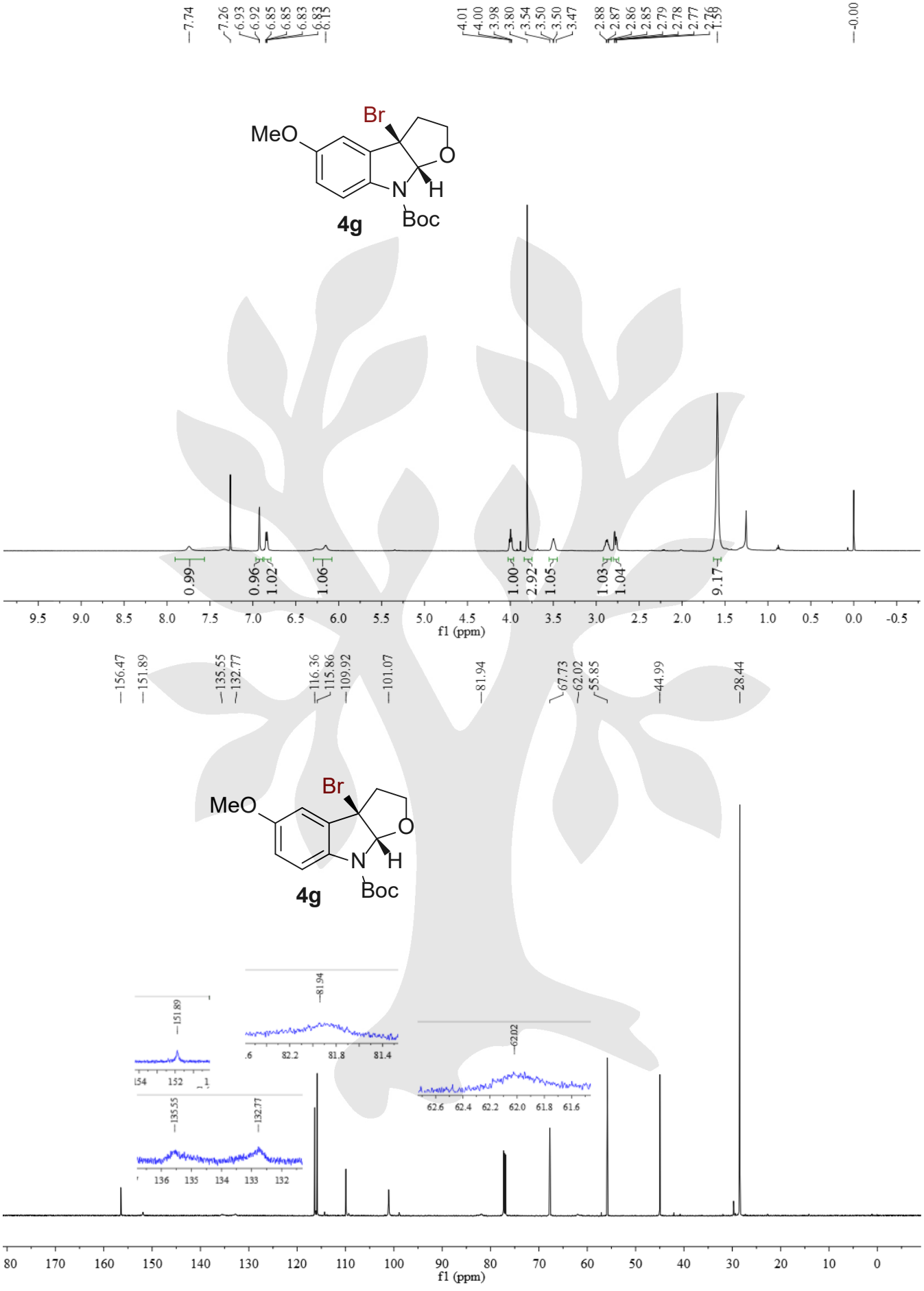

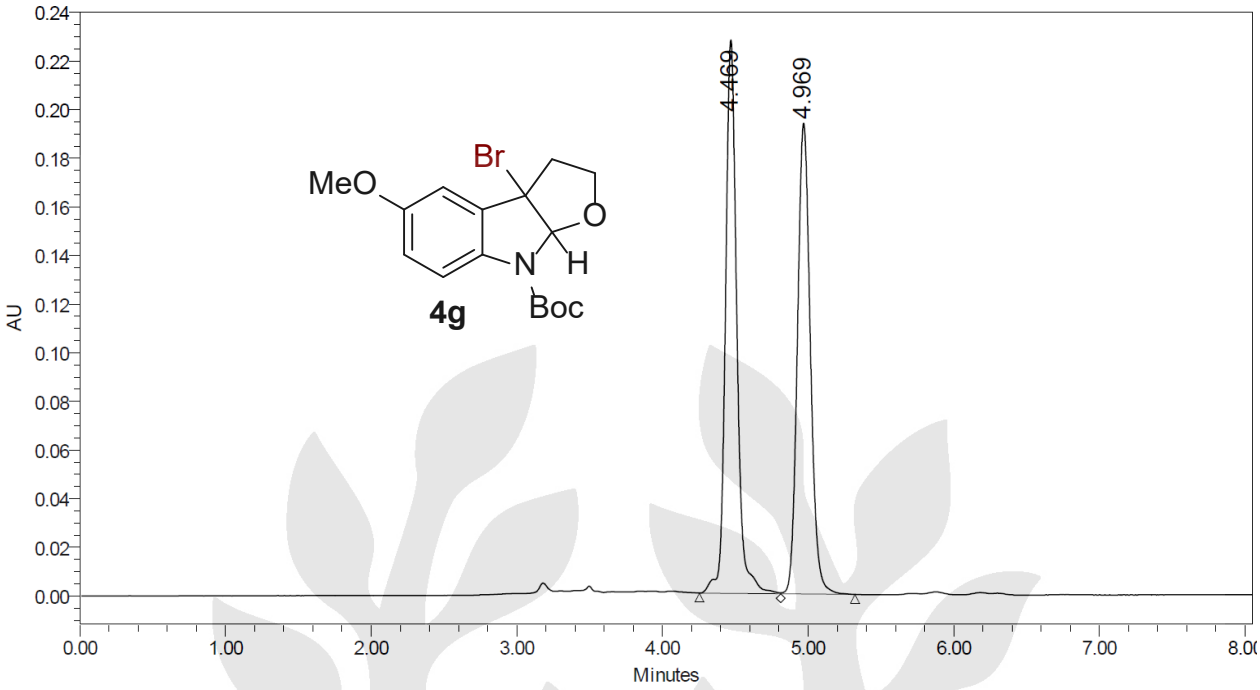

	RT (min)	Peak Type	Area (μV*sec)	% Area	Height (μV)	% Height	Integration Type	Points Across Peak	Start Time (min)	End Time (min)
1	4.469	Unknown	1238070	50.86	227659	54.04	BV	335	4.253	4.812
2	4.969	Unknown	1196232	49.14	193639	45.96	VB	306	4.812	5.322

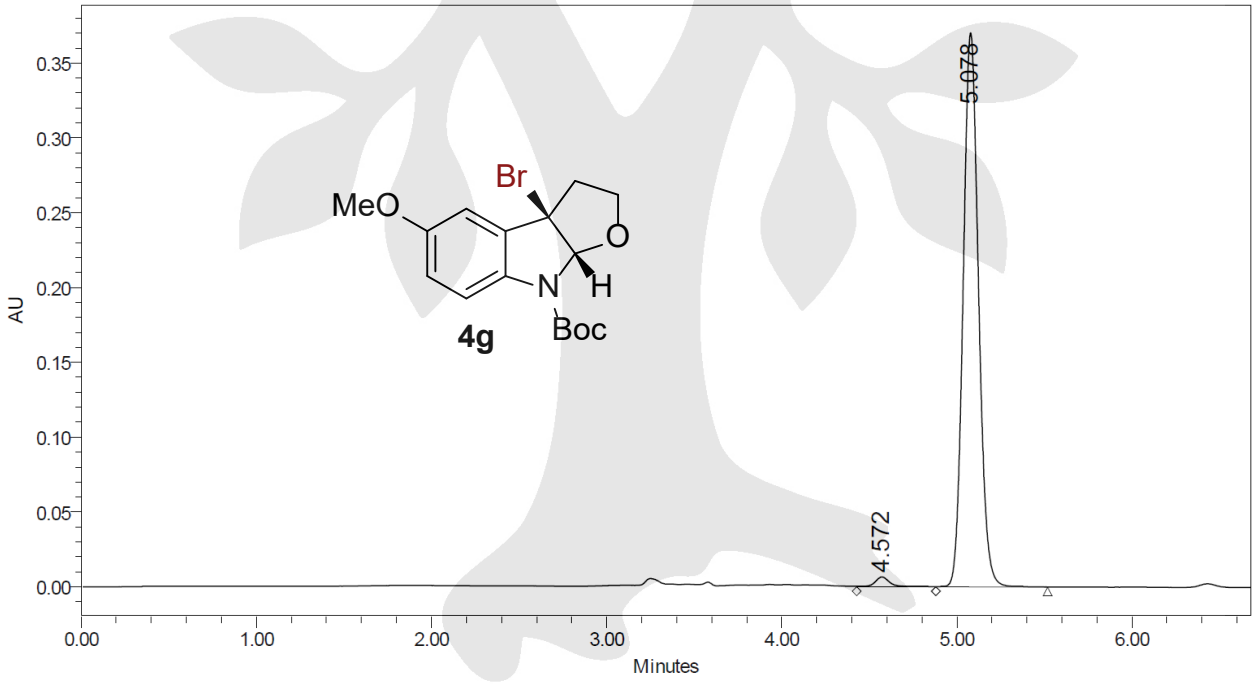

	RT (min)	Peak Type	Area (μV*sec)	% Area	Height (μV)	% Height	Integration Type	Points Across Peak	Start Time (min)	End Time (min)
1	4.572	Unknown	38937	1.70	6487	1.72	VV	271	4.428	4.880
2	5.078	Unknown	2254617	98.30	370207	98.28	VB	383	4.880	5.518

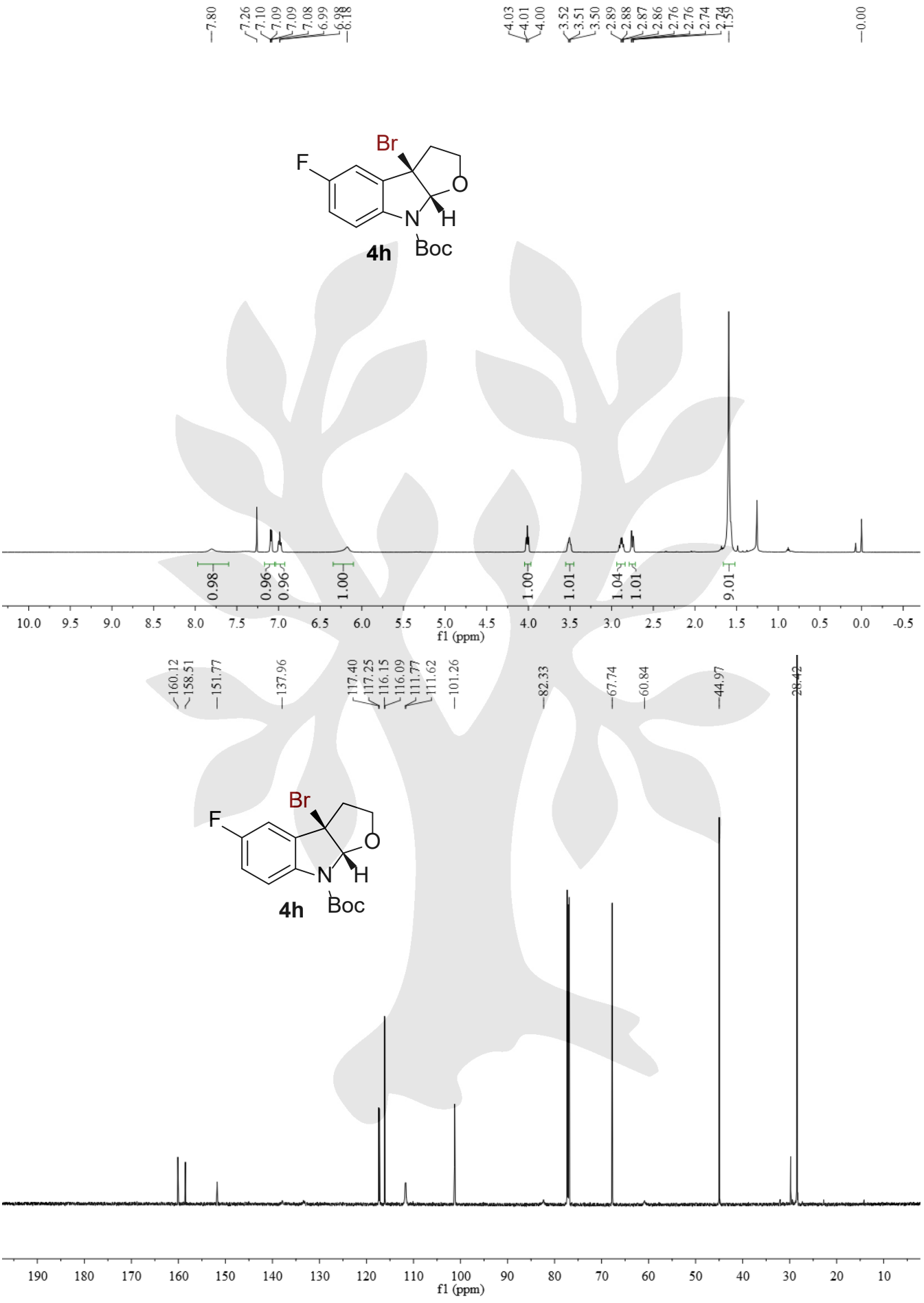

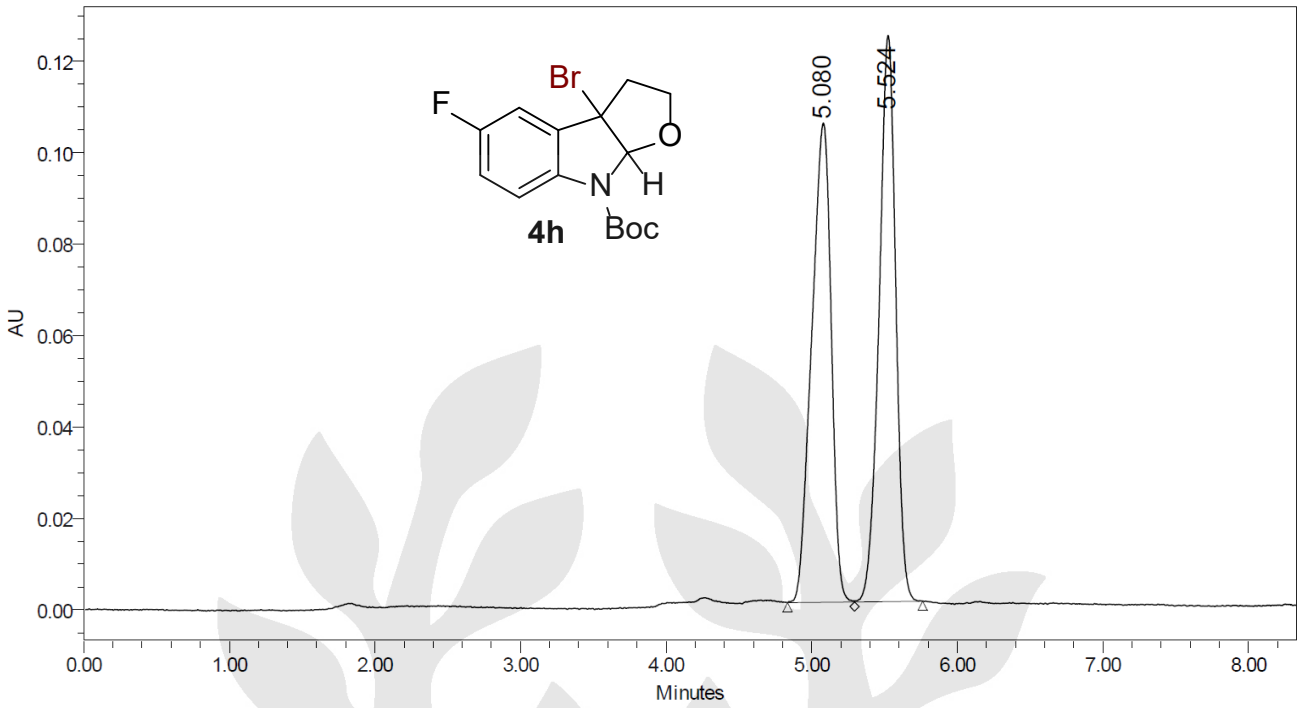

	RT (min)	Peak Type	Area (μV*sec)	% Area	Height (μV)	% Height	Integration Type	Points Across Peak	Start Time (min)	End Time (min)
1	5.080	Unknown	974611	49.78	104828	45.84	BV	276	4.833	5.293
2	5.524	Unknown	983237	50.22	123871	54.16	VB	281	5.293	5.762

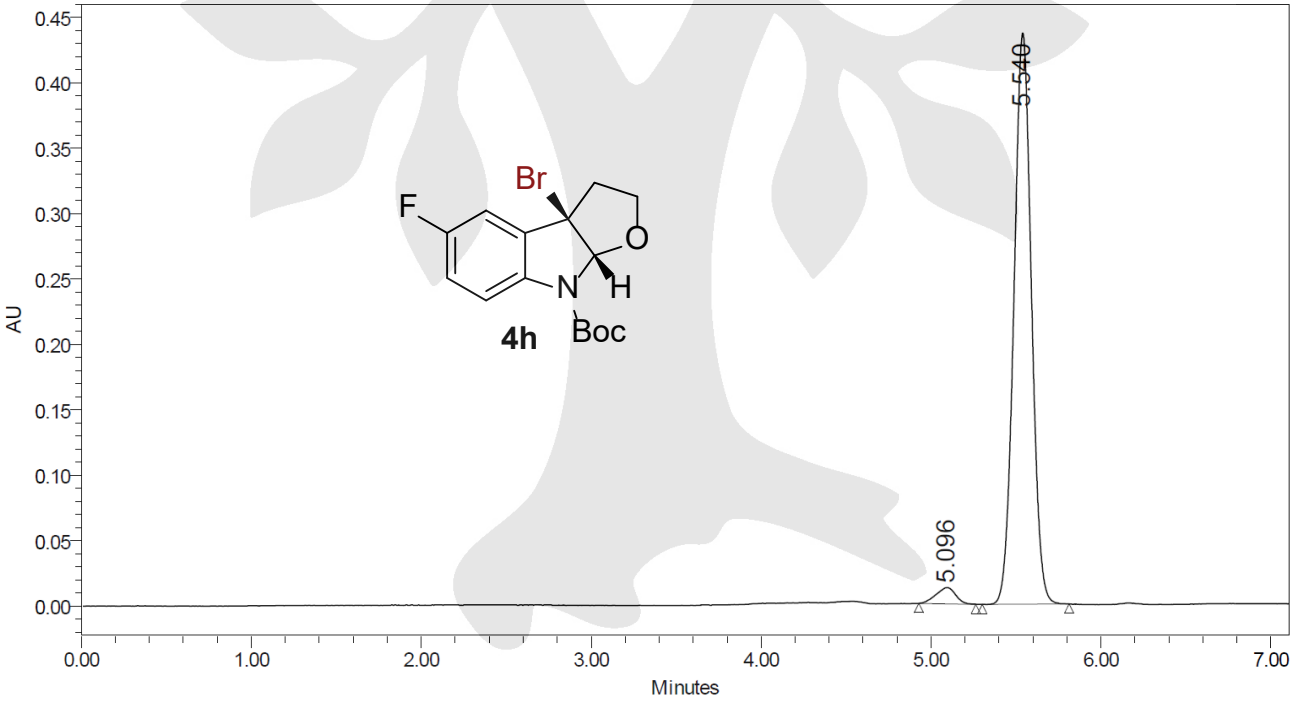

	RT (min)	Peak Type	Area (μV*sec)	% Area	Height (μV)	% Height	Integration Type	Points Across Peak	Start Time (min)	End Time (min)
1	5.096	Unknown	99659	3.10	12418	2.77	Bb	201	4.928	5.263
2	5.540	Unknown	3113194	96.90	436572	97.23	bB	307	5.302	5.813

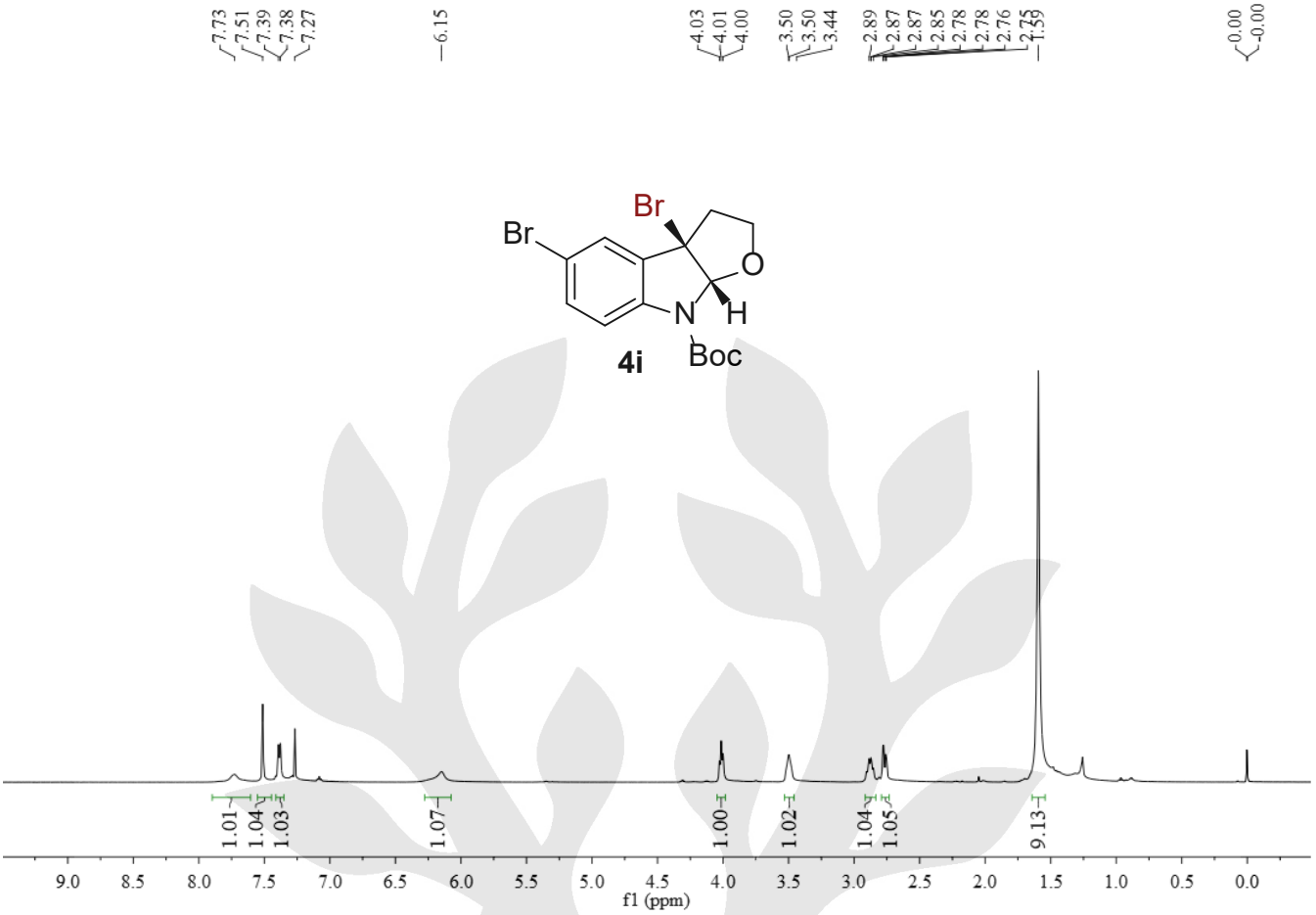

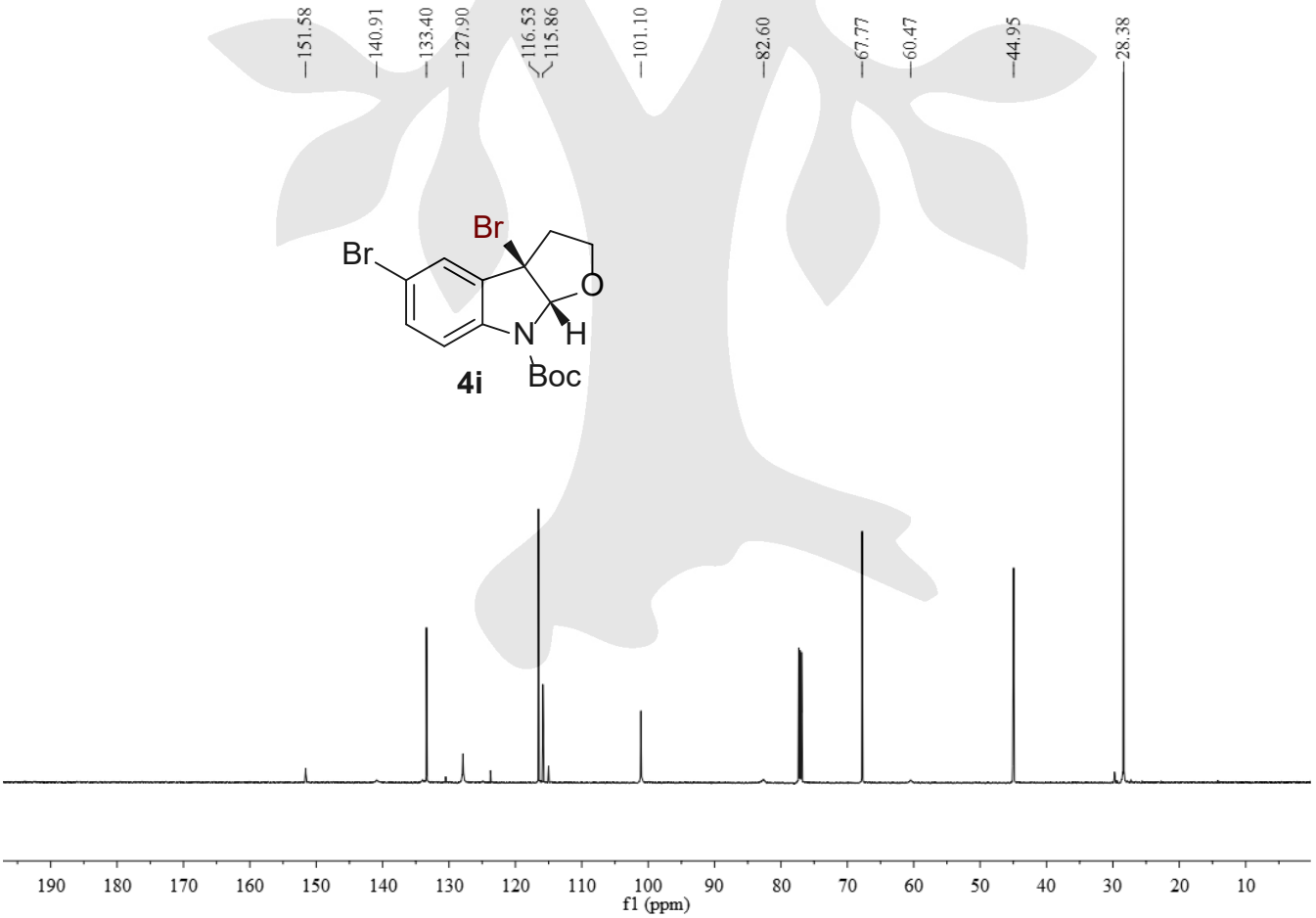

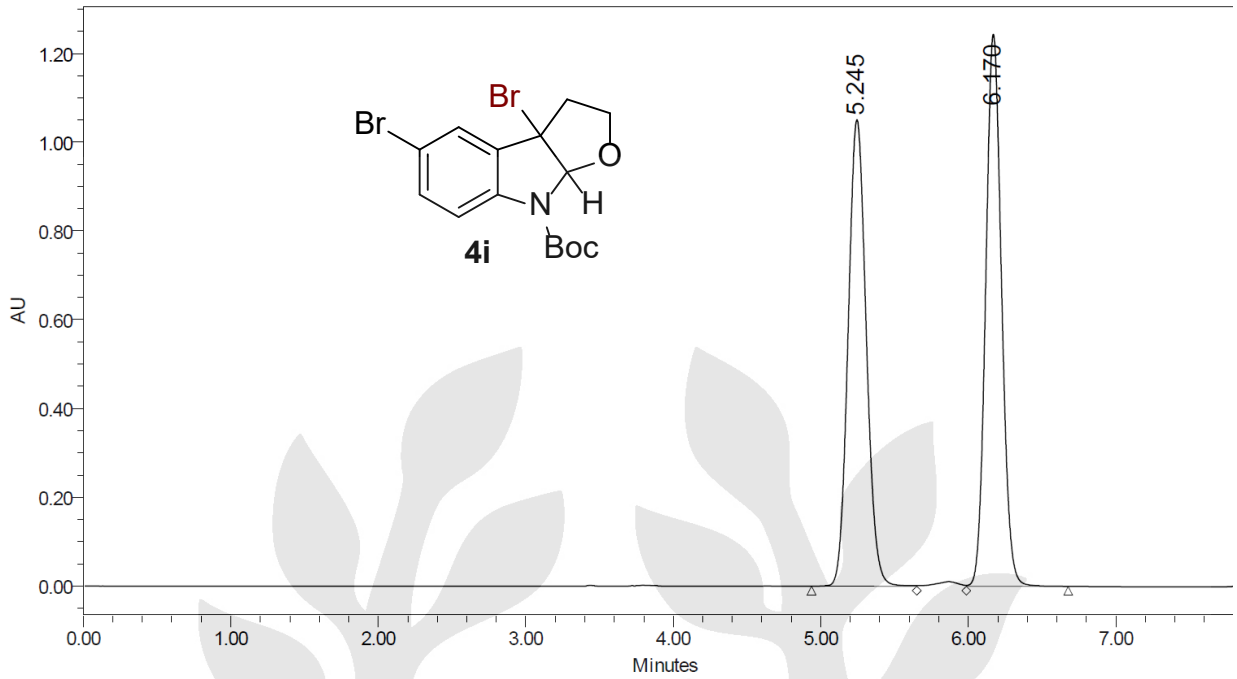

	RT (min)	Peak Type	Area (μV*sec)	% Area	Height (μV)	% Height	Integration Type	Points Across Peak	Start Time (min)	End Time (min)
1	5.245	Unknown	8960635	49.13	1050966	45.79	BV	428	4.937	5.650
2	6.170	Unknown	9276477	50.87	1244013	54.21	VB	414	5.987	6.677

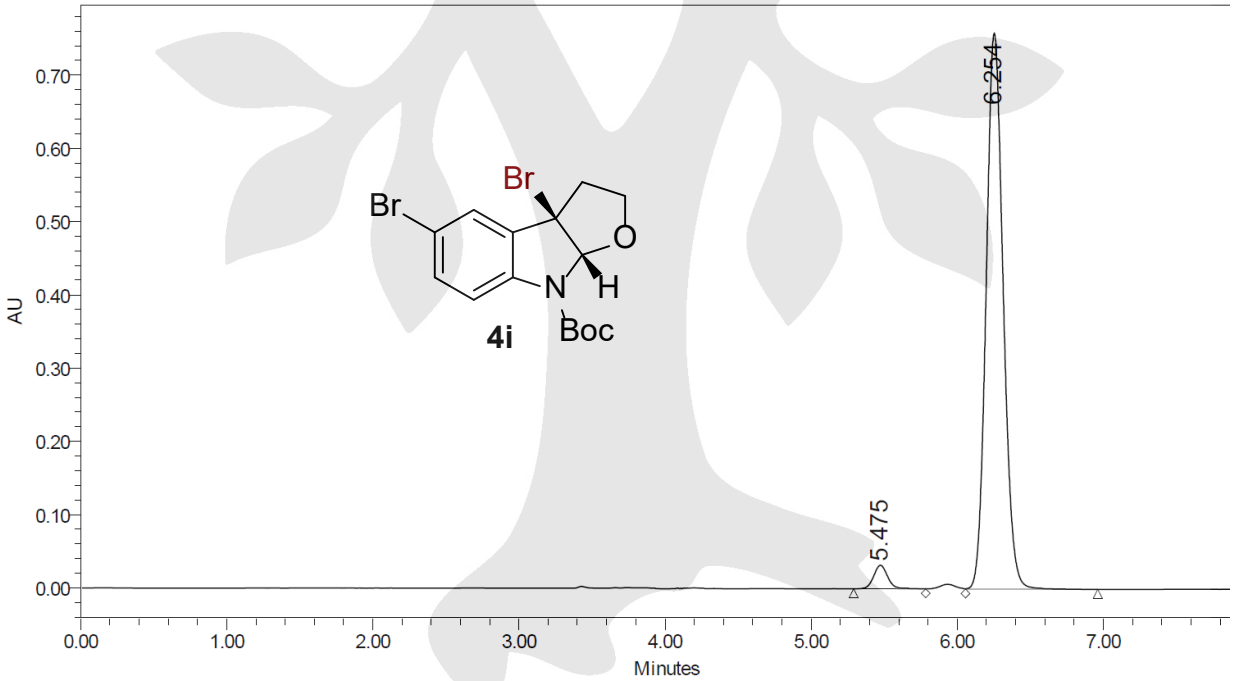

	RT (min)	Peak Type	Area (μV*sec)	% Area	Height (μV)	% Height	Integration Type	Points Across Peak	Start Time (min)	End Time (min)
1	5.475	Unknown	214131	3.37	32046	4.05	BV	296	5.292	5.785
2	6.254	Unknown	6139271	96.63	759120	95.95	VB	543	6.057	6.962

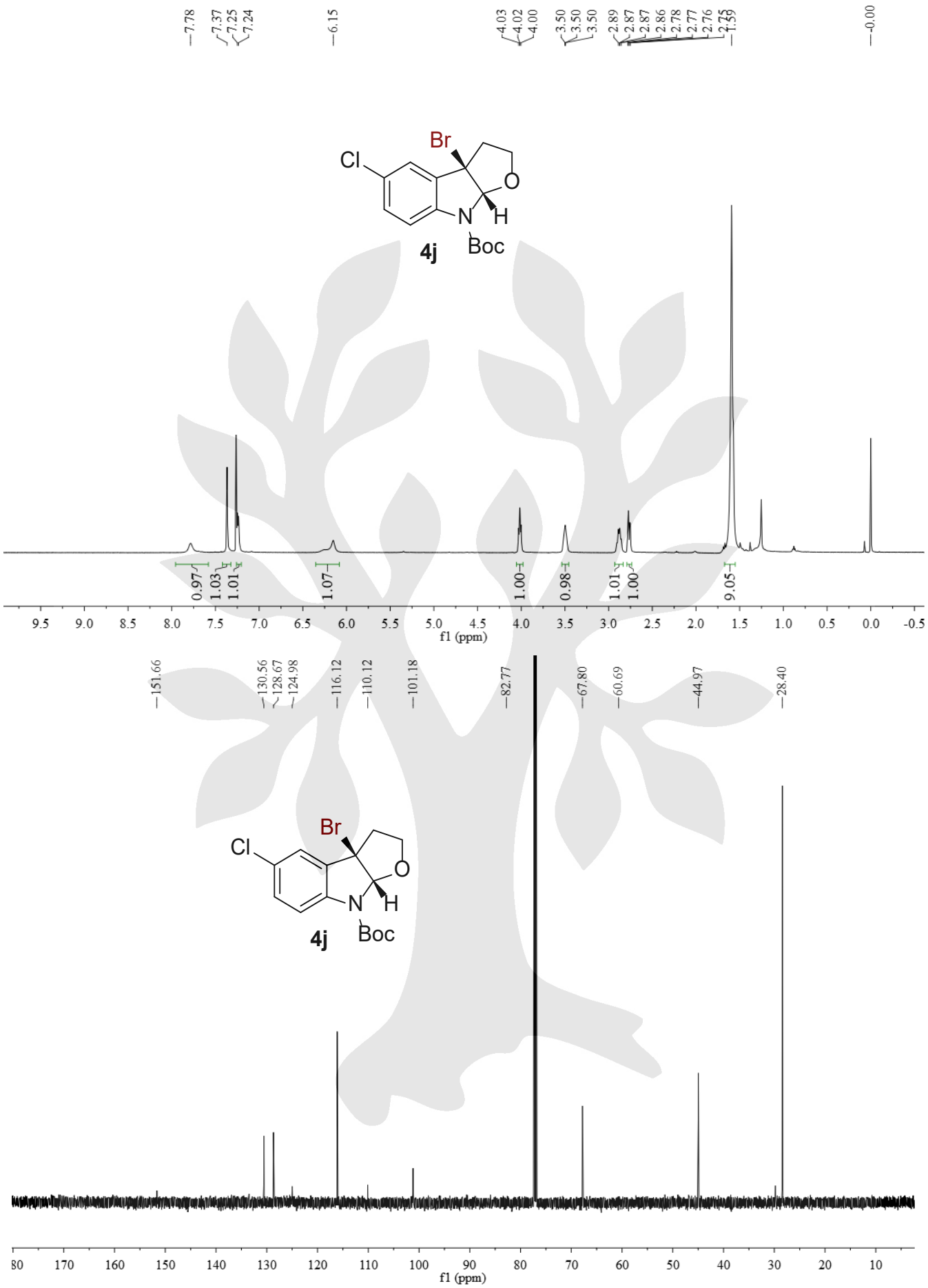

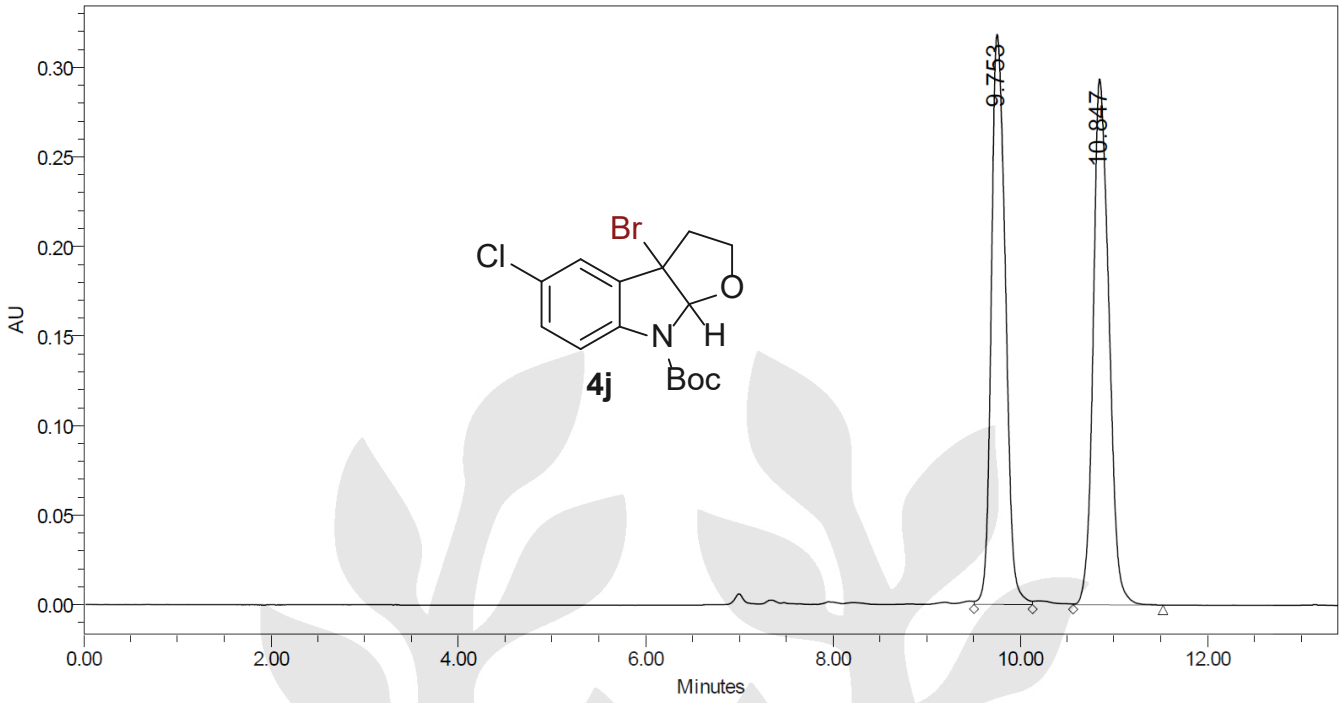

	RT (min)	Area (μV*sec)	% Area	Height (μV)	% Height
1	9.753	3346165	49.40	318427	52.02
2	10.847	3427972	50.60	293639	47.98

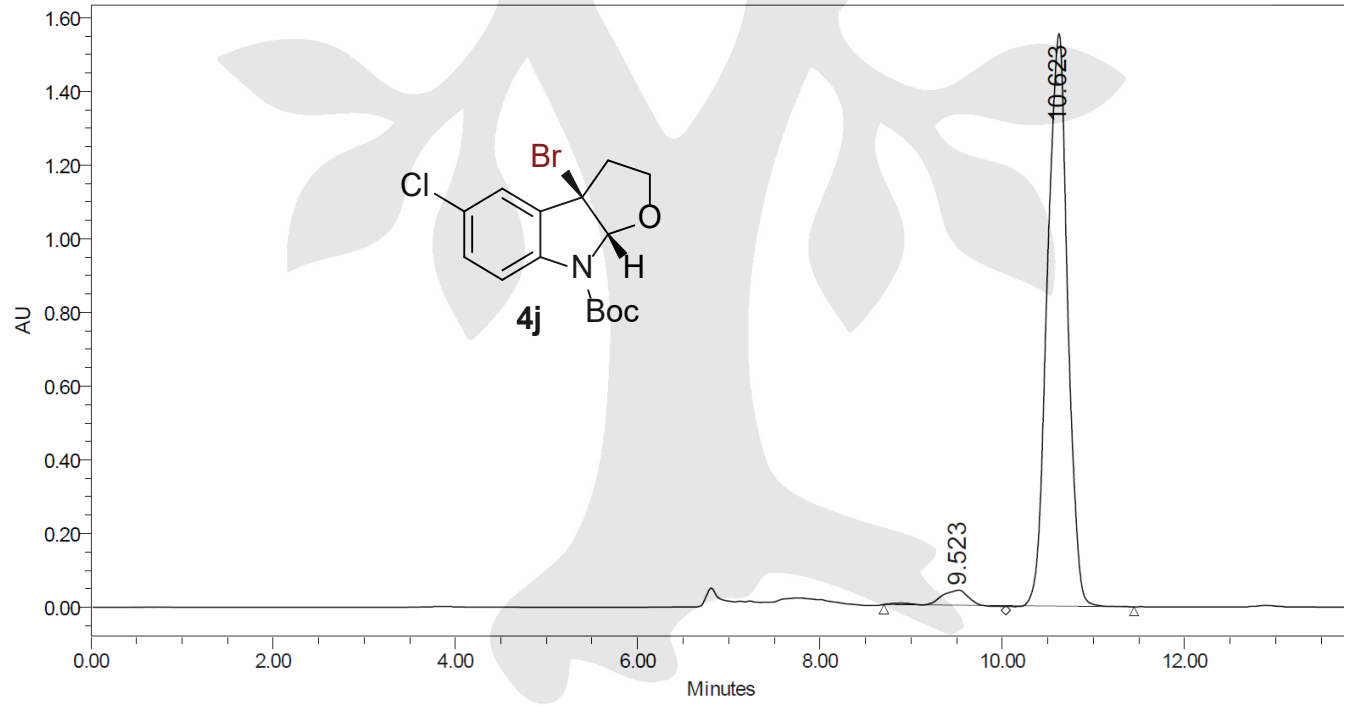

	RT (min)	Area (μV*sec)	% Area	Height (μV)	% Height
1	9.523	875875	3.52	40762	2.56
2	10.623	24027871	96.48	1553678	97.44

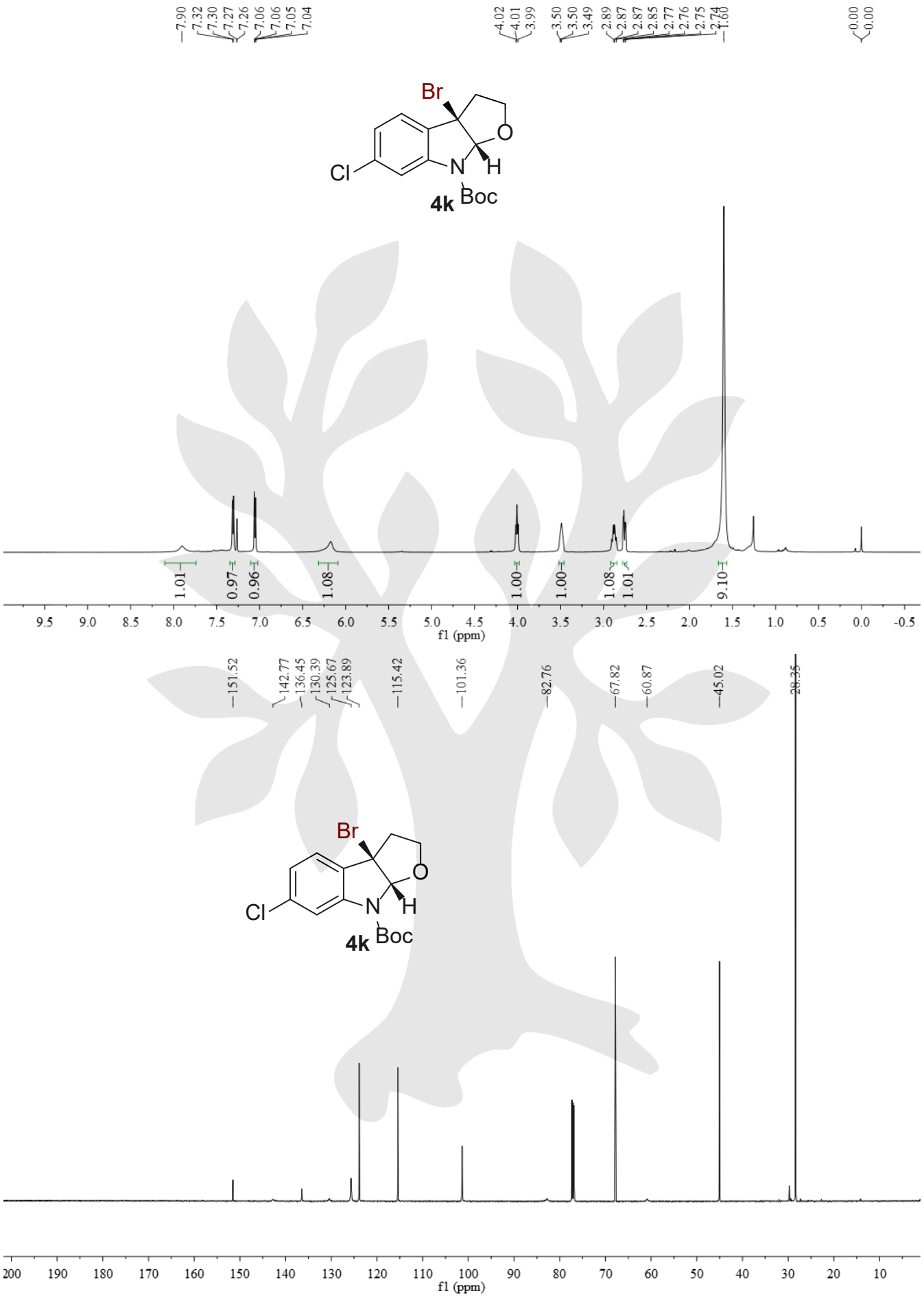

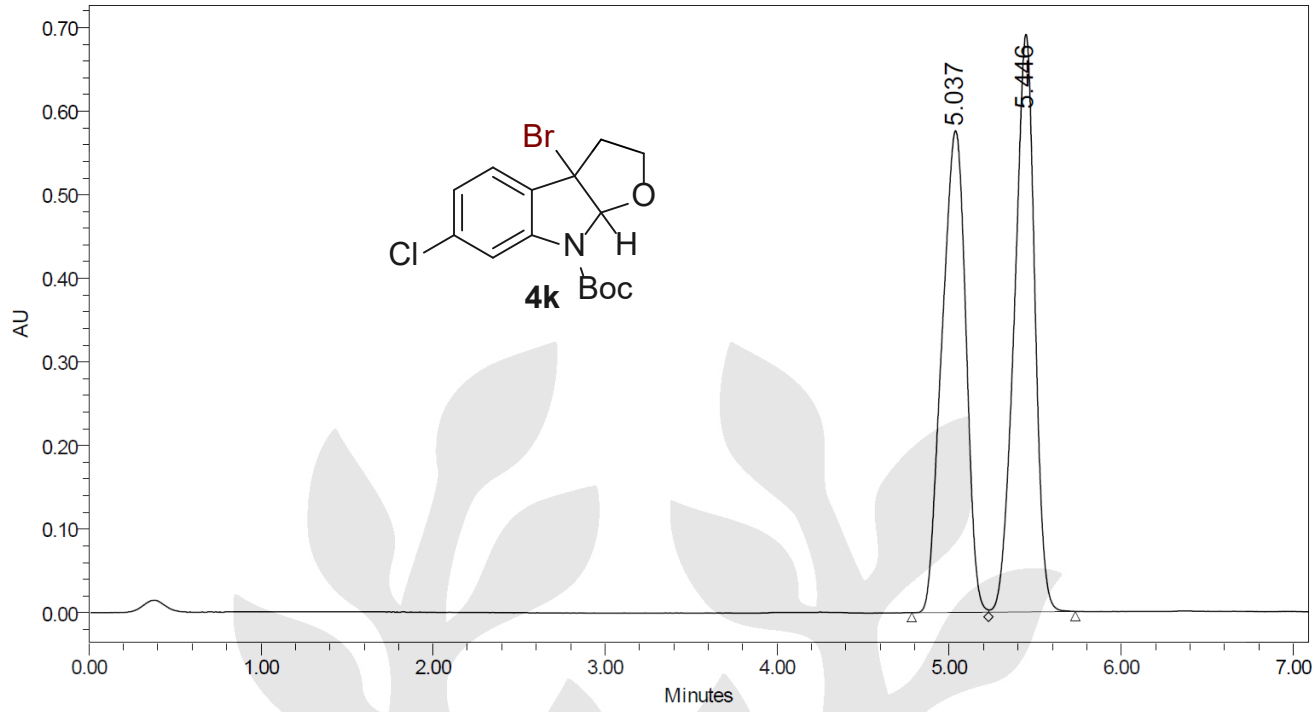

	RT (min)	Peak Type	Area (μV*sec)	% Area	Height (μV)	% Height	Integration Type	Points Across Peak	Start Time (min)	End Time (min)
1	5.037	Unknown	5572942	49.56	576266	45.47	Bv	267	4.783	5.228
2	5.446	Unknown	5671517	50.44	690952	54.53	vB	303	5.228	5.733

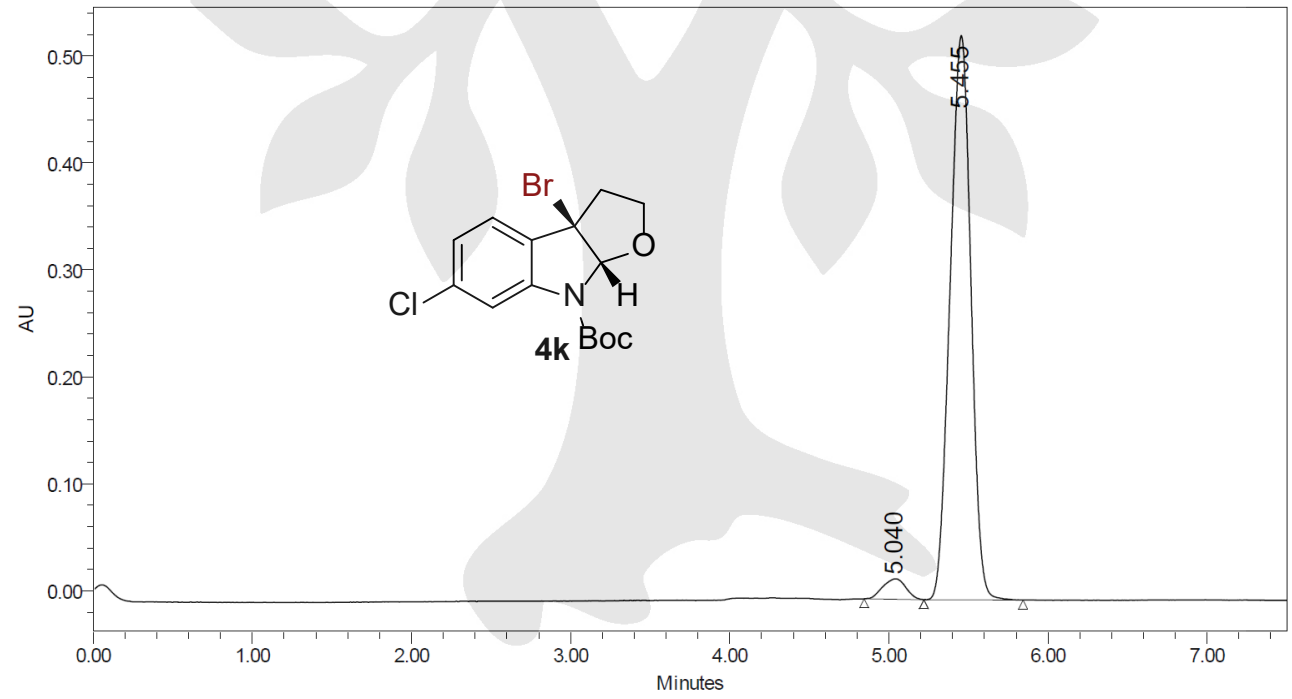

	RT (min)	Peak Type	Area (μV*sec)	% Area	Height (μV)	% Height	Integration Type	Points Across Peak	Start Time (min)	End Time (min)
1	5.040	Unknown	192249	3.87	19144	3.50	BB	225	4.845	5.220
2	5.455	Unknown	4781549	96.13	527492	96.50	BB	374	5.220	5.843

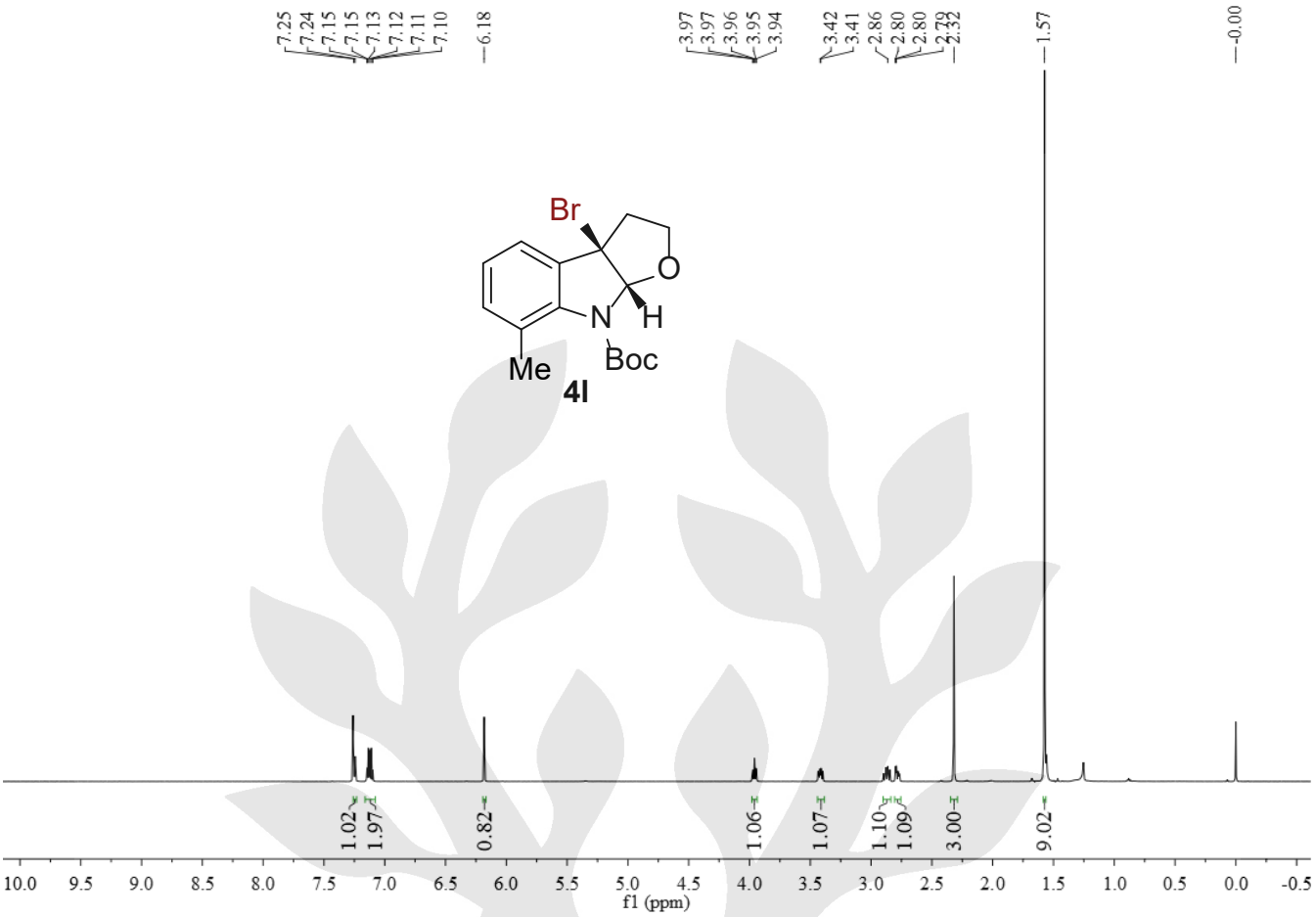

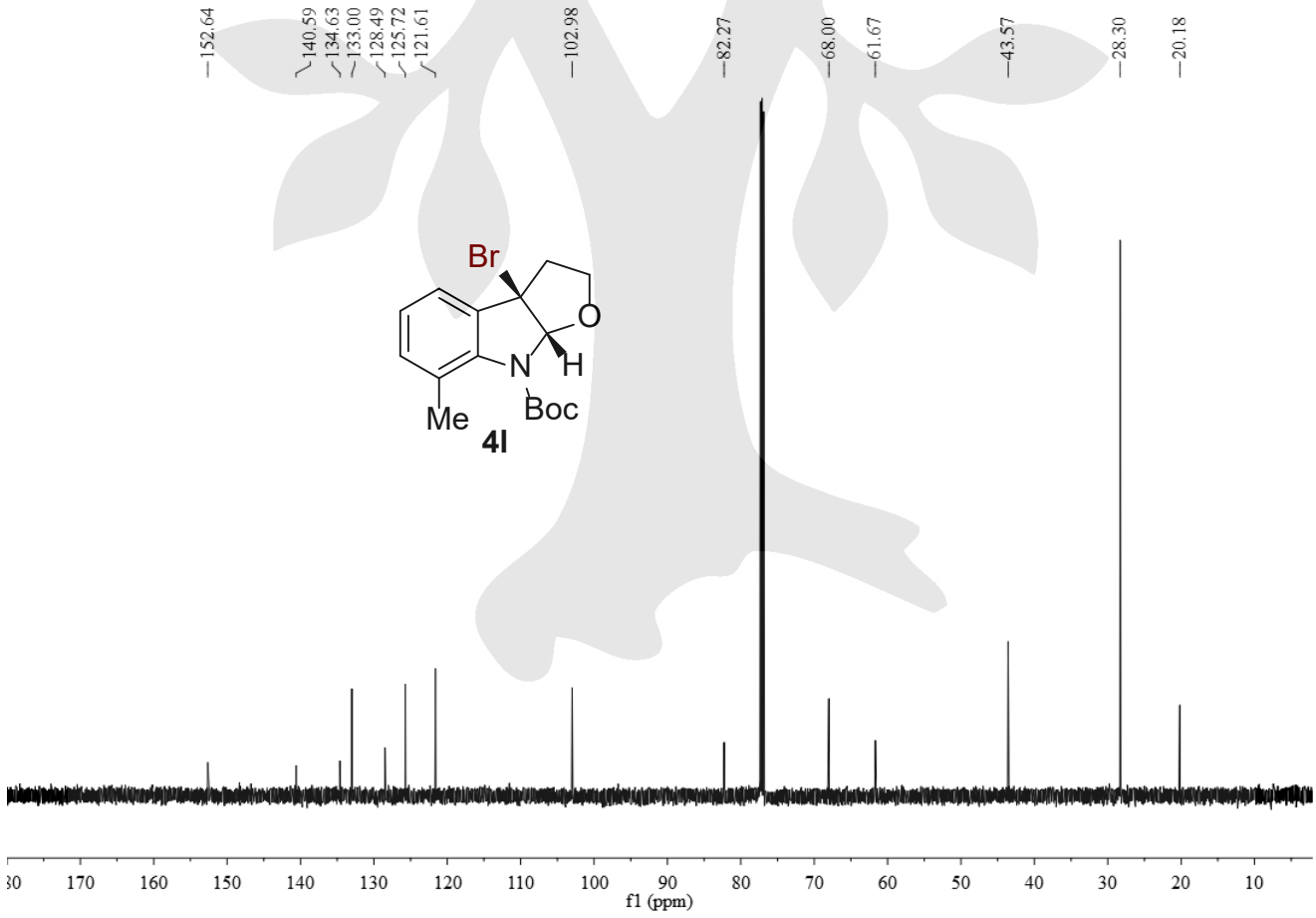

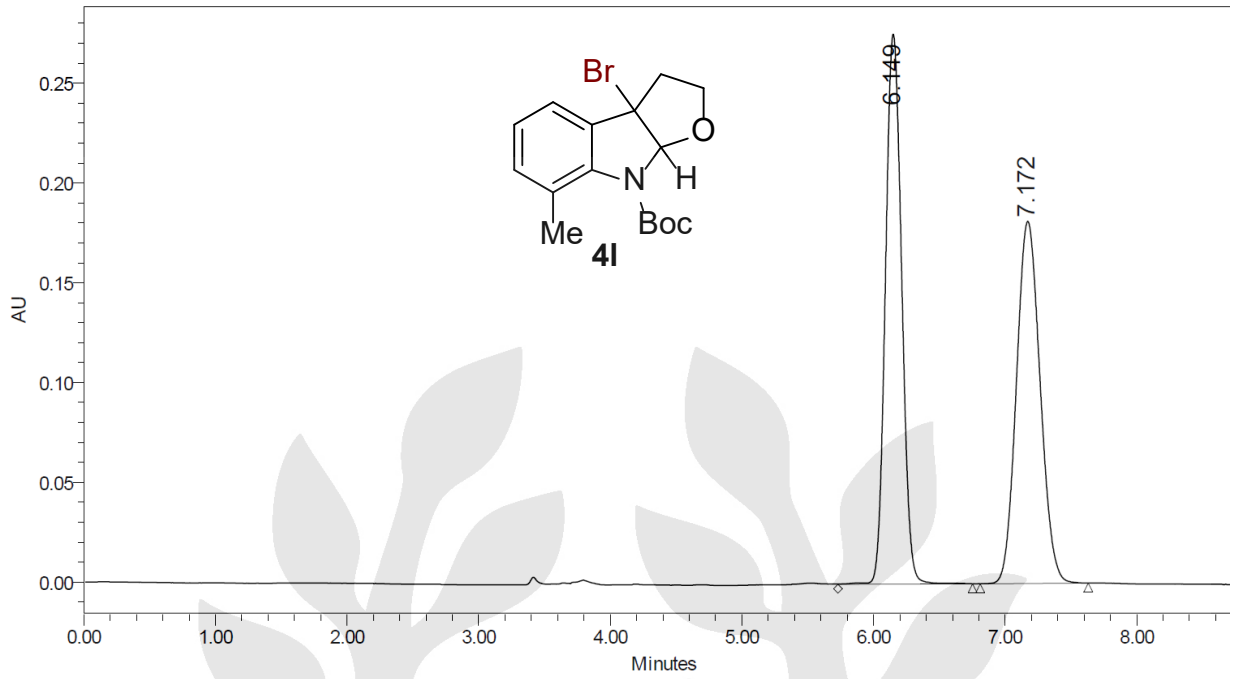

	RT (min)	Peak Type	Area (μV*sec)	% Area	Height (μV)	% Height	Integration Type	Points Across Peak	Start Time (min)	End Time (min)
1	6.149	Unknown	2362436	50.98	275633	60.30	VB	614	5.730	6.753
2	7.172	Unknown	2271482	49.02	181466	39.70	BB	493	6.810	7.632

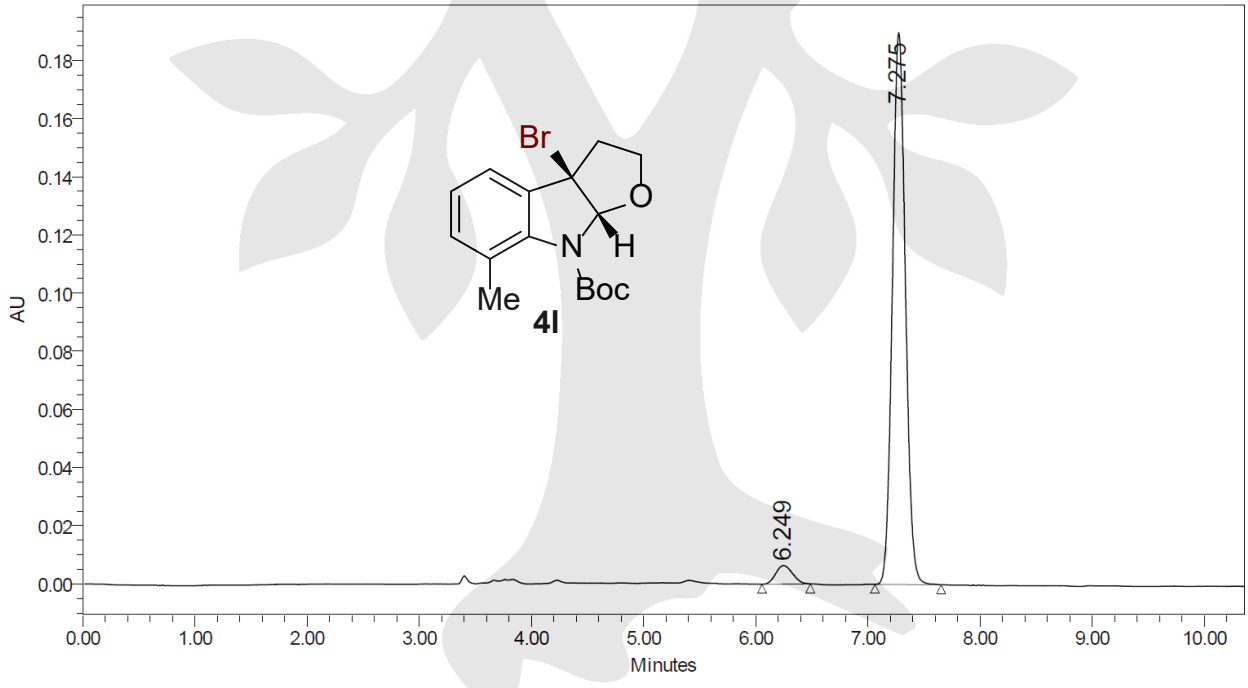

	RT (min)	Peak Type	Area (μV*sec)	% Area	Height (μV)	% Height	Integration Type	Points Across Peak	Start Time (min)	End Time (min)
1	6.249	Unknown	66365	4.17	6380	3.25	Bb	258	6.057	6.487
2	7.275	Unknown	1526081	95.83	189823	96.75	BB	355	7.062	7.653

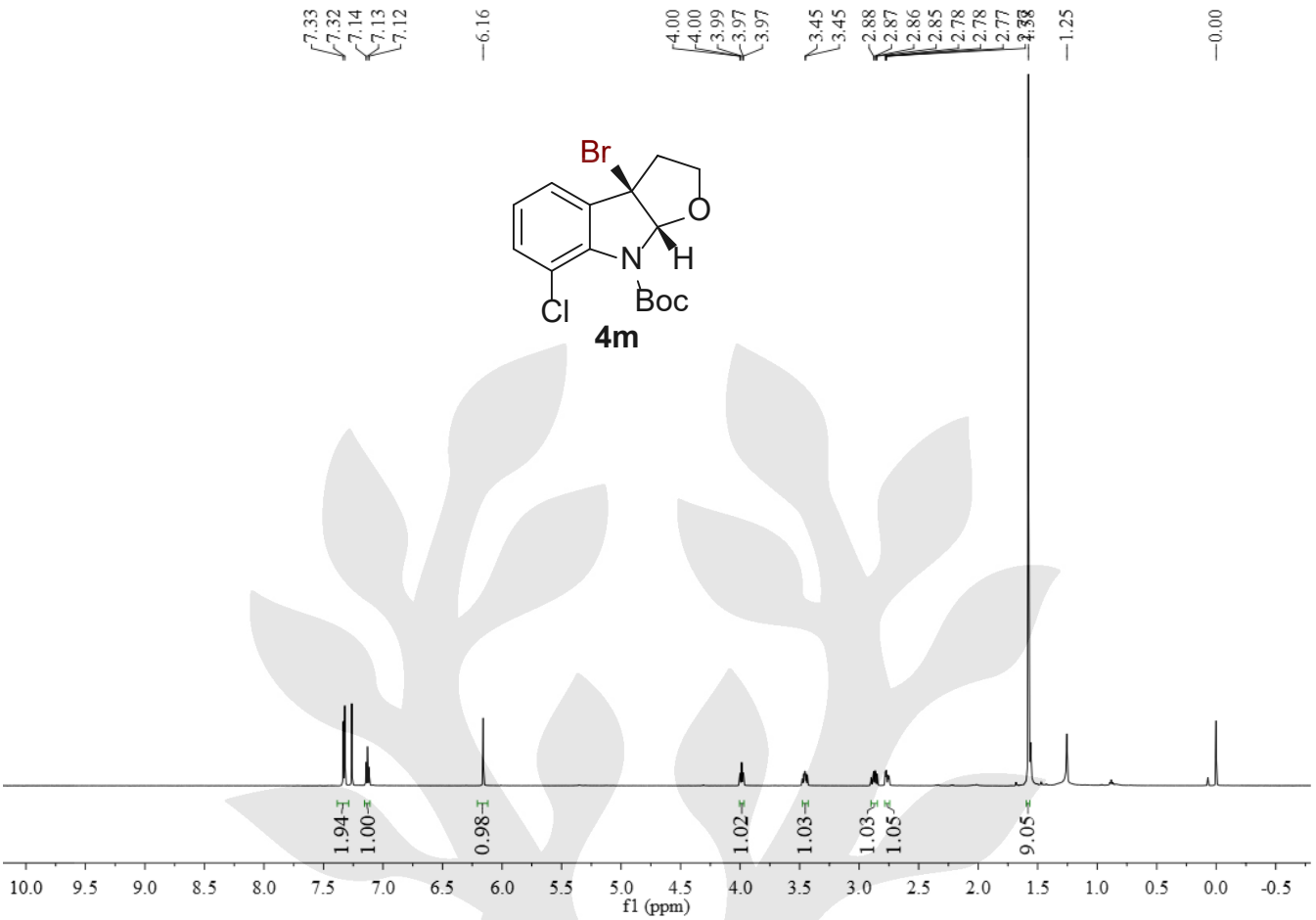

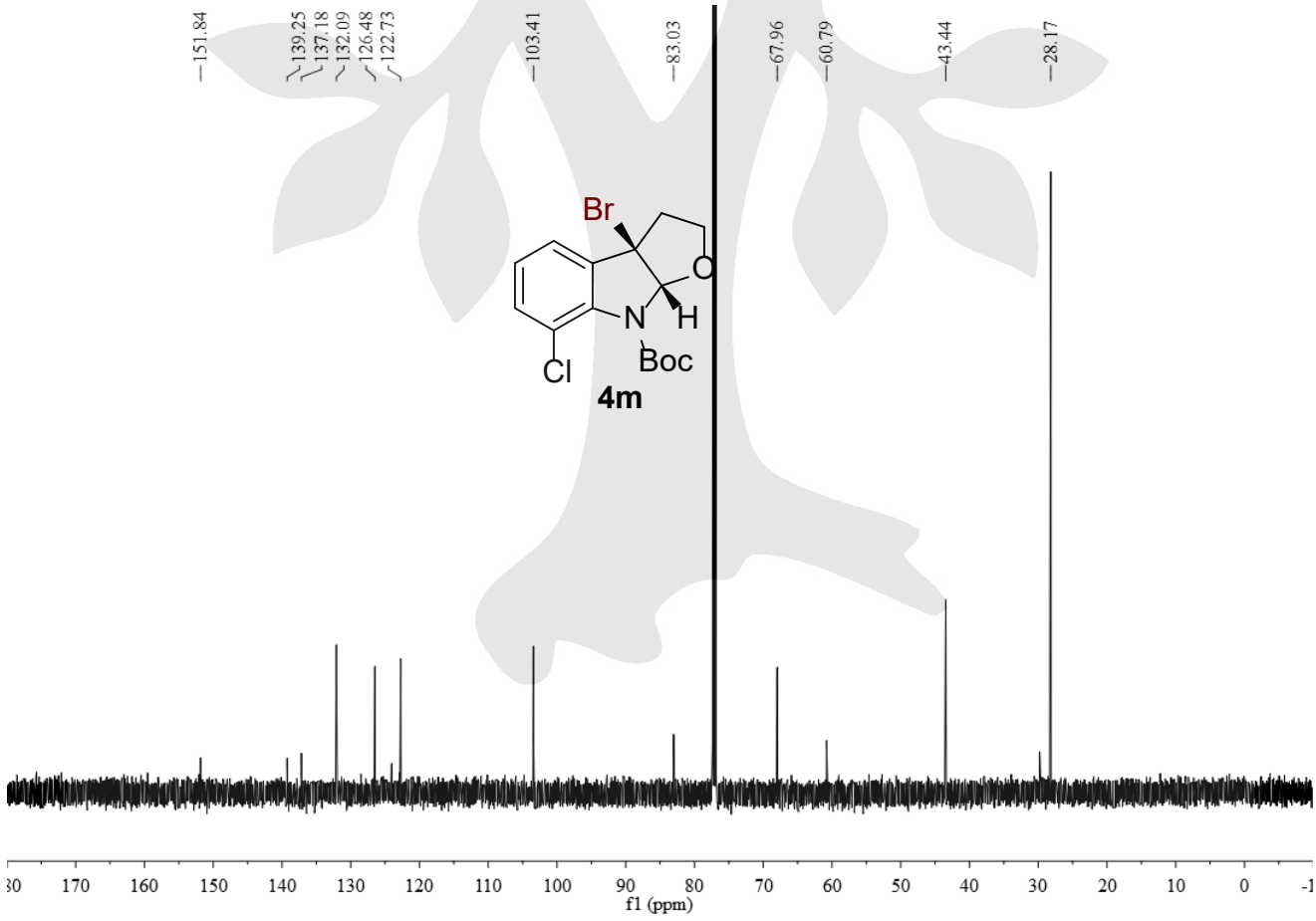

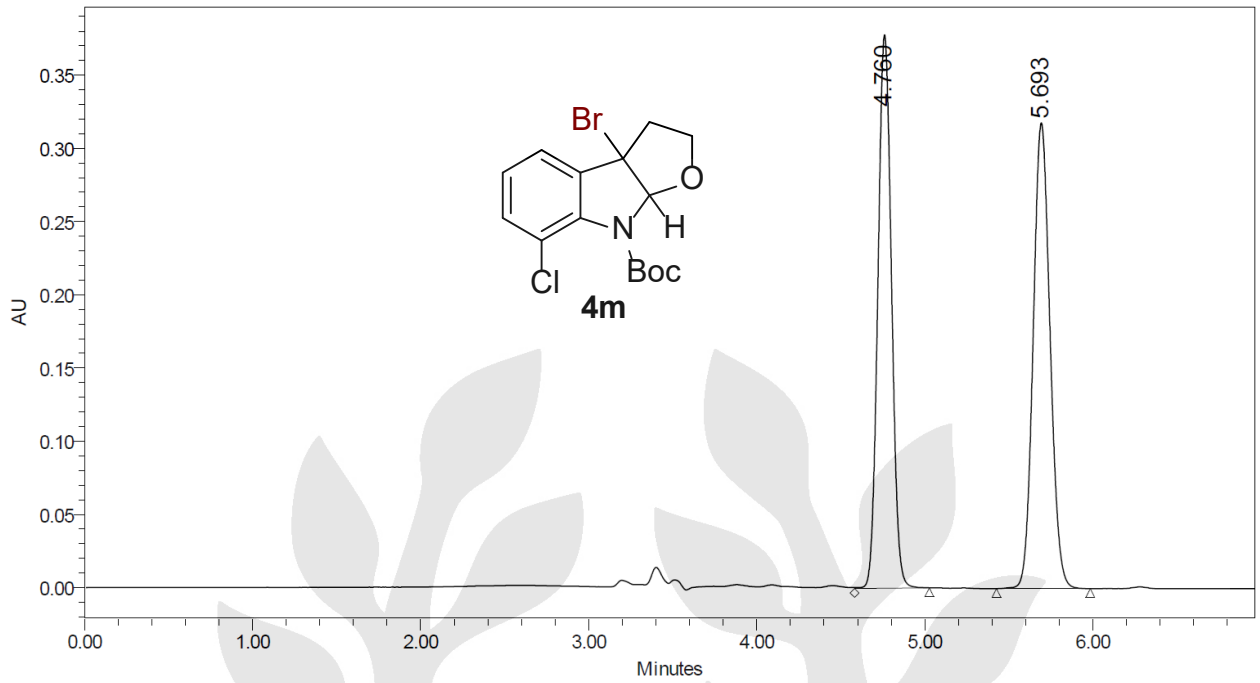

	RT (min)	Peak Type	Area (μV*sec)	% Area	Height (μV)	% Height	Integration Type	Points Across Peak	Start Time (min)	End Time (min)
1	4.760	Unknown	2126316	48.92	378002	54.30	VB	267	4.582	5.027
2	5.693	Unknown	2220449	51.08	318174	45.70	BB	335	5.427	5.985

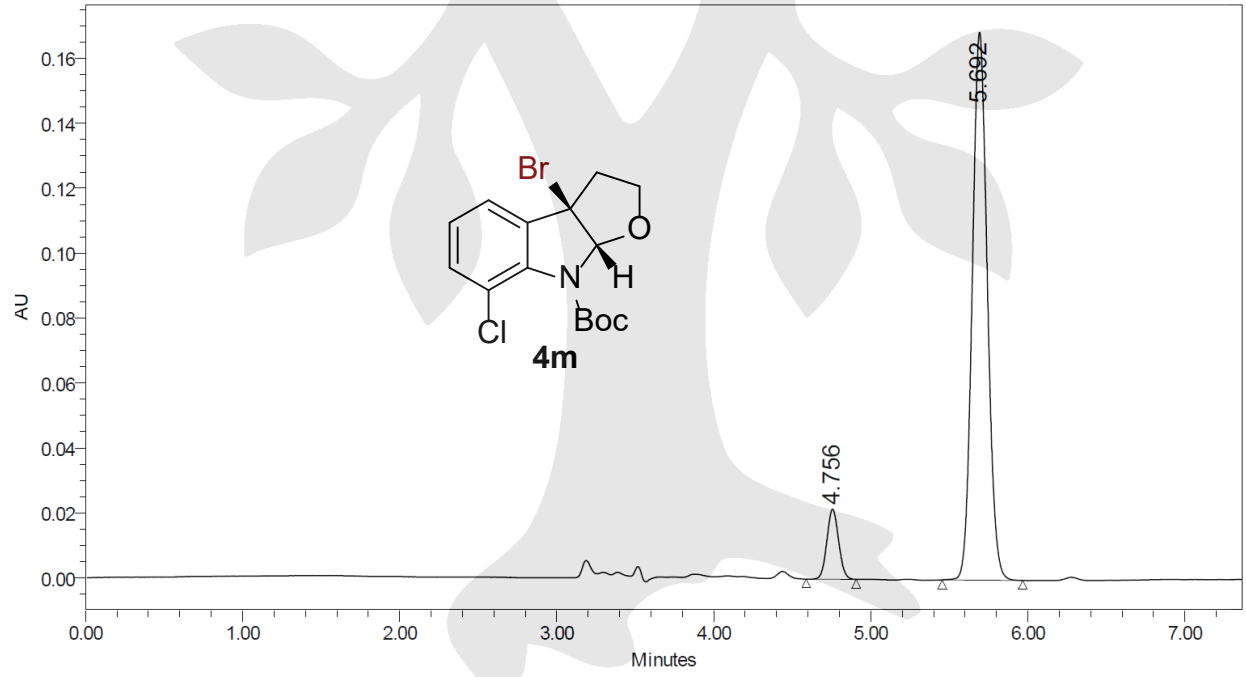

	RT (min)	Peak Type	Area (μV*sec)	% Area	Height (μV)	% Height	Integration Type	Points Across Peak	Start Time (min)	End Time (min)
1	4.756	Unknown	112557	9.11	21610	11.35	BB	191	4.588	4.907
2	5.692	Unknown	1122812	90.89	168740	88.65	BB	308	5.455	5.968

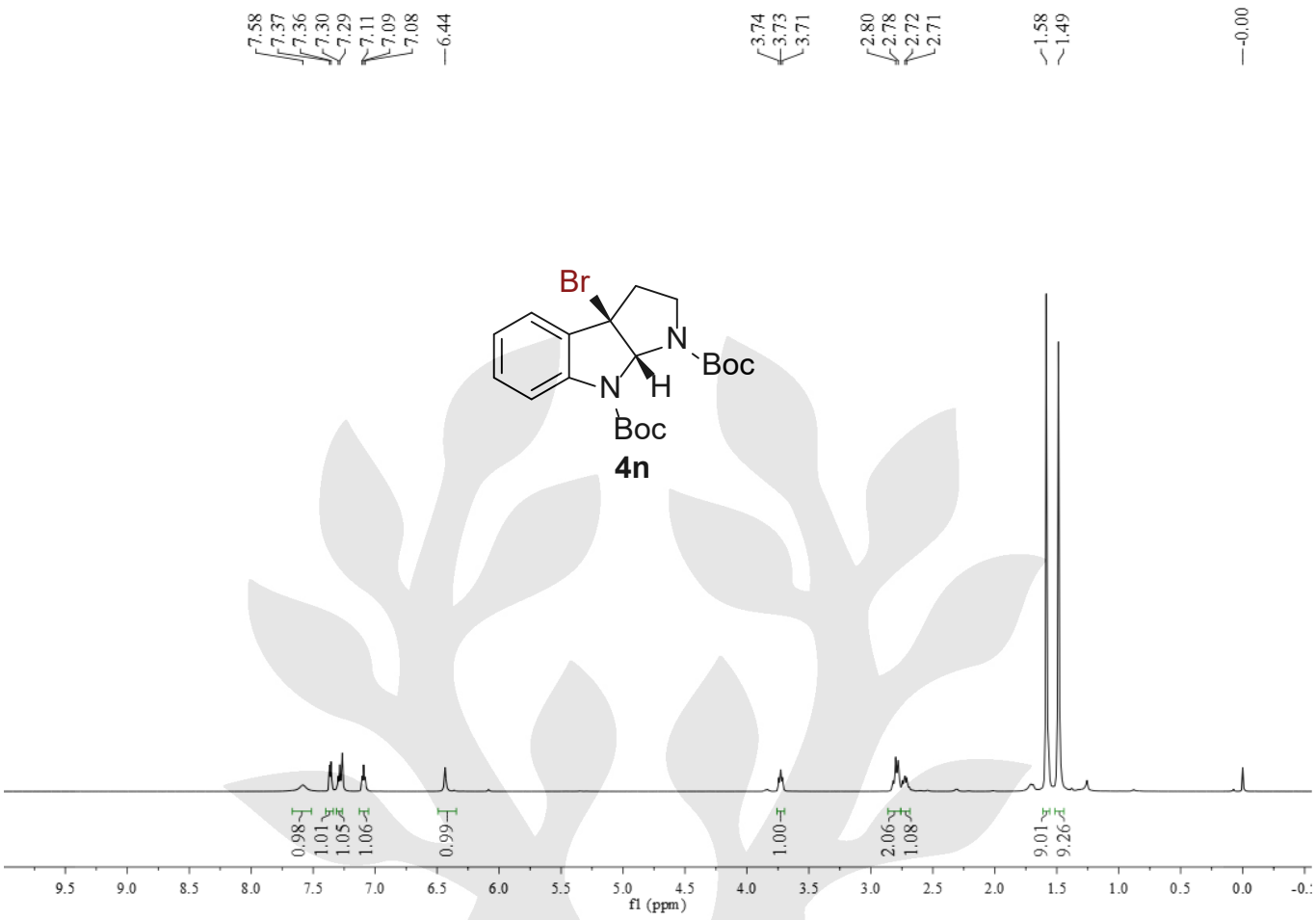

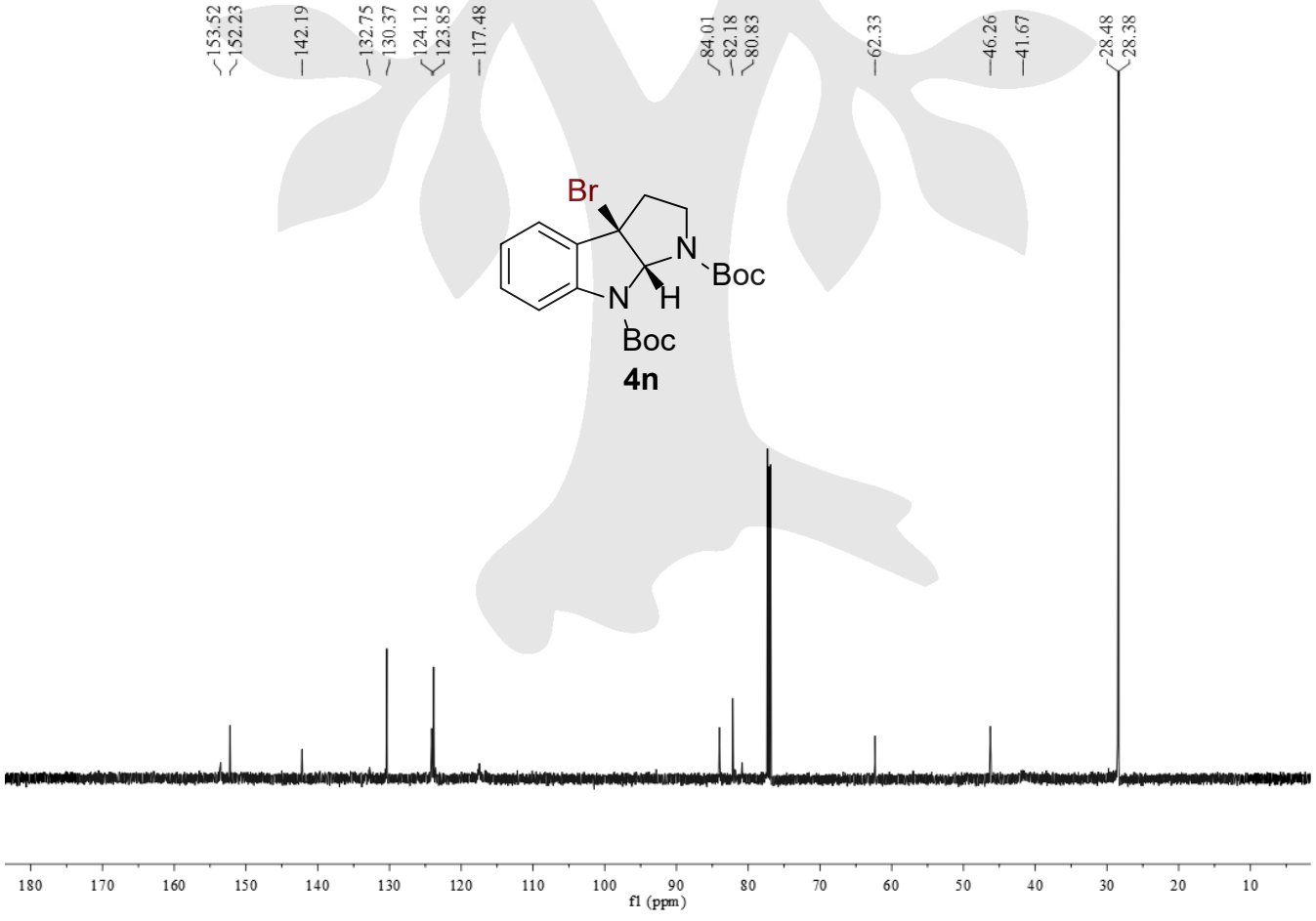

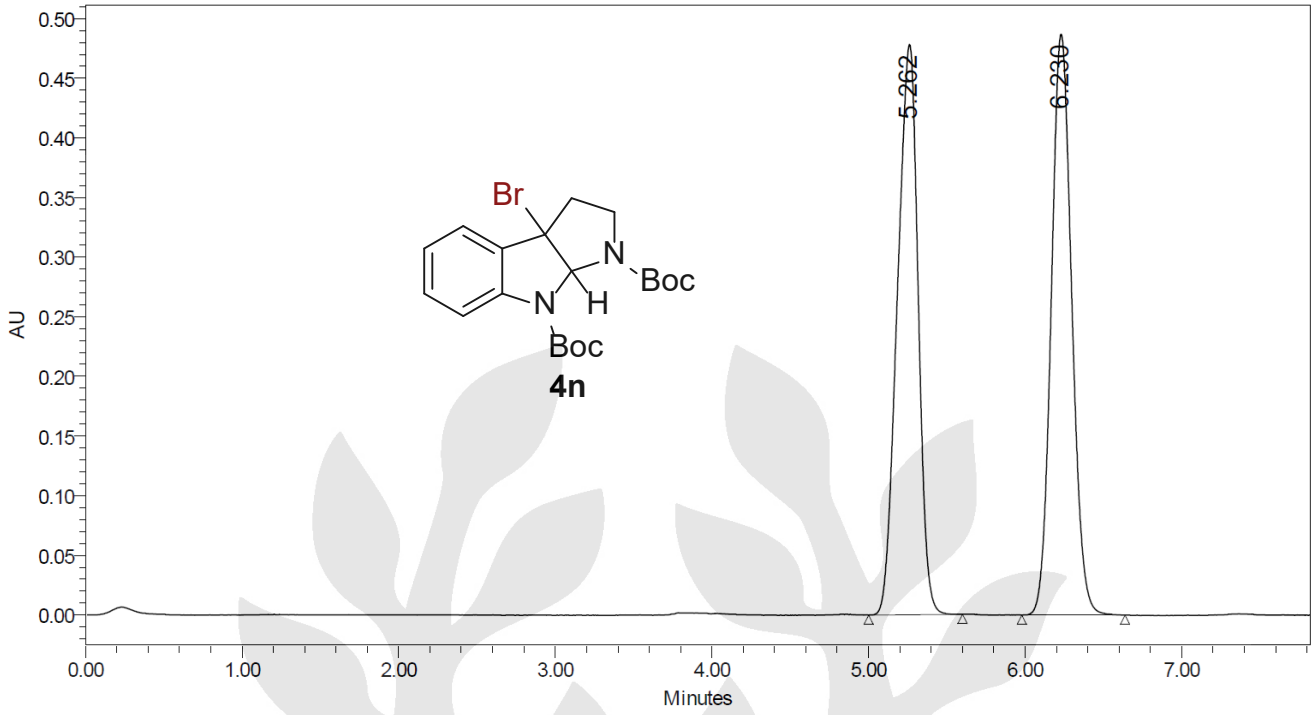

	RT (min)	Peak Type	Area (μV*sec)	% Area	Height (μV)	% Height	Integration Type	Points Across Peak	Start Time (min)	End Time (min)
1	5.262	Unknown	4401786	49.87	478247	49.54	BB	360	5.000	5.600
2	6.230	Unknown	4424784	50.13	487220	50.46	BB	396	5.978	6.638

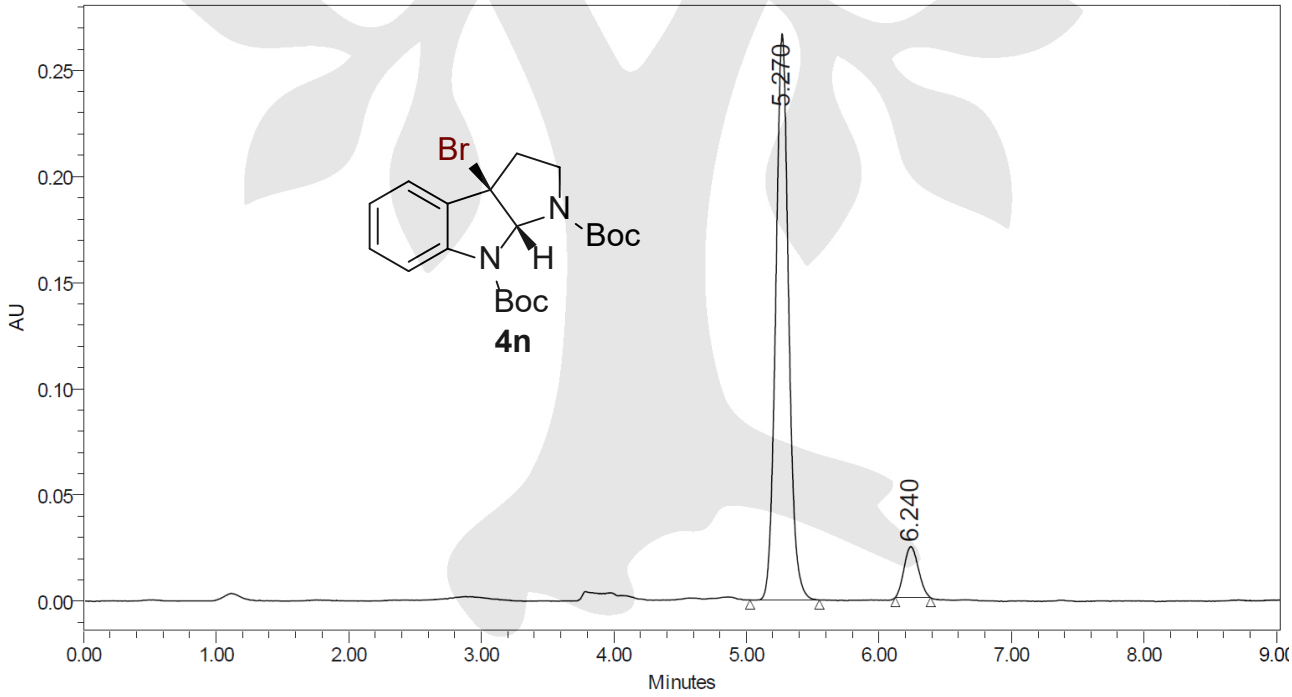

	RT (min)	Peak Type	Area (μV*sec)	% Area	Height (μV)	% Height	Integration Type	Points Across Peak	Start Time (min)	End Time (min)
1	5.270	Unknown	1807298	90.96	266743	91.75	bB	314	5.028	5.552
2	6.240	Unknown	179628	9.04	23975	8.25	bb	160	6.123	6.390

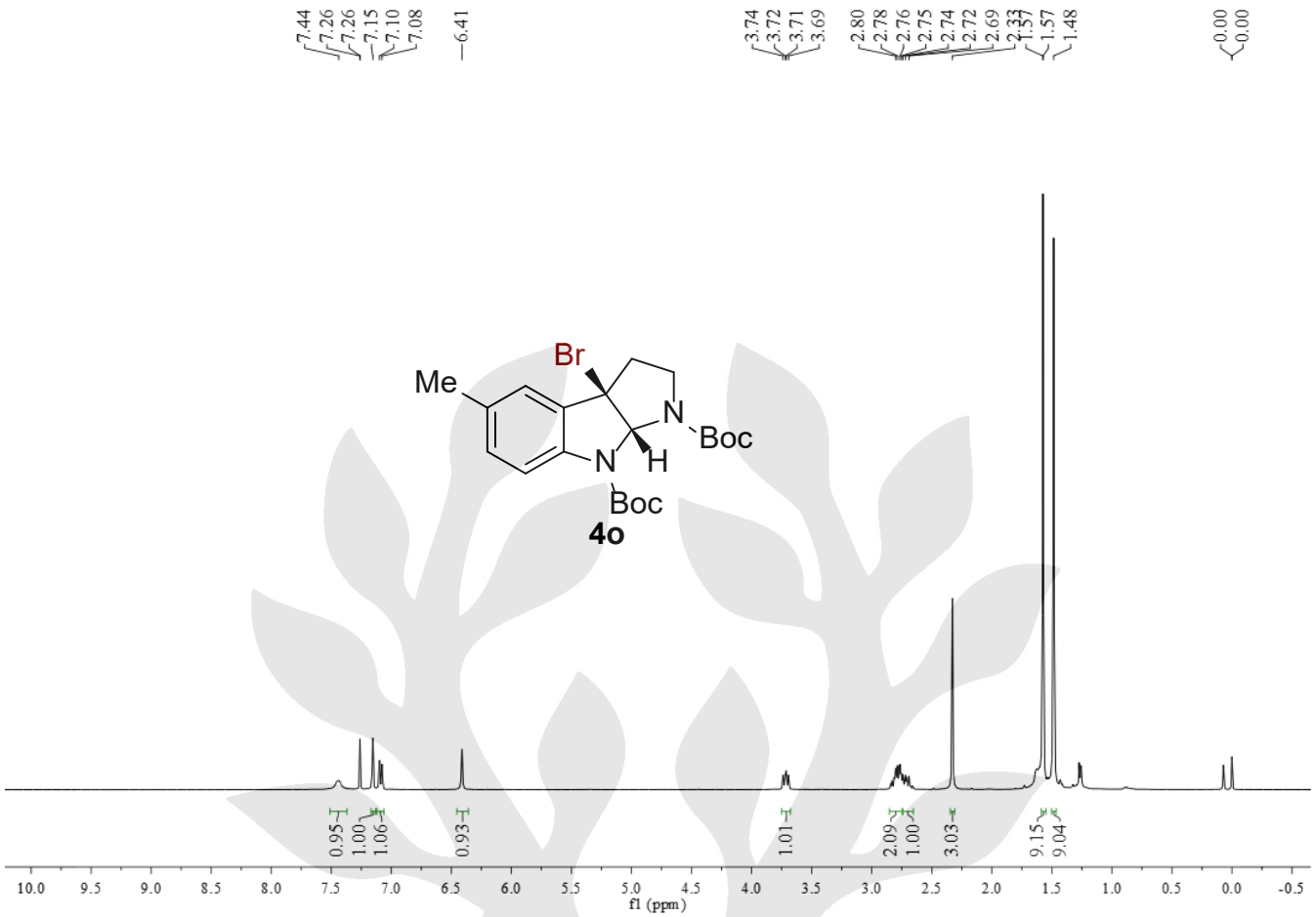

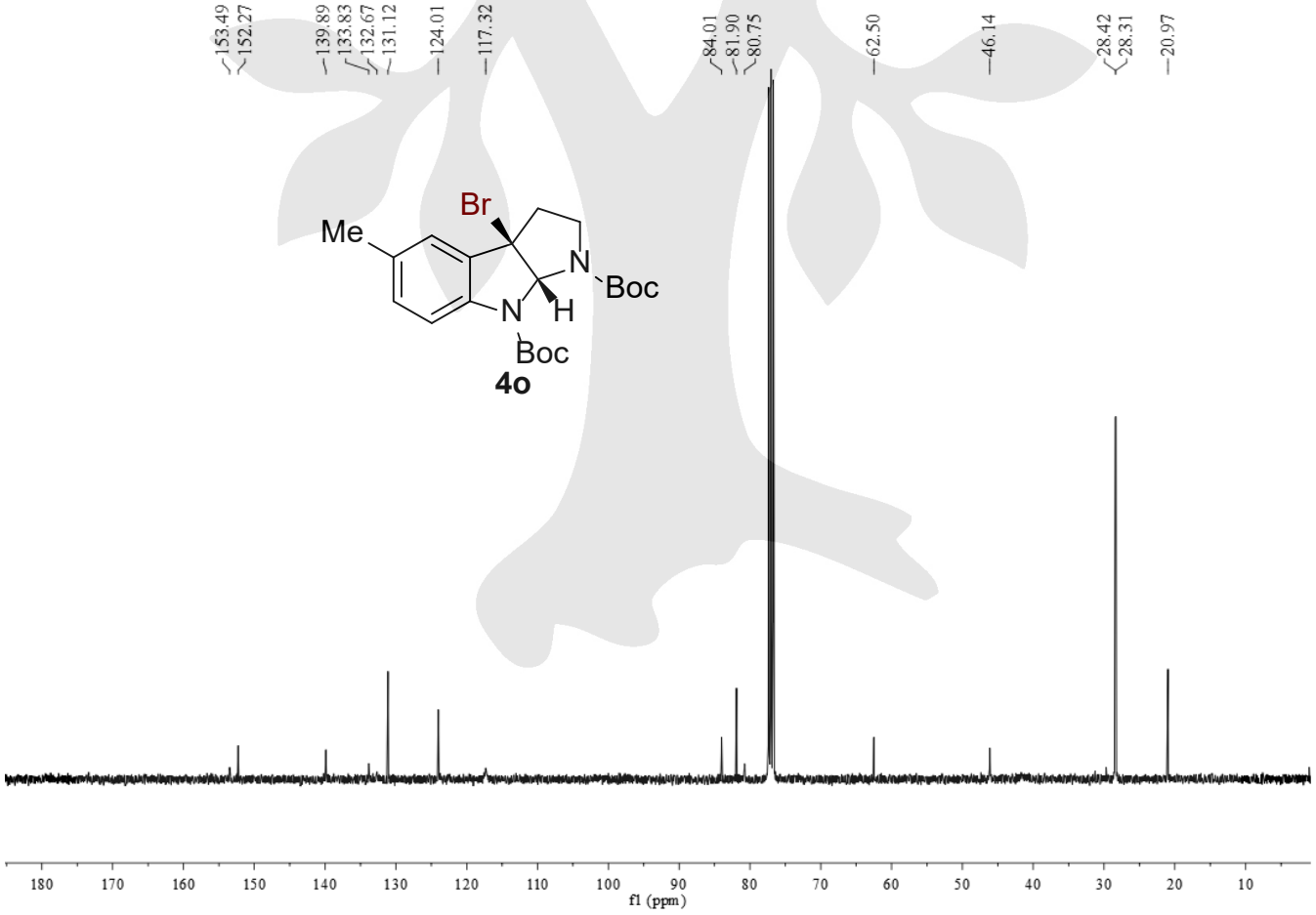

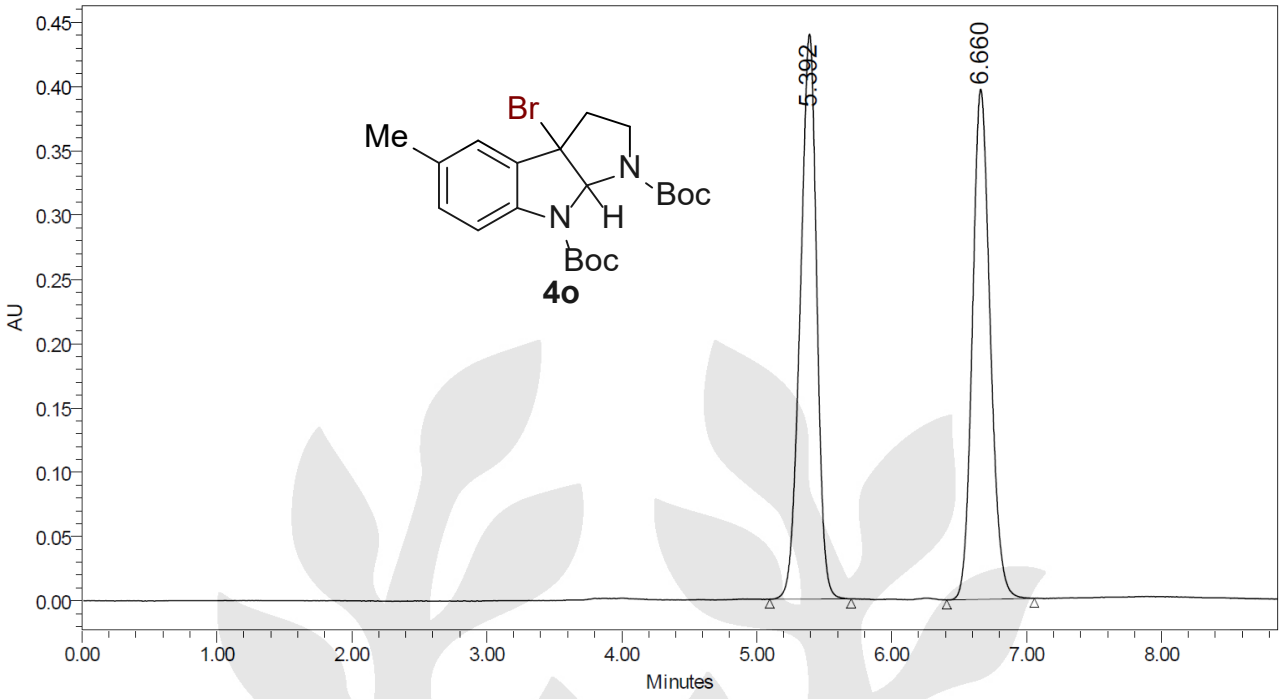

	RT (min)	Peak Type	Area (μV*sec)	% Area	Height (μV)	% Height	Integration Type	Points Across Peak	Start Time (min)	End Time (min)
1	5.392	Unknown	3742544	50.72	439366	52.56	bB	362	5.097	5.700
2	6.660	Unknown	3636483	49.28	396608	47.44	BB	390	6.408	7.058

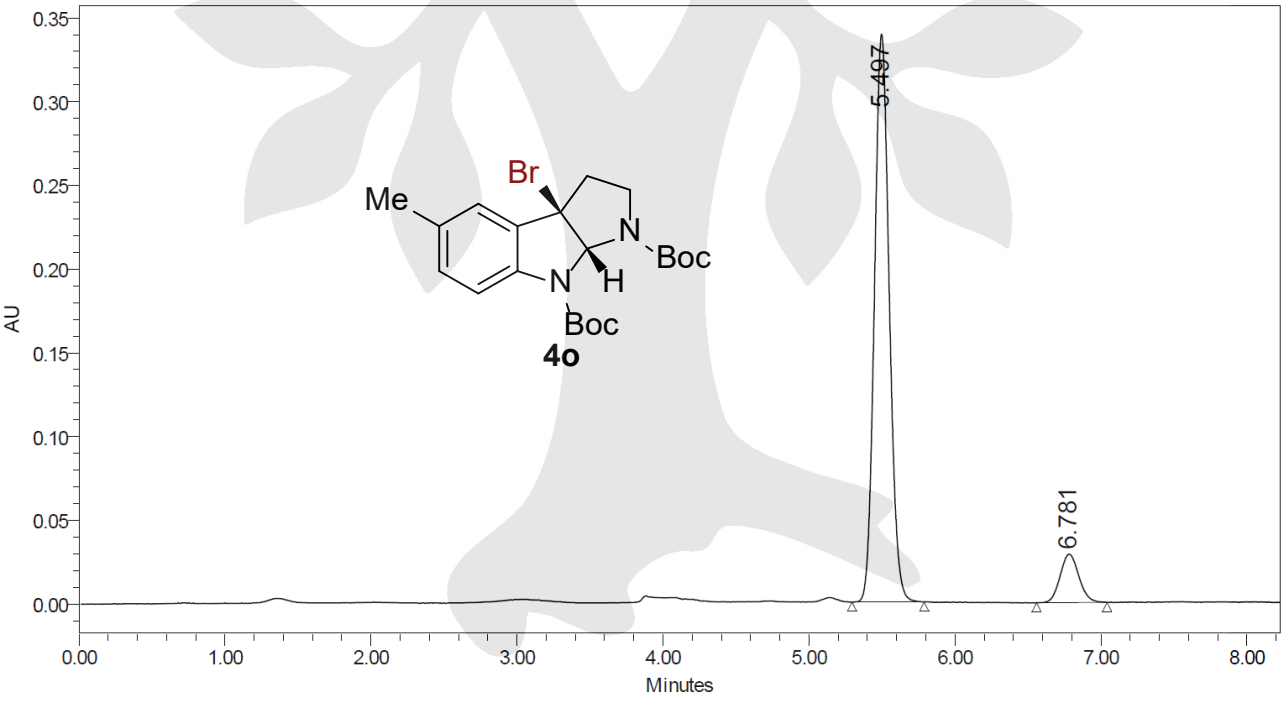

	RT (min)	Peak Type	Area (μV*sec)	% Area	Height (μV)	% Height	Integration Type	Points Across Peak	Start Time (min)	End Time (min)
1	5.497	Unknown	2388657	90.31	339215	92.16	BB	296	5.295	5.788
2	6.781	Unknown	256385	9.69	28844	7.84	bB	290	6.558	7.042

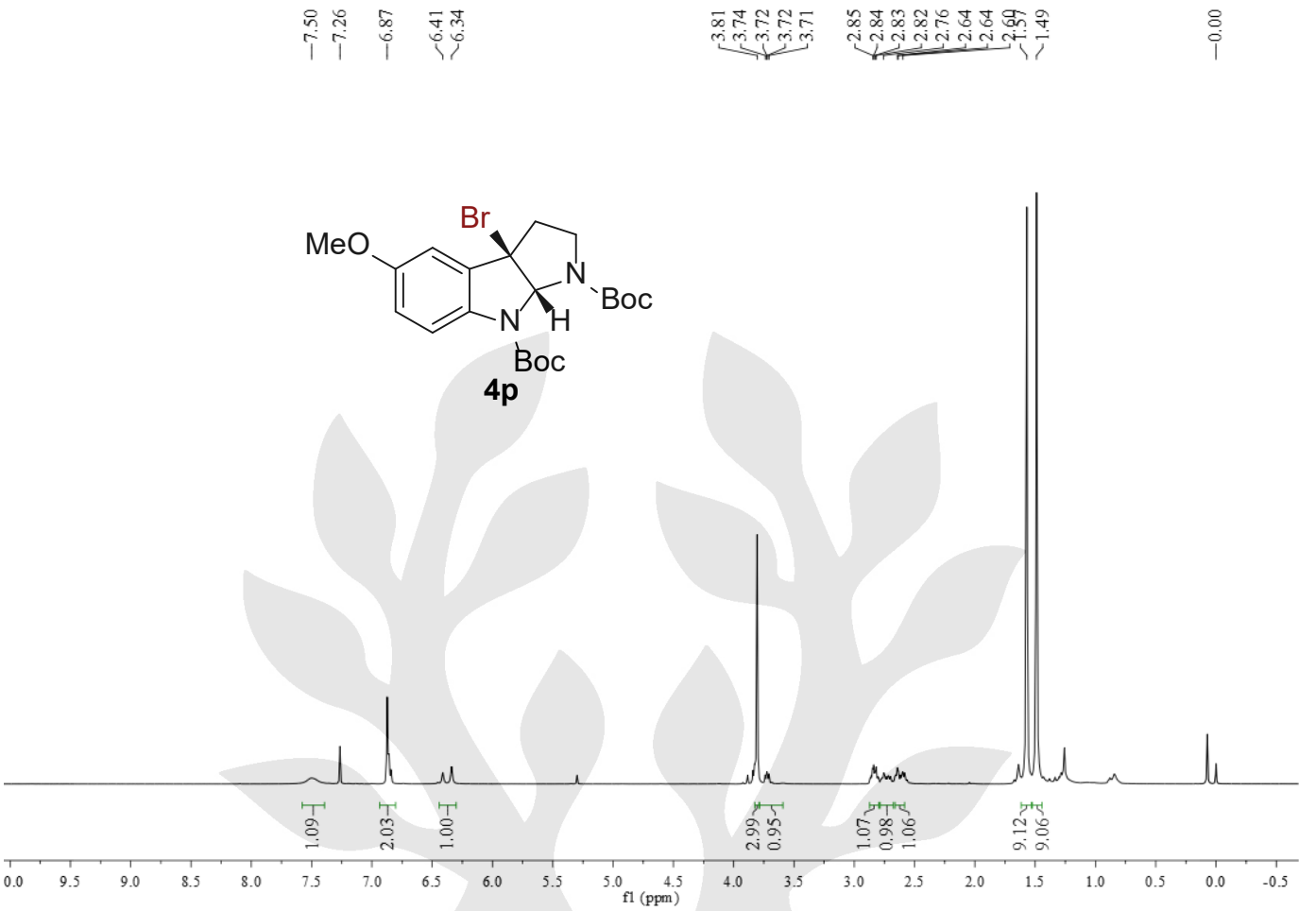

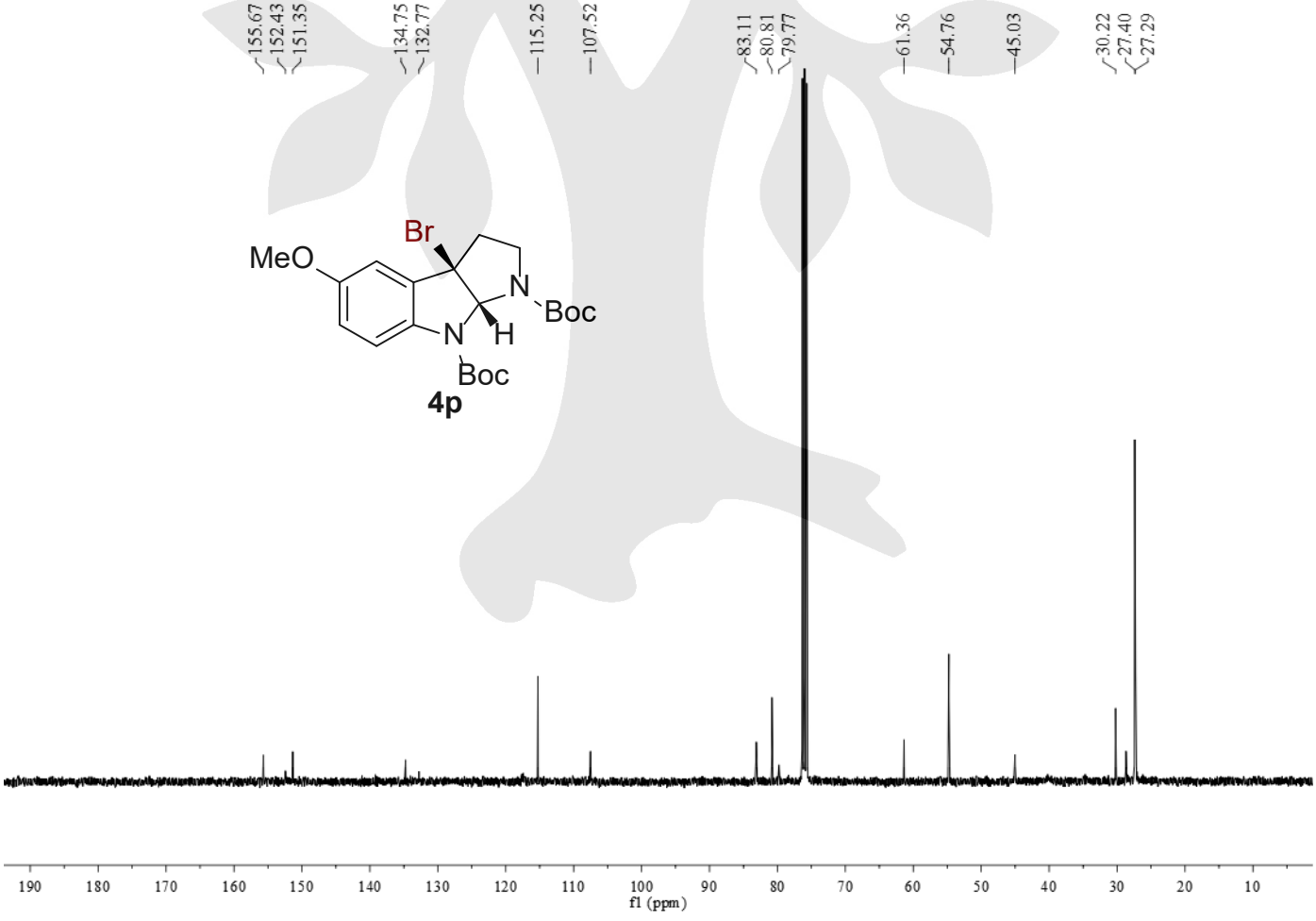

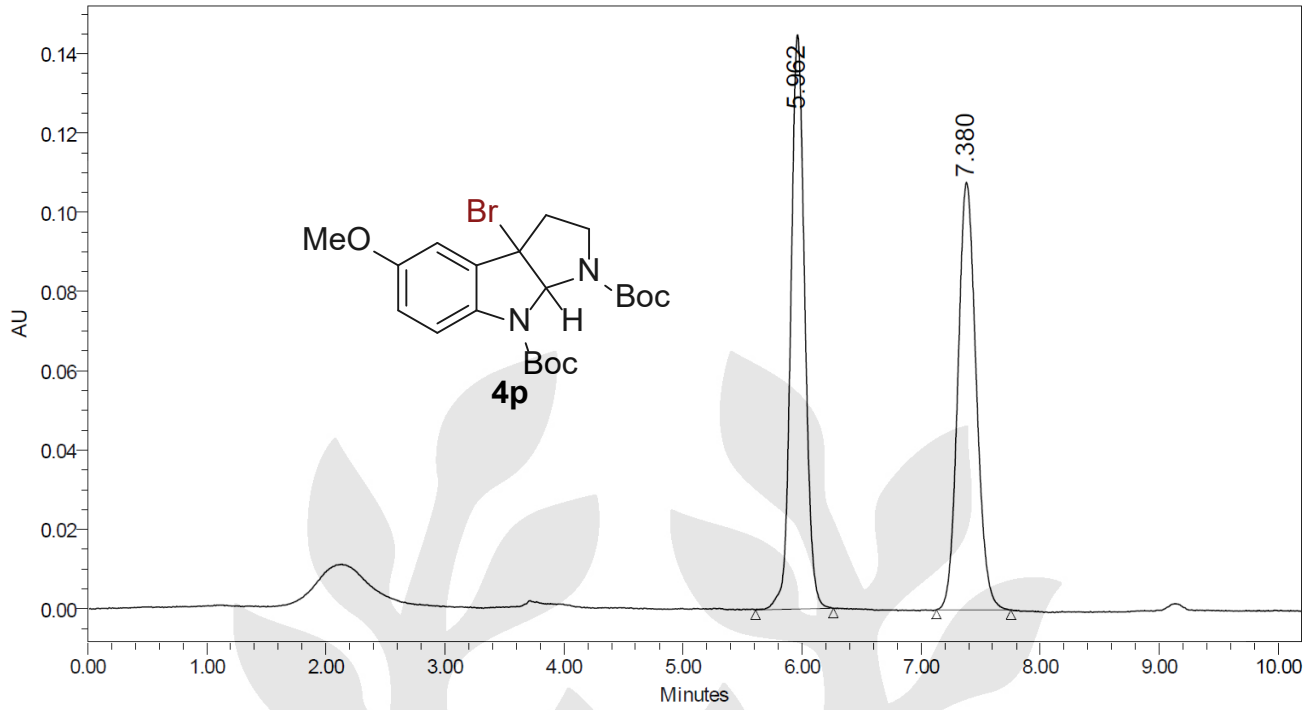

	RT (min)	Peak Type	Area (μV*sec)	% Area	Height (μV)	% Height	Integration Type	Points Across Peak	Start Time (min)	End Time (min)
1	5.962	Unknown	1185286	50.59	144910	57.33	BB	393	5.608	6.263
2	7.380	Unknown	1157649	49.41	107871	42.67	BB	375	7.128	7.753

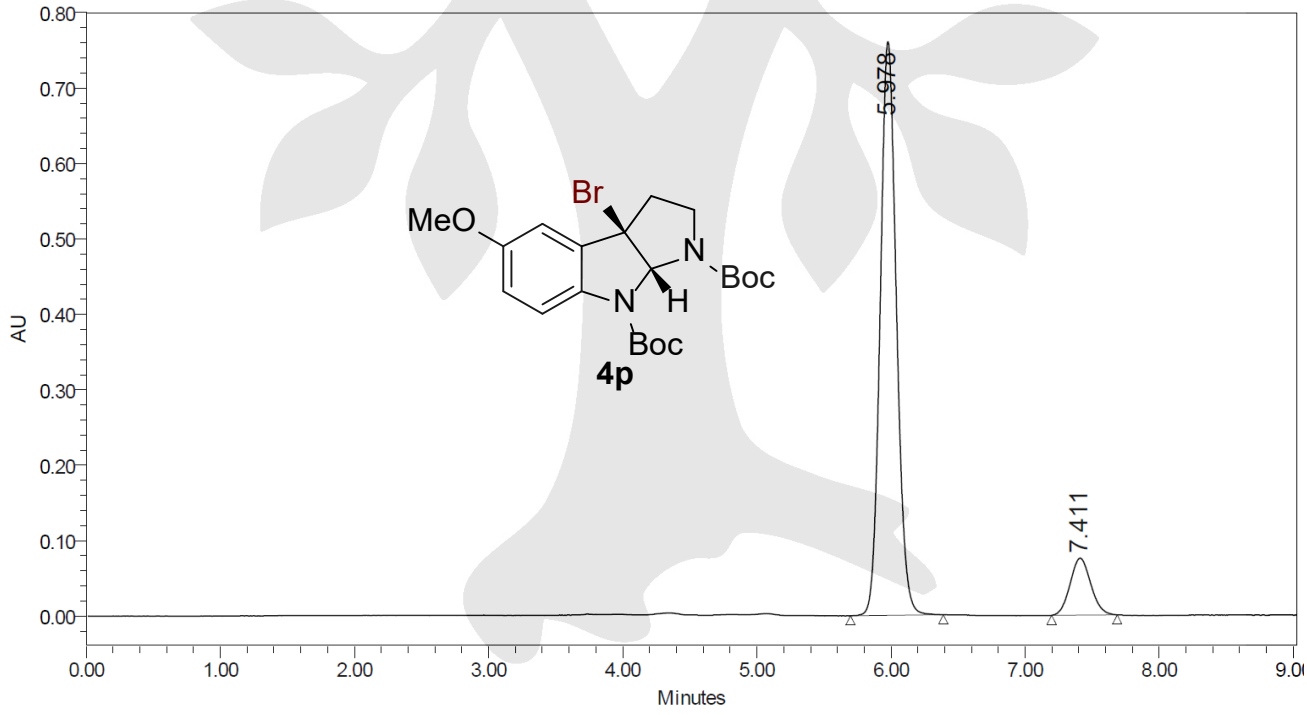

	RT (min)	Peak Type	Area (μV*sec)	% Area	Height (μV)	% Height	Integration Type	Points Across Peak	Start Time (min)	End Time (min)
1	5.978	Unknown	6392571	88.80	760640	90.98	BB	415	5.698	6.390
2	7.411	Unknown	806364	11.20	75423	9.02	bb	293	7.198	7.687

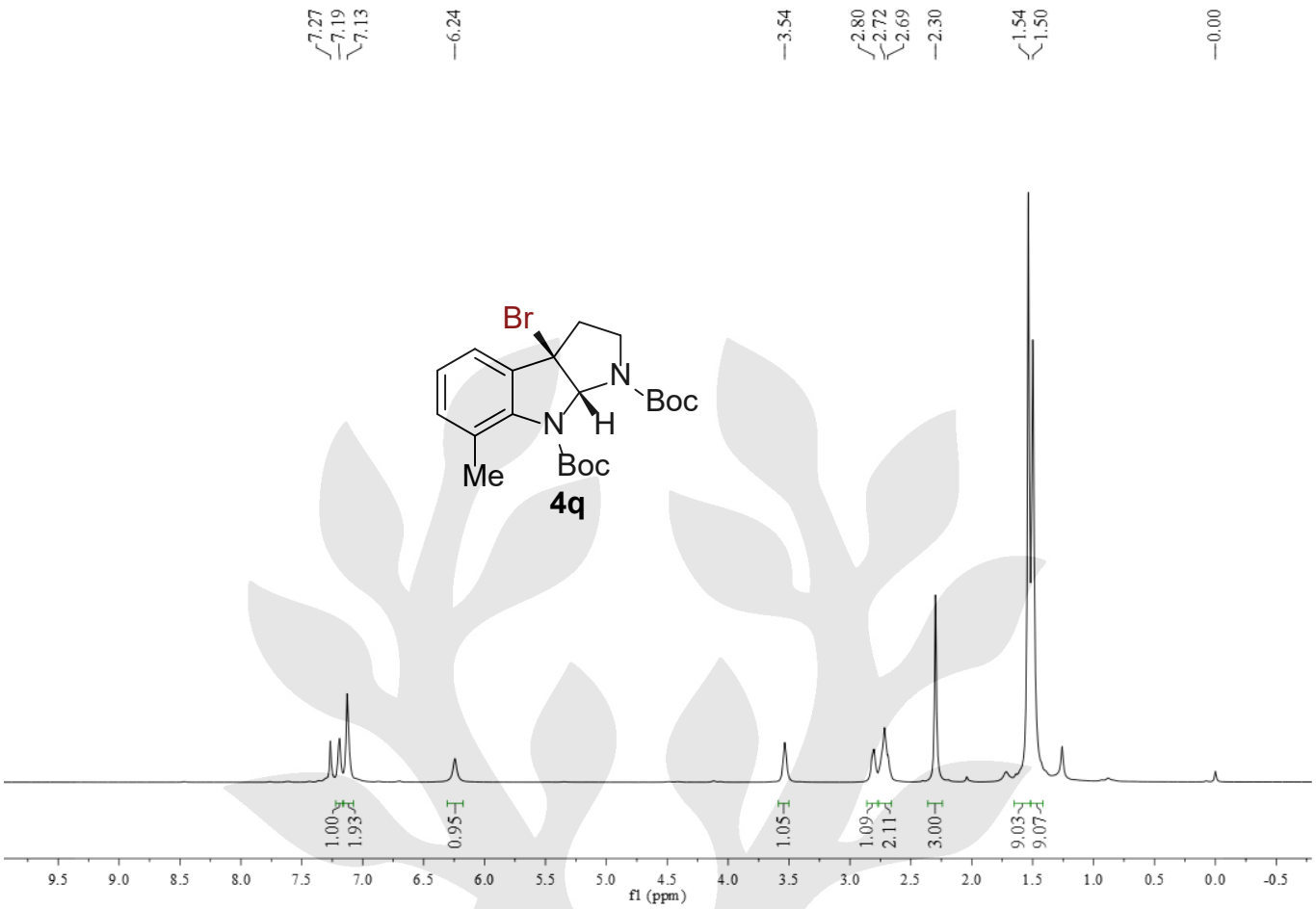

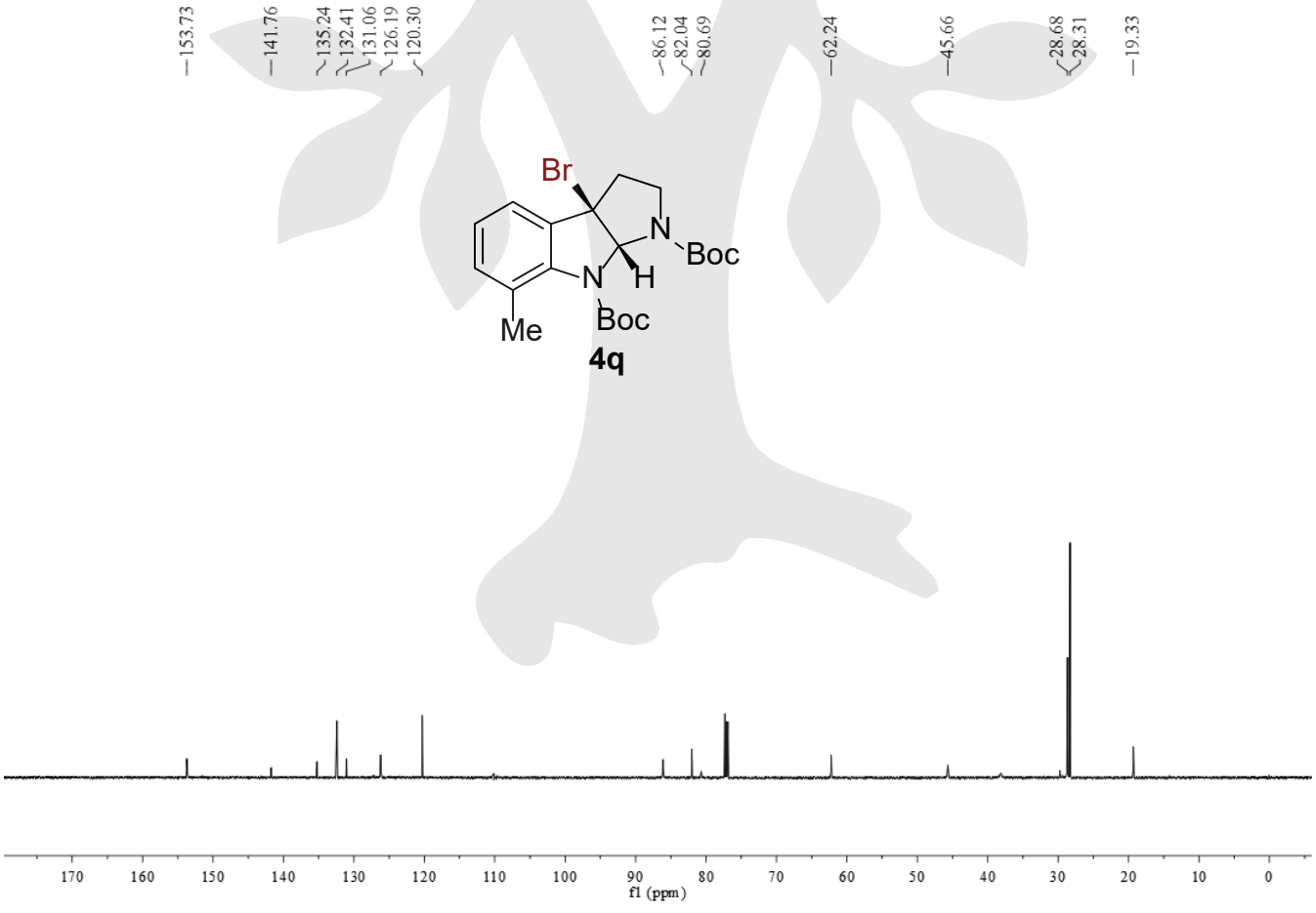

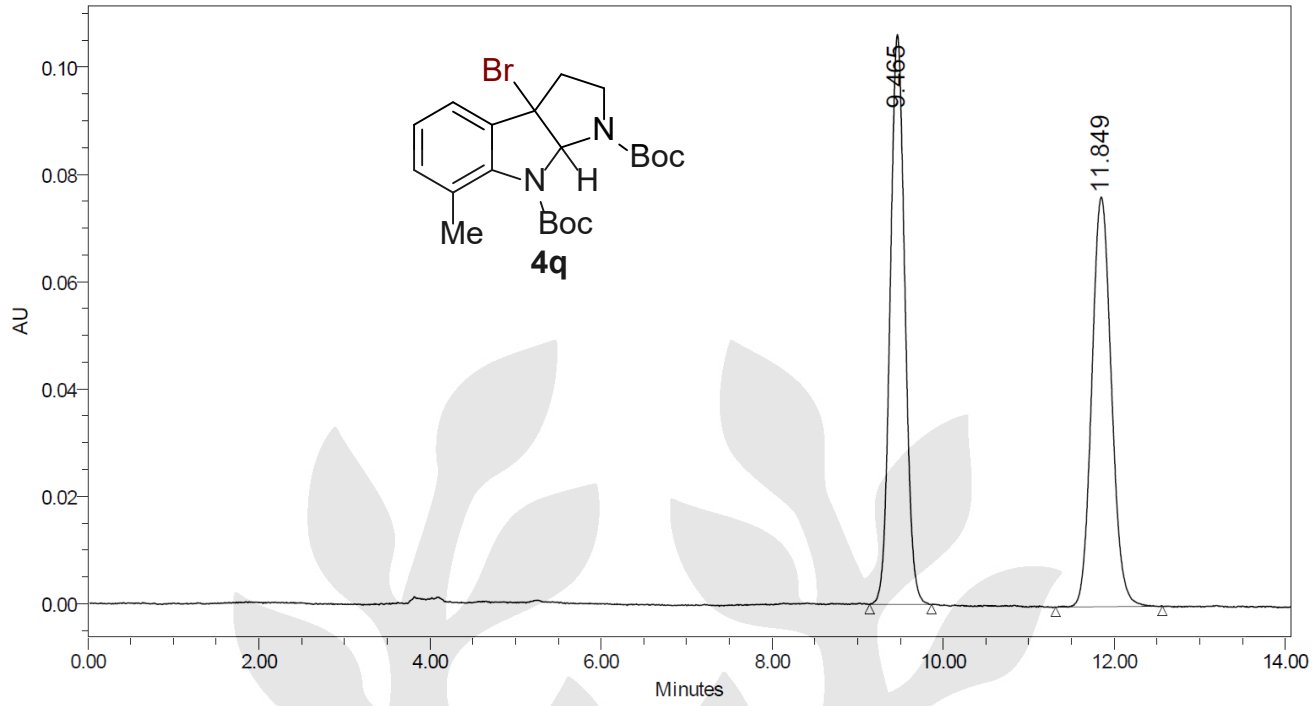

	RT (min)	Peak Type	Area (μV*sec)	% Area	Height (μV)	% Height	Integration Type	Points Across Peak	Start Time (min)	End Time (min)
1	9.465	Unknown	1271648	51.12	106212	58.19	BB	434	9.140	9.863
2	11.849	Unknown	1215898	48.88	76324	41.81	bb	749	11.315	12.563

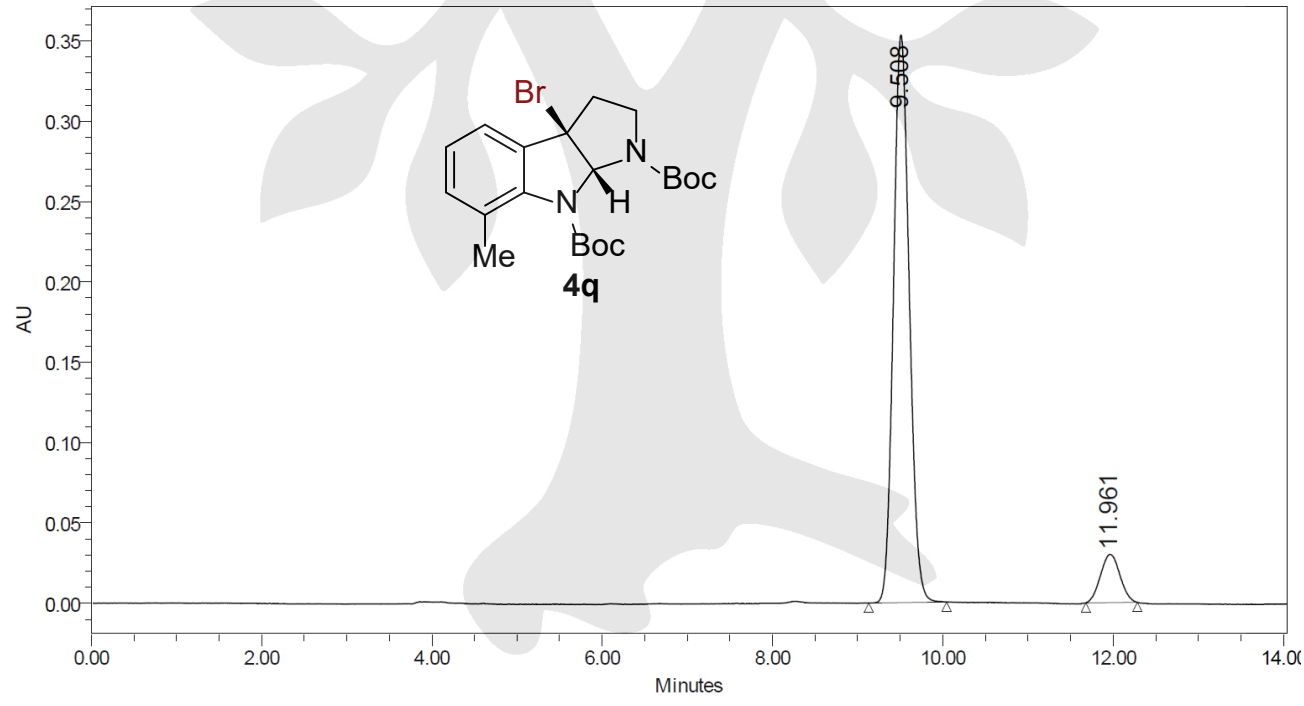

	RT (min)	Peak Type	Area (μV*sec)	% Area	Height (μV)	% Height	Integration Type	Points Across Peak	Start Time (min)	End Time (min)
1	9.508	Unknown	4555663	90.53	353349	92.16	bB	549	9.130	10.045
2	11.961	Unknown	476802	9.47	30072	7.84	bb	364	11.678	12.285

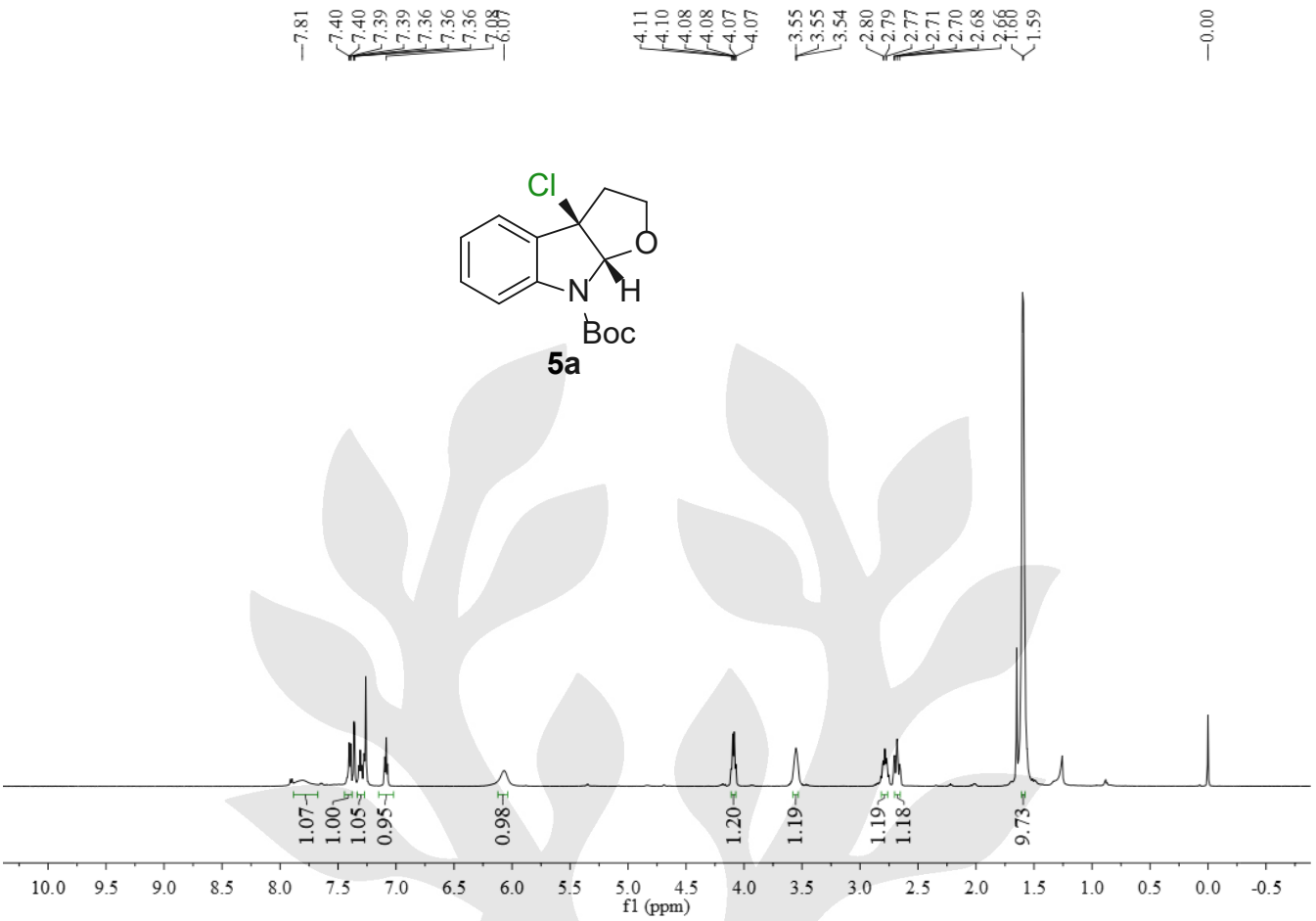

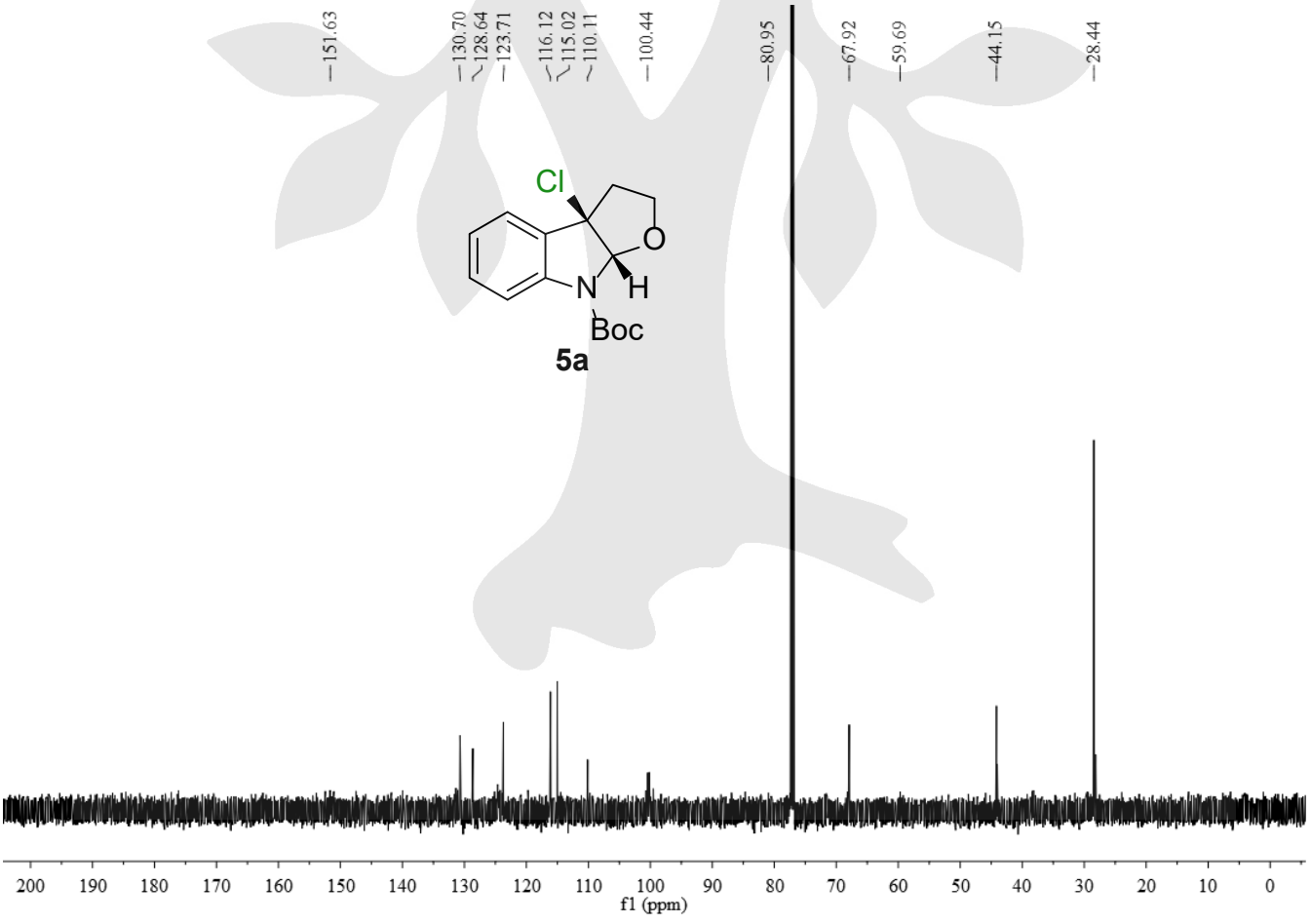

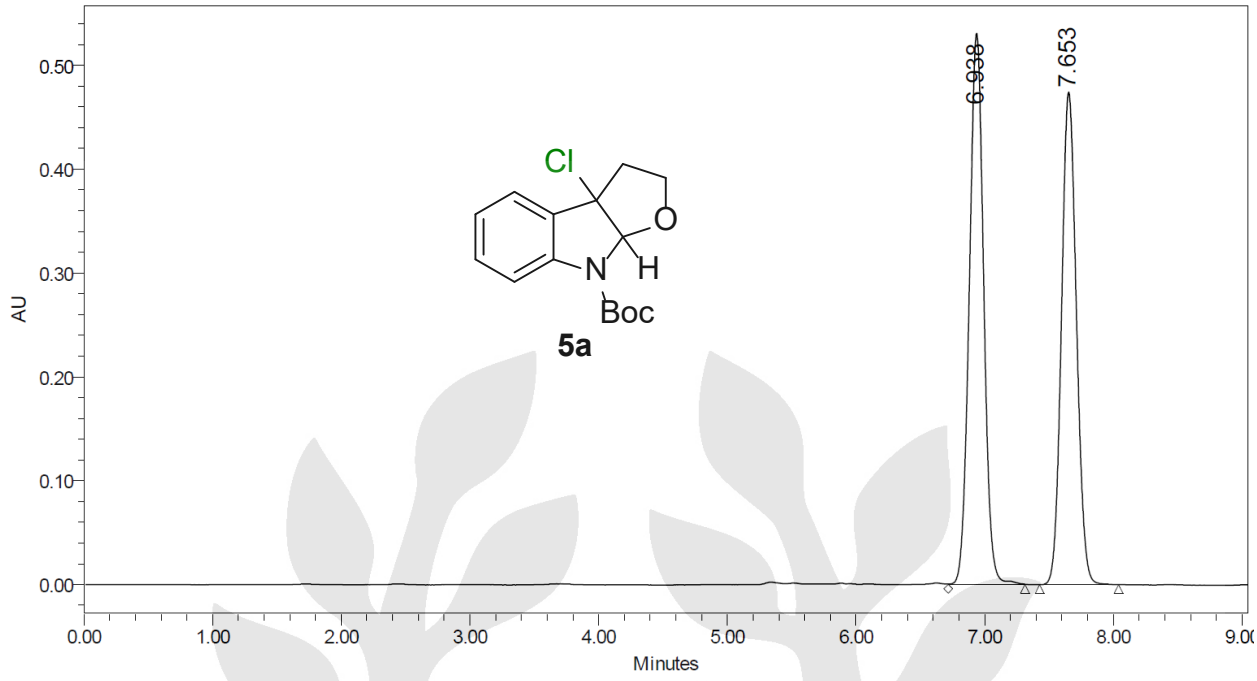

	RT (min)	Peak Type	Area (μV*sec)	% Area	Height (μV)	% Height	Integration Type	Points Across Peak	Start Time (min)	End Time (min)
1	6.938	Unknown	4122936	51.82	530660	52.80	Vb	358	6.717	7.313
2	7.653	Unknown	3832746	48.18	474349	47.20	BB	369	7.427	8.042

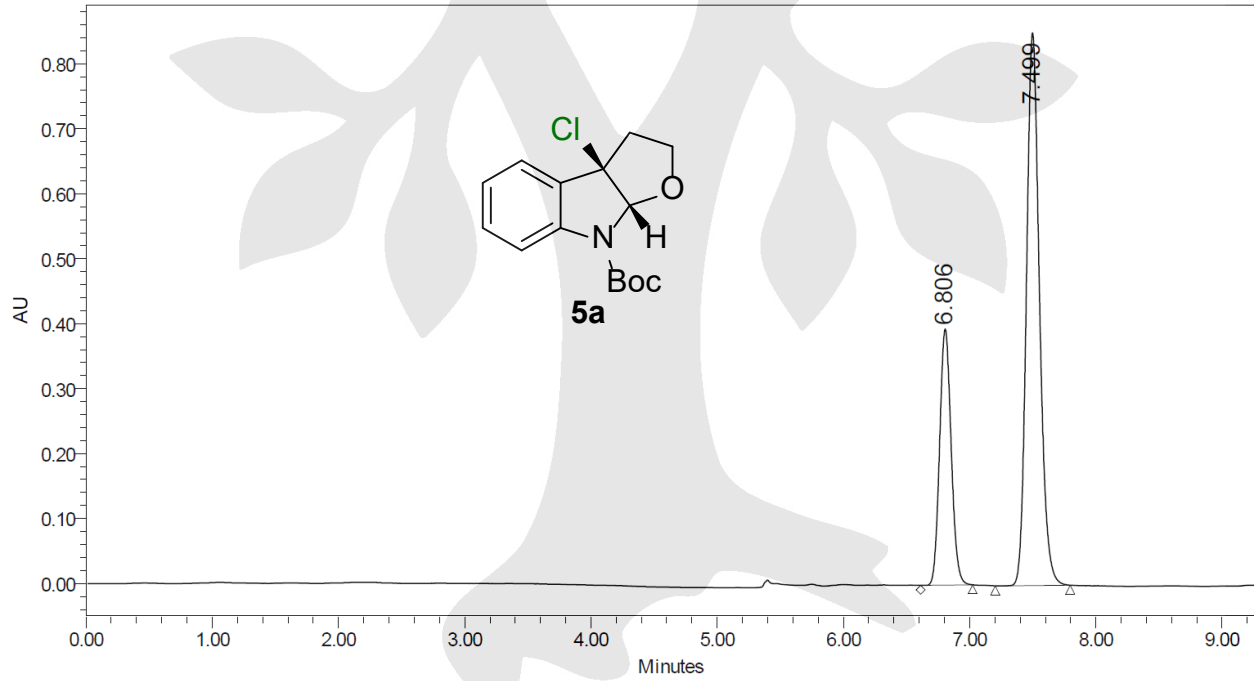

	RT (min)	Peak Type	Area (μV*sec)	% Area	Height (μV)	% Height	Integration Type	Points Across Peak	Start Time (min)	End Time (min)
1	6.806	Unknown	2508210	29.13	394203	31.66	Vb	247	6.612	7.023
2	7.499	Unknown	6101830	70.87	850886	68.34	bB	356	7.203	7.797

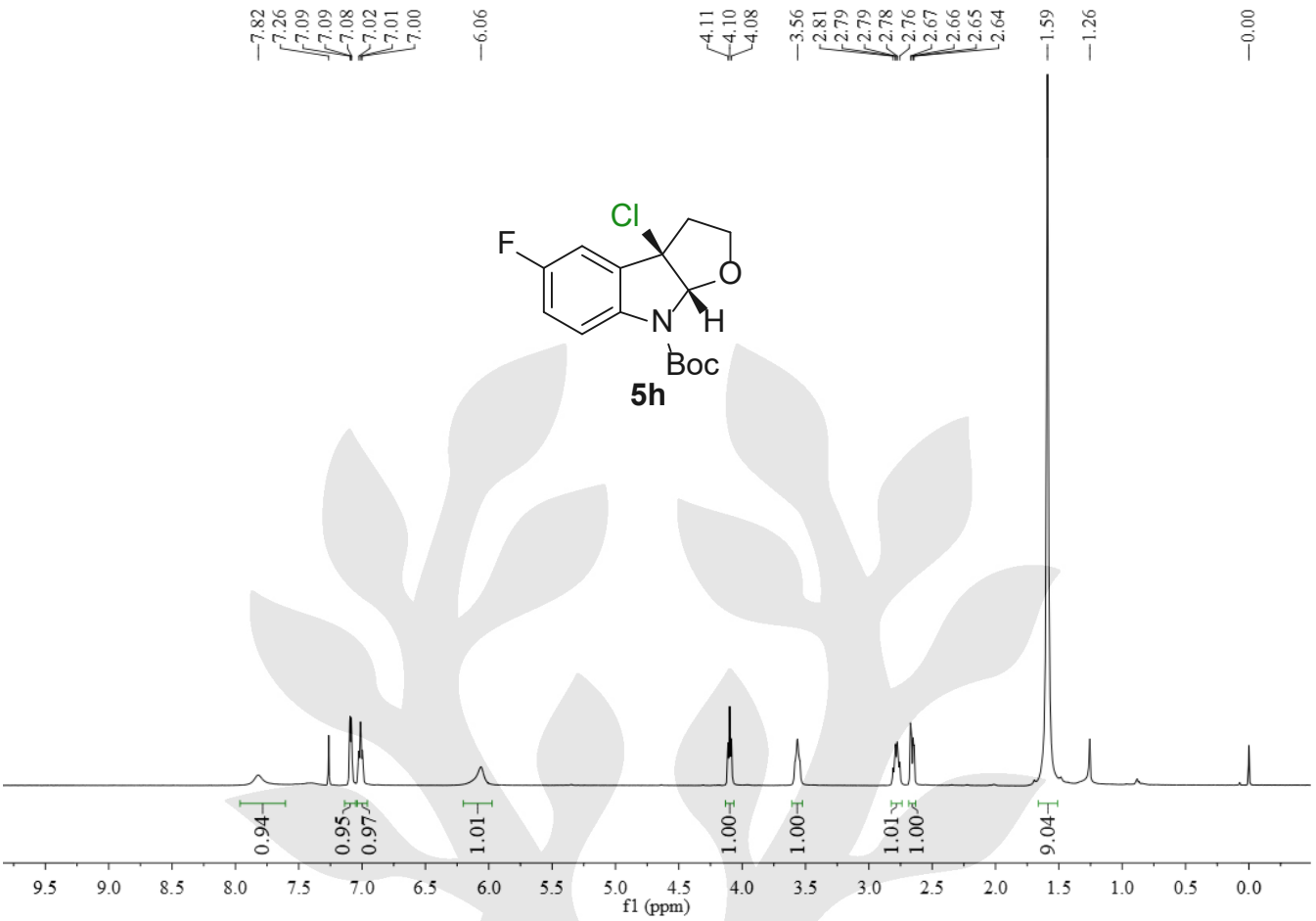

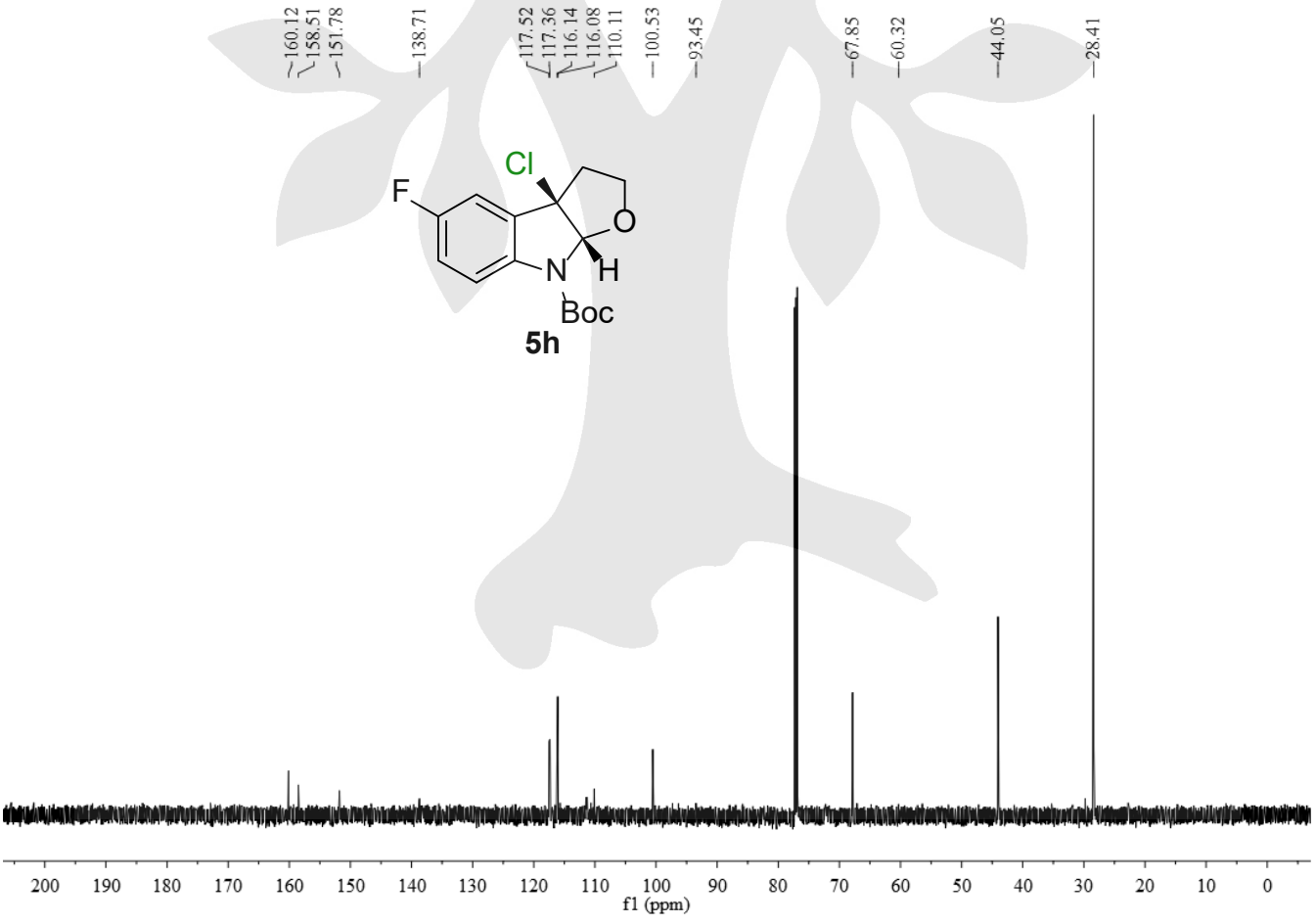

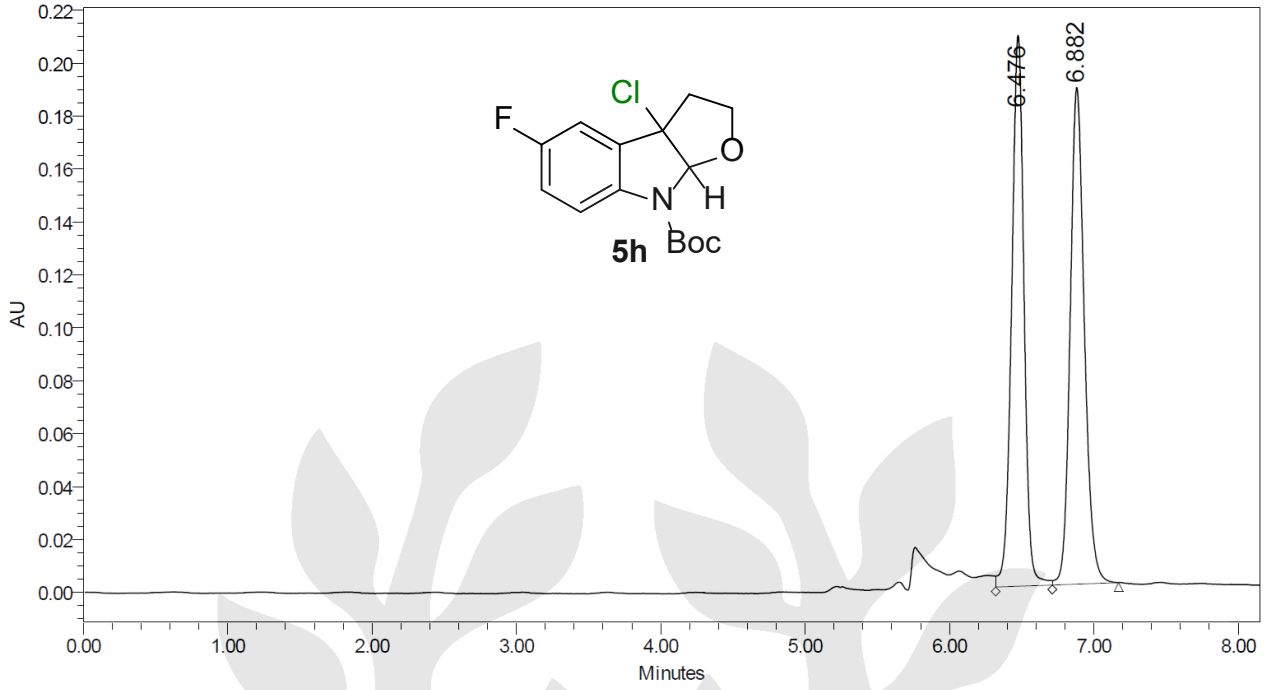

	RT (min)	Peak Type	Area (μV*sec)	% Area	Height (μV)	% Height	Integration Type	Points Across Peak	Start Time (min)	End Time (min)
1	6.476	Unknown	1241247	49.19	208225	52.59	VV	235	6.320	6.712
2	6.882	Unknown	1282182	50.81	187684	47.41	VB	276	6.712	7.172

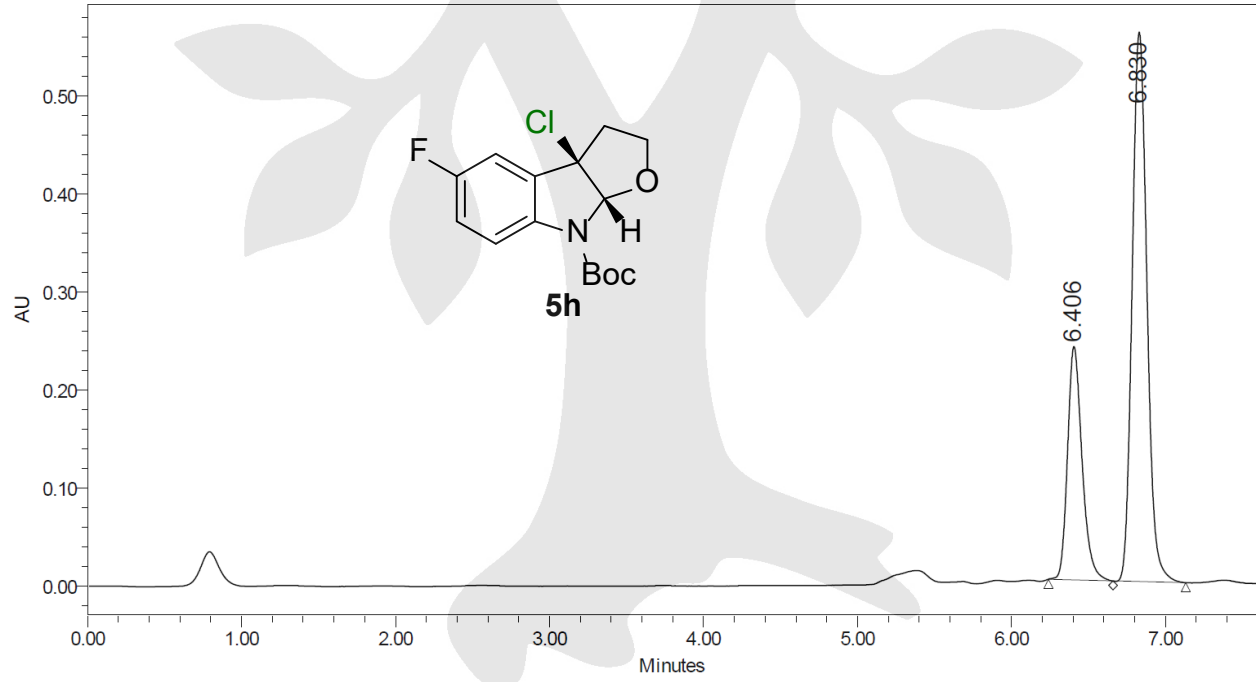

	RT (min)	Peak Type	Area (μV*sec)	% Area	Height (μV)	% Height	Integration Type	Points Across Peak	Start Time (min)	End Time (min)
1	6.406	Unknown	1560890	29.49	238152	29.81	bv	252	6.240	6.660
2	6.830	Unknown	3732650	70.51	560800	70.19	vb	283	6.660	7.132

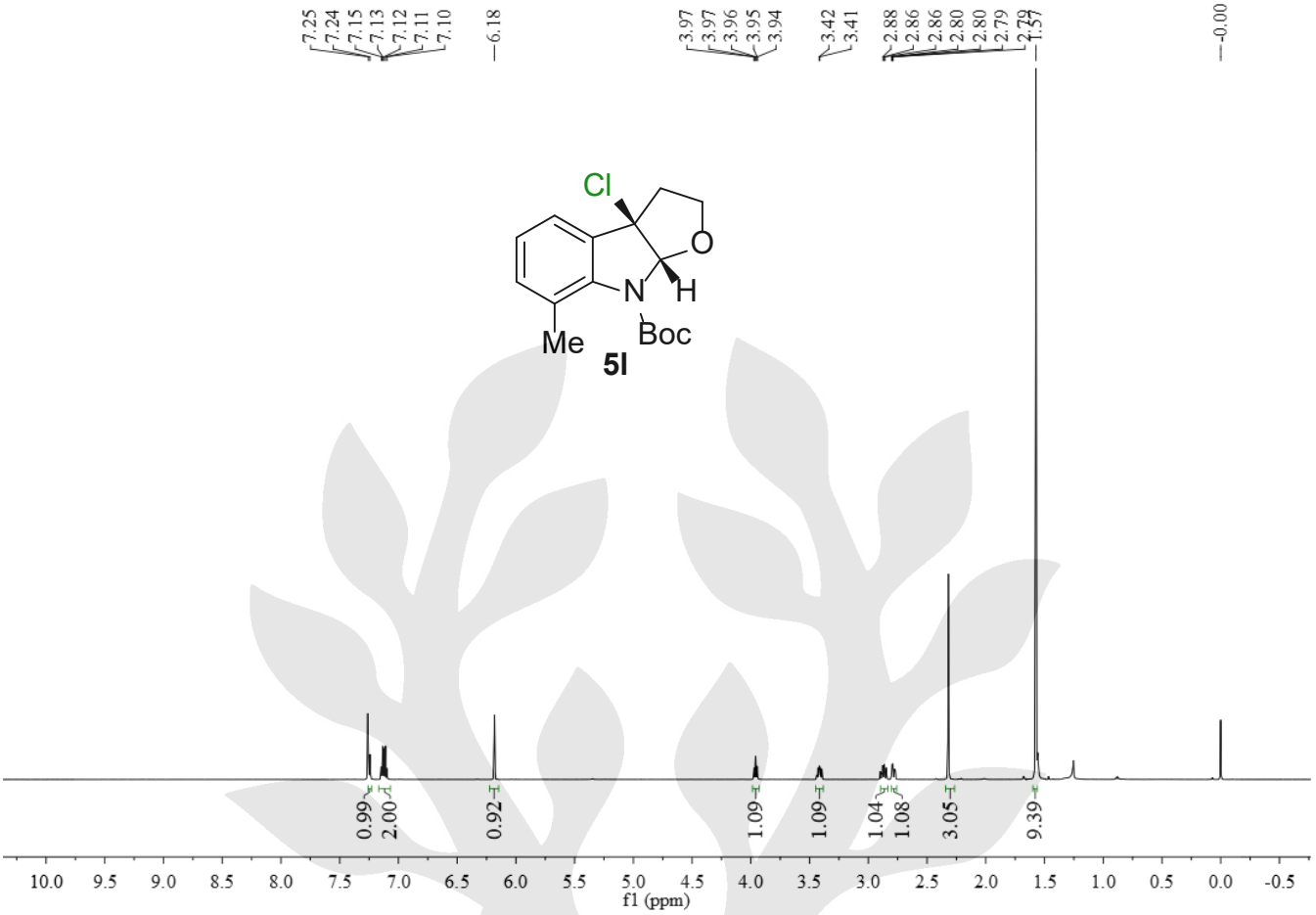

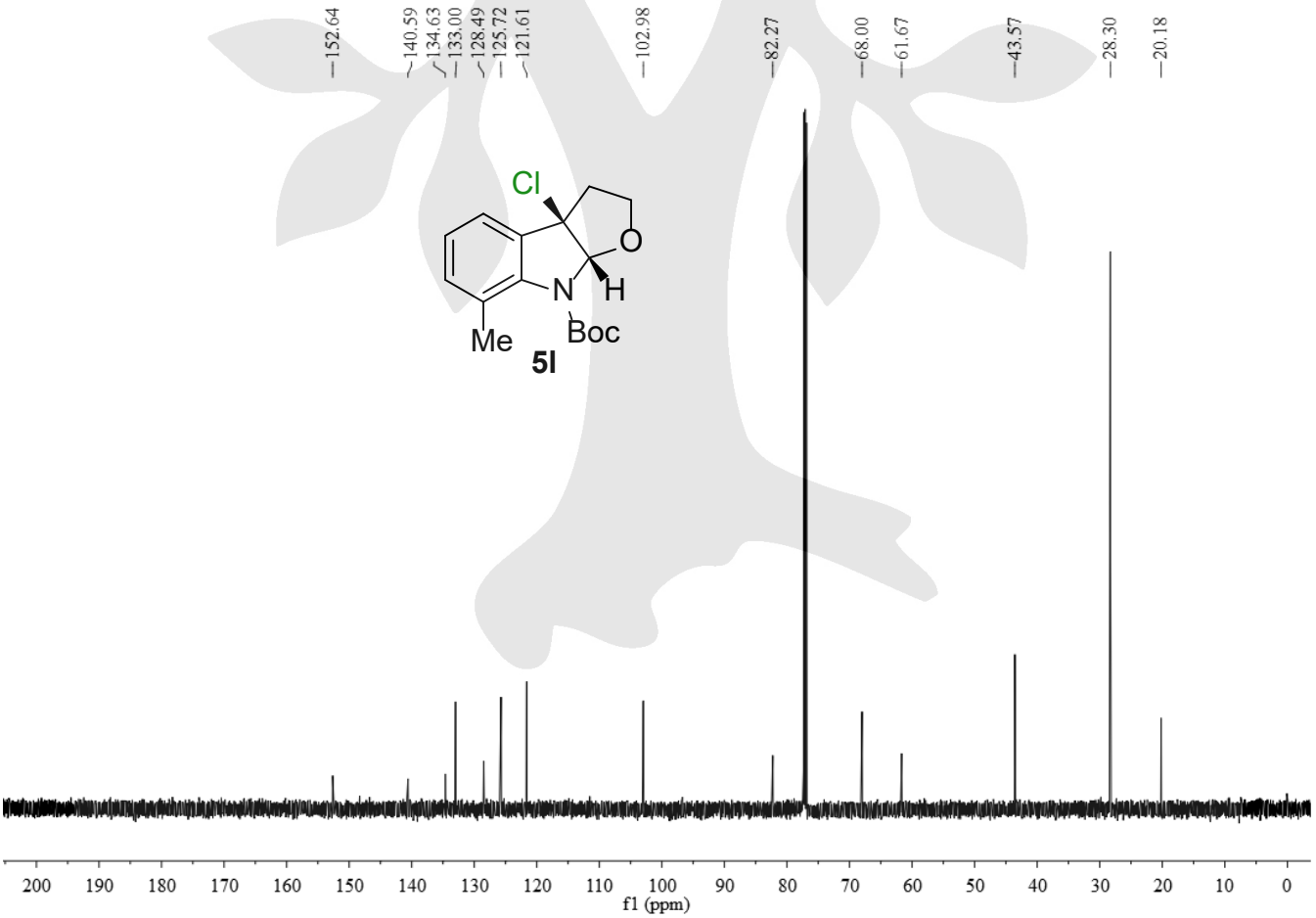

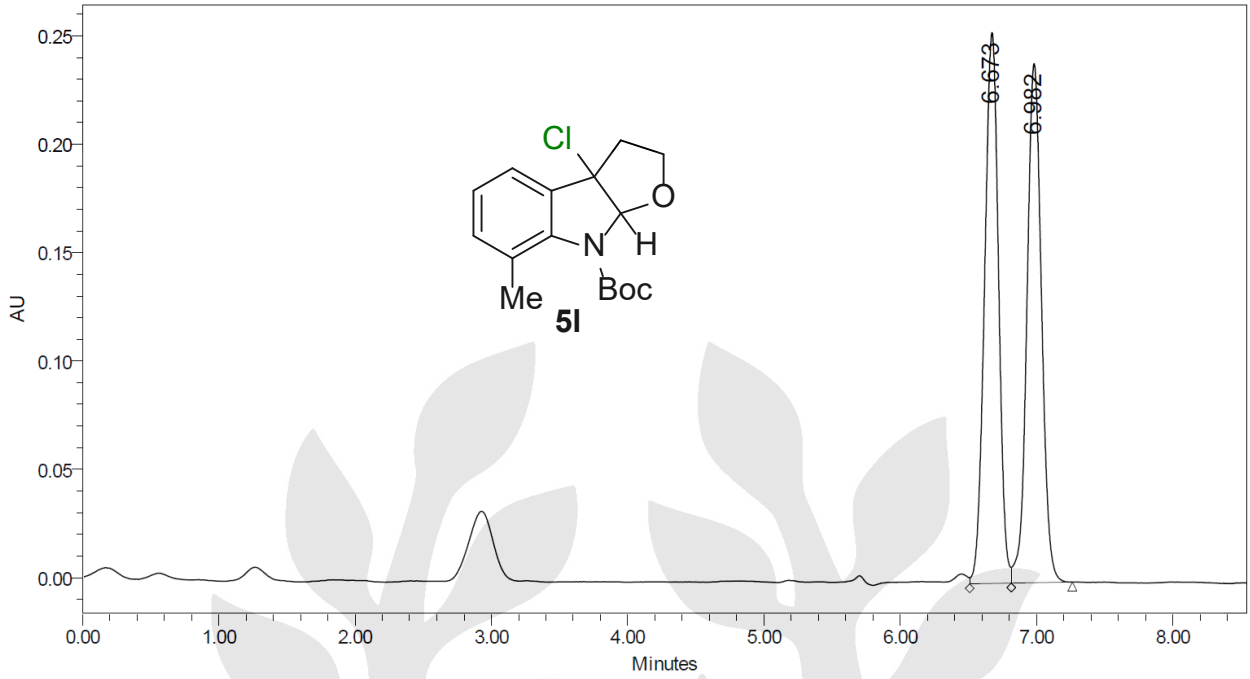

	RT (min)	Peak Type	Area (μV*sec)	% Area	Height (μV)	% Height	Integration Type	Points Across Peak	Start Time (min)	End Time (min)
1	6.673	Unknown	1814731	50.46	254224	51.48	VV	183	6.510	6.815
2	6.982	Unknown	1781959	49.54	239589	48.52	VB	269	6.815	7.263

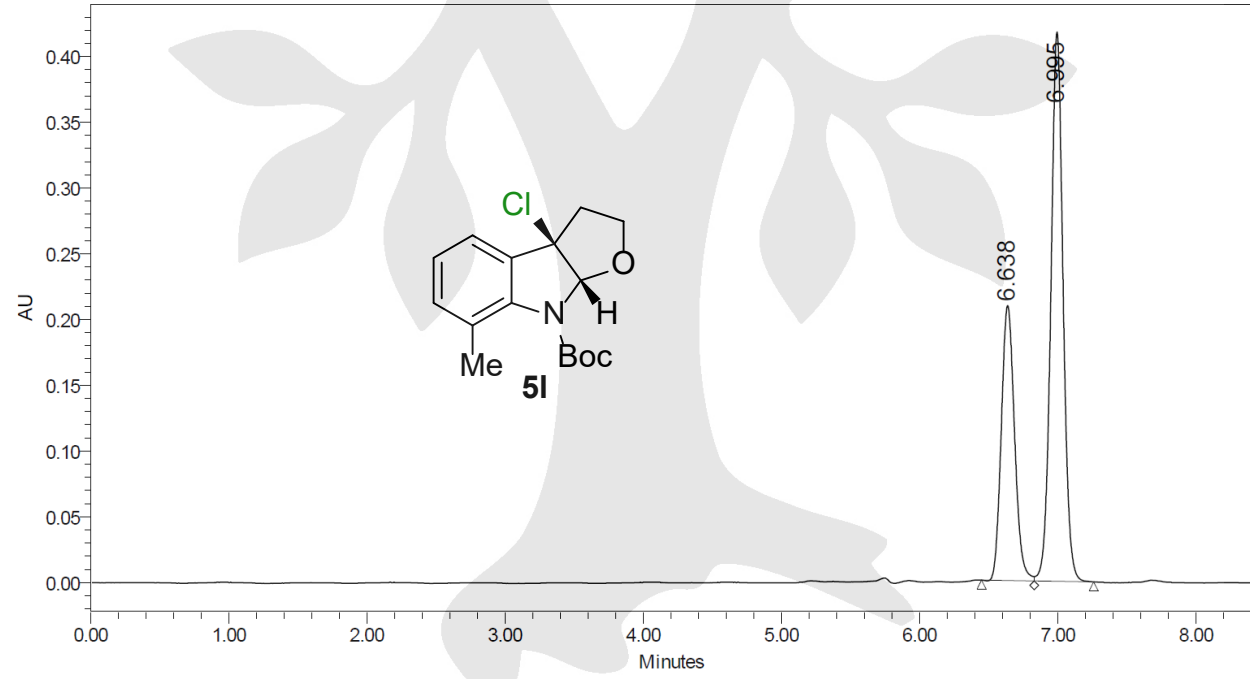

	RT (min)	Peak Type	Area (μV*sec)	% Area	Height (μV)	% Height	Integration Type	Points Across Peak	Start Time (min)	End Time (min)
1	6.638	Unknown	1395198	35.14	209005	33.35	bV	229	6.448	6.830
2	6.995	Unknown	2574764	64.86	417659	66.65	Vb	258	6.830	7.260

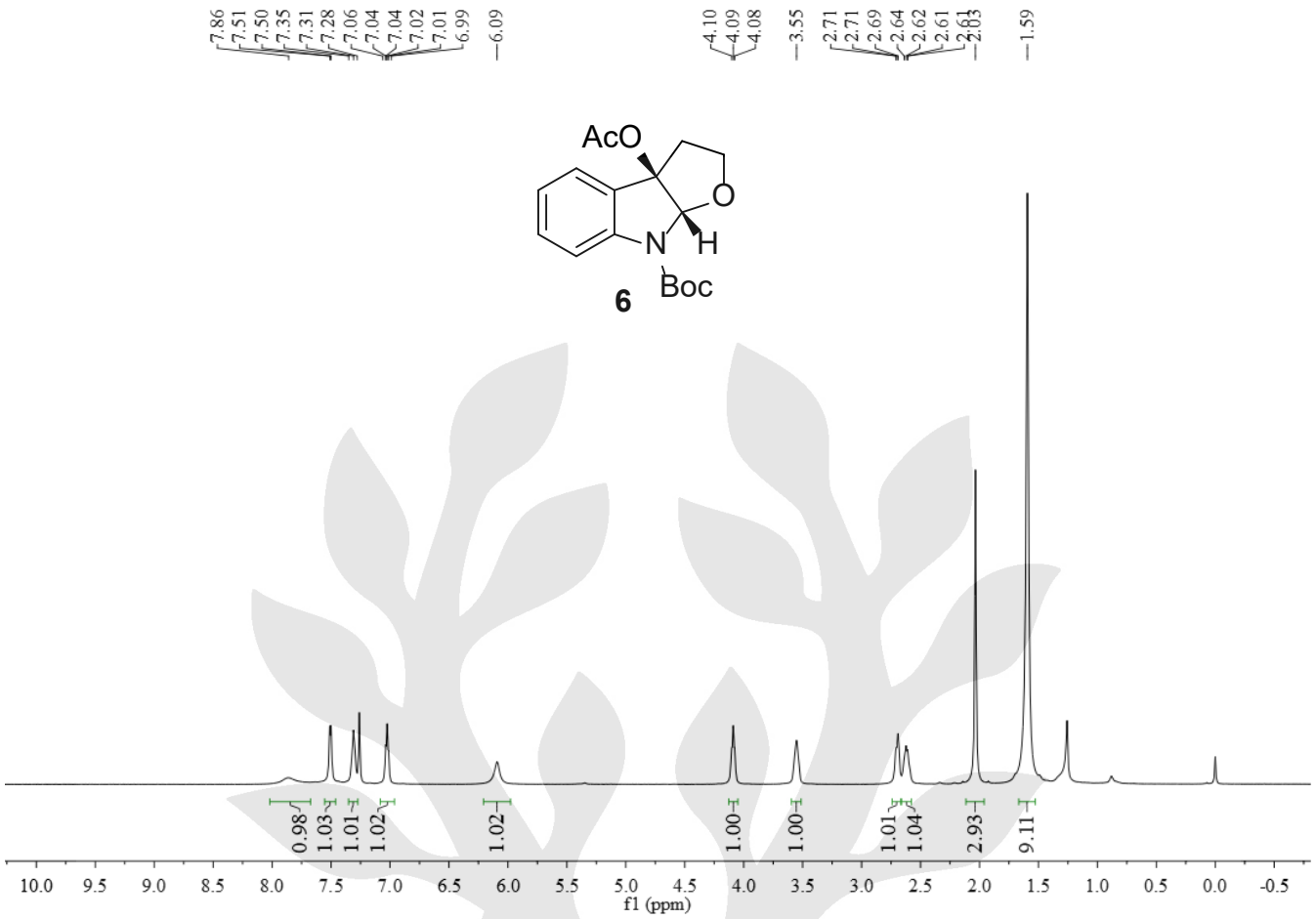

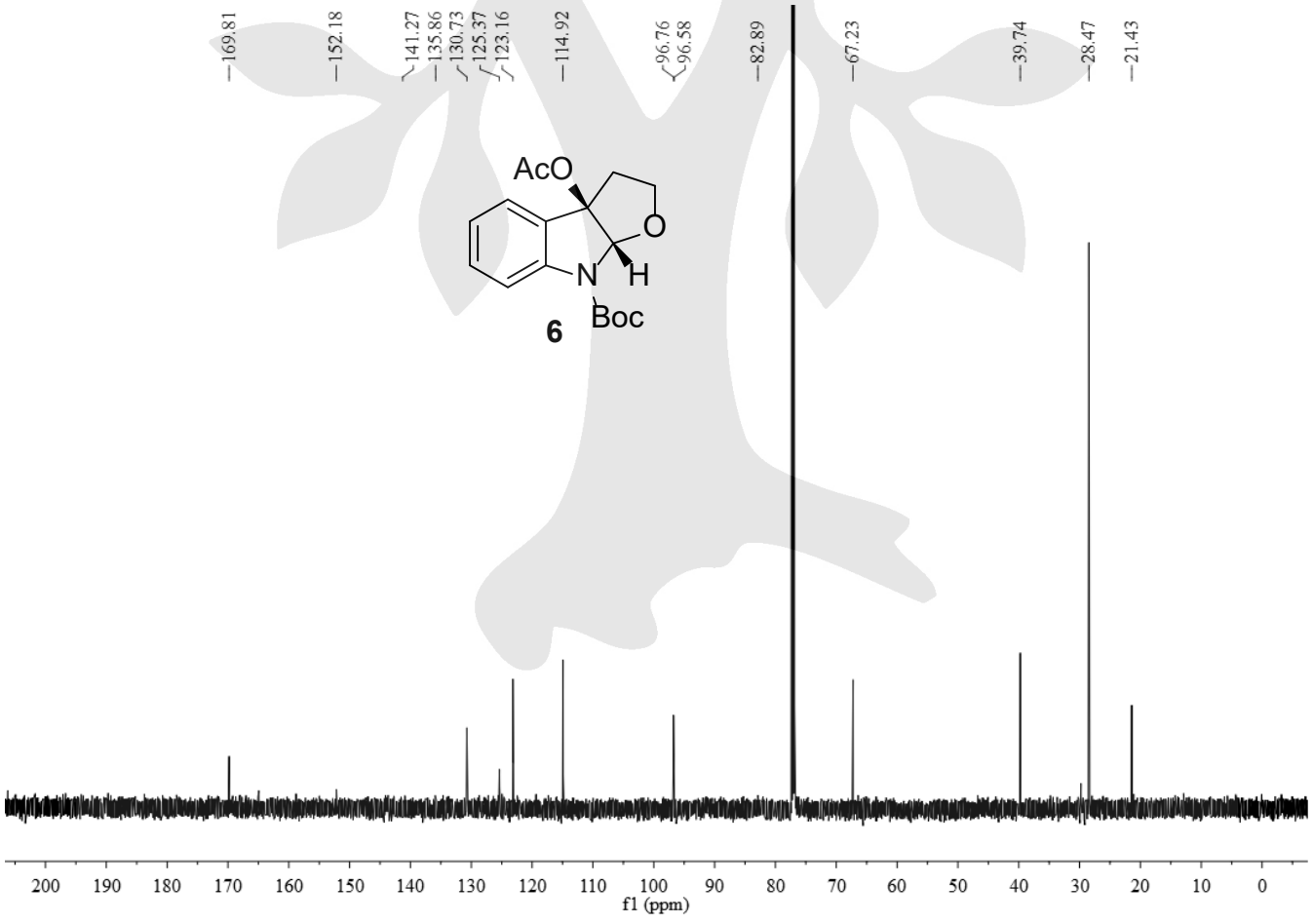

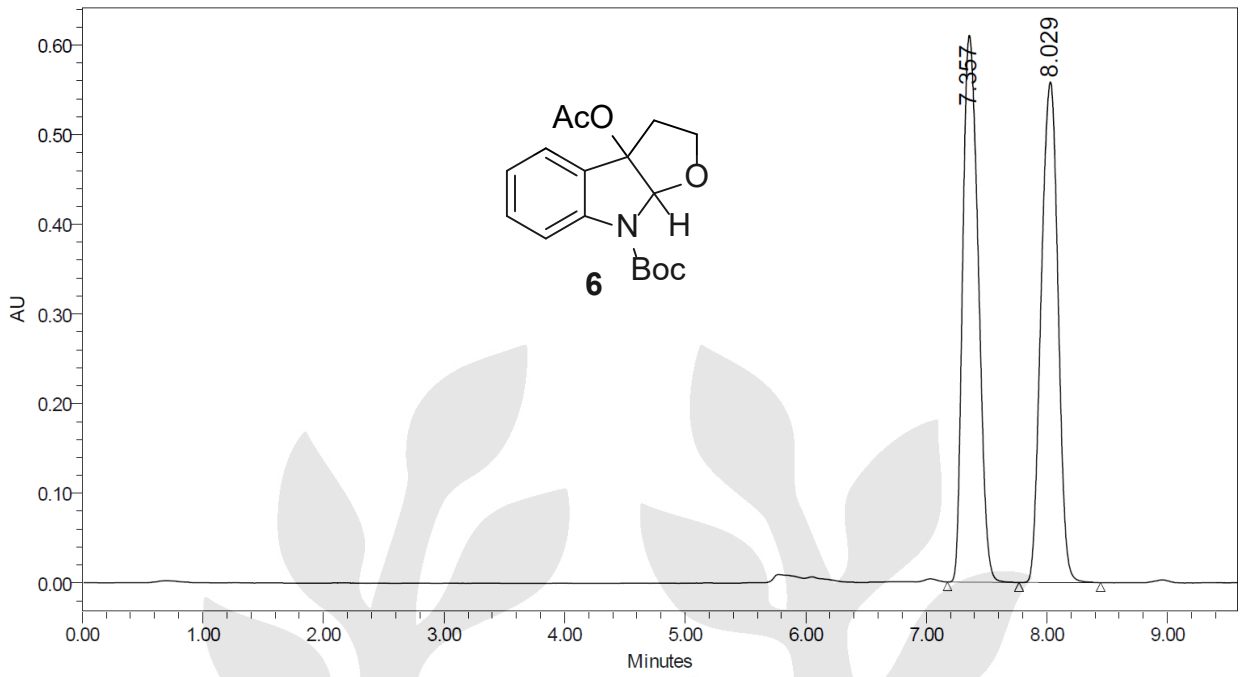

	RT (min)	Peak Type	Area (μV*sec)	% Area	Height (μV)	% Height	Integration Type	Points Across Peak	Start Time (min)	End Time (min)
1	7.357	Unknown	5478973	50.25	610134	52.22	BB	356	7.175	7.768
2	8.029	Unknown	5424305	49.75	558359	47.78	BB	406	7.768	8.445

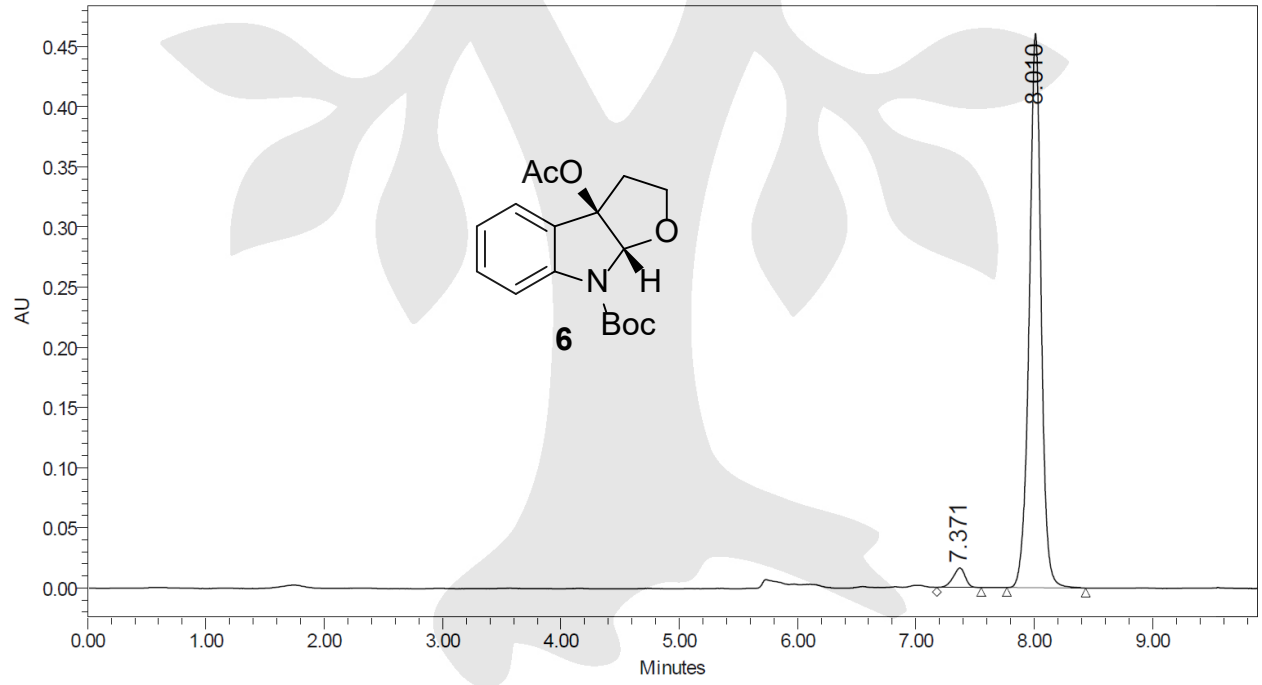

	RT (min)	Peak Type	Area (μV*sec)	% Area	Height (μV)	% Height	Integration Type	Points Across Peak	Start Time (min)	End Time (min)
1	7.371	Unknown	116433	3.49	16250	3.41	VB	225	7.177	7.552
2	8.010	Unknown	3215345	96.51	460719	96.59	BB	400	7.768	8.435